

1989

Sediment dynamics on the shore slopes of the Puget Island reach of the Columbia River, Oregon and Washington

Timothy Abbe
Portland State University

Follow this and additional works at: https://pdxscholar.library.pdx.edu/open_access_etds



Part of the [Geology Commons](#), and the [Sedimentology Commons](#)

Let us know how access to this document benefits you.

Recommended Citation


Abbe, Timothy, "Sediment dynamics on the shore slopes of the Puget Island reach of the Columbia River, Oregon and Washington" (1989). *Dissertations and Theses*. Paper 4306.
<https://doi.org/10.15760/etd.6190>

This Thesis is brought to you for free and open access. It has been accepted for inclusion in Dissertations and Theses by an authorized administrator of PDXScholar. Please contact us if we can make this document more accessible: pdxscholar@pdx.edu.


AN ABSTRACT OF THE THESIS OF Timothy Abbe for the Master of Science in Geology presented August 11, 1989.

Title: Sediment Dynamics on the Shore Slopes of the Puget Island Reach of the Columbia River, Oregon and Washington.

APPROVED BY MEMBERS OF THE THESIS COMMITTEE:


Richard E. Thoms, Chair


Ansel G. Johnson


Leonard A. Palmer


Scott Wells

Water waves generated by wind and ships; ebb tidal currents; water level fluctuations; and dredging impact sediment transport in shallow water of the lower Columbia River. Observations were made over a one-year period after sand dredged from the navigation channel was placed at three study sites in the Puget Island region, 46°15'N

123°25'W, Oregon and Washington. Sediment composition is fine to medium grained, low density dacitic volcanics with small percentages of pumice, heavy minerals, and basalt.

Sediment response to ship waves was examined on a smooth sandy beach face at specific points in shallow water using a sediment trap system. "Ship waves" include: an initial drawdown event (uni-direction flow off the shore); a surge (transverse stern) wave moving obliquely up and along the shore in the direction of ship motion; "quiet" period (water surface returns to mean conditions); and incidence of secondary ship waves. Drawdown and secondary ship waves accounted for most of the sediment flux during ship passages. Hydraulics of ship wave actions include: (sheet flow, wave orbital velocities, plunging waves, and longshore currents. Boundary conditions describing the limit of shallow water sediment flux by ship waves are at a depth of about 2.0 meters to 0.3 meters above mean water level. A model constructed to evaluate the annual impact of ship waves showed that (using maximum measured merchant ship waves and natural processes), $6,364 \text{ m}^3$ of sand eroded or 25% of the $26,197 \text{ m}^3$ of sand place at the site. Using the maximum measured sediment transport by larger naval ship waves, predicted erosion is $73,478 \text{ m}^3$ of sand per year, above the eroded volume by 2.8 times. The range of predicted values encompasses the actual eroded volume.

Error is attributed to the exponential distribution of sediment flux in the vicinity of a breaking wave that makes accurate point sampling difficult. Another source of error in the mass balance may be the lack of observations during high energy events, such as storms.

Annual cumulative energy delivered by a process to the shore is secondary to instantaneous energy the process delivers. If instantaneous energy is not enough to move sediment then the process is of little importance in sediment transport. Observed ebb tidal currents and wind waves only slightly surpassed sediment threshold conditions, so even summed over large time periods, they account for a very small quantity of sediment entrainment. Ship waves regularly supply energy in very short time intervals (1-6 minutes) well in excess of the sediment threshold conditions and account for most of the sediment transport.

Physical processes also result in a distinct set of geomorphic features and sedimentary structures: shore notches, beach scarps, and planar bedding by ship waves; alluvial fans by wind; oscillatory ripples by wind waves; trough and hummocky cross-bedding by tidal fluctuations; swash lines of pumice and heavy minerals, beheaded ripples, and reactivation surfaces by waves. Shore slope change is most rapid shortly after sand disposal, decreasing with time as slope approaches a more stable state. The greatest

shore changes occurred at sites closest to the navigation channel. Features such as shore notches can dramatically impact slope evolution, eroding into a previously stable shore. Shore notches are asymmetric sites of accelerated shore erosion associated with adjacent lower beach accretionary lobes.

In water less than two meters, fluvial and estuarine processes are overprinted by pipeline dredging operations and the passage of large ships. Ship waves modify shore morphology and remove sediment from the intertidal zone of the shore slope.

SEDIMENT DYNAMICS ON THE SHORE SLOPES
OF THE PUGET ISLAND REACH OF THE COLUMBIA RIVER,
OREGON AND WASHINGTON

by
TIMOTHY ABBE

A thesis submitted in partial fulfillment of the
requirements for the degree of

MASTER OF SCIENCE
in
GEOLOGY

Portland State University
1990

TO THE OFFICE OF GRADUATE STUDIES:

The members of the Committee approve the thesis of
Timothy Abbe presented August 11, 1989.

[REDACTED]

Richard E. Thoms, Chair

[REDACTED]

Ansel G. Johnson

[REDACTED]

Leonard Palmer

[REDACTED]

Scott Wells

APPROVED:

[REDACTED]

Ansel G. Johnson, Chair, Department of Geology

[REDACTED]

C. William Savery, Interim Vice Provost for Graduate
Studies and Research

ACKNOWLEDGEMENTS

This thesis was the largest (literally) project I've attempted in my life, something that I often thought might never become a reality. But after to many long hours and more trial and error than I care to recount, I've come to the end of this project.

I have a lot of people to thank. I'll begin with my thesis advisor, Dr. Richard Thoms, whom brought this project to light when he found I was interested in recent sedimentology and physical processes. Dick was supportive and the days he spent with me hashing through my work is greatly appreciated. Dick become one of my best friends and I look forward to keeping in close touch with Dick and Chris. Dr. Ansel Johnson was a steadfast supporter and friend helping me get through some of the mathematics and kept me moving along toward completion. I enjoyed all of Ansel's classes and I have become much better at quantitative methods through his tutoring. Ansel's help and encouragement allowed me to present some of my results at several scientific meetings.

The U.S. Army Corps of Engineers employed me during the interim in which this thesis was completed and without the professional help, economic support, and field support

this thesis would never have become reality. I express special thanks to my supervisor, Dick Vetter for his confidence and support. Mr. Steve Chesser often offered me encouragement and read through my manuscripts, I greatly appreciate all his help. After rough seas at first meeting Karl Eriksen, I believe we've become good friends and I greatly appreciated Karl's professional advice and guidance. Mark Korsness has been a awesome colleague and friend, what more can I say? Thanks Mark! And I'd like to add a thanks to my second boss at the Corps, Ron Mason. Ron is the kind of boss most of us only hope we'll ever work for, thanks for your support Ron!

I greatly enjoyed my classes in civil engineering, and hope to pursue many more C.E. classes. Much of this incentive is due to the great C.E. professors I had at Portland State. Special thanks go to Dr. Scott Wells who provided me encouragement, advice, was a great teacher and a source of inspiration of what people can do to make a better world!

Dr. Palmer provided valuable advice on my research and showed that a professional can do a lot to help the community in which they live. I'd like to thank Dr. Michael Cummings. Mike was often ready to critique my work and presentations. Mike opened up an opportunity to me when I first arrived at PSU and was always a source of

inspiration, Mike was one of the finest teachers I've ever had.

And a very special thanks go to my closest friends; Ruth and Stephani Onisko, Karen Boelling, Tom Taylor, Ellen Eberhardt, and my brother Cleve. The final manuscript is a testimony to the help Tom gave me in the anagonizing final weeks. All my friends, especially Stephani put up with a lot of my stressed out behavior, and I am indebted forever. Thanks Stephani, you'll always be my best friend! All my friends, colleagues, and professors are the most important part of this thesis.

This thesis means a lot to me, for it took perserverance I didn't think I could muster. My graduate studies at Portland State University have enabled me to become a better geologist, more organized, and the happiest I've ever been in my life! I'm looking forward to a challenging and productive career in environmental geology and engineering.

TABLE OF CONTENTS

	PAGE
ACKNOWLEDGEMENTS.....	iii
LIST OF TABLES.....	ix
LIST OF FIGURES.....	xii
 INTRODUCTION	 1
Synopsis of the Problem	1
Geology of the Study Region.....	5
The Columbia River.....	14
Geomorphology.....	17
Human Actions.....	21
Shore Features.....	24
Ship Waves	24
Hypothesis	31
 METHODS	 34
General Methodology.....	34
Shore Monitoring.....	36
Aerial Image Analysis.....	36
Profiles.....	37
Observations of Beach Characteristics.....	42
Geomorphology.....	42
Ship Passage	43
Background Conditions.....	43
The Ships.....	44
Sediment Analysis.....	45

Sediment Transport	51
RESULTS	56
The Study Sites.....	56
Shore Erosion.....	59
Aerial Image Analysis, Price Island.....	62
Aerial Image Analysis, Puget Island.....	62
Aerial Image Analysis, Gull Island.....	67
Shore Profiles, Price Island.....	69
Shore Profiles, Puget Island.....	71
Shore Profiles, Gull Island.....	77
Observations of Beach Character.....	79
Geomorphic Features.....	79
Constructing a Shore Nourishment.....	84
Shore Slope Morphology.....	88
The Shore Notch.....	93
Sedimentary Structures.....	104
Physical Factors/Processes.....	112
Water Level Fluctuations.....	112
Channel Geometry.....	115
Wind.....	118
Wind Generated Water Waves.....	121
Effect of Wind on Beach Morphology.....	124
Background Hydraulics.....	127
Ships.....	130
Predicting Ship Wave Height.....	130
Sediment Transport.....	144
Process Delineation and Transport	
Prediction.....	144
Effect of Tidal/River Currents.....	145
Effect of Ship Drawdown Wave.....	149
Effect of Secondary Ship Waves.....	150
Longshore Currents by Secondary Ship Waves..	158
Field Sampling.....	163
Sediment Character.....	183
Sediment Density.....	186
Sediment Size Distribution	186

Sieved Versus Settling Tube Grain Size Analysis.....	188
Petrography.....	191
CONCLUSION	198
Shore Erosion.....	198
Geomorphic Observation and Development.....	199
Sediment Transport.....	200
Ship Waves.....	201
Sediment Transport by Ship Induced Water Motions.....	202
Mass Balance of Measured Values and Sources for Error.....	205
Sediment Character.....	211
Future Work.....	212
REFERENCES	214
APPENDICES	
A SHORE PROFILES.....	232
B SEDIMENTARY FEATURES.....	252
C SHIP WAVES.....	267
D SAND TRANSPORT ON A BEACH FACE.....	306

LIST OF TABLES

TABLE		PAGE
I	Sediment Contribution of Cowlitz River to the Columbia River after the Eruption of Mt. St. Helens.....	7
II	Discharge of the Columbia River.....	16
III	Major Human Influences on the Lower Columbia River.....	<u>22</u>
IV	Set of Water Motions Associated with Ship Passage in a Confined Channel.....	<u>27</u>
V	Profiling Error.....	40
VI	Error in Strip Chart Recorder.....	46
VII	Site Location and Distance to Navigation Channel.....	57
VIII	Aerial Imagery Analysis of Erosion 1939-1983.....	<u>58</u>
IX	Changes in Volume at the Price Island Site.....	71
X	Changes in Volume at the Puget Island Site.....	75
XI	Example of Beach Face Slope.....	<u>76</u>

TABLE

PAGE

XII	Changes in Volume at the Gull Island Between July 31, 1987 and June 7, 1988.....	83
XIII	Descriptive Transect Normal to Shore Slope.....	90
XIV	Water Levels at Puget Island Site.....	114
XV	Columbia River Cross-Sections.....	<u>117</u>
XVI	Average Winds at Astoria, Oregon.....	120
XVII	Symmetrical Eolian Dune Orientations....	121
XVIII	Ship Passages.....	131
XIX	Calculated Values of Secondary Ship Ship Wave Height.....	<u>134</u>
XX	Wave Description, Merchant Ship Passages.....	<u>142</u>
XXI	Critical Unidirectional Flow Velocities.....	<u>145</u>
XXII	River-Tidal Sediment Transport.....	<u>148</u>
XXIII	Predicted Threshold Velocities and for Depths.....	152
XXIV	Linear Wave Predictions.....	<u>152</u>
XXV	Predicted Threshold Velocities and Depths for Lower Columbia River Sand.....	154

TABLE

PAGE

XXVI	Sediment Transport Data Collected by Shallow Water Sediment Trap Array for the Upstream Passage of the Bulk Carrier, Magnolia, 17Sep87...	159
XXVII	Shallow Water Sediment Transport by Merchant Ship Waves.....	176
XXVIII	Sediment Densities.....	187
XXIX	Puget Island Sand Characteristics.....	188
XXX	Graphical Statistics of Columbia River Sands.....	189
XXXI	Grain Size Statistics.....	191
XXXII	Linear Regression: Plagioclase and Grain Size.....	195
XXXIII	Linear Regression: Opaque Minerals and Grain Size.....	196
XXXIV	Study Site Erosion.....	199

LIST OF FIGURES

FIGURE		PAGE
1.	The lower Columbia River, USA.....	3
2.	Geology of Price and Puget Island Reach.....	9
3.	Geologic cross-section.....	11
4.	Local geology.....	12
5.	Discharge of the Columbia River.....	15
6.	Quaternary history of the lower Columbia River valley.....	19
7.	Puget Island study site from Cathlamet, Washington	20
8.	Holocene sea level rise.....	20
9.	Flow duration curves.....	23
10.	Beach profile-related terms (USACE, 1984).....	25
11.	Sediment and bedform characteristics of a coastal near-shore zone, features also observe along the lower Columbia River beach nourishments (Reading, 1978).....	25
12.	Waves in the breaker zone.....	28
13.	Shore protection.....	32
14.	Surveying beach slope.....	38
15.	Typical shore profile.....	39
16.	Shore profile changes over time.....	40

FIGURE		PAGE
17.	Calibration curves.....	48
18.	Settling tube.....	50
19.	Shallow water sediment trap	53
20.	Sediment trap sampling array.....	54
21.	Removal of sand from sediment bag.....	54
22.	Sites observed in shore slop sediment dynamics study	57
23.	Columbia River soundings, 1913.....	60
24.	Columbia River soundings, 1913.....	61
25.	Price Island erosion.....	63
26.	Changes at Price Island.....	64
27.	Computer imagery of Puget Island site.....	65
28.	Computer imagery of Puget Island site.....	66
29.	Computer imagery of the Gull Island site....	68
30.	Price Island site profile grid.....	70
31.	Puget Island profile grid.....	72
32.	Puget site before sand disposal.....	74
33.	Puget site after sand disposal	74
34.	Puget Island site profile 7.....	76
35.	Puget Island site profile 10.....	77
36.	Gull Island site profile grid.....	78
37.	Gull Island site before sand disposal.....	80
38.	Gull Island site after sand disposal.....	80
39.	Representative silt-clay bank bordering the lower Columbia River channel.....	81

FIGURE

PAGE

40.	Price Island bankline erosion.....	82
41.	Shoreline at high tide at the south end of the Puget Island site.....	85
42.	Apex of shore notch at Puget Island study site, July 23, 1987.....	85
43.	Pipeline dredging operation.....	86
44.	Beach face on Wallace Island, Oregon.....	89
45.	Beach face at Puget Island site, looking north from profile 12.....	89
46.	Large beach scarp.....	92
47.	Excellent example of an active beach scarp that has been cut into a previously smooth beach face.....	94
48.	Grain size on a beach dace.....	95
49.	1987 Puget Island shore notch.....	97
50.	Vista Park (RK WA-54.7) shore notch.....	97
51.	1988 Puget Island shore notch.....	98
52.	1988 Puget Island shore notch.....	99
53.	Puget Island shore notch.....	99
54.	Sample locations.....	100
55.	Mean grain size across shore notch.....	101
56.	Water motions at a shore notch.....	102
57.	Profiling 1987 Puget Island shore notch.....	104
58.	Trough cross-bedding.....	105

FIGURE	PAGE
59. Three shore sedimentary facies.....	107
60. Shore stratigraphy.....	108
61. Rippled lower beach face.....	110
62. Beach face after ship waves.....	110
63. Tidal terrace at low tide.....	111
64. Tidal terrace bedding surface.....	111
65. Tidal terrace trench.....	113
66. Tidal terrace stratigraphy.....	113
67. Combined flood frequency	115
68. Columbia River cross section at Puget Island site.....	116
69. Hjulstrom (1939) Curve for estimating critical threshold velocity of quartz grain (sp. gr. 2.65) for range of grain sizes (Sundborg and Norrman, 1963).....	119
70. Eolian slope, beach scarp.....	125
71. Puget Island profile 4.....	126
72. Model results of ebb flows.....	129
73. Predicted versus measured ship wave heights.....	135
74. Channel cross-section with ship.....	136
75. Ship wave record.....	136
76. Ship wave.....	138

FIGURE	PAGE
77. Observed sequence of ship waves.....	139
78. Plunging breaker (ship wave).....	140
79. Wave run-up after breaking.....	140
80. Wave run-up.....	141
81. Beach scarp formation.....	141
82. Estimating sediment motion.....	157
83. Predicted longshore current velocities, as estimated by Equation (20) (Komar, 1975).....	161
84. Predicted longshore current distribution through the surf zone.....	162
85. Ship drawdown wave.....	164
86. Plunging ship wave.....	167
87. Wave breaking in the plunging form, characteristic of most secondary ship waves observed, but spilling, surging, and collapsing breakers were observed..	168
88. Shallow water sediment transport by the ship waves of "Leandros".....	170
89. Shallow water sediment transport by the ship waves of "Coast Range".....	172
90. Shallow water sediment transport by the ship waves of the "U.S. Gray".....	173

FIGURE

PAGE

91.	Sediment flux distribution normal to the shoreline for the ship "Coast Range".....	175
92.	Results of studies by the Beach Erosion Board, 1933 (in: King, 1972, p. 251).....	177
93.	Simple linear model illustrating ship wave sediment transport in shallow water as measured by shallow trap array.....	180
94.	Ship passages in the lower Columbia River.....	184
95.	Calibration curves, Puget Island sand.....	185
96.	Sediment size distribution curves.....	190
97.	Settling velocities, Puget Island sand.....	192
98.	Petrography of lower Columbia sand.....	193
99.	Relationship between grain size and petrography in lower Columbia sand.....	197
100.	Surf zone sediment flux distribution.....	204
101.	Mass Balance.....	206

INTRODUCTION

SYNOPSIS OF THE PROBLEM

What processes move sediment in shallow water along the shores of the lower Columbia River? How much bankline material sand is lost over time; how much sand is moved during events caused by ship passage? What is the shore and sediment response to processes observed? These are questions that have been addressed in this thesis.

Sand transport is an important physical phenomena in fluvial and coastal studies, directly impacting engineering endeavors within these settings. The lower Columbia River hosts a major deep draft navigation channel that is maintained through continual dredging. The source of shoaling sediments into the navigation channel has been a question engineers and scientists have attempted to answer for several decades. Local sediment sources within the river have only recently been considered the possible source for much of this shoaling (Eriksen, 1989).

The shallow near-shore zone may be a possible sediment reservoir (supplier) for channel shoaling and act as a geomorphic and sedimentologic recorder of the dominant physical processes. This hypothesis is examined using aerial imagery, surveying, sedimentology, sediment

transport studies, and established theory to evaluate the problem.

Lower Columbia sands exhibit a range of distinct sedimentary structures that result from a variety of distinct petrographies, physical processes, and grain size differences. The sites investigated were in shallow water inter- and supratidal regions along sandy shores of the lower Columbia River. Sediment transport initiated by water motions associated with the passage of ships was observed and analyzed.

The primary physical processes of the study region include: currents generated by tidal fluctuation and river discharge and wave actions generated by wind and ship passage.

The study setting is in northwest Oregon and southwest Washington between Columbia River Kilometers (RK) 54 to 88 (River Miles, RM, 34-55). See Figure 1. This area lies well upstream of maximum spring tide salinity penetration into the Columbia Estuary during low fresh water discharges, reaching RK 32 (Jay, 1984).

Many of the sandy shores along the banks of the Columbia are not natural, but disposal or "nourishment" sites constructed during dredging operations to maintain the Federal Navigation Channel. Dredging of the lower 178 kilometers of the Columbia has been going on since the late 1800's. The approximate mean annual volume of sediment

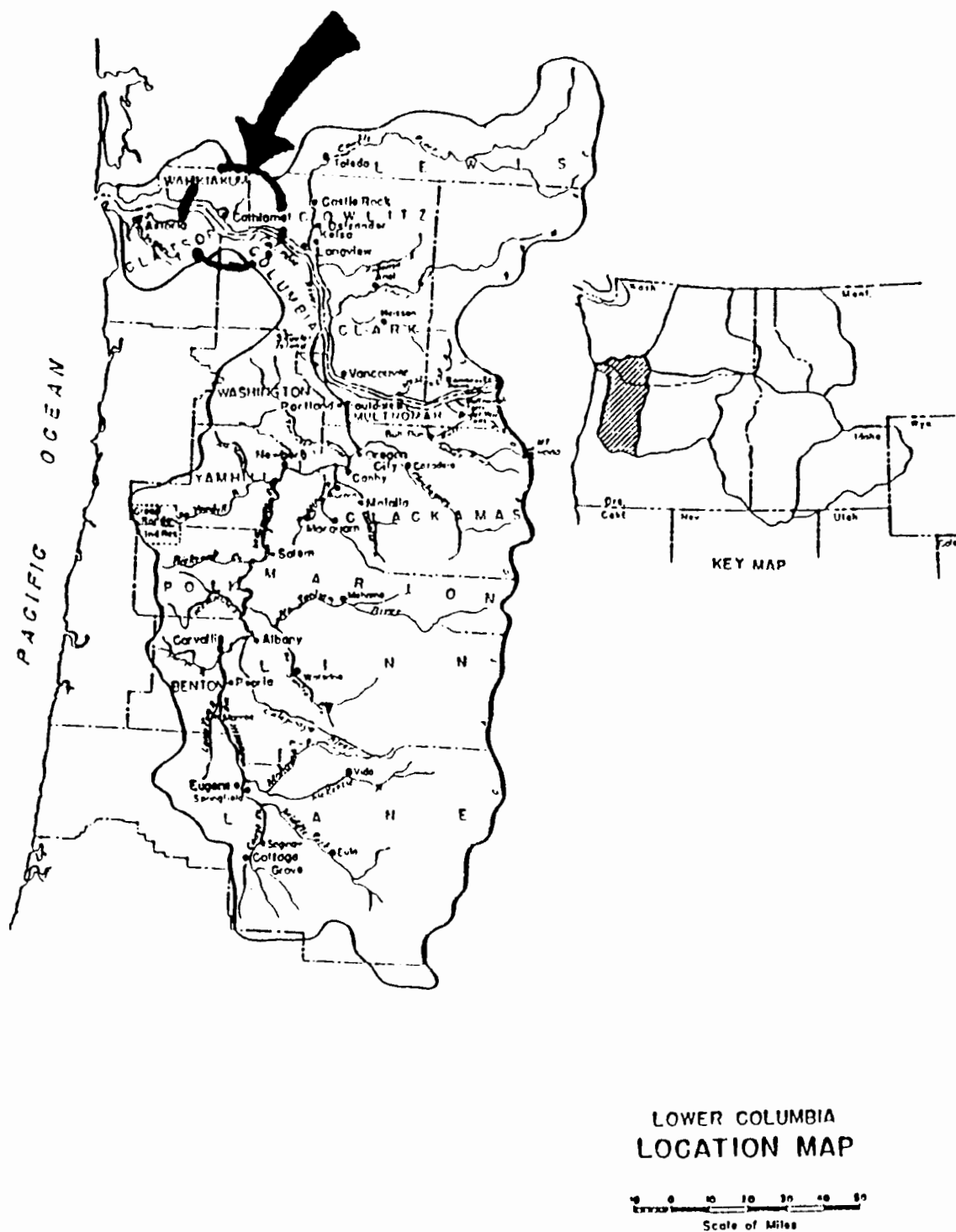


Figure 1. The lower Columbia River, USA. From USDI, 1947.

dredged from the Columbia River since the 1970's is between 5 to 6 million cubic meters (USACE, 1988b). In order for channel maintenance procedures to be cost-effective and environmentally sound, the physical processes responsible for channel shoaling need to be understood. One facet of this comprehensive understanding is addressed by the observations and accompanying analysis of this study.

Currently there exists some question regarding the origins of the sediment responsible for channel shoaling: is the sediment derived from up-river sources or is it derived locally? Work by Eriksen (1988, 1989) suggests that most sediment responsible for shoaling is derived from local sources and enters the channel through side slope motion (for description of possible mechanics of this process, see; Ikeda, 1982). Shoaling may be due to natural bar migration and/or the erosion of unstable side slopes. Unstable side slopes are an artificial phenomena created by channel dredging and shore nourishments. If dredging operations are a precursor to mobilizing sediment back into the channel, then shoaling might be controlled by better dredging and nourishment practices. Eriksen (1988) reports that total sediment volumes produced in river dredging far exceeds average annual predicted sediment yields transported in the system.

GEOLOGY OF THE STUDY REGION

The study region lies at the margin between the North American continental plate and the subducting Juan de Fuca oceanic plate. The result of this collision has been active sedimentation, tectonic, and volcanic activity in the Pacific Northwest region for the last 55 million years (Lowry and Baldwin, 1952). Uplift in the northwest during the last five million years has resulted structural deformation (folds) and extensive faulting of the bedrock geology. The Coast Range of northwest Oregon and southwest Washington has been part of an accretionary prism for at least 45 m.y. (Heller and others, 1987).

The Holocene alluvial stratigraphy of the Columbia River valley is poorly documented, but in general consists of fine to medium grained volcanic sands interbedded with lenses of clay-silts.

Bedrock geology presents a record of deep to shallow water and subaerial deposits intercalated with basaltic sequences going back 50-60 million years ago (m.y.a.). The volcanic Cascade Range developed approximately 35 m.y.a. and has been the primary source terrain for sands transported through the lower Columbia River. Columbia River sand petrology is predominantly volcanic rock fragments (dacite and basalt) and plagioclase (Clemens and Komar, 1988; Abbe, 1988a; Sherwood and others, 1984; Whetton and others, 1969).

The May 8, 1980 eruption of Mount St. Helens is an example of the dramatic influence recent volcanism of the High Cascades has had on influx of sediments into the Columbia River; Hubbell and others, 1983, estimated that 27.5 million m³ of sediment was contributed during the first 24 hours after the eruption. This sediment input reduced the 12.2 meter deep navigation channel to 4.3 meters at the mouth of the Cowlitz River, RK 109. The deposits spread 3.2 km downstream and 11.2 km upstream in the Columbia River (Hubbell and others, 1983). Table I presents the estimated sediment contributions of the Cowlitz River to the Columbia between 1980 and 1986 (USACE, 1988). Cowlitz River sediment is primarily clay, silt, or very fine sand. These fine sediment grains only account for a small fraction (<5% by weight; Hubbell and others, 1983) of the Columbia River sediment population composing the channel bed. The contribution of sediment by the Cowlitz to the Columbia is about two-thirds fine sand (.0625-.125mm) and one-third medium sand (.25-.50mm) (Eriksen, 1989).

Bed material is defined as the rock or sediment composing the channel bed. Bed material includes sediments transported as bedload (particles saltated along the bed) and suspended above the bed.

The lower Columbia's sediments coarsen upstream (Hubbell and others, 1983; Whetton and others, 1969). This trend generally lies within one standard deviation.

TABLE I

SEDIMENT CONTRIBUTION OF COWLITZ RIVER TO THE COLUMBIA
RIVER AFTER THE ERUPTION OF MT. ST. HELENS

Columbia River Kilometer 109.5

Water	Sediment yield in millions of m ³		
<u>Year</u>	<u>Total</u>	<u>Bed Material</u>	<u>Bed % of total</u>
1980	30.6	N/A	N/A
1981	N/A	N/A	N/A
1982	17.59	0.76	4.3
1983	16.06	2.29	14.3
1984	7.65	1.53	20.0
1985	4.59	1.53	33.3
1986	3.82	1.53	40.0
1987	3.82	1.53	40.0

where bed material is grains larger than very fine sand (> 3 ϕ or .125mm, excluding v. fine sand).

Water Year = October to October

The Columbia River's western drainage basin (west of 122° longitude) is the primary source of coarse sediments (>.0625mm, sand and larger) found in the lower Columbia (Whetton and others, 1969). The construction of Bonneville Dam at RK 234 km has exaggerated this boundary and serves as the approximate upstream boundary of the "lower Columbia."

The lower Columbia has done extensive scouring (Allen, 1987) into the surrounding rocks, clearly evident

in the large basalt cliffs and canyons along the river's course. In the post-glacial period from about 18,000 years ago, the behavior of the river has probably been drastically different, filling in some of the valley that it had carved. A series of catastrophic floods about 13,000 years ago were responsible for much of the Columbia River's geomorphic expression.

















The bedrock geology in the Price Island, Washington, region is exhibited in Figure 2 (Walsh, 1987). The region is characterized by volcanogenic sedimentary rocks and flows. A geologic cross section through the Columbia River valley at Price Island, WA (N46°15') is presented in Figure 3. The cross section shows a shallow, yet distinctly asymmetrical syncline. Strata on the Oregon side exhibit a relatively constant northerly dip of 10°, while the north limb of the syncline steepens from about south 10 degrees at Skamokawa, WA to about south 35 degrees 5 km to the north (Figure 3). The local bedrock foundation is partly composed of inclined strata of the Miocene Grande Ronde Basalt and underlying very fine to medium grained carbonaceous, micaceous sands of the Lower Astoria Formation (Figure 4).

The Columbia River Basalt Group is composed of a sequence of tholeiitic rift basalts that originated in Eastern Washington during the Miocene epoch. These basalts covered much of the Northwest, over an area of 163,721 km²,



Figure 2. Geology of Price and Puget Island Reach. See key on next page. Adapted from Walsh (1987).

KEY TO GEOLOGIC UNITS PRESENTED IN FIGURE 2

STRATIGRAPHIC UNIT	AGE m.y.a.
 Qal (Quaternary alluvium).....	<2
 Qls (Quaternary landslide debris)	<2
 Qt (Quat. terraced sediments).	<2
 Tsp (Saddle Mtns. Basalt)	16.6-11.2
 Tgc (Gnat Creek Formation)....	" "
 Tasu (Upper Astoria Formation)	" "
 Twf (Wanapum Basalt, ... Frenchman Springs mem.)	" "
 Tiwf (Intrusive Frenchman)	" "
 Tgr (Grande Ronde Basalt)	" "
 Tigr. (Intrusive Grande Ronde Basalt)	" "
 Tasc (Cannon Beach mem. Astoria Fm-Niem & Niem, 1985)	24.0-11.2
 Tasw (Wickiup Mtn. mem. (Niem and Niem, 1985))	" "
 Tasl (Lower mem. of Wells) ..	" "
 Tsmc (Smuggler Cove Fm. of ... Niem and Niem, 1985)	30.0-17.0
 Tlcs (Lincoln Creek Fm. sandstone member)	38.0-39.0
 Tsc (siltstone of Skamokawa Creek of Wells, 1981)	40.0-36.6

*An Interpretative Geologic Cross Section Across the Columbia River,
Price Island Region, Washington and Oregon*

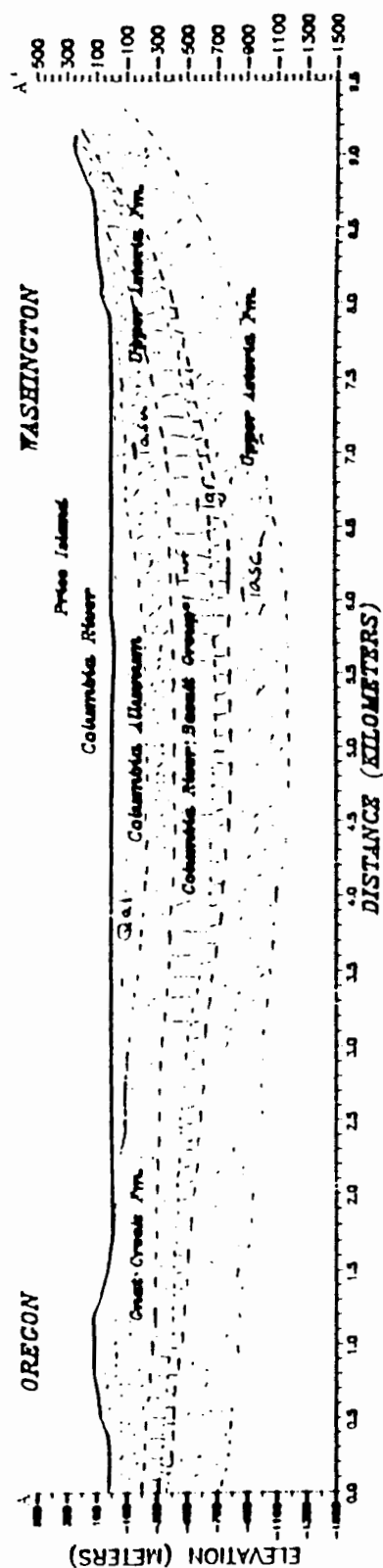


Figure 3. Geologic cross-section. Through Price Island, Washington.



Figure 4. Local geology. Steeply dipping bedding east of Cathlamet, WA; north of Puget Island along Washington Route 4. Grande Ronde basalt overlying sands of Upper Astoria Formation.

and have an estimated cumulative volume of 170,649 km³ (Tolan and others, 1987). Some of these flows used the ancestral Columbia River basin as their primary flow path to the west. Thus, the morphology of the Columbia's ancestral valley limited the lateral extent of the basalt flows and the flows subsequently influenced the river's course (McKee, 1972).

On the Oregon side of the Columbia River across from Puget Island, the Gnat Creek Formation outcrops above approximately 40 meters of the Frenchman Springs basalt member of the Columbia River Basalt Group. The Gnat Creek Formation (Tgc) consists of friable, cross-bedded or bioturbated, micaceous and carbonaceous feldspathic sandstone, pebbly, coarse grained feldspathic sandstone, thick bedded massive sandstone with slumped siltstone blocks in channels cut into laminated carbonaceous mudstone, and rare lignite, a low grade coal (Walsh, 1987). The Gnat Creek Formation appears to be correlative in general lithology and age to the Upper Astoria Formation on the Washington side. The Gnat Creek Formation overlies the Frenchman Springs Basalt member of the Columbia River Basalt Group. The friable, poorly lithified nature of the Gnat Creek and Astoria Formations is characteristic of much of the sedimentary stratigraphy in Northwest Oregon and Southwest Washington.

THE COLUMBIA RIVER

The Columbia River drains an area of $671,000 \text{ km}^2$ ($259,000 \text{ mi}^2$), flowing from the Canadian Rockies to the Pacific Ocean. Columbia River discharges for the study period are presented in Table II. Fresh water flows generally range from 4,000 to $15,000 \text{ m}^3/\text{s}$. Salt water intrusion can directly impact sediment transport by increasing the water density and thus transport potential (Dyer, 1986). Salt intrusion into the Columbia Estuary can reach RK 38 (RM 24) during the low flow season, but is downstream of Astoria during high freshwater flows (Jay, 1984). Figure 5 presents monthly mean discharges for the time periods listed in Table II.

In any hydrologic and sediment transport study in the nearshore boundary region of a river, it is important to establish channel geometry and water surface elevation. Flood events will raise the water level on the shoreline and thus where currents and wave actions will occur. Much of the shoreline damage in coastal regions occurring during storms is not by the increase in water level, but the elevated wave actions (USACE, 1984; MuirWood and Fleming, 1980; Bascom, 1980). The frequency in which particular elevations are subjected to shoreline processes can be predicted using stage elevation estimates for combined flood events. (USACE, 1986). Floods increase sediment

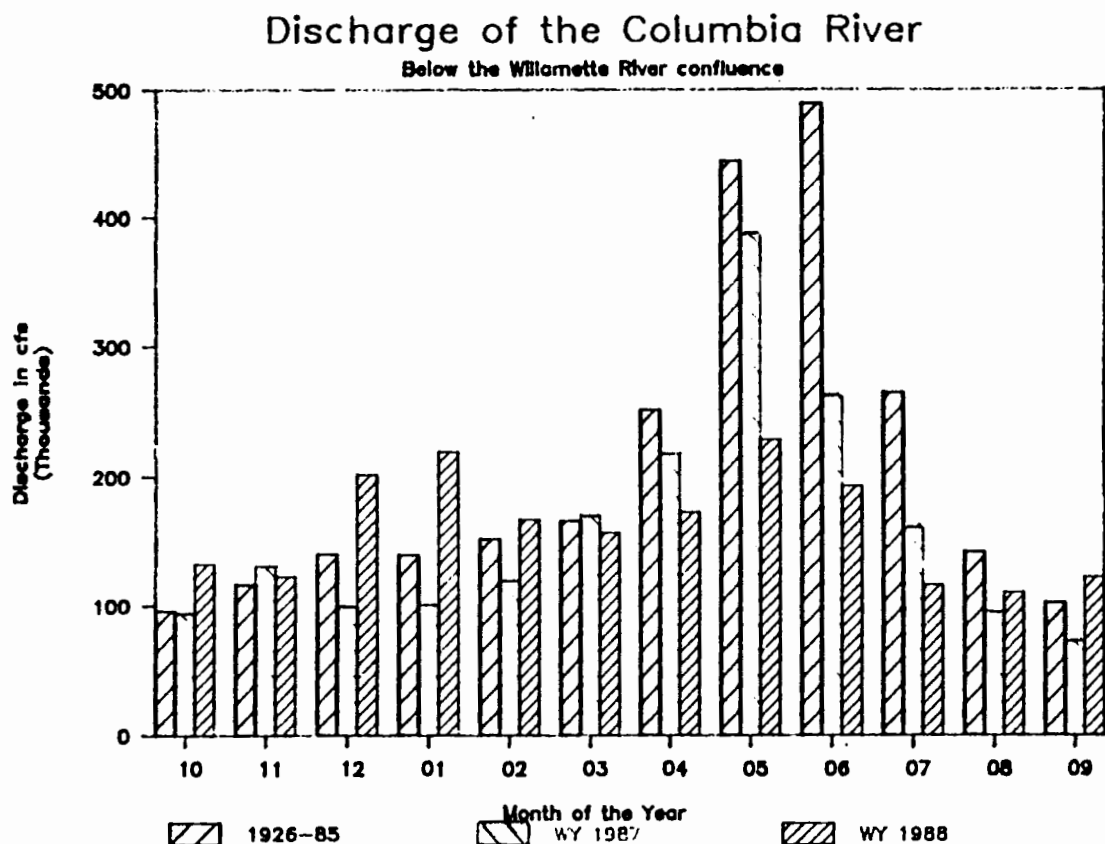


Figure 5. Discharge of the Columbia River. Water years 1987 and 1988. Monthly average discharge from 1926 to 1985.

TABLE II
DISCHARGE OF THE COLUMBIA RIVER

Downstream of the Confluence with the Willamette River

<u>Water Year</u> <u>(Oct. to Sept.)</u>	<u>Mean Annual</u> <u>Discharge</u>	<u>Maximum</u> <u>Discharge</u>	<u>Minimum</u> <u>Discharge</u>
1926-1985 ¹ average	5,905 m ³ /s (208,516cfs)	13,837 m ³ /s (488,651cfs) (June)	2,717 m ³ /s (95,944cfs) (October)
1987 ¹	4,503 m ³ /s (159,030cfs)	10,926 m ³ /s (385,860cfs) (May)	2,026 m ³ /s (71,530cfs) (September)
1988 ²	3,845 m ³ /s (135,866cfs)	6,938 m ³ /s (245,013cfs) (May)	2,223 m ³ /s (78,551cfs) (July)

¹CRMWG, 1988

²USGS, 1989

transport and elevate shoreline processes to regions otherwise unexposed to these actions.

Other processes associated with flood events include increased bed shear and sediment transport. Bedload transport in the Columbia only becomes appreciable with significant discharges. If the Columbia has a discharge of 7,080 m³ (250,000 cfs), predicted bedload is less than 1 ton/day; at 8,500 m³ (300,000 cfs) predicted bedload is about 1.5 metric tons per day or about 2 m³ of sand/day (USACE, 1986).

Tides in the region are mixed semidiurnal. Every day there are two high tides of distinctly different elevations, likewise for the low tides. The average

maximum difference between lower low tide and higher high tide is about 2 meters during neap tides and up to 4 meters during spring tides. Tidal effects are felt all the way up the Columbia River to Bonneville Dam, RK 234.1 (RM 145.4). Tides are very important in the evaluation of sediment dynamics because they control water elevation, cross-sectional channel area, salt water intrusion, and the velocity regime of the river.

High and low water slack correspond to static water conditions in the river, which are the times between ebb and flood flow. Slack conditions do not coincide with high and low water surface elevations in the Puget Island Region. Slack water is when current velocity is zero. Maximum flood and ebb currents occur 1 to 2 hours before high tide and low tide, respectively. Slack water occurs 1 to 2 hours before and after peak flood flow.

GEOMORPHOLOGY

The Lower Columbia flows through a confined alluvial plain from the Cascade Mountains to the Pacific Ocean. The Lower Columbia is characterized by large curves extending to the sides of its valley. Structural features such as fault trends and basalt outcrops apparently control much of the river's lateral migration. The strong influence of geology upon the river's character is attributed to active tectonics. The sedimentary stratigraphy of the lower

Columbia River valley is a fascinating record of Pleistocene to Recent geologic processes. The most dramatic sedimentary processes that have affected the river's morphology and sediment transport have been:

- o a series of extremely large floods called the Bretz Floods that occurred in the late Pleistocene and Early Holocene (Allen, 1986);
- o the rise in sea level since the Flanarian Stage of the Wisconsin Ice Age 18,000 years ago;
- o Holocene (pre-human influence) flood events;
- o human influences (though the time period has been very short in comparison and evaluation is difficult).

Sea level rise has the same general sedimentologic effect as damming a river. The river responds by aggrading its bed in an upstream direction, illustrated with a simplified cartoon in Figure 6. Alluvial sands were found to depths of at least 90-100 meters in Cathlamet channel (Figure 7), providing some evidence that the lower Columbia became a sediment trap due to the backwatering effect of a sea level rise (Washington State, 1986). An aggradation of approximately 100 m of recent sediments corresponds to sea level changes in the last 18,000 years. Shepard (1963) used C^{14} dates of peat, wood, and shells deposited near sea level and now submerged, to estimate a rise of approximately 100m in sea level. Curray (1965) had come to

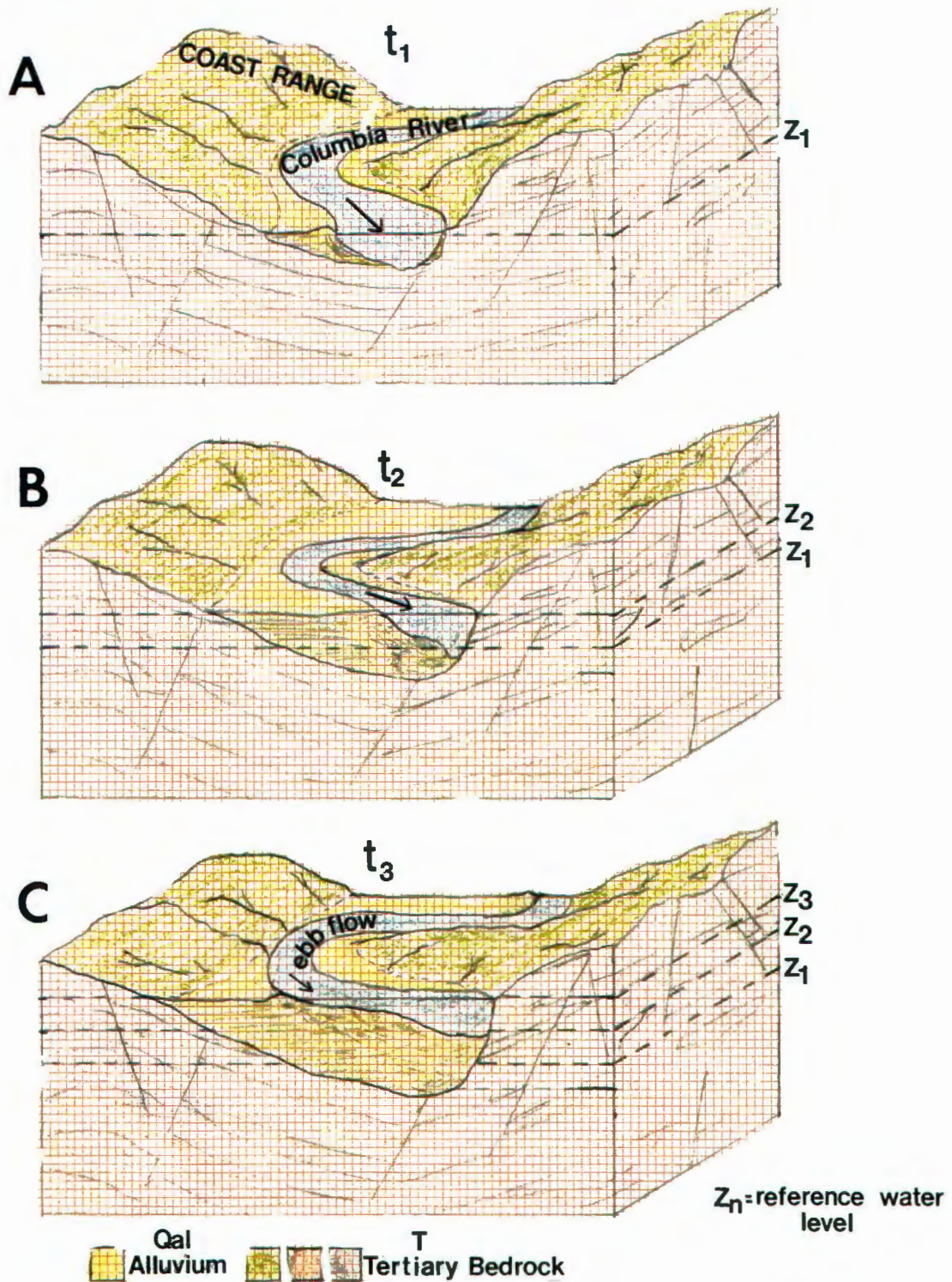


Figure 6. Quaternary history of the lower Columbia River valley. In this hypothesis the Columbia River remained entrenched in the same approximate location on the alluvial plain throughout the rise in sea level.

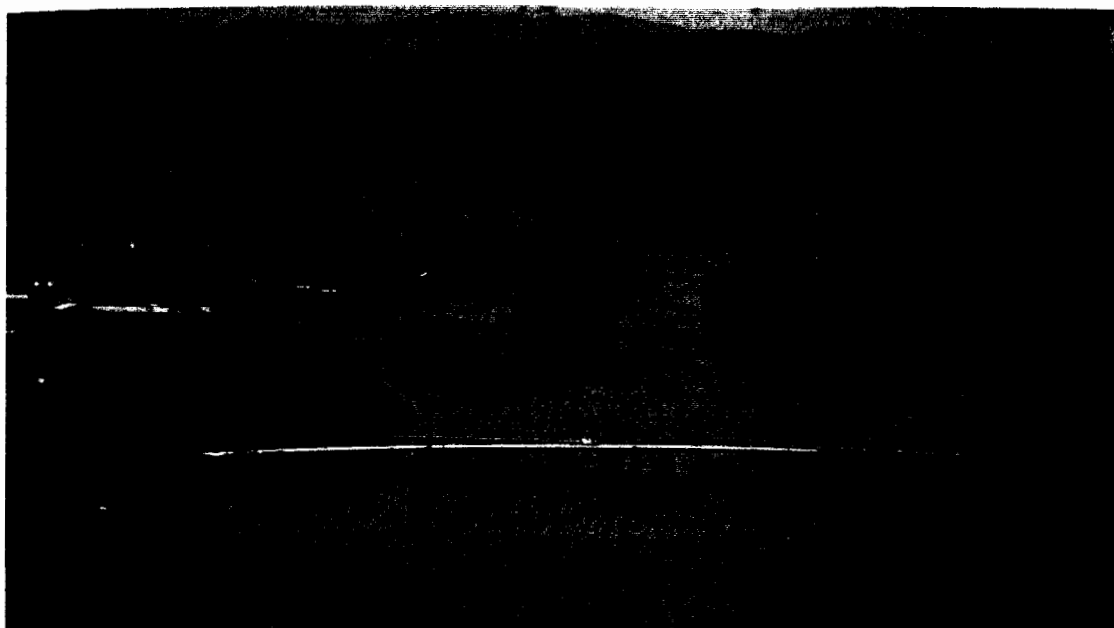


Figure 7. Puget Island study site from Cathlamet, Washington. In foreground is new Puget Island Bridge, from which piling logs recorded Columbia River sand (Holocene) to depths of slightly less than 100m (285 ft). Main channel flows left to right just above center of photograph. Cathlamet Channel is in center foreground.

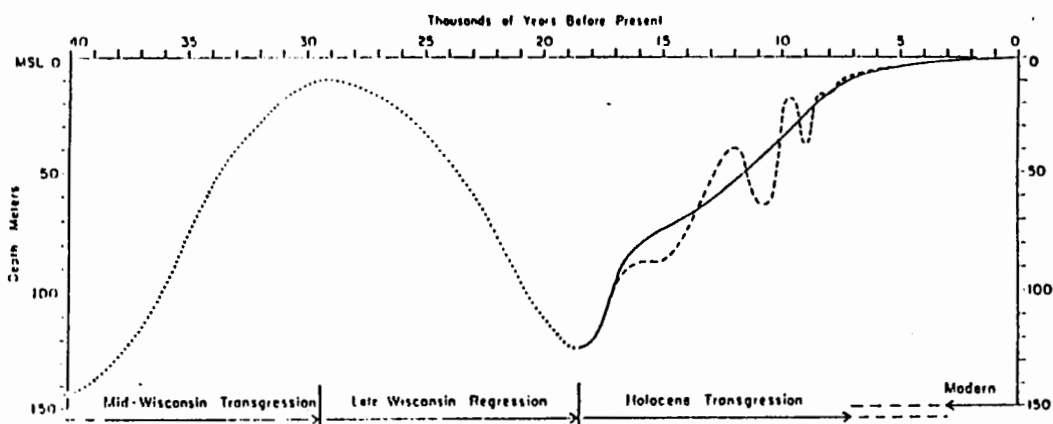


Figure 8. Holocene sea level rise. Since the Wisconsin Ice Age. From Curray (1965).

a similar estimate, graphically illustrated in Figure 8 (Komar, 1976). The rate of sea level rise have been estimated at about 5-7 mm/yr following the retreat of the last glaciation 9,000-5,000 years ago (Curry, 1965); rates that have been proportional to the rate of sedimentation in the lower Columbia River valley. Further evidence of the rise in sea level and aggradation in the lower Columbia River valley (thus lack of sand flux to the coast) comes from studies of sands along the Oregon Coast (Clemens and Komar, 1988; Peterson and others, 1985). Clemens and Komar (1988) concluded that the Columbia has not provided a sediment supply to the Oregon coast south of Cape Flattery since the Pleistocene.

Human Actions

Human activities have been extensive and have affected the behavior of the lower Columbia River. Table III lists chronologically major engineering projects on the Columbia River system. An extensive reservoir network regulates flows to produce electricity and provide flood control. Flow regulation cuts down the number of major flood events responsible for the greater part of sediment transport in a river. The impact of engineered structures on the Columbia is illustrated in the flow duration curves from 1878-1962 and 1972-1977, (Figure 9). The Columbia River's estimated average annual sediment yield at Vancouver has been reduced by the regulation (Figure 9)

TABLE III

MAJOR HUMAN INFLUENCES ON THE LOWER COLUMBIA RIVER

<u>DATE</u>	<u>ACTIVITY</u>
pre 1885	Sporadic, minimal dredging
1885	30 ft (10m) Entrance Project initiated
1905	40 ft (12m) Entrance Project initiated
1938	Bonneville Dam
1945	Regular annual dredging initiated
1954	48 ft (14.6m) Entrance Project initiated
1977	52 ft (16m) Entrance Project initiated

Modified from: Sherwood and others, 1984.

from «10,700,000 m³ before 1962 to 1,530,000 m³ by the late 1970's (USACE, 1986). After the May 1980 eruption of Mt. St. Helens, the sediment budget has greatly increased for the Columbia downstream of the Cowlitz River confluence from 5,350,000 m³ to 19,110,000 m³ (with a bed material fraction of between 1,070,000 m³ and 2,750,000 m³ a year).

Pre-1980 sediment predictions were about 1,530,000 m³ with a bed material fraction between 306,000 m³ to 459,000 m³ (20-30% of the total) (USACE, 1986).

Extreme events in fluvial systems (floods) that occur about 5% of the time and account for 90% of the sediment discharge. About 80% of the time, base flow conditions of a river contribute virtually nothing to its overall sediment discharge (Dyer, 1986). Water regulation also

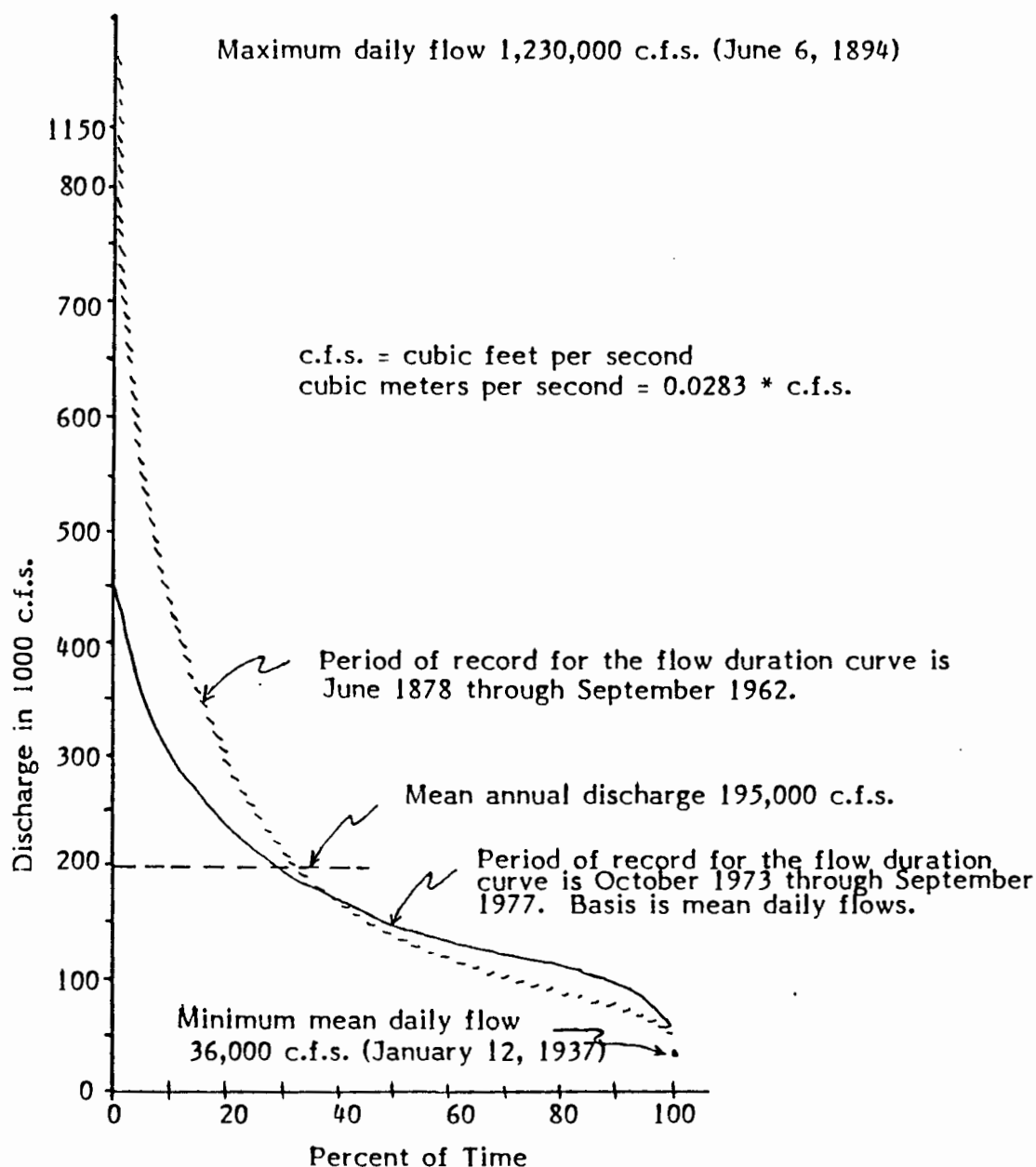


Figure 9. Flow duration curves. Columbia River at the Dalles, Oregon before and after regulation (USACE, 1986).

affects the water elevation, thus affecting where nearshore processes will occur.

To maintain the Federal navigation channel to the current specified dimensions of 40 x 600 feet (12.2 x 182.9 meters), the U.S. Army Corps of Engineers uses both hopper and pipeline dredging operations. The majority of river dredging (upstream of the Columbia River mouth) is done by the pipeline method which uses shore sites for depositing channel sands.

Shore Features

Shorelines exhibit distinct geomorphic characteristics dependent on the sediment composing them and the processes acting upon them. The shore slope is controlled by the energy assault upon it and the sediment particle size (Komar, 1979). These subenvironments and associated features in the near-shore shallow water region presented in Figures 10 and 11 (definitions from Bagnold, 1963; and Komar, 1976).

SHIP WAVES

When discussing the physical processes acting in the Lower Columbia, those originating from the passage of a large vessel cannot be ignored. The Lower Columbia is a major international shipping lane, with the highest bulk export tonnages on the west coast and second largest (in

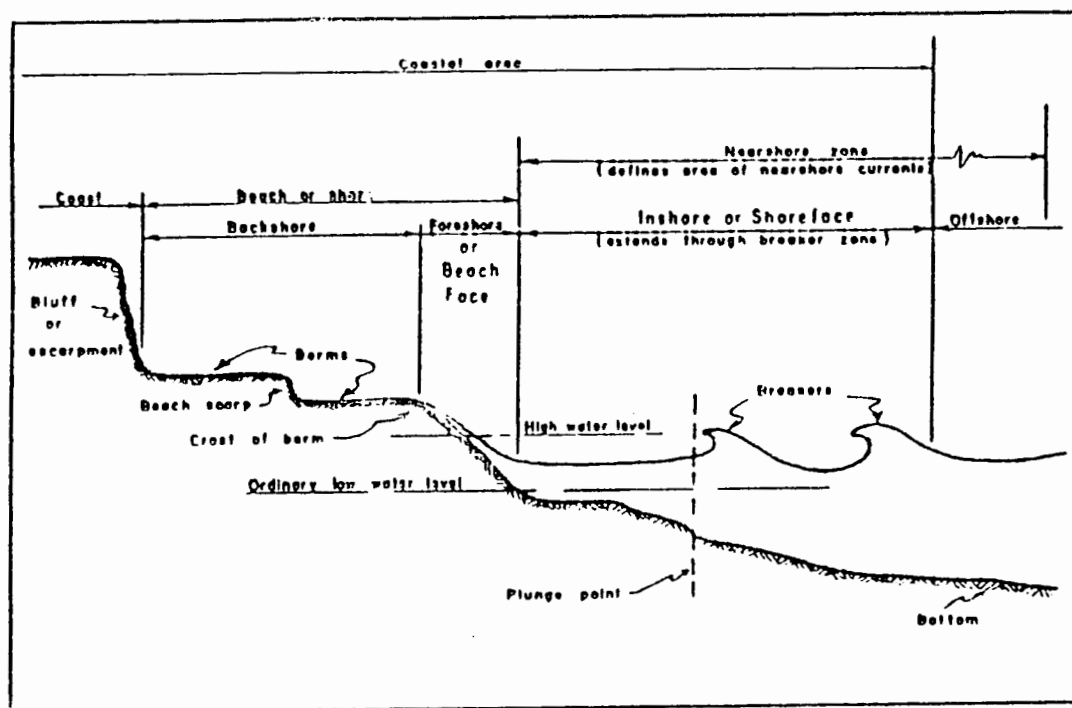


Figure 10. Beach profile-related terms (USACE, 1984).

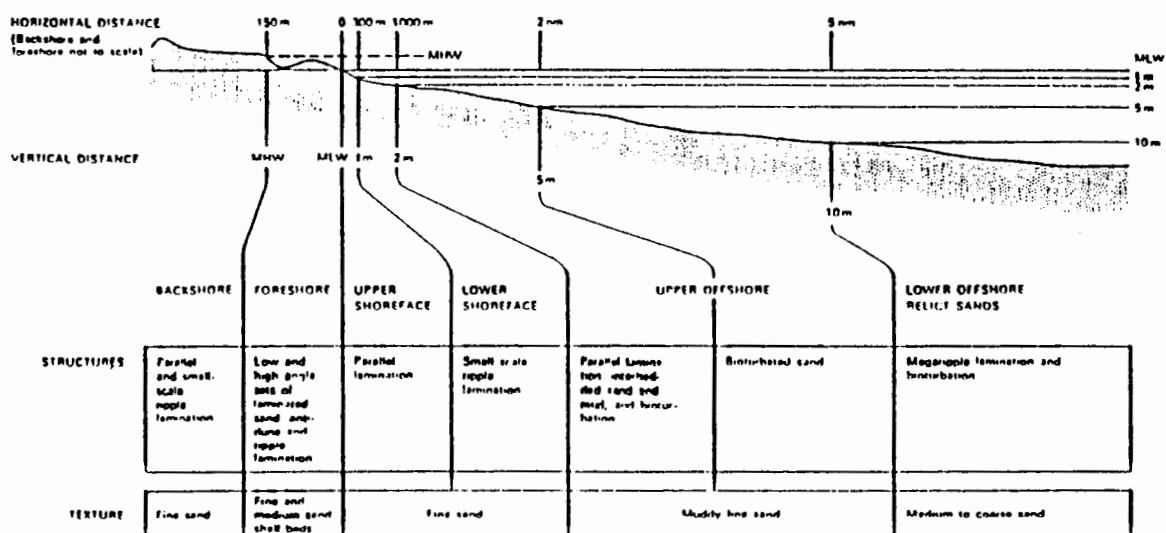


Figure 11. Sediment and bedform characteristics of a coastal near-shore zone, features also observe along the lower Columbia River beach nourishments (Reading, 1978).

tonnage) inland navigation system in the United States. The number of deep draft ships using the Columbia navigation channel increased sharply after the official channel enlargement in 1976 (Port of Portland, 1986).

When a large ship moves through a confined channel, a complex set of water waves occur. This set of waves moves with the velocity of the ship along the banks of the channel, with a wide range of behavior that is dependent on the channel geometry and shallow water region close to shore. Water motions associated with vessel passage in a confined channel are presented in Table IV (Span and others, 1981). The behavior of water waves attacking a shoreline has been documented in coastal studies (Figure 12) and can be used as an analogy in evaluating the behavior of ship waves.

The magnitude of ship waves is a function of several variables; as presented below (Ofuya, 1970):

$$H_{\max} = f(L_s, Y_s, V_s, d, D, B, g) \quad (1)$$

where: $f()$ = function of ...

Y_s = distance from ship's sailing line

L_s = length of ship

V_s = velocity of ship

d = depth of water in channel

D = ship's draft

B = width of ship (beam)

g = acceleration of gravity

TABLE IV

SET OF WATER MOTIONS ASSOCIATED WITH
SHIP PASSAGE IN A CONFINED CHANNEL

- 1) the return flow between the ship and the canal bottom and banks.
- 2) the drawdown (depression of water surface) caused by the return flow, sometimes called the primary ship wave.
- 3) the transverse stern wave, being the transition between the drawdown alongside and the (slightly raised) water surface behind the vessel. When pronounced, such a wave is comparable to a surge wave.
- 4) the slope-supply flow providing water over the canal slopes to restore the original water level immediately after the ship has passed.
- 5) the secondary ship waves (predominantly bow and stern waves).
- 6) the propeller race.

(Span and others, 1981)

a similar estimate, graphically illustrated in Figure 8 (Komar, 1976). The rate of sea level rise have been estimated at about 5-7 mm/yr following the retreat of the last glaciation 9,000-5,000 years ago (Curry, 1965); rates that have been proportional to the rate of sedimentation in the lower Columbia River valley. Further evidence of the rise in sea level and aggradation in the lower Columbia River valley (thus lack of sand flux to the coast) comes from studies of sands along the Oregon Coast (Clemens and Komar, 1988; Peterson and others, 1985). Clemens and Komar (1988) concluded that the Columbia has not provided a sediment supply to the Oregon coast south of Cape Flattery since the Pleistocene.

Human Actions

Human activities have been extensive and have affected the behavior of the lower Columbia River. Table III lists chronologically major engineering projects on the Columbia River system. An extensive reservoir network regulates flows to produce electricity and provide flood control. Flow regulation cuts down the number of major flood events responsible for the greater part of sediment transport in a river. The impact of engineered structures on the Columbia is illustrated in the flow duration curves from 1878-1962 and 1972-1977, (Figure 9). The Columbia River's estimated average annual sediment yield at Vancouver has been reduced by the regulation (Figure 9)

TABLE III

MAJOR HUMAN INFLUENCES ON THE LOWER COLUMBIA RIVER

<u>DATE</u>	<u>ACTIVITY</u>
pre 1885	Sporadic, minimal dredging
1885	30 ft (10m) Entrance Project initiated
1905	40 ft (12m) Entrance Project initiated
1938	Bonneville Dam
1945	Regular annual dredging initiated
1954	48 ft (14.6m) Entrance Project initiated
1977	52 ft (16m) Entrance Project initiated

Modified from: Sherwood and others, 1984.

from «10,700,000 m³ before 1962 to 1,530,000 m³ by the late 1970's (USACE, 1986). After the May 1980 eruption of Mt. St. Helens, the sediment budget has greatly increased for the Columbia downstream of the Cowlitz River confluence from 5,350,000 m³ to 19,110,000 m³ (with a bed material fraction of between 1,070,000 m³ and 2,750,000 m³ a year).

Pre-1980 sediment predictions were about 1,530,000 m³ with a bed material fraction between 306,000 m³ to 459,000 m³ (20-30% of the total) (USACE, 1986).

Extreme events in fluvial systems (floods) that occur about 5% of the time and account for 90% of the sediment discharge. About 80% of the time, base flow conditions of a river contribute virtually nothing to its overall sediment discharge (Dyer, 1986). Water regulation also

The importance of these processes differs with regard to bottom and slope loading as a function of speed, canal dimensions, and ship's size.

This statement has been reiterated in regard to specific situations throughout the world both in canals and natural river systems. Johnson (1958, p. 666) stated;

Ships moving through water generate surface waves which in many navigation channels cause severe wave-wash damage to the bank.

Hertzberg (1954, p 628) found wave-wash damage along narrow unprotected foreshore of the Mississippi River: "Destructive waves in the river are caused by wind and passing ships." Hertzberg (1954) suggested that shore debris such as logs enhance erosion. This debris is common along the Lower Columbia River. Ship generated water motions have been recognized as a significant set of forces eroding the boundaries of many of waterways in the Soviet Union.

Bekendam and others (1988, p. 21) evaluated barge traffic in the River Rhine for the Netherlands Government in an extensive study of the channel-vessel physical processes. The study concluded that:

Navigation has a big impact on the natural environment of the river bank. To prevent further degradation of the natural environment and the particular river landscape, measures are necessary to reduce wave attack and the force of currents (Bekendam and others, 1988).

Their investigation was instigated because of an increase in the size of barges using the navigation route.

The state of Maryland Coastal Resource Division (1981) studied the impacts of small boats on banks and found that in constricted channels having no speed limits, the boat wakes played an active role in bank erosion.

Ship waves in the lower Columbia have been recognized (Abbe, 1988, 1989; Abbe and Phan, 1987; Beeman, 1985a, b; USACE, 1960, 1986) as an agent in shore erosion. Figure 15 exhibits shore protection installed by a land owner on Puget Island, WA, to protect a rapidly retreating beach scarp that jeopardized the land owner's residence. Most of the studies to date described the secondary wave train of vessels and did not present the complete set of processes occurring with a ship passage such as drawdown and return wash (surge) or the relative impact of these forces on sediment transport and shore morphology (PIANC, 1987).

Shore protection at the Puget Site is at the apex of a "shore notch" (site of accelerated bank erosion) that was threatening a house (Figure 13). Sand accumulated on the shoreward side of the structure. Ship surge and waves eroding the shore notch at this site carry sediment from downstream (right to left), building out a beach accretionary lobe to the left. This longshore transport is also suggested by the accumulation of sand behind the structure. The structure did aid in preventing further transgression of the beach scarp.

Much of the theoretical model work and field work examining ship generated hydraulics in a confined channel is based on a canal setting. The canal is a designed structure with a static morphology through which flow velocities are usually negligible. The static-steady state nature of canals differentiates them from rivers. The natural river's morphology is controlled by its geologic setting, sediment load and basin hydrology. In the United States, the vast majority of the navigable waterways are natural rivers. Structures have been built in these navigable rivers to obtain a more consistent and predictable behavior of the river. Groins, pile dikes, and shore revetments attempt to train thalweg currents into a consistent position to protect shorelines and maintain a navigable channel. Reservoir networks further control rivers by regulation of discharge and sediment retention.

HYPOTHESIS

This study investigated the hypothesis that shore nourishment stability is expressed in the shore's morphology with respect to time and the physical processes attacking the site. Three important concepts are presented in this hypothesis:

- 1) Shoreline sedimentary features reflect the prevailing physical processes.



Figure 13. Shore protection. Installed by ... land owner at Puget Island site, at the upper left portion of the beach below the residence.

- 2) The primary processes are water motions due to river and tidal currents and wave actions due to wind and ship passage.
- 3) Shoreline stability can be predicted by understanding these physical processes.

In order to establish the significance of this hypothesis, the study has described examples of: shore morphology, shore changes over time, the effect of dredged channel sand disposal and the disposal (or nourishment) response to specific processes, shore sediment, and sediment transport induced by ship generated water motions. Using site specific observations, the study presents part of the sedimentology and hydraulics in a shallow water

setting of a tidally affected river hosting extensive human activity.

METHODS

GENERAL METHODOLOGY

The study utilized several different investigative methods at several different scales to approach and solve the problem. Background data in the form of aerial imagery and topographic/bathymetric maps were examined over time. Sites chosen for examination were surveyed over a one year period. Physical processes were observed at the sites and ship waves were quantitatively measured. Geomorphic features and sedimentary structures were observed and recorded. The sediment was analyzed for size distribution and petrography.

The first step in the methodology to investigate sediment transport was to apply appropriate theoretical and empirical relationships to see if measured physical processes in the study region were likely to be responsible for sediment transport. The second step was to measure sediment transport in the regions of concern. Physical measures made of wave heights, beach slope, wave period, depth and wave incidence were plugged into established expressions describing wave hydraulics and sediment transport to predict the thresholds of sediment motion.

Methods used in this study to evaluate sediment dynamics on the shore slopes of the lower Columbia are as follows:

- 1 - Establish site locations and document site evolution.
- 2 - Observation and description of sedimentary forms and their creation and destruction.
- 3 - Establishment of processes occurring and their basic parameters.
- 4 - Description of sediment population to obtain basic information necessary for to evaluate of sediment transport.
- 5 - Use of basic wave and current measurements to see if threshold conditions are expected to be surpassed. Make predictions of the relative importance of sand transport due the various processes observed.
- 6 - Design of sampling scheme to evaluate sediment transport.
- 7 - Measurement of sediment transport on beach face and develop simple model to estimate total transport.

To examine shore slope sediment dynamics, specific sites needed to be chosen. Selection of these sites was based on the following criteria:

- o A current beach nourishment site

- o Location along the navigation channel
- o Accessibility

Field reconnaissance and review of dredging operations lead to the selection of four study sites. These sites were then further divided by the detail in which they would be examined. The most accessible site would be examined with the most detail; profiling, geomorphic records, current and tidal records, ship wave records, and sediment transport observations. Two other sites would be include profiling and geomorphic observations and the fourth site would include only occasional visual observations.

SHORE MONITORING

Aerial Image Analysis

Aerial imagery was used to see long-term trends along the shores of the study sites. The images were stereoscopic black and white or color infrared photographs at a scale of 1:11,111. Images were equilibrated to the same scale using a zoom transfer scope. Polygons representing the change in area over time were digitized to find their areas. Only polygons of area change on the navigation side of Price Island were used in determining the area loss over time. Other areas were determined to experience minimal change and were not evaluated.

Profiles

Shore profiling is an essential component of most coastal and fluvial problems. Simple level and rod surveys were used to describe the shore sites. A surveying reduction software package (Birkemeir, 1988) and hand calculations were used to derive and present shore changes over time.

- 1) Field surveys (level and rod).
- 2) Stereoscopic orthophotography (from aerial photographs).

A simple leveling profile, as presented in Figure 14 is a quick, inexpensive and accurate technique for documenting slope evolution. Profile data such as that illustrated in Figure 15 were digitally input into a computer for analysis and graphical presentation. These profiles were plotted on a planimetric grid so that three dimensional analysis of beach sediment volume changes could be done. Each profile had an established benchmark stake.

When these profiles are entered into a database with appropriate elevation corrections, the development of slopes can be analyzed for distinctive trends (Figure 16). These trends can lead to empirical expressions that could be used in predictions and modeling.

Level and rod profiles of the beach nourishments were done for a period of approximately one year to show slope and volume changes over time. Beach slope is an integral

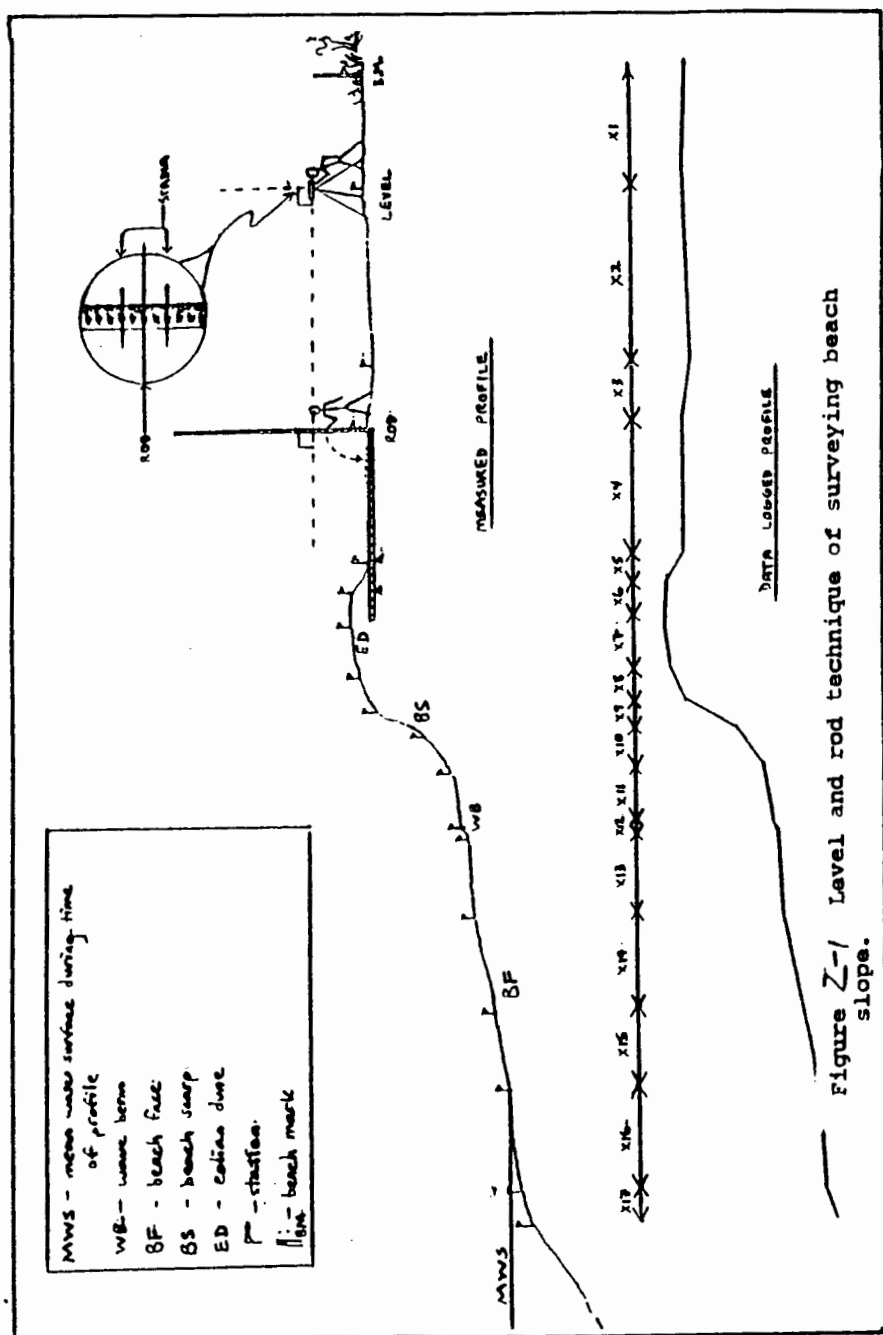


Figure 14. Surveying beach slope.

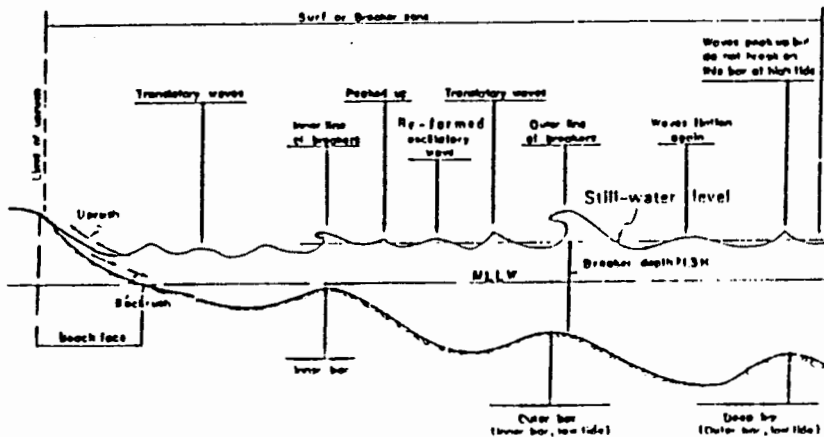


Figure 12. Waves in the breaker zone. From USACE (1984).

The importance of ships moving in inland waterways is brought out clearly in this excerpt from Fuehrer, Romisch, and Engelke (1981, p. 30):

In last the two decades (1960-80) the problem of the hydraulic loading on the bottom and slopes of navigation canals by shipping traffic has gained an increasing politico-economic importance on the account of the rapid development of inland navigation. The inland waterways are exposed to an increased hydraulic loading by:

- increasing size of ships
- increased power and thus speed of ships

In canal reaches with heavy traffic the above mentioned development leads to suddenly increasing damage of the bottom and slopes, thus causing rather high maintenance cost.

The following hydraulic effects produced by the moving ship are above all responsible for the destruction of the canal boundaries:

- wave motion caused by ships
- displacement current (backwash)
- flow processes caused by propeller (jet)

Profile for Wave Analysis, October 29, 1987
 80 minutes before high low tide
 Beach face slope = 1:16.5 (3.5 degrees)

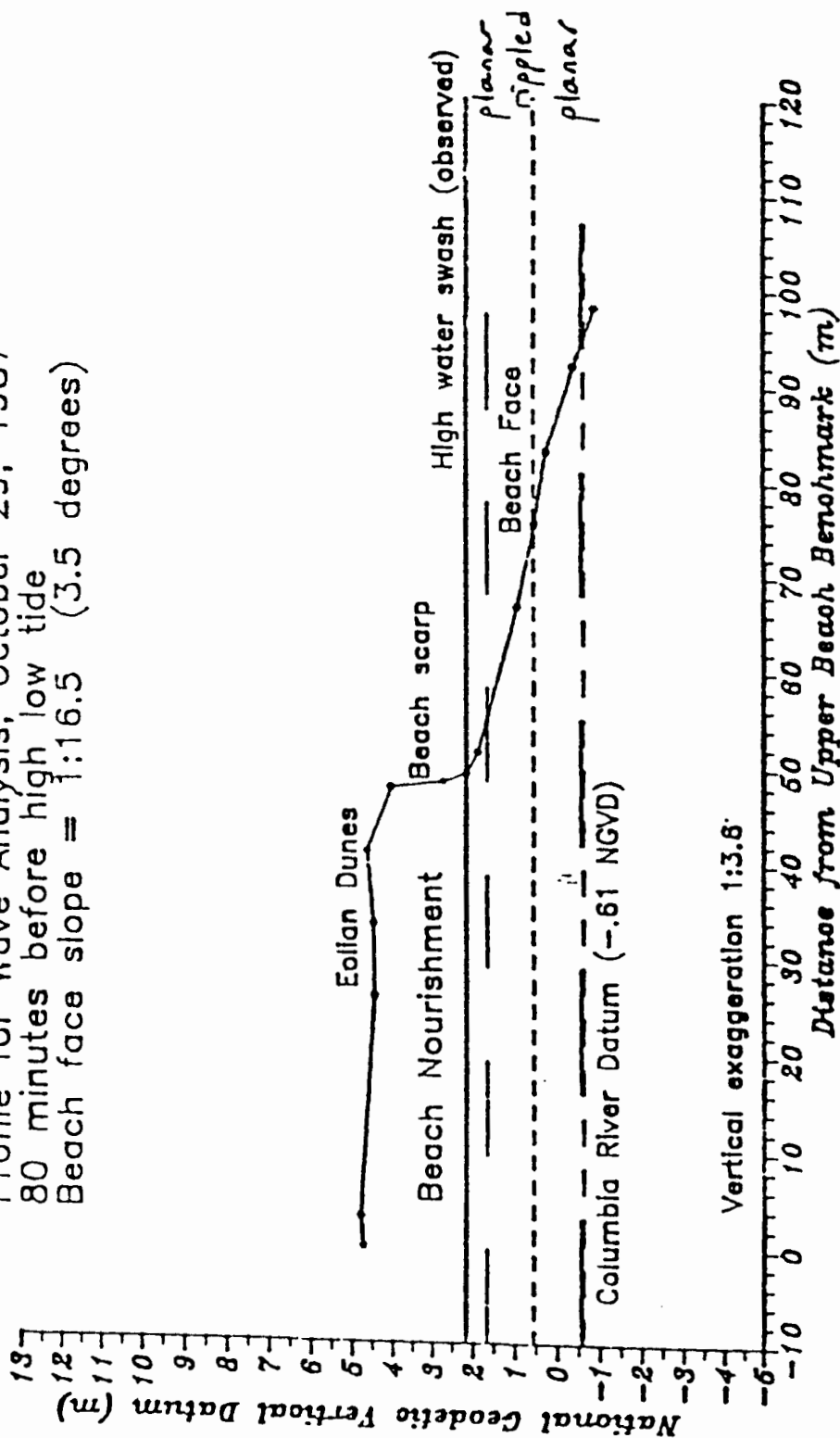


Figure 15. Typical shore profile. As presented from rod and level profiling data.

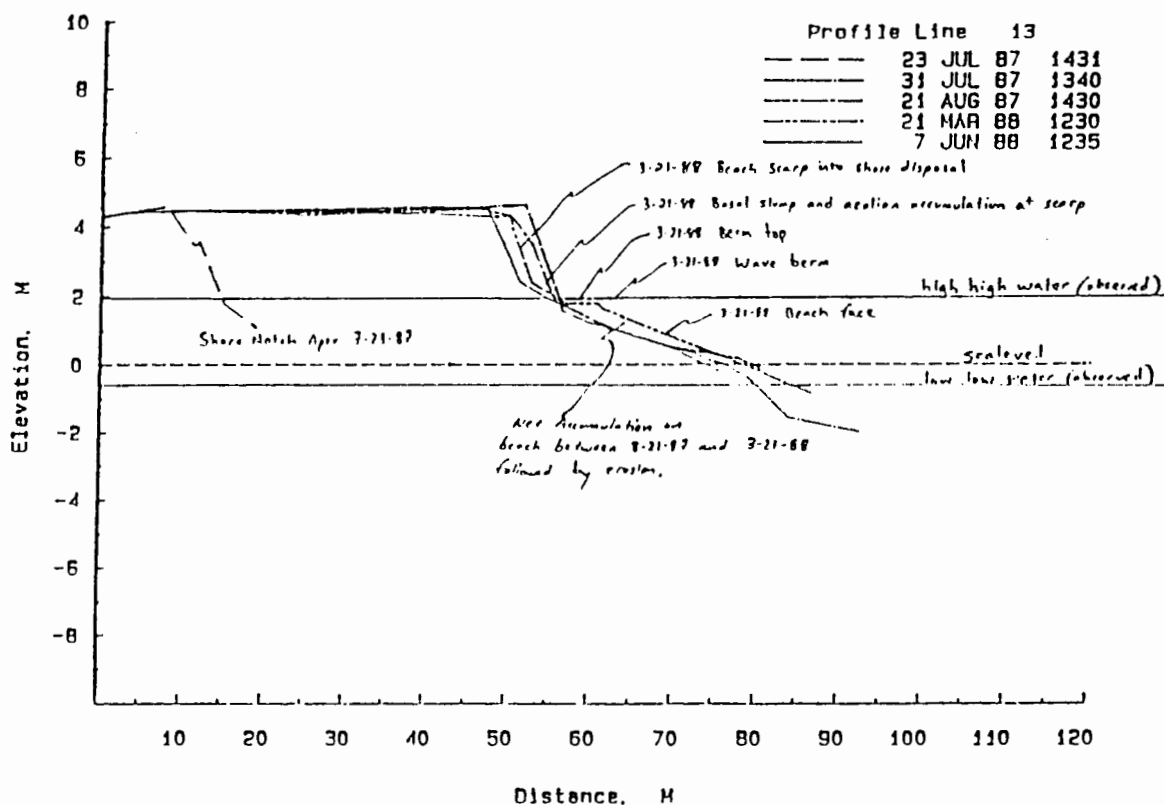


Figure 16. Shore profile changes over time.
Puget Island site.

TABLE V

PROFILING ERROR

Profile	A (area, m ³)	$V = A - A_{\text{mean}} / A_{\text{mean}}$
1	124.9	0.0015
2	122.1	0.0241
3	126.2	0.0082
4	127.3	0.0175

$$\begin{aligned}
 V_{\text{mean}} &= 0.0128 = 1.28\% \\
 V_{\text{max}} &= 0.0241 = 2.41\% \\
 V_{\text{min}} &= 0.0015 = 0.15\%
 \end{aligned}$$

part of any sedimentary environment, and a direct factor in the behavior of energy delivered to the shore, in wave breaking, and in sediment transport (USACE, SPM, 1984; Bascom, 1951).

Error analysis was done on the level and rod method by surveying the same profile four times with two different combinations of surveyors. The area under each profile above a zero datum (NGVD=0) was calculated and each compared. Table V exhibits the error that was found in the method of surveying used in the study.

Limitations concerning interpretations of the data and analysis in this study are as follows:

- A. The data was collected over a limited period that did not include large hydrologic events that are important in any hydrology study used to make long-term interpretations.
- B. The data was collected at unequal time intervals which may have not been the best increment or descriptive enough for certain seasons. These are factors beyond the control and scope of this investigation.
- C. An error exists in the data collection, an error that is analyzed and presented in this section. Interpretations are only valid then based on changes that occur outside the error range.

- D. The processes acting on these slopes are described as observed in this study, but only some of these were quantified to any degree of integrating into a model or analytic solution descriptive of slope evolution and sediment transport.
- F. The interpretations and derivations presented in this study are based on foundations presented in this thesis, with conclusions that must be viewed in this light. Conclusions present a scientific description based on the small amount of data representative of a complex system. Thus, analysis of data was integrated with the theoretical/laboratory work of others as much as possible to make realistic interpretations.

OBSERVATIONS OF BEACH CHARACTERISTICS

Geomorphology

Visual observations recorded with photographs and sketches provided qualitative descriptions of shore features that characterized the study site and its development. During profiling, specific shore features were recorded where they were found on the profile. Some geomorphic forms such as the distinct topographic wave created "shore notch" feature were also described by sampling the structure to define any distinct grain size differences.

A sediment grain exposed to a distinct hydraulic regime behaves according to its shape, size, and density. When a variety of grains of varying size, shape, and density are present, they each may have a different response to the same hydraulic regime. Distinct mineral banding and structures can result. A grain's behavior is also dependent on its relative size in comparison to the grains around it (Komar, 1987b). The cumulative grain response of a sediment population results in an assorted variety of distinct bedding structures. These structures can be described by their appearance, location on the shore slope, and by the hydraulic process which formed them. Structures were photographed or sketched, the probable process responsible for the structures' formation was noted, and their positions on the beach face were recorded.

SHIP PASSAGE

Background Conditions

The lower Columbia River has a complicated set of hydraulic actions occurring in its channels. Water motions are controlled by: freshwater discharge, tidal range, wind waves, ships and channel geometry. All these processes were observed, but impacts of ship waves in shallow water were examined with most detail. Thus, the simplest background conditions would occur when all other variables are neglected occurs when: the river current velocity, $u =$

0, the time of low and high water slack; and where and when wind effects are negligible. To establish background conditions, near shore surface velocities were taken and wind waves described.

The Ships

The Columbia River Pilots Association provided the following vessel descriptors; length over-all (LOA), beam or breadth extreme, and mean draft during passage. Draft or the submerged depth of a ship is influenced by the pitch of the vessel. Pitch is the rotation of the ship upon a horizontal axis that bisects the ship perpendicular to the ship's long axis, identical to a "rocking-horse". A high pitch would correspond to a high standard deviation about the ship's mean draft. It is assumed that the mean drafts obtained from the Pilots is representative of a ship with no pitch or a level keel. General ship descriptors such as dimensions and net displacements were obtained from the Lloyd's Ship Register (1987-88) and Jane's Fighting Ships (1987-88), such as dimensions and net displacements. The information acquired was inadequate to describe the hull geometries of the vessels quantitatively. This is a problem other studies have had (Sorensen and Weggel, 1984). It is assumed that draft and speed of the vessel will outweigh the other factors in the net effects upon the shore slopes. But the correlation of the ship factors with

actual impacts upon the shoreline and resulting sediment transport is complex. Much of the interpretation and conclusions of this study were drawn from analogy using established expressions and case studies presented in the literature (PIANC, 1987; Johnson, 1966; Ofuya, 1970; Sorensen, 1973; Sorensen and Weggel, 1984; Brebner and others, 1968; and others listed in references).

To describe a ship wave event a single low pressure transducer [transmetrics P21C 0-15 psi] was placed in water 1-2 meters of depth in proximity to the sampling array. The transducer was attached to a two channel strip chart recorder that recorded the signal. Each day sampling was done, the transducer was checked and calibrated by raising and lowering the transducer through the water column. The system usually worked well. Error estimation and calibration of the transducer-strip chart recording system was done to establish the precision of the method. The strip chart record was run at either eight or sixteen inches per minute, but the lower speed was found to create fewer problems in paper binding. The strip chart recorder was tested each day operated to establish the recorder's precision. Error is presented in Table VI.

SEDIMENT ANALYSIS

Sediment characteristics such as specific gravity, the average unit weight of the population, grain size and

TABLE VI
ERROR IN STRIP CHART RECORDER

Time Calibration			
Strip-Chart <u>Record</u>	<u>Minimum Error</u>	<u>Maximum Error</u>	<u>Mean Error</u>
8 in./min (.13"/sec)	0.0%	3.0%	1.5%
16 in./min (.27"/sec)			
Transducer Depth			
Measurements	0.0%	13.0%	3.0%

shape affect the sediment population's behavior when exposed to a hydraulic regime.

Unit weights of the dry loose sand were obtained by splitting the sample, weighing the split and determining it's volume with graduated cylinder. The average grain density was obtained by weighing a dry sample and then finding the sample's volume by the displacement of water in a graduated cylinder.

Two methods were utilized in grain size analysis: mechanical sieving and settling tube analyses. Each method provides a very distinct analysis. Sieving, because it uses square openings, is also a measure of grain shape. A grain's intermediate diameter will govern whether or not it will pass through the sieve. Standard preparation of the samples was followed in the analysis of grain size (Blatt and others, 1980).

Mechanical sieving involved first wet sieving the 1-2 kg sample with a 325 mesh sieve to remove any silts and clays from the sample and then placed in an evaporating oven. Grains of silt size and finer account for less than 0.01% of the beach sand samples. The sample was then dry sieved using one, one-half, or quarter phi intervals. Wet sieving is a more precise technique when the population has a significant portion of fine sand and smaller particles. The water releases these surface tension tending to hold these very small particles together. When wet sieving was used, the sample fractions were then dried and weighed. Dry sieving was done with a roto-tap machine for 15-20 minutes. Each fraction was then removed and weighed.

The settling tube technique provided a more rapid and continuous recovery of the sample distribution of sediment falling velocities and approximate grain size distribution. To obtain a realistic presentation of the sediment's size distribution with the settling tube, a mechanically sieved sample at quarter phi intervals was used to calibrate the process. Each interval was run on the settling tube and the median settling time, t_{50} , plotted for each size fraction, as exhibited in Figure 17. Samples are first split to obtain a representative sample of approximately 2 grams. Calibration of sediment samples enables the settling tube system to rapidly give the user continuous data describing a sediment population. The logarithmic

SETTLING TUBE CALIBRATION COLUMBIA RIVER SEDIMENTS AND GLASS BEADS

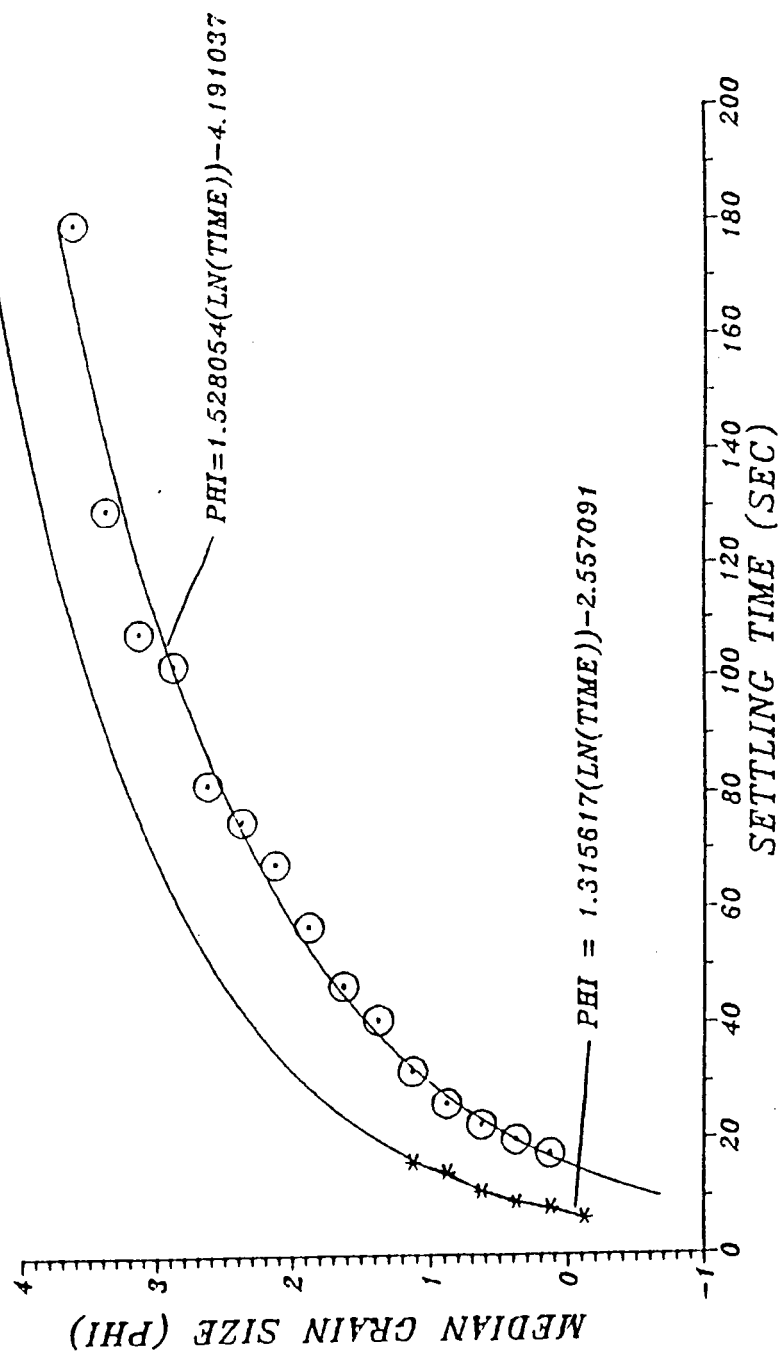


Figure 17. Calibration curves. Two mechanically sieved data sets. Stars represent glass beads (spheres) and the circles represent unreworked Puget Island dredge spoil sand, sampled in September 1987. Logarithmic curves were used to convert settling time from settling tube to an estimate of grain size, enabling grain size distribution acquisition from the settling tube system.

line of best fit was used to derive an equation converting settling time to size and the computer generated data file thus could include an approximate estimate of grain size. This data file was constructed with a BASIC program that used digital data converted from an analog signal. The analog signal is sent from the strain gage in the settling tube measuring the accumulation of sediment on a plate. The entire settling tube process is shown in Figure 18.

The interpretation of sediment size distributions has been of critical importance and debate in engineering and geologic disciplines since the early 1900's. Stochastic descriptions of a sediment population enable researchers to correlate sediment behaviors to specific in situ and sediment transport conditions that enables realistic interpretation of a sediment response. A statistical description of a sediment size population has become increasingly important in sediment transport theory (Einstein, 1972; Komar, 1987a, 1987b; Gomez and Church, 1989).

The most simple model of a sediment size distribution is the Gaussian or normal distribution. Statistical description of a sample based on graphical parameters (Folk and Ward, 1957) have been widely used in geological research and are applied in this study. Moment measures were also calculated for representative samples.

SETTLING TUBE SYSTEM

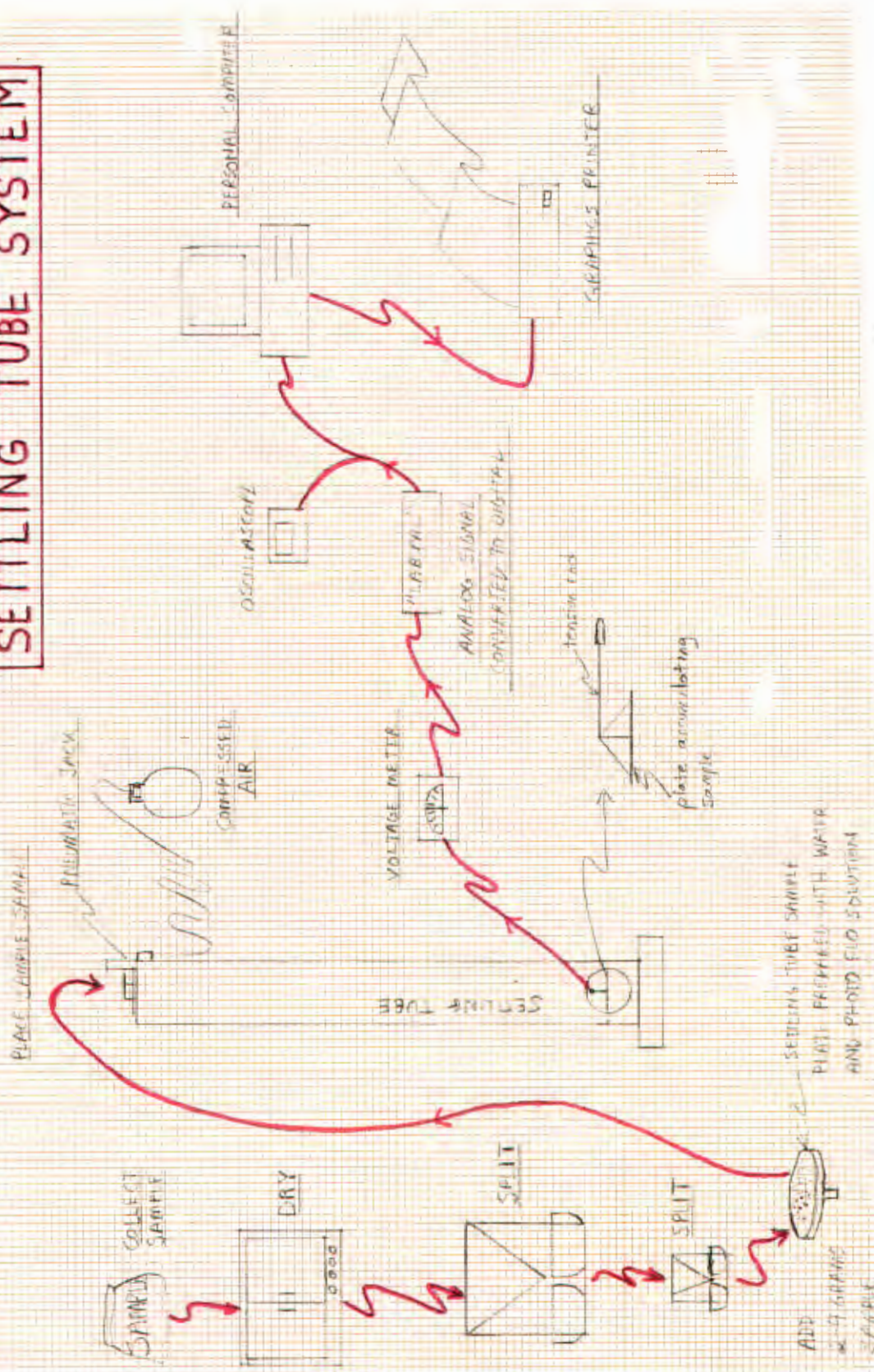


Figure 18. Settling tube. Cartoon of the two meter settling tube system in the PSU sediment laboratory.

SEDIMENT TRANSPORT

To evaluate the magnitude, direction, and rate of sediment transport across the beach face a field apparatus was needed that could collect sediments during a given event. The only systems found in the literature that were designed to meet similar criteria were used in the surf zone along the Japanese coast and along a North Carolina barrier beach (Katori, 1982; Katori, 1983) and (Kraus, 1987; Kraus and Dean, 1987b), respectively. These experiments presented an example of shallow water sampling in a surf zone. But because of constraints in economy, labor, and physical factors, a system had to be designed that would not only give a representative sample of longshore sediment transport as in the works of Katori and Kraus, but also give transport vectors on the beach face.

An effective method with minimal requirements for equipment and personnel was designed to document sand movement near the bed partially based on work by Hubbell and others (1986). Little such sampling has been done to date (Kraus, 1987). The design encompassed the following criteria: a minimum of hydraulic turbulence or interference; several sampling positions in the water column at the same lateral position; the potential to sample several transport directions; easily transportable; remain secure in desired position during most events; support sample bags of desired mesh for maximum flow; and

easy removal of sediment sampled. The trap mouths were made from square steel piping modified with a slightly flared exiting port, with an entry to exit ratio of 1:1.23, slightly less than the recommended 1:1.4 ratio for the Helley Smith bedload sampler (Hubbell and others, 1986). Design of the sampler set and array is presented in Figures 19 and 20, respectively. A nylon 105 micron mesh sieve cloth was used for the sample collection bags. The traps proved quite successful in collecting sediment put into motion during sampling events. Collected samplers are exhibited in Figure 21.

A low pressure transducer and strip chart recorder was used to numerically document the wave event during sampling. Other studies (Kraus, 1987; USACE, Portland District, 1986) video taped a staff gage(s) placed in the water near the sampling point or across the surf zone and then did spectral analysis, a labor intensive and costly procedure. The transducer offered a simpler method adequate for this study. When possible a video camera was used to record the event, providing verification and records of some of the events.

Problems with the sediment trap array system include stability during the turbulence of extreme events, (e.g. an out-going container ship the "Verrazano Bridge" caused a 1.52 meter drawdown and strong surge of approximately a meter that resulted in four of six trap array rods being

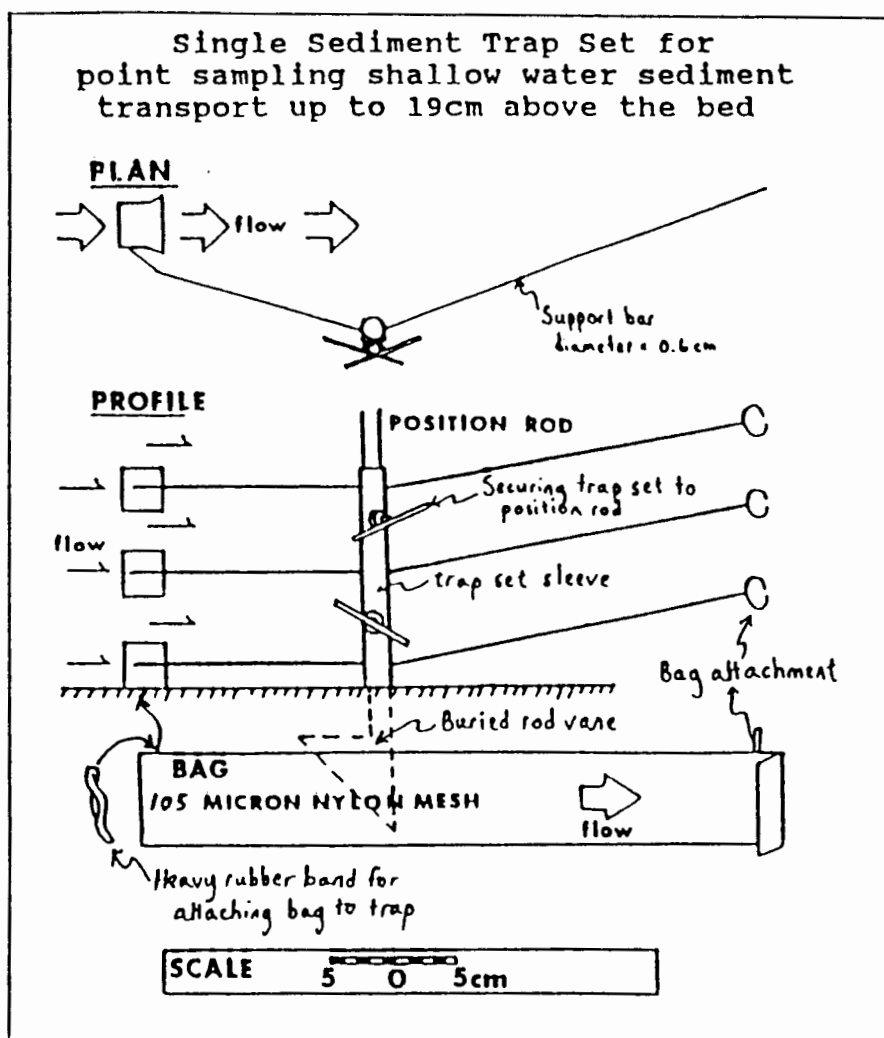


Figure 19. Shallow water sediment trap.

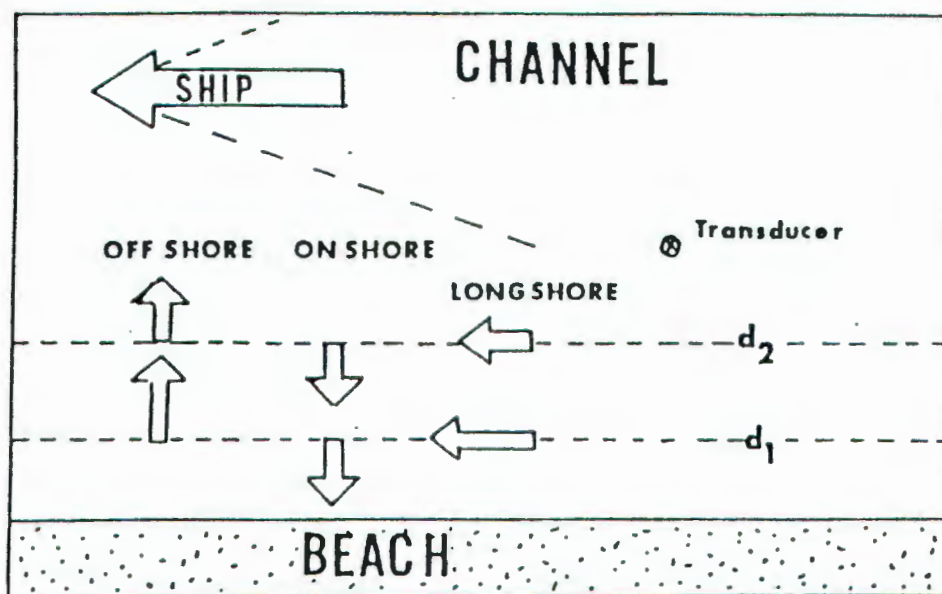


Figure 20. Sediment trap sampling array.



Figure 21. Removal of sand from sediment bag.

knocked over. Early problems with the arrays spinning on the vertical rod axis due to wave shear was remedied by welding a stabilizing steel plate to the bottom of the rod that is driven into the bed. To decrease the influence the traps themselves had on the hydraulics of the event, they were made small and the trap arrays were placed approximately three to five meters from one another. This introduces some error because interpretations are made using the entire array of several trap arrays covering a distance of up to eighteen m² along the shore to represent a point. This interpretation is valid if the shore geometry is relatively constant in the vicinity of the nearshore array.

RESULTS

THE STUDY SITES

Four beach sites were examined: Price Island, Washington, River Kilometer (RK) 55; Puget Island, Washington, River RK 62; Wallace Island, Oregon, RK 76.5; Gull Island, Oregon, RK 88. The principle study site was the northwestern tip of Puget Island, Washington, at $46^{\circ}12'12''$ N $123^{\circ}25'25''$ W. Figure 22 displays the location of the study sites. Each site is located adjacent to the navigation channel. Table VII lists the approximate distance from the mean water level line at each site to the center of the navigation channel.

Because the channel is maintained to a width of 183 meters, ninety-two meters can be subtracted from the distances given in Table VIII to give the minimum distance a ship will come to the shore. The average slope from shore to channel, assuming a channel depth of 13.7 m (45 ft.= advanced maintenance dredging, USACE 1989). The distance from the navigation channel to a site is critical in evaluating potential erosion. By design, the navigation channel approximately defines the river thalweg, thus is the region of highest current velocities and steepest side slopes. Ikeda (1982) showed that the side slope of a

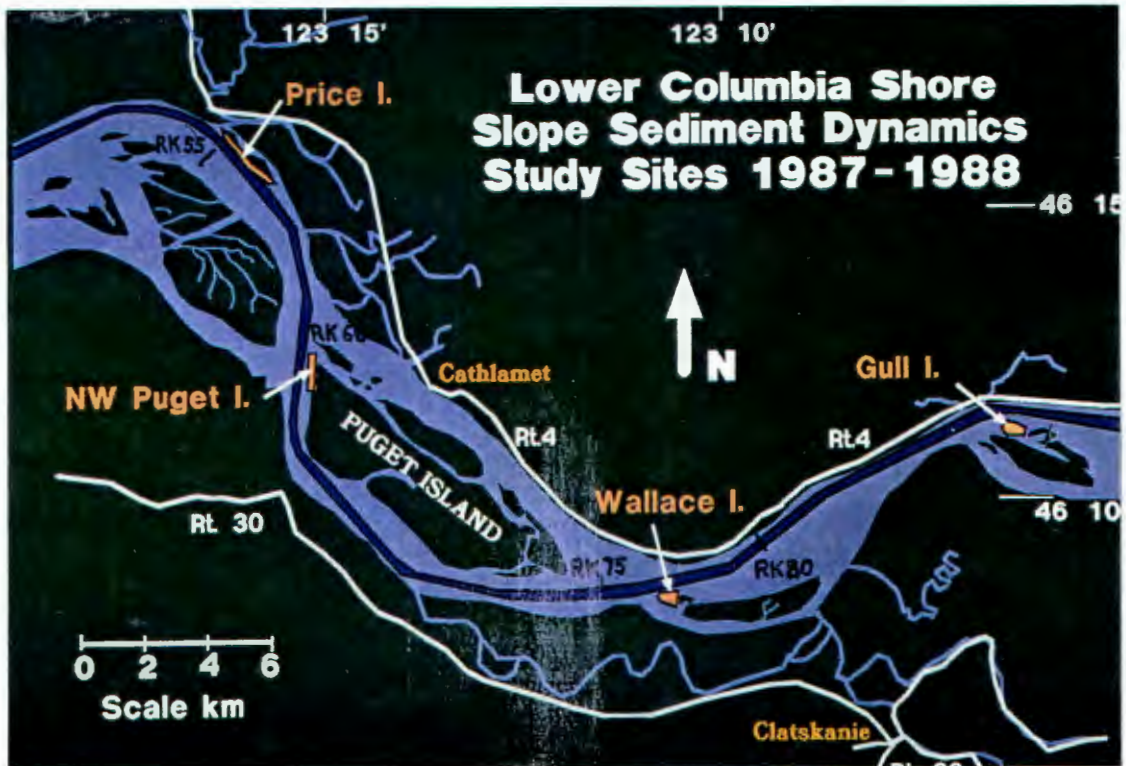


Figure 22. Sites observed in shore slope sediment dynamics study. Puget - RK WA-62; Price Island Site, RK WA-55.4; Wallace Island Site, RK OR-76.9; and Gull Island Site, RK OR-88.4.

TABLE VII

SITE LOCATION AND DISTANCE TO NAVIGATION CHANNEL

<u>Site</u>	<u>RK</u>	<u>Distance to channel center line</u>
Price	WA-55.4	215m (channel parallel to shoreline)
Puget	WA-62.3	270m (channel parallel to shoreline)
Wallace	OR-76.9	305m (channel parallel to shoreline)
Gull	OR-88.4	280-350m (channel oblique to shore)

TABLE VIII

AERIAL IMAGERY ANALYSIS OF EROSION 1939-1983

West bank of Price Island (square meters)
Cumulative Area

<u>Year</u>	<u>Eroded</u>	<u>Years</u>
1939	0.00	0
1948	60,299	9
1957	119,788	18
1961	130,310	22
1966	145,284	27
1968	163,090	29
1970	187,169	31
1973	204,570	34
1974	223,591	35
1978	250,301	39
1979	270,940	40
1983	329,620	44

channel can play an important role in lateral bedload transport leading to channel shoaling. Shore slope at depths less than one half of the deepwater wavelength of water waves controls wave refraction and reflection in transitional and shallow water (USACE, 1984) and thus the incidence and magnitude of ship waves (Johnson, 1968).

Price Island, Washington at RK 55.0 (River Mile, RM, 34.4) and Gull Island, Oregon at RK 87.8 (RM 54.9) were both profiled, observed, and sampled during 1987 and 1988;

no quantitative measurements of sediment transport were made. Visual observations of sedimentary structures, geomorphic features, and ship wave behavior were made at Wallace Island, Oregon at RK 76.5 (RM 47.8).

SHORE EROSION

Historic records of the study region offer information that more closely represents the "natural" conditions of the river than are observed today with the extensive modifications that have occurred in the last century by human development. These modifications include: shoreline levees, wetland drainage, beach nourishments, dredging, reservoir construction, and pile dike fields. Figure 23 presents a 1913 navigation chart of the Price Island and Puget Island study reach. The deepest water soundings (Figure 23) approximately trace the river's thalweg. Shallow water soundings delineate regions of natural shoaling, areas that have been utilized as sand disposal sites (USACE, 1989).

Figure 24 presents 1913 soundings in the vicinity of Gull Island (north of Grimms Island, Oregon). Gull Island was much smaller in 1913 than today as a result of continued sand disposal and a relatively low energy environment. Gull has traditionally been a site of deposition or shallow water sand bar. Price and Puget Island sites are land masses lying above mean highest high water.

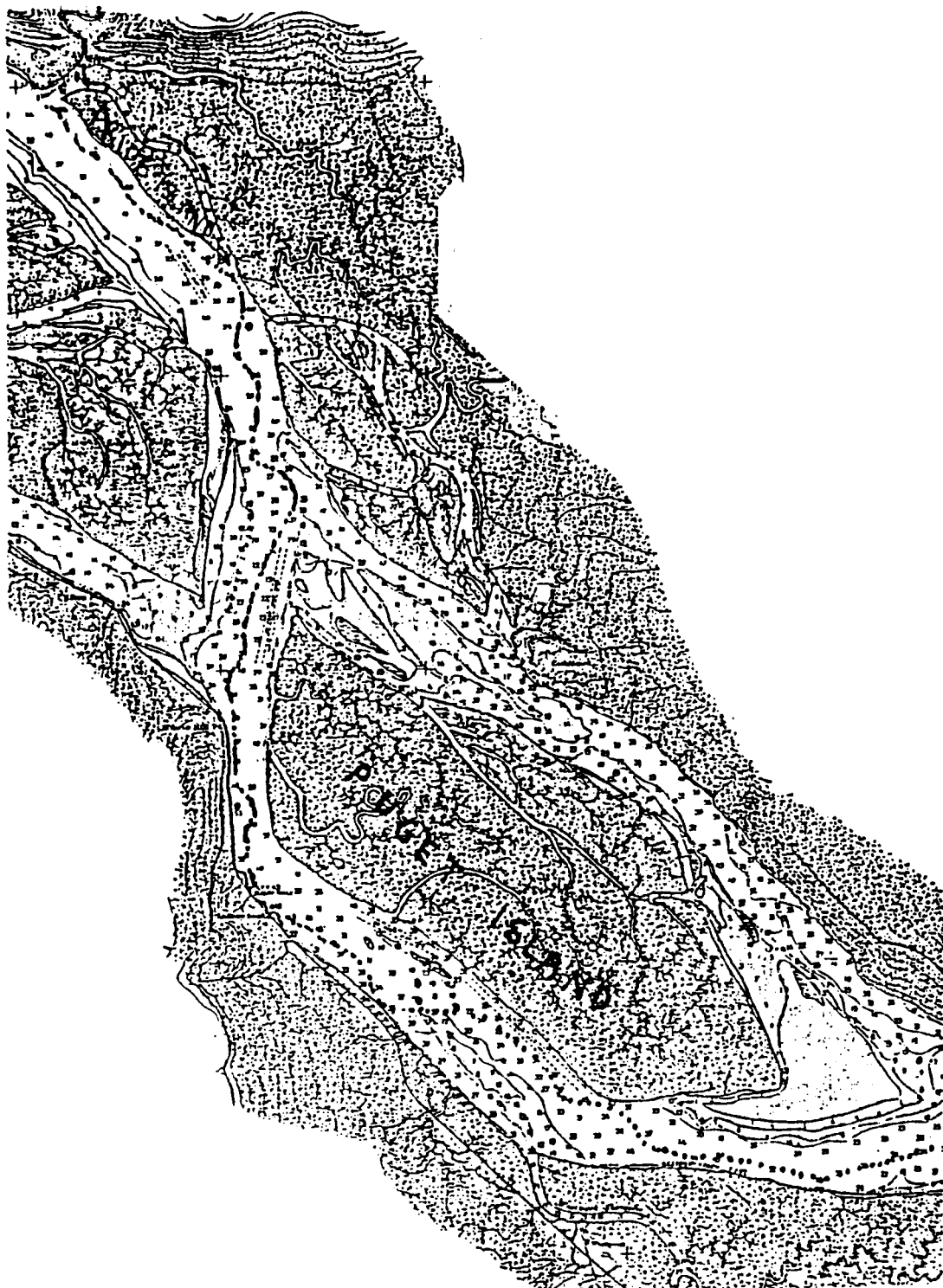


Figure 23. Columbia River soundings, 1913.
Price Island and Puget Island reach (NOAA,
1913).

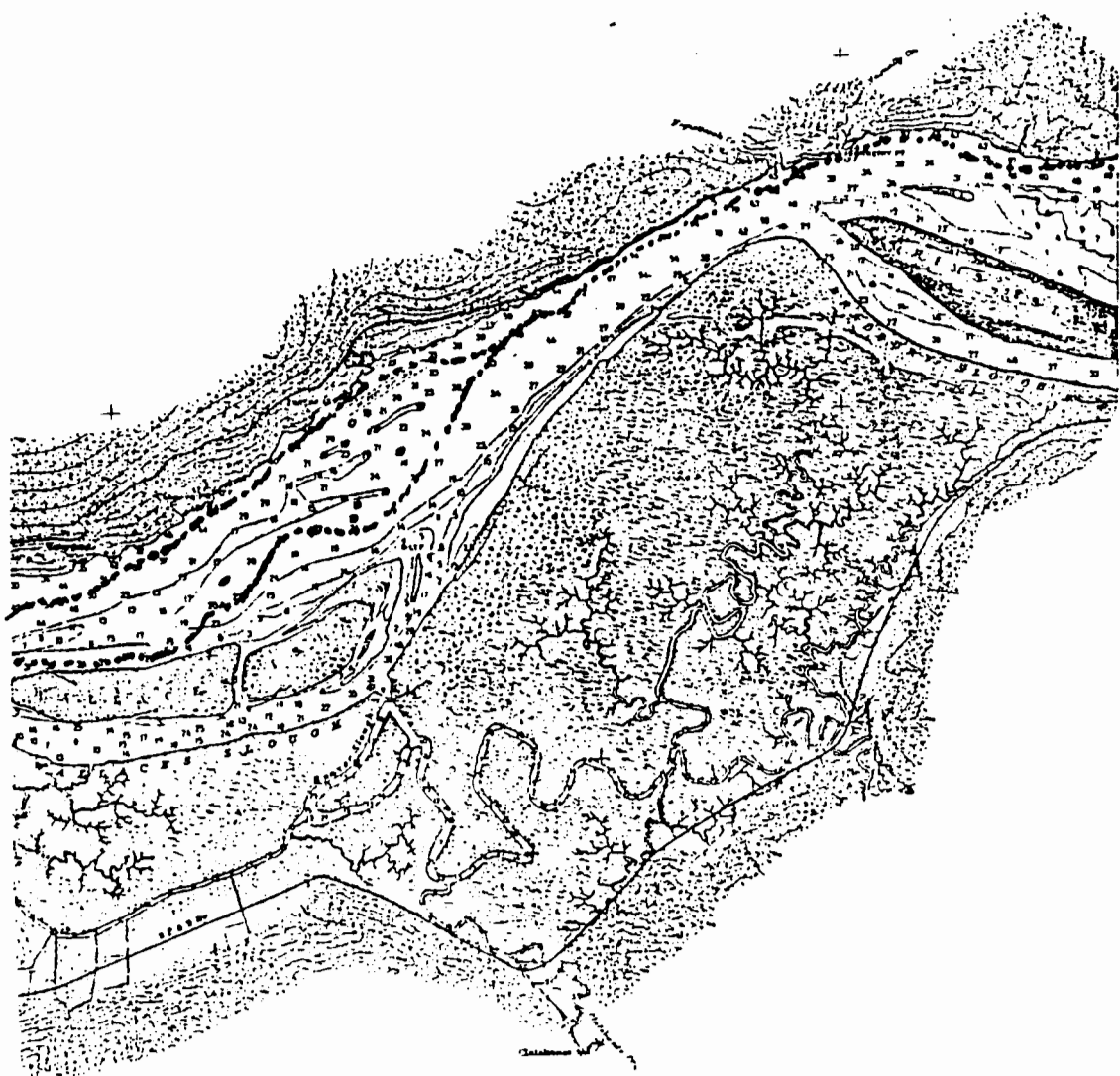


Figure 24. Columbia River soundings, 1913. Grimms and Gull Islands, Oregon (NOAA, 1913). Note Gull Island is primarily a shoal with a large shallow water intertidal region north of Crims Island. This region of shoaling is now mostly above mean highest high water due to continued site nourishment from dredging operations.

Aerial Image Analysis, Price Island

7,204,800 m³ (9,423,000 yd³) of sand was dredged from the Skamokawa reach of the lower Columbia between 1906 and 1986 (USACE, 1988b). To dispose a portion of this sand, beach nourishments have been made since 1959 on the southwest side of at Price Island. The site lies adjacent to the navigation channel as illustrated in location map in Figure 22. Erosion along Price Island was evaluated using aerial imagery and survey profiling (Abbe, 1988a). The beach nourishments may have slowed erosion on the southwest flank of the island, a factor that should be considered in evaluating aerial imagery with respect to time.

Aerial imagery at a scale of 1:11,111 was stereoscopically analyzed by Abbe (1988a) to determine shoreline changes from the 1939 to 1983. The changes in the Island's area have been dramatic, with a loss of approximately 330,000 m². Figure 25 presents an overlay of the cumulative changes at Price Island between 1939 and 1983, clearly showing extensive erosion in this period. Erosion plotted as a function of time is exhibited in Figure 26, portraying the rate loss of material in the resultant curve. Table VIII presents areal differences computed from the aerial image analysis.

Aerial Image Analysis, Puget Island

The Puget Island site was examined only for long-term changes with aerial imagery. Because of extensive historic

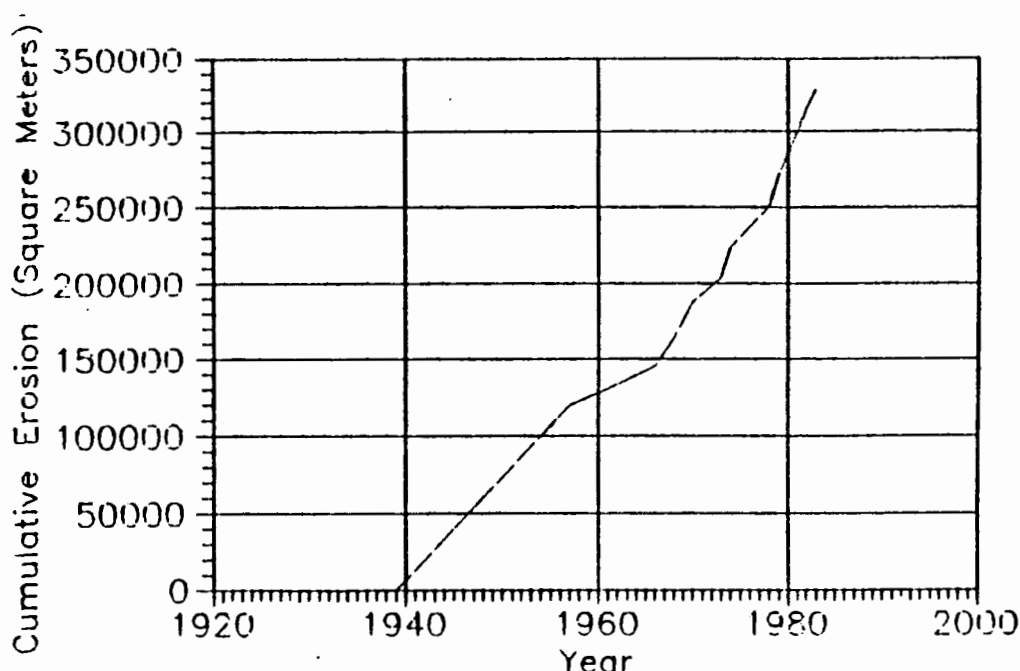


Figure 25. Price Island erosion. West flank of Price Island from 1939-1983.

sand disposal, changes have not been as dramatic as at the Price Island site WA-34. Figures 27 and 28 are computer generated images from the aerial photographs that summarize changes at the Puget Island Site between 1939 and 1983. The Puget site has had a net loss even with constant nourishment of sand by dredged sand disposal (USACE, 1988b).

Using the computer images digitized from aerial photographs, estimates of erosion and accretion at the northwest end of Puget Island were made. Between 1939 and 1983 approximately 56,795 m² of shore has eroded from the island adjacent to the navigation channel, immediately north of the Puget site. No shore nourishments or sand disposals had been placed at this location directly north

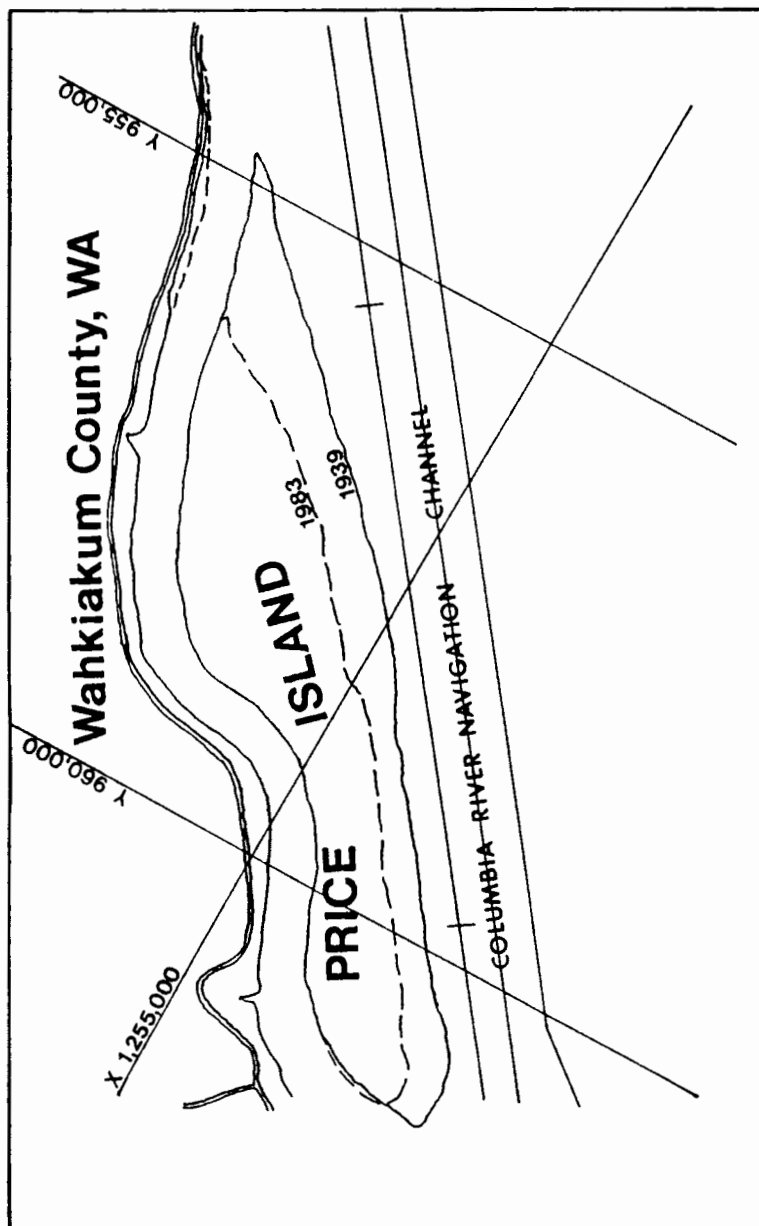


Figure 26. Changes at Price Island. Change along Price Island's western flank during the period from 1939 to 1983. The central portion of the Island's west bank has received sand nourishment since 1959.

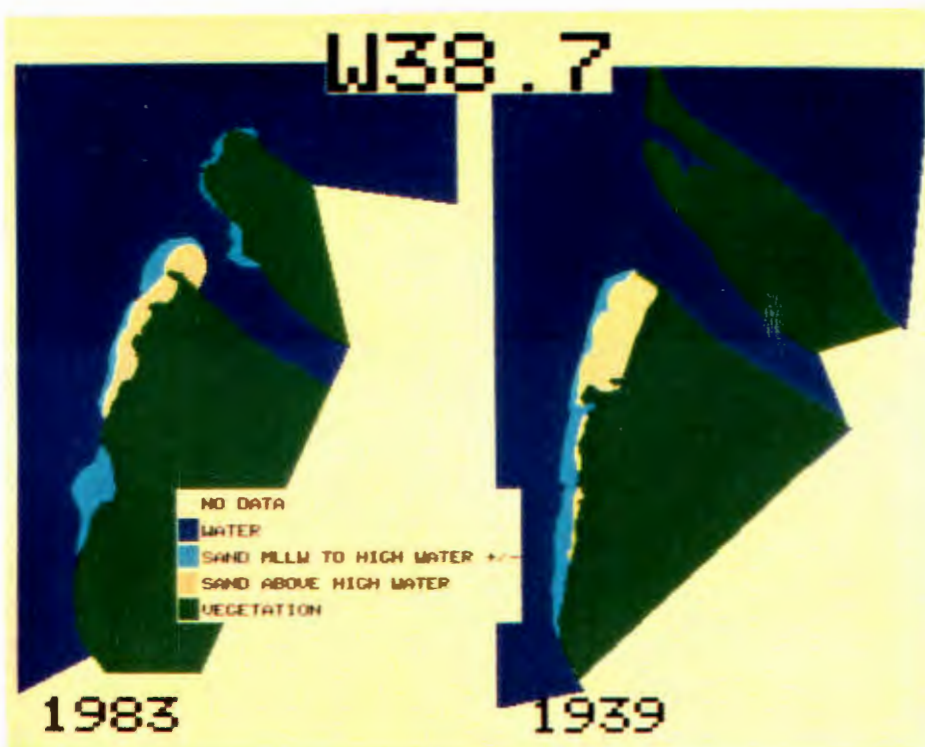


Figure 27. Computer imagery of Puget Island site. Based on aerial photographs, 1939-1983. Note erosion of small island north of Puget site.

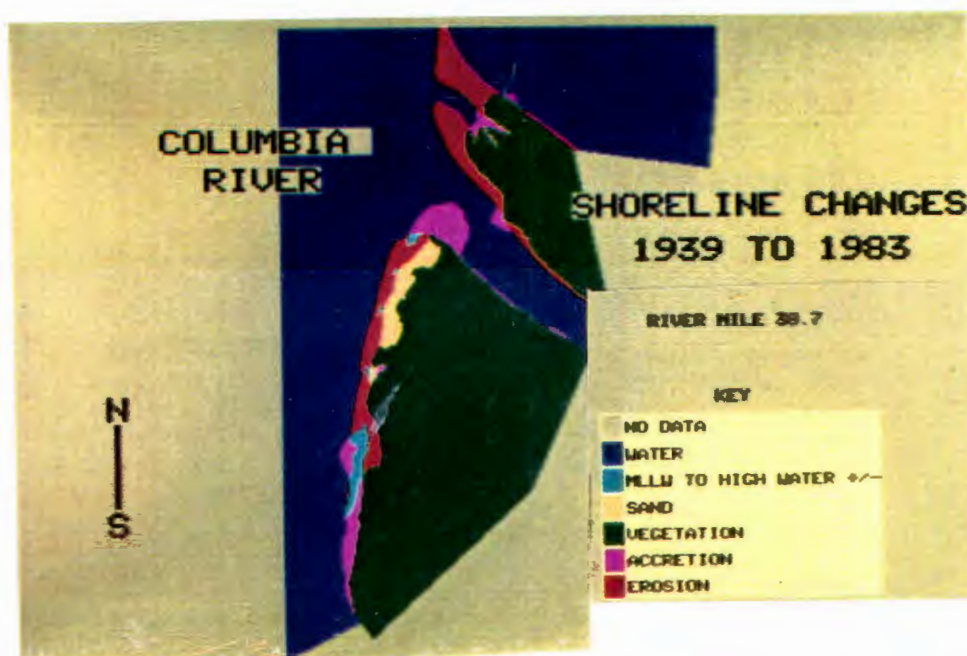


Figure 28. Computer imagery of Puget Island site. Digitized from aerial photographs, 1939-1983. Net erosion evident even though site has received a minimum of two million cubic yards ($1.5 \times 10^6 \text{ m}^3$) of sand during this period.

of the Puget site and it offers a suggestion of possible erosion at the Puget site had not extensive shore nourishments been made. A minimum estimate of the volume of sand contained in the accreting lobe north of the Puget site with a 1.0 meter accumulation, as interpreted by the difference between present topography and the 1913 soundings produces a volume of $33,528 \text{ m}^3$ of sand. The average accretion would be 761 m^3 per year. The source of this sediment has been the continued disposal of sand at the Puget site. The volume of sand nourished at the Puget Island site during the same period 1939-1983 far exceeds the minimum estimated mass stored in the accretionary lobe. During only the fifteen year period from 1968-1983 $1,450,000 \text{ m}^3$ ($1,897,000 \text{ yd}^3$) of sand was disposed at the Puget site (USACE, Portland District, 1988b). The evidence of net erosion at the site even with sand disposal and storage estimates in the accretionary lobe suggest that a considerable portion of this sediment is transported completely out of the local shallow water region encompassing the Puget disposal site.

Aerial Image Analysis, Gull Island

The Gull Island site ($46^{\circ}11'15''\text{N}$ $123^{\circ}09'00''\text{W}$) was examined for long-term changes with aerial imagery. Figure 29 is a computer imagery based on aerial photographs of the cumulative changes at Gull Island between 1939 and 1983, exhibiting net aggradation of the site. Gull Island is

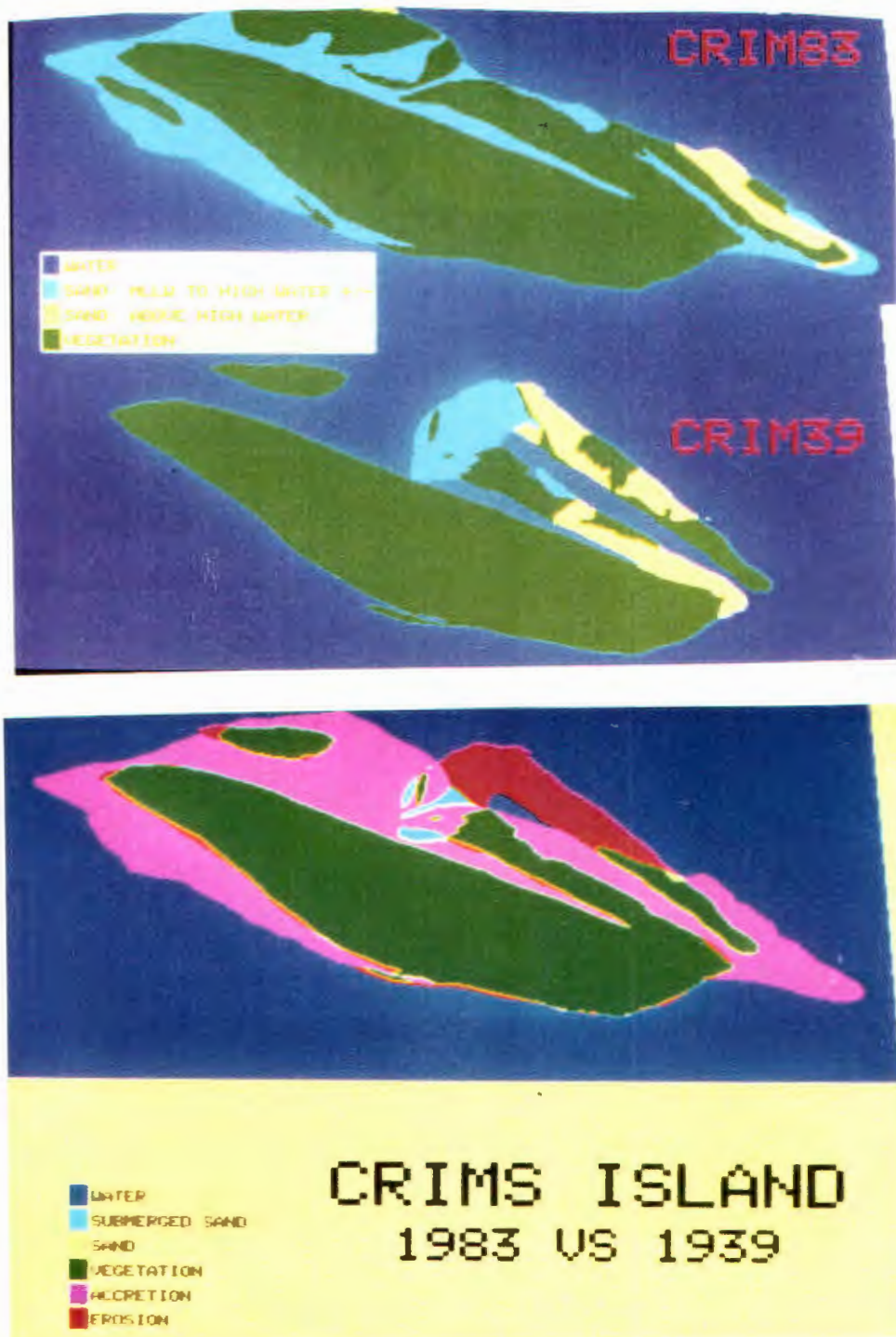


Figure 29. Computer imagery of the Gull Island Site. Digitized from aerial photographs, 1939-1983. Gull is the small island lying northwest of Crims Island.

north of Crims Island. Figure 29 shows the development of Gull Island from a shallow water bar to a well developed Island, the result of continued shore disposals of dredged sand from 1939 to the present.

Shore Profiles, Price Island

The shore slope of a river is defined as the region from the levee crest to 2 meters below the level of lowest low water. The river shore slope is an ever changing-responding geomorphic feature. Describing a shoreline as a function of time is an important part of many coastal studies done to establish volume changes and slope development. During periods of prolonged "steady-state" conditions shore slopes may display a stable form in "equilibrium" with the acting processes. But if this slope is exposed to a new set of processes or change in magnitude of existing processes, the shore will adjust to suit changing conditions. Processes include wind, currents, waves, and dredging.

Profiles compiled for Price Island (RK 54) during 1987 and 1988 show distinct erosion. Figure 30 presents the four profile lines used at the Price Island site.

Using profiles, a cumulative estimate of sand lost in the Price Island grid (Figure 30) is presented in Table IX.

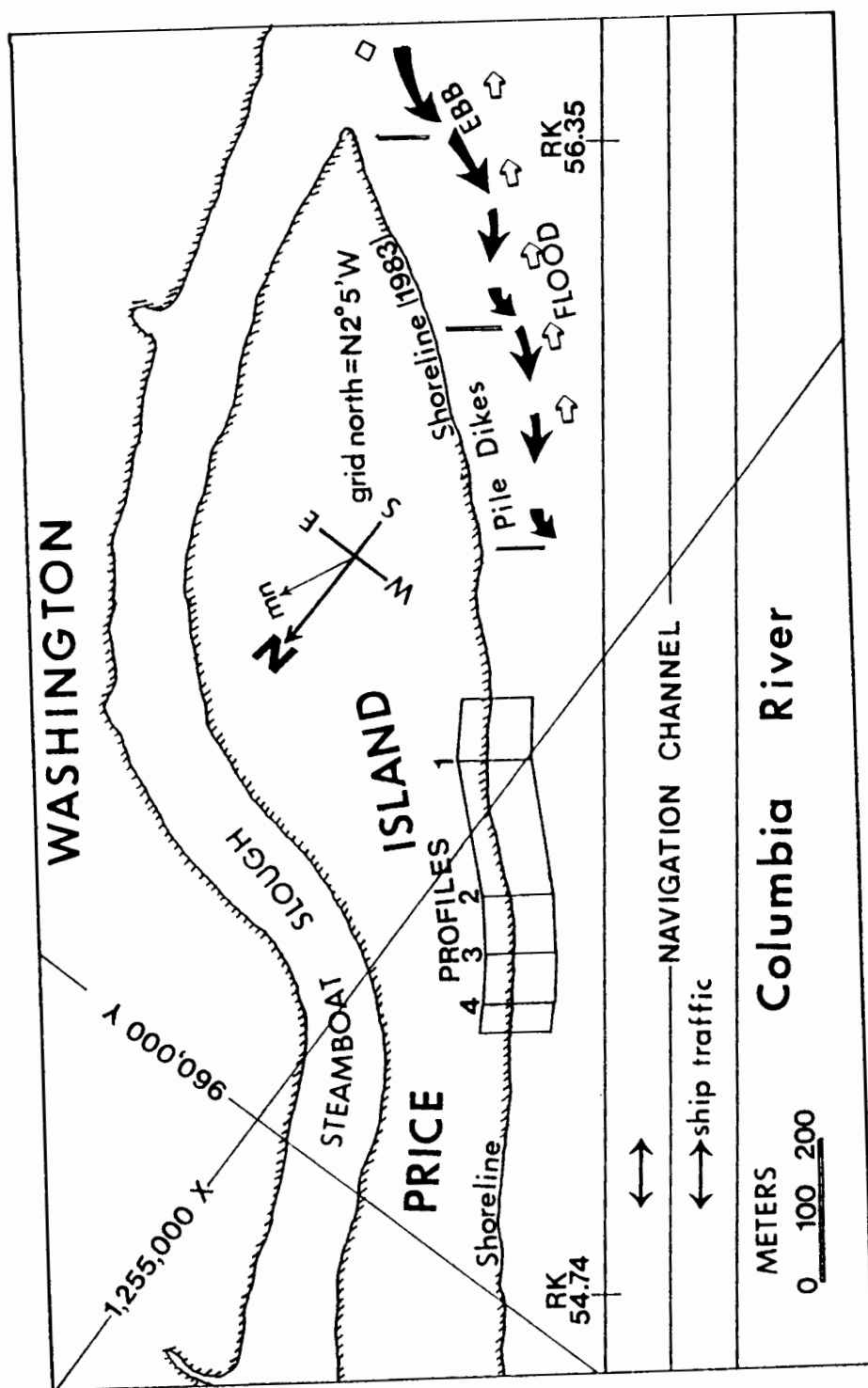


Figure 30. Price Island site profile grid.

TABLE IX
CHANGES IN VOLUME AT THE PRICE ISLAND SITE
Between June 15, 1987 and June 29, 1988

Profile	Cell width(m)	Cell Volume Change (m^3)	Relative Cell Change m^3/m
1	157	- 4,370	- 27.8
2	135	-11,718	- 86.8
3	76	- 4,720	- 62.1
4	52	- 6,920	-133.1

Total Estimate -27,729

Total nourishment June 1-10, 1987 = 178,687 m^3

Estimated loss = 15.5%

Error_{max} = +/- 631 m^3

Shore Profiles, Puget Island

The twenty-one profile lines surveyed at the Puget Island site (RK 62) were used to document slope changes and calculate volume changes over time at the site. Figure 31 presents a plan view of the Puget site monitoring layout.

Twice during the study period the Puget Island Site was nourished twice during 1987-1988 with channel dredged sands of the adjacent Puget Island Reach Channel. Between the 24th and 29th of July, 1987 approximately 97,903 cubic meters (128,045 yd^3) of sand were placed at the site. Between the 30th of July and 6th of August in 1988 196,738 cubic meters (257,308 yd^3) were laid down at the Puget site (USACE, 1988c). The dramatic changes a site undergoes after receiving a beach nourishment are illustrated in

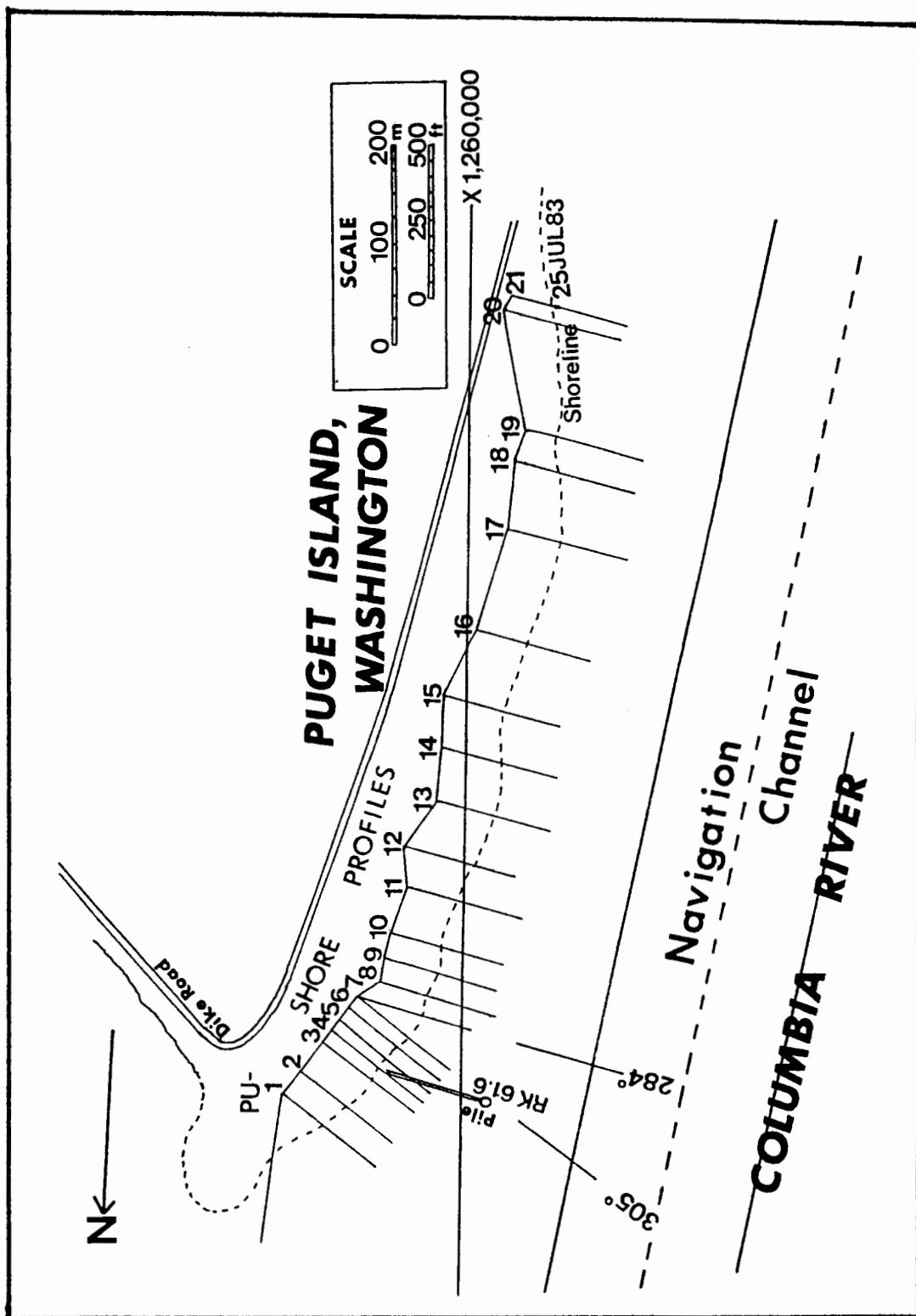


Figure 31. Puget Island profile grid.

Figures 32 and 33 which exhibit before and after views of the Puget site for the July 1987 nourishment.

Table X exhibits the computed volumes of sand eroded or deposited on the profiled beach slopes at the Puget Island site over about eleven months. After the 1987 nourishment at the Puget site through the period of July 31, 1987 to June 7, 1988 the estimated loss of sand from the Puget Island site was $26,197 \text{ m}^3$, about twenty-seven percent of the $97,903 \text{ m}^3$ quantity placed at the site during the July 24-29, 1987 nourishment. The eroded volume is equivalent to a daily flux out of the Puget site cell grid of about $72 \text{ m}^3/\text{day}$.

Slope development of the beach is illustrated in profile development with time, as displayed in Figure 34 (profiles in Appendix 1). Profile PU-7 had a slope of 1:55 or 1.0° on June 23, 1987 prior to the July 1987 nourishment. This slope is probably approaching an equilibrium slope angle for the Puget site with time (under the mean wave and current regimes during the slope development). After nourishment, on July 31, 1987 the beach face had a greatly exaggerated slope of 1:7.14 or 8° . By August 21, 1987 the beach face slope was 1:12.7 or 4.5° . Shore slope development is presented in Table XI. The upper beach is eroded and sand is deposited on the lower beach, typical of a low energy wave regime (USACE, 1984). If the water level reaches a two meter elevation it can be



Figure 32. Puget site before sand disposal. Looking north, from profile line 13. Photo: 23JUL87.



Figure 33. Puget site after sand disposal. Looking from about same site as in 32. Site was nourished with 97,903 m³ of sand between July 24 to 29, 1987. Use trees at right for reference. Photo: 16SEPT87.

TABLE X
CHANGES IN VOLUME AT THE PUGET ISLAND SITE
Between July 31, 1987 and June 7, 1988

<u>Profile</u>	<u>Cell width(m)</u>	<u>Cell Volume Change (m³)</u>	<u>Relative Cell Change m³/m</u>
3	44	-4,812	-109.4
5	29	-5,035	-173.6
7	31	-4,702	-151.7
8	26	-3,148	-121.1
9	24	-1,577	- 65.7
10	38	-2,065	- 54.3
11	38	- 527	- 13.9
12	41	-1,015	- 24.8
13	53	- 356	- 6.7
14	53	- 975	- 18.4
15	62	- 560	- 9.0
16	88	+1,871	+ 21.3
17	87	- 830	- 9.5
18	49	- 462	- 9.4
19	76	-2,003	- 26.4

Total Estimate = -26,197m³

Total nourishment July 24-29, 1987 = 97,903m³

Estimated loss = 27.0%

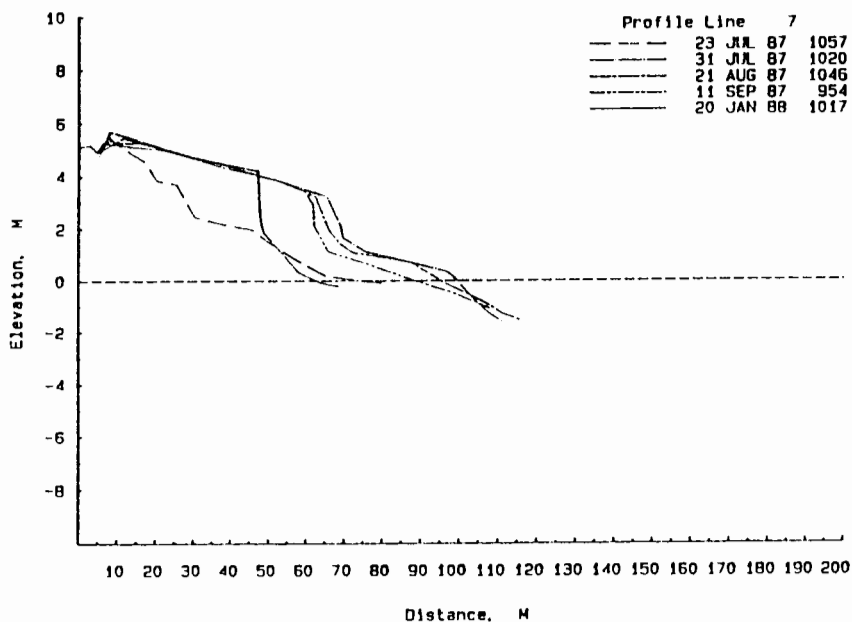


Figure 34. Puget Island site profile 7. Showing shoreline retreat. 23JUL87 before nourishment, 31JUL87 after nourishment.

TABLE XI

EXAMPLE OF BEACH FACE SLOPE

Development at Puget Site Profile No.7

<u>Date</u>	<u>Location</u>	<u>Slope</u>	<u>Notes</u>
07-23-87	Lower Beach	0.02	preceding nourishment
07-31-87	Lower Beach	0.14	directly after nourishment
08-21-87	Lower Beach	0.10	
01-20-88	Lower Beach	0.03	

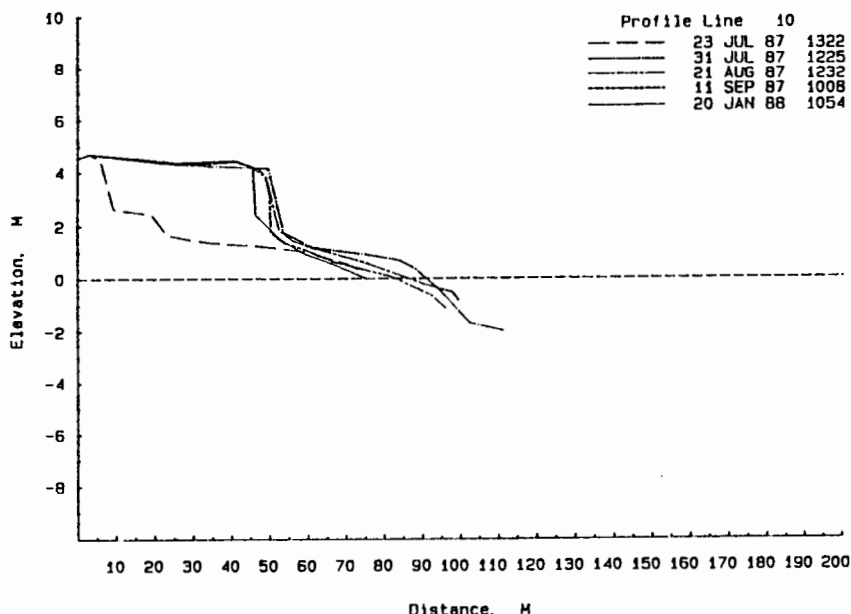


Figure 35. Puget Island site profile 10. Showing shoreline retreat and slope development.

expected that the beach slope will develop as a function of water actions (such as ship waves) up to that point. Extrapolating the "equilibrium slope" riverward from the high water level can yield an estimate of what sand that may be eventually lost to erosion. An example of shore slope steepening is seen in Figure 35, where the June 7, 1988 upper beach face is distinctly steeper than the January 20, 1988 upper beach face slope, the result of a shore notch.

Shore Profiles, Gull Island

The Gull Island site profile grid is presented in Figure 36. Gull Island was nourished with approximately 151,192 m³ (197,740 yd³) between July 29 to August 1, 1987.

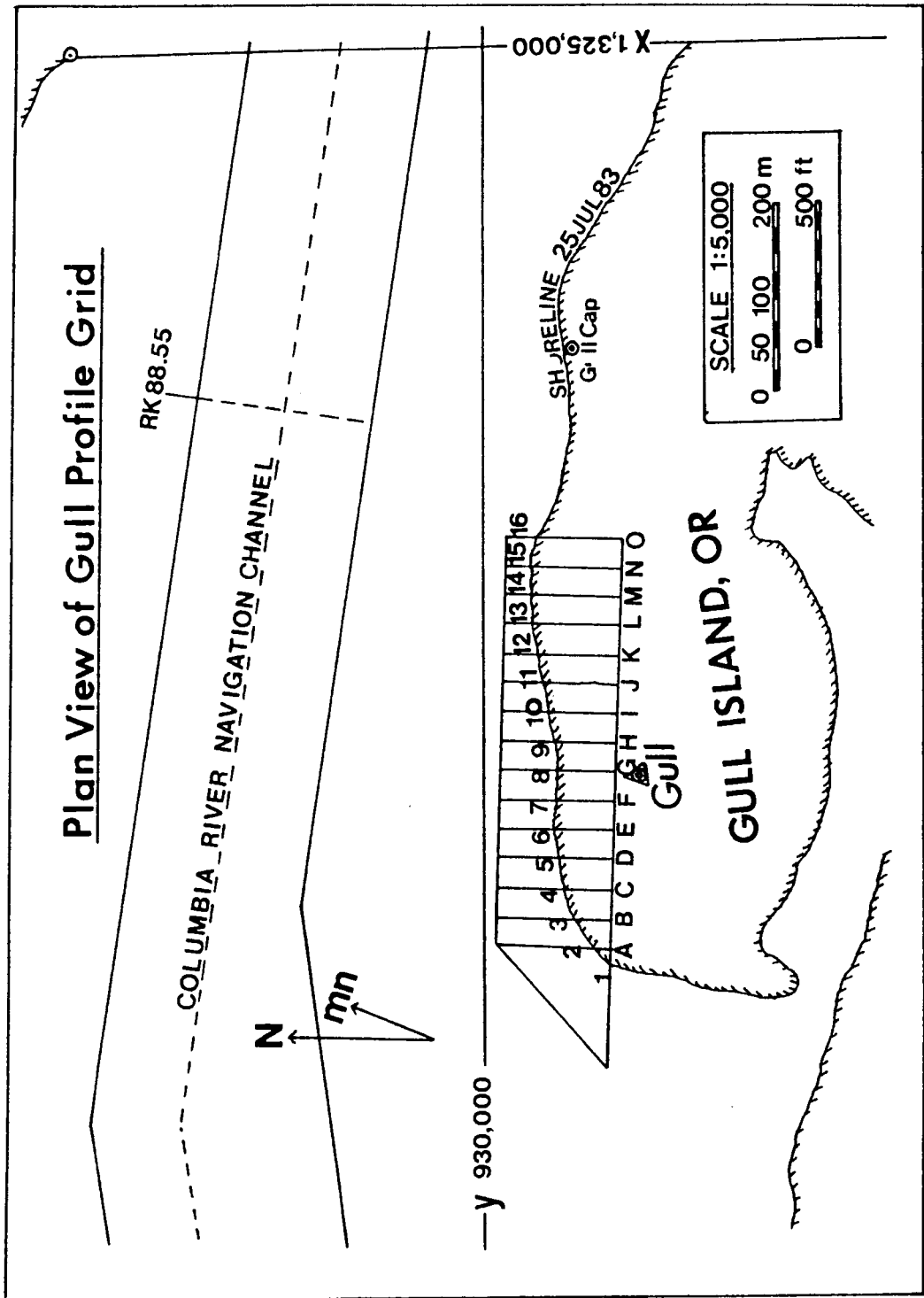


Figure 36. Gull Island site profile grid.

Figure 37 shows the Gull site before nourishment and Figure 38 shows it after the 1987 shore nourishment. Results from profiling at Gull Island suggest it is a relatively stable site, showing the least change of the sites examined. Table XXII presents the results of profiling at the Gull Island site.

OBSERVATIONS OF BEACH CHARACTER

Geomorphic Features

Geomorphic observations (Bekendam and others, 1988) can provide strong analogous evidence suggesting the dominant processes in bank erosion. The lower Rhine River has a bank morphology that has been directly impacted by the actions of ship waves (Bekendam and others, 1988), a bank that is similar in composition and morphology to banks of the lower Columbia (USACE, 1960; USACE, 1986; Abbe, 1989).

Figure 39 displays a "native" (natural) Columbia River bankline of silty clay, and exhibits a distinct wave terrace. Silty clay deposits constitute the native lower Columbia banks and a major Holocene Columbia River deposit occurring since the Wisconsin ice age. Much of the lower Columbia's native clay banks have been buried under sandy shore nourishments (USACE, 1988b). Figure 40 is a descriptive diagram illustrating geomorphology on channel and slough side of a "native" clay lower Columbia River



Figure 37. Gull Island site before sand disposal. Looking east from west end. Note abundant vegetation colonizing the upper beach face and no beach scarps, evidence of a stable shore. Photo: 28JUN87.

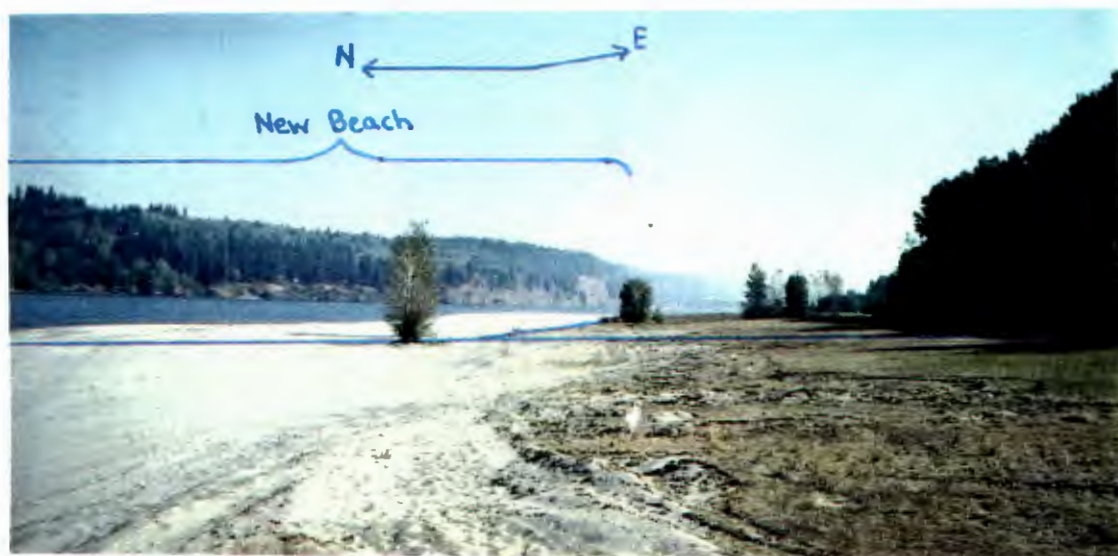


Figure 38. Gull Island site after sand disposal. View from approximately 60 meters behind Figure 37 photo. Photo taken 08AUG87.



Figure 39. Representative silt-clay bank bordering the lower Columbia River channel. Note the distinct wave cut terrace, debris, and eroding character.

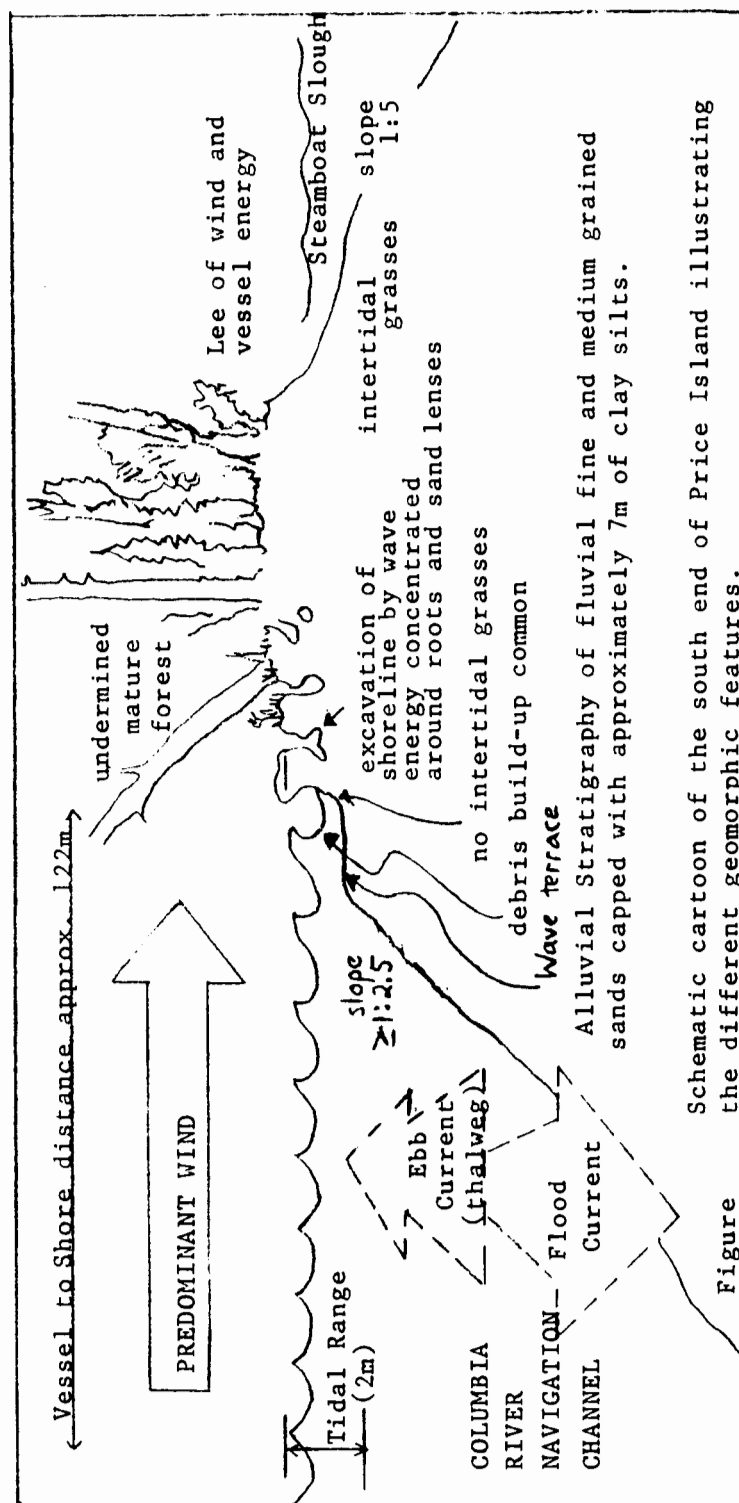


Figure 40. Price Island bankline erosion.

TABLE XII

CHANGES IN VOLUME AT THE GULL ISLAND SITE BETWEEN
JULY 31, 1987 AND JUNE 7, 1988

Estimated Using Profile lines and unit cells

<u>Profile</u>	<u>Cell width(m)</u>	<u>Cell Volume Change (m³)</u>	<u>Relative Cell Change m³/m</u>
2	15.2	- 368	-24.0
3	30.5	- 234	- 7.7
4	30.5	- 341	-11.2
5	30.5	- 113	- 3.7
6	30.5	+ 656	+21.5
7	30.5	- 207	- 6.8
8	30.5	- 55	- 1.8
9	30.5	-1128	-37.0
10	30.5	+ 235	+ 7.7
11	30.5	- 241	- 7.9
12	30.5	- 12	- 0.4
13	30.5	- 85	- 2.8
14	30.5	+ 43	+ 1.4
15	30.5	-1357	-44.5
16	30.5	-1067	-35.0
TOTAL ESTIMATE	-4,266		

Total nourishment July 29 - August 1, 1987 = 151,192 m³
Estimated loss = 3.0%

bankline, using the southeast end of Price Island at the present time as a model. The bankline on the channel side displays distinctive erosion, while the slough side lacks erosive characteristics. Several points along the Puget Island site prior to the 1987 nourishment exhibited severe erosion, as presented in Figures 41 and 42.

Constructing a Shore Nourishment

The method in which a sand shore nourishment is emplaced on a beach plays an important factor in the subsequent beach dynamics. Two distinct methods are employed to deposit channel dredged sand to nourishment sites.

The first method is an unrestricted slurry or hyperconcentrated discharge, that is directed across a shore. The sediment settles out when it reaches the river's edge. This technique builds locally large beach lobes with gentle slopes, but a considerable quantity of sand re-enters the river at points controlled by the water elevation during disposal. The majority of that sand settles out soon after re-entry into the relatively calm nearshore water.

The second method is called "beach diking," a technique in which bulldozers work steadily to maintain and direct the hyperconcentrated flow (slurry) with a sand dike riverward of the outflow. Figure 43 displays this commonly used method. The sand diking enables the dredge crew to



Figure 41. Shoreline near high tide at the south end of the Puget Island site. This shore is eroding despite an extensive vegetated cover, 08/87.



Figure 42. Apex of shore notch at Puget Island study site, July 23, 1987. Located at profile PU13. Vegetative cover slows, but does halt erosion.



Figure 43. Pipeline dredging operation. Shore nourishment at Puget Island site.

cover much more shoreline using the same quantity of sand and less time using unrestricted slurry discharge. This technique creates a steep, large berm near the water's edge, producing an unstable beach.

Because of the significant tidal variation, constructed beaches can result in a sinuous configuration when viewed from above (plan view), with the water surface controlling the location and slope riverward of the constructed sand dike or berm. The sinuous pattern results because the constructed dike follows the water-shore interface, thus during the tidal cycle the dike moves up and down the pre-existing shore slope (while migrating alongshore). A straight diked beach can be best constructed by constructing the dike at or above the high water contour to occur during the disposal. This beach configuration will control wave incidence on the beach by the refraction of waves approaching a site. Thus sediment transport by waves will be directly affected because of significant variations in longshore currents. If the sand dike were built above high high water, this beach would probably be very stable unless exposed to extreme flood conditions. But usually the dikes are built at or near the water surface. In both methods of shore nourishment the disposal pile is usually leveled off with bulldozers after the pumping has ceased. These two different beach nourishment techniques are clearly delineated in profiles

taken after the nourishment: low beach face slopes for the slurry method and a steep beach scarp near the water with the diking method.

Shore Slope Morphology

Several such characteristic coastal features which have been observed and presented in publications (USACE, 1984; Komar, 1976; King, 1972) were found along the shore nourishment beaches of the lower Columbia River. All of the features listed in Table IV are observed along the beaches of the study sites. Examples of beaches with many shore features along the same profile are displayed in Figures 44 and 45, at Wallace Island and Puget Island, respectively.

The shore or bankline profile characteristic of lower Columbia shore nourishments has a set of features, described in Table XIII from shore to river. The sedimentary features present on a shore slope reflect the sediment response to physical processes. Wave actions cut beach scarps and berms. Ship surge cuts beach scarps and carries sediment in the direction of ship motion, constructing accretionary lobes on the lower beach face. Wind generated waves deposit bands of heavy minerals above the high water berm and construct oscillatory ripples on the beach face. Tidal recession of the water surface will behead and sometimes destroy ripples. Ship waves



Figure 44. Beach face on Wallace Island, Oregon. Northwest end of site, looking due east. Note small scarp at right and heavy mineral accumulation along upper beach swash zone. Inclined slope of nourishment pile to far right suggests it has been above highest water (no vertical scarps). Photo: 24JUN88.



Figure 45. Beach face at Puget Island site, looking north from profile 12. Note scarp at far right, suggesting entire beach face is active. Pumice in center is accumulated by

TABLE XIII

DESCRIPTIVE TRANSECT NORMAL TO SHORE SLOPE

<u>Shore Slope Position</u>	<u>Feature(s)</u>
Upper beach	Level (supratidal zone) topography, vegetation, and aeolian dunes Upper Beach Scarp Largest aeolian dune, directly above and shoreward of beach scarp
Beach Scarp Face	Vertical incision into the shore profile Beach Scarp Toe Set of collescing fans ("micro-bajadas"), steep inclined slope, wave cut berm Upper Beach Face Debris zone from wave swash, wave cut berm, heavy mineral banding, slope less than scarp toe, but steeper than beach face
Beach Face	gentle to moderate slope ($1-5^{\circ}$), pumice banding, symmetrical oscillatory ripples with flattened crests and pumice in troughs, planar, smooth sand surfaces. Lower Beach Face Limit of lowest low water elevation, small (2-12cm) berm constructed and maintained by wind generated water waves, oscillatory

TABLE XIII
DESCRIPTIVE TRANSECT NORMAL TO SHORE SLOPE
(continued)

<u>Shore Slope Position</u>	<u>Feature(s)</u>
	ripples in shallow water (.1-1.5m), steepening of slope directly off shore.
Subtidal region	transition from oscillatory ripples parallel to shore to asymmetrical current ripples normal to shore (>1m depths), steepening of slope.

obliterate ripples and deposit planar cross-beds. Wind constructs dunes and ripples above higher high water, and alluvial fans at the base of beach scarps. Ship wave surge, secondary ship wave swash, and wind generated wave swash deposit bands of pumice grains at the upper limit of water actions on the beach face.

Beach scarps were commonly observed, when present, at the shoreward end of a beach profile. Beach scarps along the lower Columbia are often dramatic features, as seen in Figure 46. Vertical beach scarps are a important response to active wave erosion. Beach scarps are most stable when exposed to wave processes, maintaining a near vertical slope. During periods of little or no wave action the slope of the scarp face tends to decrease, taking on the character of a foredune (Komar, 1976) or becoming



Figure 46. Large beach scarp. Scarp is eroding into 1988 Puget shore nourishment at profile 5. Site is apex of 1988 "shore notch," an active site of erosion.

integrated back into the beach face. Beach scarps were observed to form in previously smooth beach faces, such as that presented in Figure 47.

Sediment grain size distribution across a beach face (Puget Island profile 11) is presented in Figure 48. The histogram illustrates weight percents of four samples down the shore slope and shows that the mean grain sizes increase toward the waterline. This is consistent with most of the established relationships in the literature (Muir Wood and Fleming, 1981; Komar, 1976; USACE, SPM, 1984) which have shown that beaches exhibit long-term sorting of grains normal to slope. Sediment grain size coarsens toward the mean water level from both the landward and riverward directions.

The Shore Notch

One geomorphic feature that was not found in any of the published literature reviewed is the "shore notch." The shore notch is a distinct asymmetric incision into the shore slope with an accretionary lobe in the direction of the incision (Figures 49 to 53). The shore notch appears to be the result of ship wave actions and is the locus of much shore erosion.

Water motions in a shore notch appear analogous to, beach cusps. Beach cusps have been observed on a variety of shorelines (Komar, 1976; Dyer, 1986). Cusps and shore

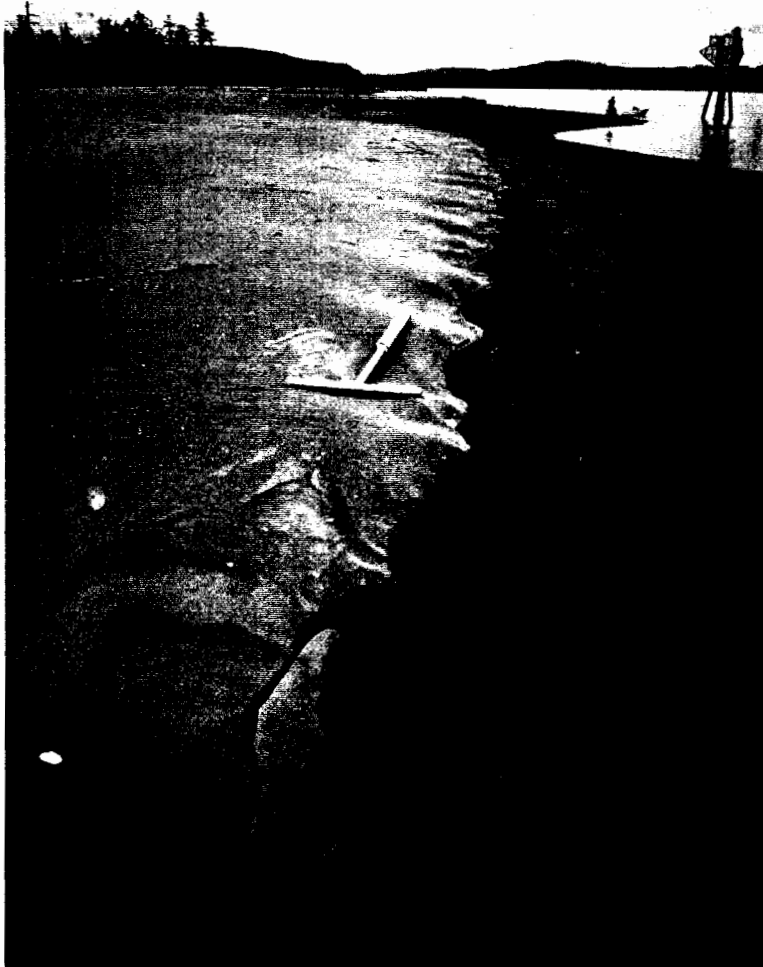


Figure 47. Excellent example of an active beach scarp that has been cut into a previously smooth beach face. Note surface expression of sand above scarp is aeolian, while below is wave swash. Ship wave surge acts similar to wave run-up, attacking the scarp and leading to rapid erosion, as seen in the slump structure near failure in the left foreground. Price Island, 27JUN87.

GRAIN SIZE ANALYSIS, PUGET—JUNE 1987

4 samples, water—shore (100' respec.)

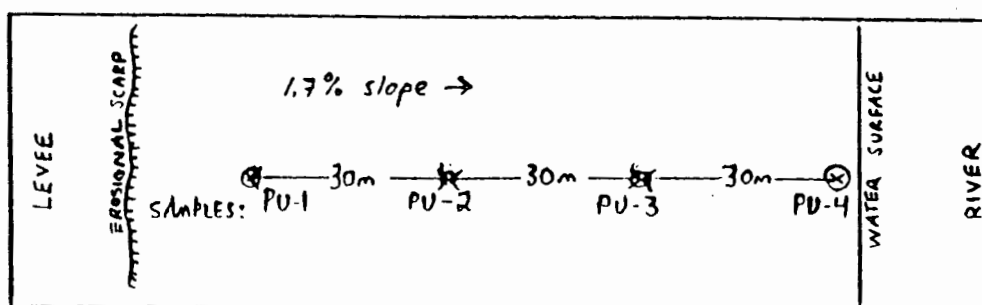
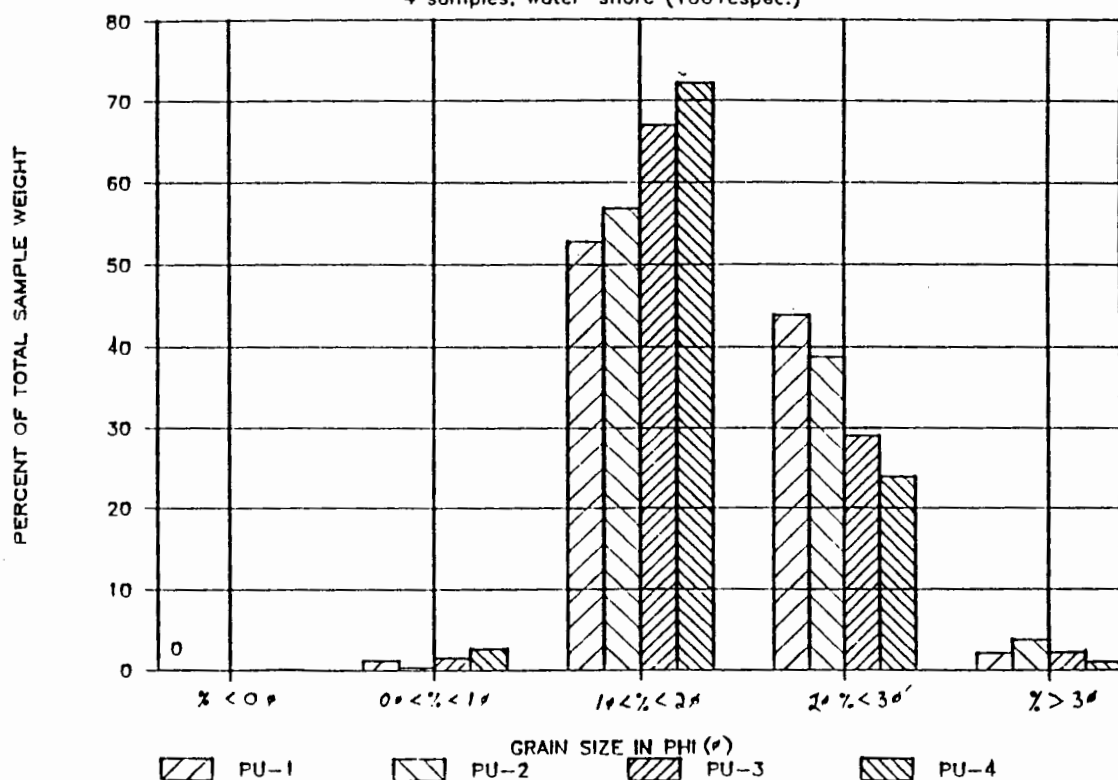


Figure 48. Grain size on a beach face. Grain size variation down a beach face toward the water's edge. Samples are surface grabs on a well developed beach face at the Puget Island site prior to the 1987 nourishment. Note coarser nature and higher kurtosis of sand closest to the water's edge, with fining and lowering of kurtosis of sand population up the beach to samples that have experienced less reworking.

notches are examples of wave refraction over a topographic surface (Komar, 1976; King, 1972; Dyer, 1986). On a low slope beach a spilling wave is refracted so that the wave travels fastest up the cusp valley, or the analogous shore notch, spreads out at the head of the valley, and then travels riverward along the flank of the cusp before dying away. The sediment-laden swash flows along the horns or accretionary lobes, causing them to lengthen. This is apparently the case on the accretionary beach lobes adjacent to the shore notch.

All of the sites profiled, as well as Vista Park, RK WA-54.7 exhibited development of these shore notches. Surge and wave impacts are concentrated at the shore notch.

Figures 49, 50, 51, 52, and 53 all illustrate some of the shore notches observed in this study. Samples were taken at intervals across the 1988 Puget Island shore notch to examine grain size variations (Figure 54). A distinct grain coarsening occurs approaching the apex of the shore notch, as presented in the variation of mean grain size parallel to the shoreline across the shore notch (Figure 55). This grain size distribution corresponds to the distribution of the wave energy across the shore notch. Figure 56 presents a schematic drawing of the relative magnitude of water motions during wave assault at a shore notch. A profile was run parallel to the shoreline at the 1987 Puget Island shore notch to evaluate erosion and



Figure 49. 1987 Puget Island shore notch.
Viewed from profile 14, looking north.



Figure 50. Vista Park (RK WA-54.7) shore notch. Note coarser grains accumulating in the notch where the magnitude of incident energy is greatest, and dissipates downstream, resulting in deposition. Thus large grains settle first, closest to the notch, August 26, 1987.



Figure 51. 1988 Puget Island shore notch.



Figure 52. 1988 Puget Island shore notch. Notch developing at profiles PU-4 to PU-8. Looking north-northwest at accreting lobe of beach downstream of notch, June, 1988.



Figure 53. Puget Island shore notch. Looking north, up apex of 1988 notch. Note runnels at base of steep upper beach face below the active beach scarp at the upper right, June 9, 1988.

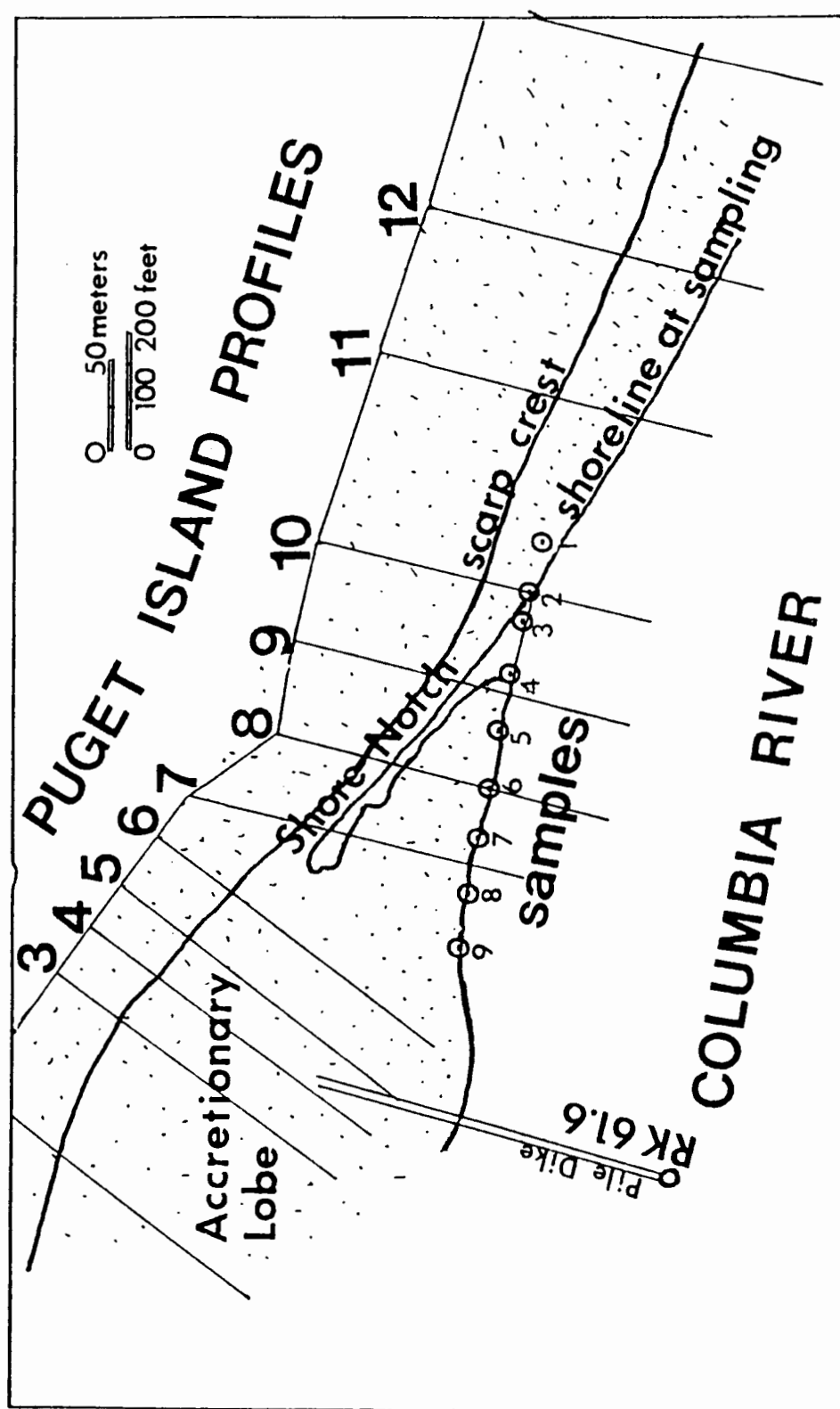


Figure 54. Sample locations. Grain size variation across shore notch (Figure 55).

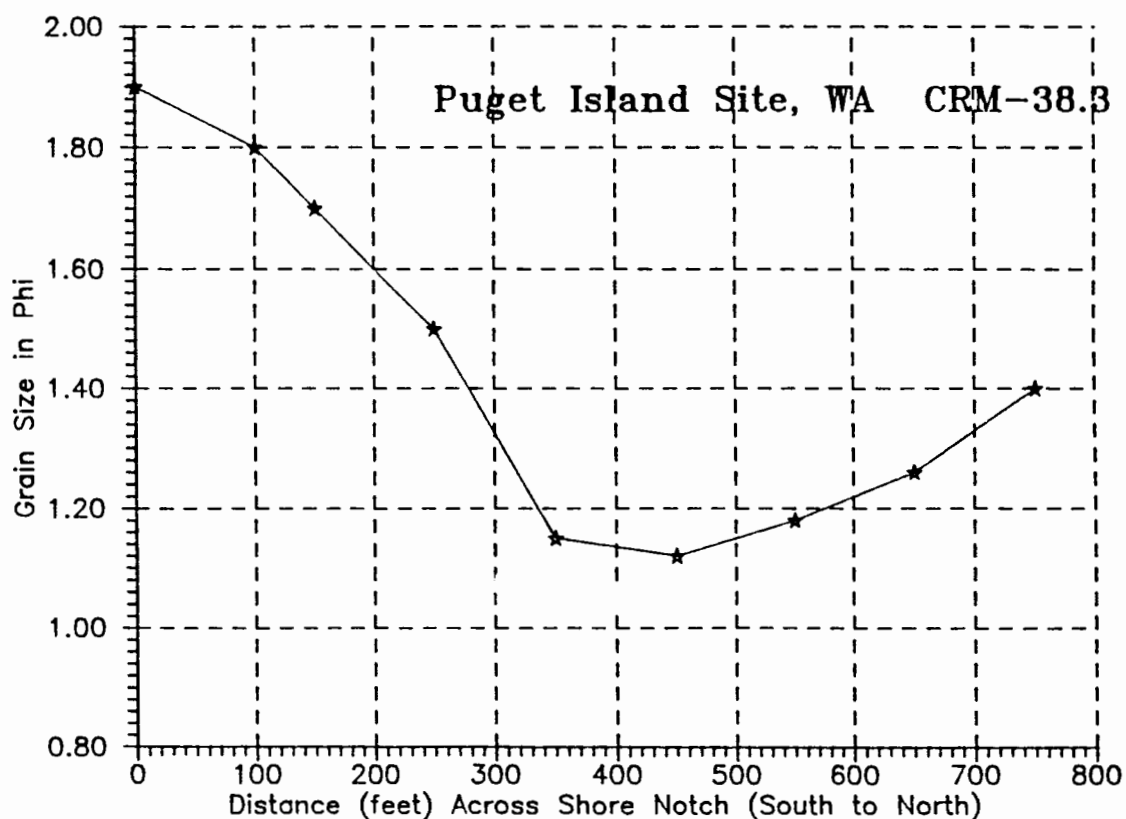


Figure 55. Mean grain size across shore notch. Surface samples taken across an active shore notch (1988 Puget Island site). Graph shows distinct coarsening trend moving across the shore notch. Sample locations are presented in Figure 54.

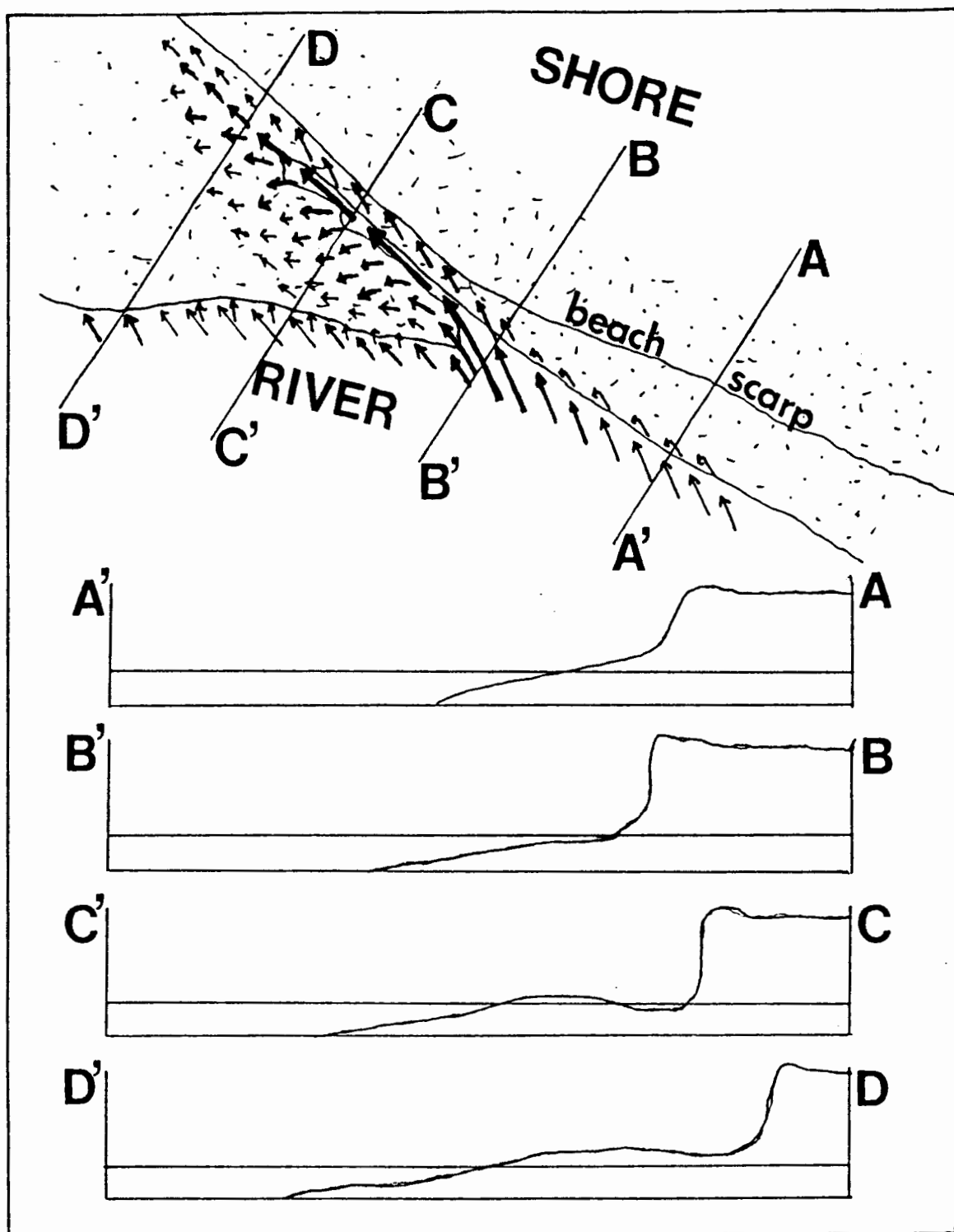


Figure 56. Water motions at a shore notch. Relative magnitude of water motions during wave assault a shore notch and schematic profiles across the shore notch.

accretion. The results of changes seen in one week are presented in Figure 57. Figure 58 shows the accretionary lobe of the 1987 Puget Island site shore notch in the foreground and the zone of accelerated erosion to the upper left.

The headward erosion of a shore notch and deposition of adjacent accretionary lobe was seen in profiling at the 1987 Puget Island shore notch (Figure 57). A breakwall structure at the Puget site made of 5cm * 25cm * 3m wood planks was installed by the landowner with a residence next to the active shore notch. The structure was partially effective in retarding erosion by allowing sediment to accrete on its shoreward side, also providing evidence of a northward longshore drift of sand (in the direction of the notch). The 1987 Puget Island shore notch was buried by a shore sand disposal operation the last week in June, 1987. A new notch developed approximately 300 meters north of this location.

A simple derivation of the volume loss in a unit cell section of the 1987 shore notch produces the following estimations.

$$\begin{aligned}
 &8.5 \text{ (m}^2\text{*m width)}/7 \text{ days} = 1.2 \text{ m}^2\text{*m/day} \\
 &1.2 \text{ m}^2\text{*m/day} * 365 \text{ days} = 443 \text{ m}^2\text{*m/yr} \\
 &443 \text{ m}^2\text{*m/yr} * 10 \text{ m width of shore notch} \\
 = &4,430 \text{ m}^3 \text{ of sand eroded by shore notch and moved} \\
 &\text{onto accretionary lobe.}
 \end{aligned}$$

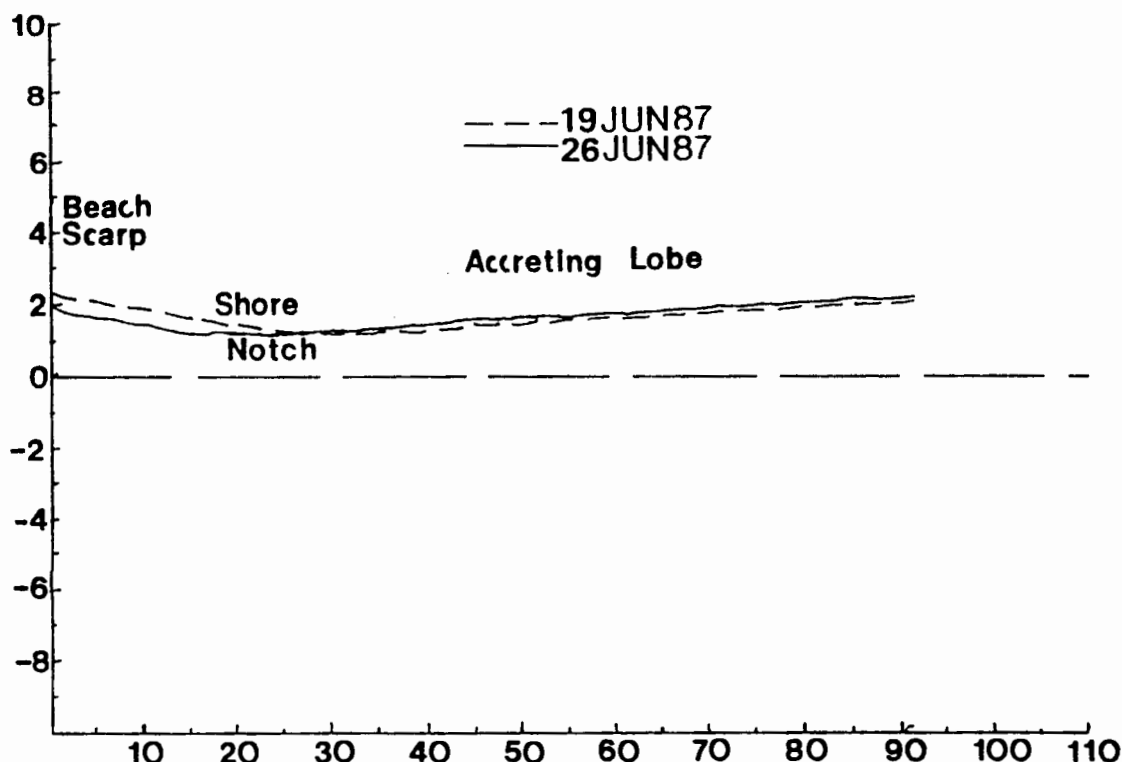


Figure 57. Profiling 1987 Puget Island shore notch. Profiles parallel to shoreline, across the shore notch. Headward erosion is moving upstream.

This estimate of sand transferred from the nourishment to the beach face at the shore notch over a one year period would be equivalent to 17 percent of the sand loss recorded at the Puget site in 1987-1988 (26,197 m³).

Sedimentary Structures

Observation of sedimentary structures can aid in describing a depositional environment and in determining sediment response to the primary physical processes. The sedimentary character of deposits at shore notches can be

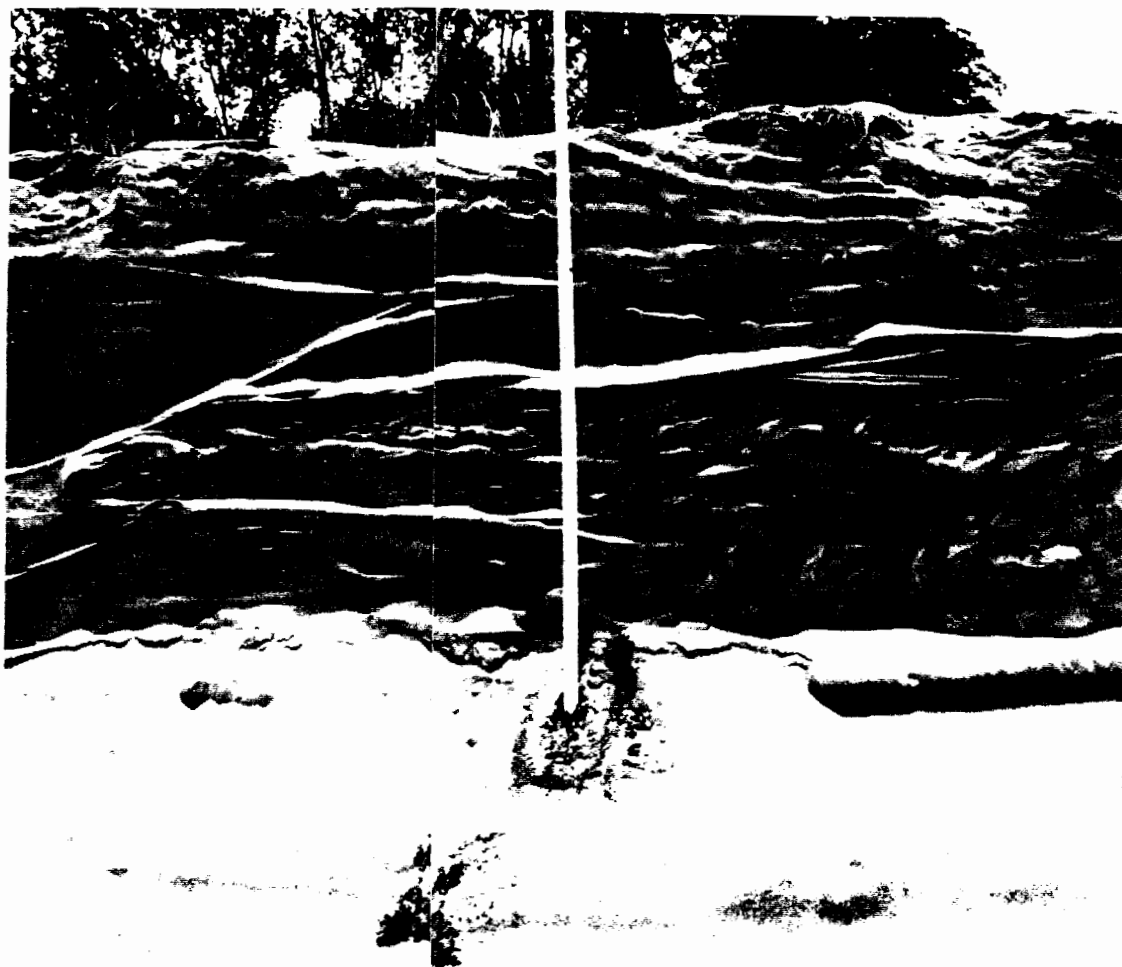


Figure 58. Trough cross-bedding. Trough cross-bedding revealed in beach scarp is characteristic of pipeline sand disposal. Same pattern is exhibited normal to this cut. Puget site profile 10, 17JUN88.63

ascertained by observing exposed sections or by trenching the beach.

The original shore nourishment deposit has a characteristic trough cross-bedding as displayed in the beach scarp of Figure 58. These bedding structures

distinguish the original nourishment from deposits of subsequent reworking. Figure 59 presents a three facies assemblage in the scarp toe cross-section of Puget profile PU-10. Swash lamination can be seen in the top eight cm of the upper beach face trench displayed in Figure 60. Swash laminae are underlain by cross bedding of the original nourishment. The recent nourishment deposition is underlain by low angle planar bedding of the previous beach face. This buried beach shows distinct mineral separation, rippled units, and reactivation surfaces.

Beach features observed at the lower Columbia study sites are presented in Appendix B and are similar to sedimentary structures found in wave and tidal deposits (Reading, 1978; Scholle and Spearing, 1982; Blatt and others, 1980; Araya-Vergara, 1986).

Distinct beheaded ripples (flattened crests) are found in the intertidal zone of the beach face. The ripples are created on the shore slope during high water periods by wind generated waves. As the water level proceeds to lower, wave actions (swash) at the shore-water interface obliterates the ripple crests. The faster the drop in the water level, the better preservation of the ripple forms and as the rate of water elevation change slows (low tide) all ripples are destroyed. Thus ripple preservation is a function time (relative to the tidal curve), wind waves, and ship waves. If a ship passes



Figure 59. Three shore sedimentary facies.



Figure 60. Shore stratigraphy. Riverward of beach scarp. Note reactivation surfaces on oscillatory wave ripples (middle of section) in stratigraphy (characteristic of tidal environment) and heavy mineral laminae (characteristic of tidal peaks).

during the period between a high tide and low tide, the ship waves destroy all of the ripples, precluding preservation. Figure 61 shows a rippled beach at the Puget site and Figure 62 shows the same spot less than one minute later, after one set of ship waves assaulted the beach. Thus considering ships pass a rate of about ten per day (USACE, 1979-1985), it is the norm that the beheaded ripple facies will be destroyed and not be preserved. This is supported by sedimentary sequences observed in shore trenches. The fact that ripples commonly form on shore slopes, but are rarely preserved provides geomorphic evidence of the significant role of ship waves on the shore slopes. Only one rippled bedding surface is preserved in stratigraphic sequence of the trench presented in Figure 59. Measurements of laminae thickness in the upper beach face trench are presented in Appendix B.

Trenches also reveal the stratigraphic character of other distinct environments, such as a tidal flat at the north end the Puget Island site, shown in Figures 63 and 64. Tidal flats characteristically exhibit features such as hummocky bedding; laminae of mud/clay settling out in within troughs; and very low angle shore slopes (Reading, 1978; Scholle and Spearing, 1982). Trenches in the tidal flat reveal settling structures (convolute bedding resulting from differential pore pressures instigated by tidal changes in water level) and pumice swash deposits



Figure 61. Rippled lower beach face. Puget Island, 1988.



Figure 62. Beach face after ship waves. Same exact site as 61, less than 2 minutes later after ship wave assault on the beach face. Ripples are rarely preserved on beach face and in the stratigraphy probably because of the frequency in which ships pass.



Figure 63. Tidal terrace at low tide. Accretionary beach lobe at northern end of Puget Island site. 02AUG88, looking south.

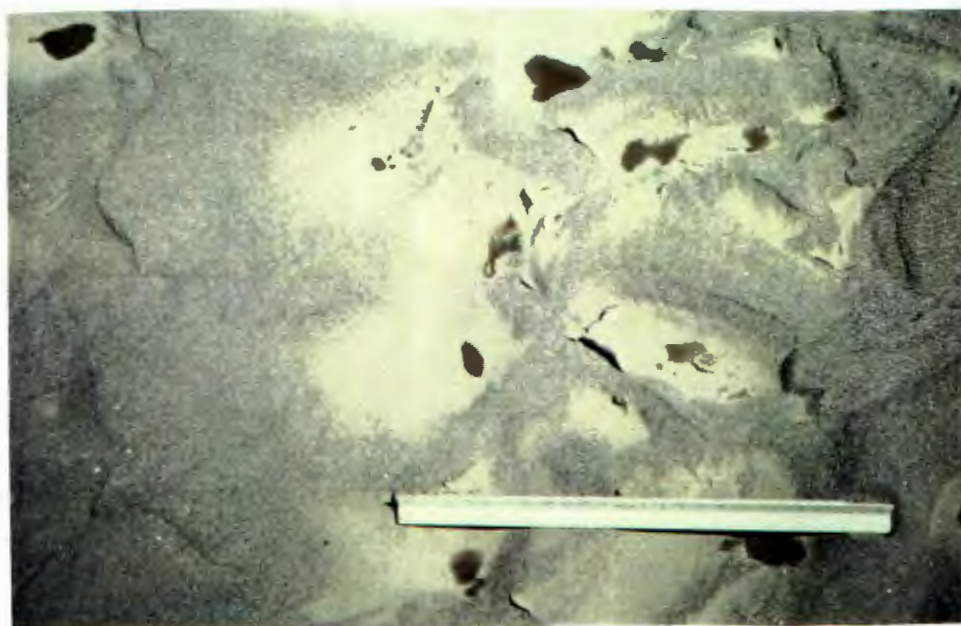


Figure 64. Tidal terrace bedding surface. Same location as 63, this irregular, cusate trough bedding surface with clay laminae is suggestive of the fluctuating water elevations associated with a tidal environment.

(resulting from wave surge) in the stratigraphy, as seen in Figures 65 and 66.

PHYSICAL FACTORS/PROCESSES

Water Level Fluctuations

Water level changes were derived by linearly interpolating data received from the NOAA tide gauges at Skamokawa, Washington (RK 55) and Wauna, Oregon (RK 72). Water elevations recorded during days on which ship waves were monitored are presented in Table XIV. Flood elevations have been extrapolated by the U.S. Army Corps of Engineers (1988d). Flood events have been well established in coastal science and engineering as a mechanism which enables wave energy to be delivered to the shoreline on an elevated water surface platform (Komar, 1976; MuirWood and Fleming, 1981; USACE, 1984). This action increases the volume of sediment reservoir potentially available to erosion. Floods also bring higher current velocities that can potentially create boundary shear sufficient to cause bank erosion (Dunne and Leopold, 1978). Flood events vary from 3.3 to 4.0 meters above the Columbia River Datum (CRD), as displayed in Figure 67. Geomorphic forms such as beach scarps are indicative of the highest high water elevation on an eroding shore.



Figure 65. Tidal terrace trench. Puget Island, 02AUG88.



Figure 66. Tidal terrace stratigraphy. Convolute bedding, overlying planar bedding more characteristic of a wave dominated beach face.

TABLE XIV

WATER LEVELS AT PUGET ISLAND SITE

Measured on days of ship wave monitoring.
Elevations above National Geodetic Vertical Datum (NGVD)

<u>Date</u>	High High Water (m)	Low Low Water (m)	Tidal Range <u>dZ(m)</u>
09-15-87	1.13	-0.53	1.66
09-16-87	1.30	-0.40	1.70
09-17-87	1.12	-0.60	1.72
09-18-87	1.30	-0.53	1.83
10-29-87	1.67	-0.57	2.24
10-30-87	1.67	-0.57	2.24
06-08-88	1.70	-0.27	1.97
06-09-88	1.93	-0.20	2.13
06-13-88	1.80	-0.63	2.43
06-14-88	1.83	-0.60	2.43

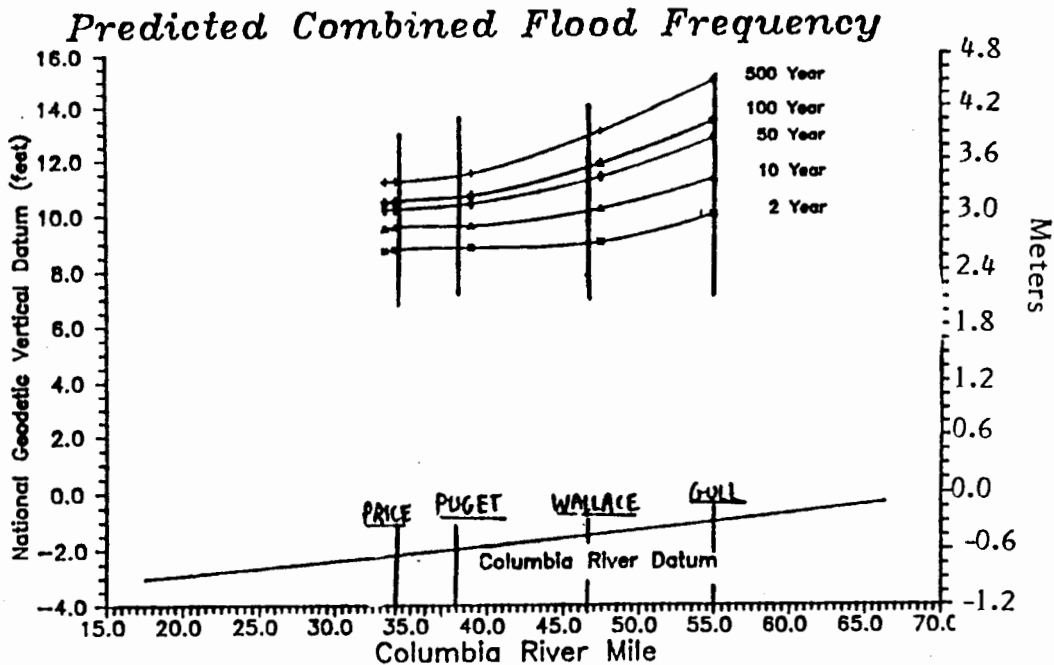


Figure 67. Combined flood frequency. Lower Columbia River. NGVD (1 ft = .3048 m) versus Columbia River Mile (CRM, 1 mi = 1.61 km). Columbia River Datum (CRD) is given for reference (Navigation channel depth is maintained in reference to the CRD).

Channel Geometry

The geometry of a river channel will directly control velocity regimes, ship waves, and wave decay, reflection, and refraction along the shore. Figure 68 presents the channel cross-section of the Columbia River adjacent to the Puget Island site. Table XV presents the variation in lower Columbia river channel size based on thirty-one cross-sections from River Kilometer 59.9 to 102.3.

Describing flow in a channel must account for the channel boundaries. A small fraction of river's boundary is the region was examined. The channel morphology

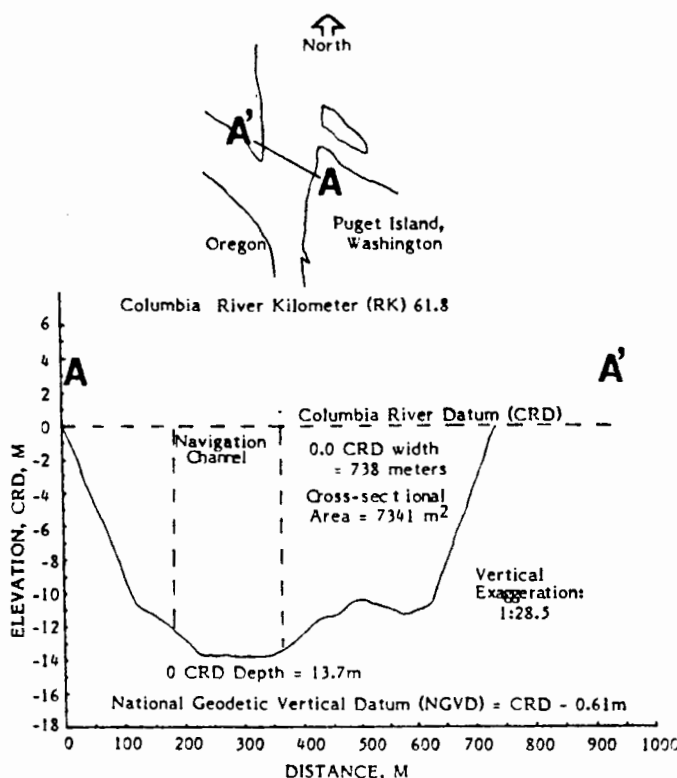


Figure 68. Columbia River cross section at Puget Island site. Data for cross section is from January 13, 1988 bathymetry by the U.S. Army Corps of Engineers, Portland District.

directly affects the hydraulics of both flow velocities and ship waves. When channel cross-sectional area increases, flows tend to decrease (illustrated in historical bathymetric maps of the river), a relationship presented quantitatively in Mannings Equation (2):

$$V = C_m / n * A * R^{0.75} * S^{0.50} \quad (2)$$

where:

- C_m = 1.0 (SI units)
- R = A/P (hydraulic radius)
- P = wetted perimeter of channel
- A = cross sectional area of channel

TABLE XV
COLUMBIA RIVER CROSS-SECTIONS
River Kilometers 59.9 to 102.3

Surface width of channel at 0 CRD

n	=	31
n_{\max}	=	564 m
n_{\min}	=	206 m
μ	=	377 m
m	=	381 m
σ	=	92 m
R	=	358 m

Cross-sectional area at 0 CRD

n	=	31
n_{\max}	=	11,260 m ²
n_{\min}	=	6,612 m ²
μ	=	8,889 m ²
m	=	8,927 m ²
σ	=	1,171 m ²
R	=	4,648 m ²

where n = number of sections

μ = mean of sections

m = median of sections

σ = standard deviation

R = range of values

w = surface width of river

- V = average velocity
n = absolute roughness coefficient
S = slope of channel bottom

Ship wave magnitude will be dampened with channel cross-sectional area (Sorensen and Weggell, 1984; Brebner and others, 1966; Johnson, 1968). The confluence of the main river channel with the Clifton Channel west of the northwest end of Puget Island increases the cross sectional area of the river, decreasing water velocities and resulting in a region of historical shoaling.

The threshold of sediment motion is partially a function of water velocity, as presented in the Hjulstrom curve (Hjulstrom, 1939) shown in Figure 69. Flow velocities are a function of channel geometry, discharge, water surface slope, and tide.

WIND

Winds in the study region builds dunes up to several decimeters in height and sort sand grains. Examination of dunes suggest that winds predominantly blow from the west, northwest. Average monthly wind velocities gaged at Astoria, Oregon between 1941 and 1976 show a two dominant wind directions; from the west, northwest in the spring and early summer; from the east, southeast in the fall and winter (Table XVI). The annual mean wind velocity at Astoria, Oregon is 3.75 m/s. Using this mean velocity

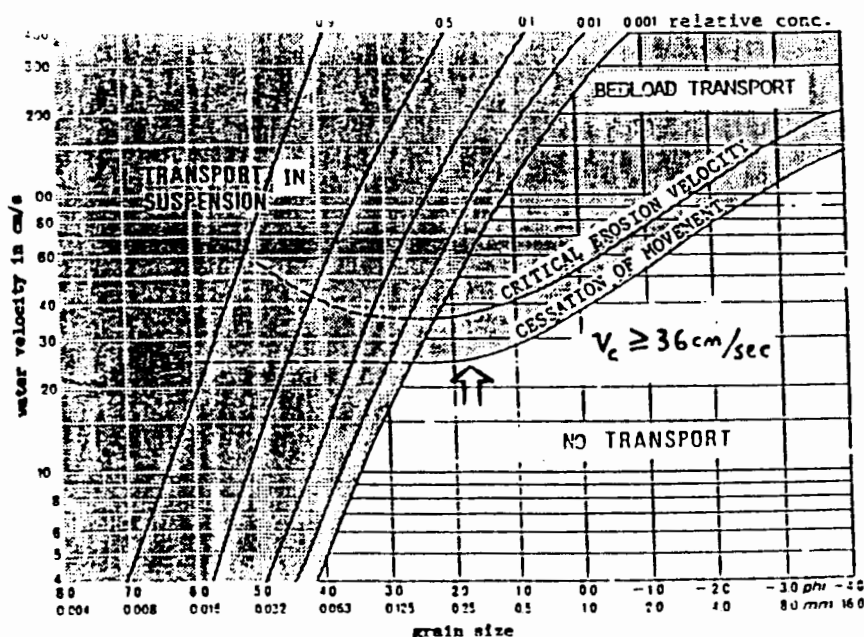


Figure 69. Hjulstrom (1939) Curve for estimating critical threshold velocity of quartz grain (sp. gr. 2.65) for range of grain sizes (Sundborg and Norrman, 1963).

estimated mean annual surface current generated by wind shear at the surface of the water is 0.11 m/sec, producing near bed velocities well below the threshold of sand.

Table XVII presents orientations of dunes recorded the summer of 1988 at the Puget Island site, which consistently presented evidence of a dominant westerly or northwesterly wind direction (blowing from the west/northwest).

Dune crests are composed of distinctly coarser grains than dune troughs. The coarser grains generally are too large for existing wind shear whereas the small grains can be more easily moved. The small grains migrate to areas of decreased wind shear (conditions below threshold).

TABLE XVI
AVERAGE WINDS AT ASTORIA, OREGON

<u>Month</u>	<u>Prevailing Direction</u>	<u>Velocity (m/sec)</u>
January	E	4.20
February	ESE	3.93
March	SE	3.98
April	WNW	3.84
May	NW	3.75
June	NW	3.66
July	NW	3.75
August	SE	3.49
September	SE	3.26
October	SE	3.35
November	SE	3.75
December	ESE	4.07

(Beeman, 1985)

TABLE XVII
 SYMMETRICAL EOLIAN DUNE ORIENTATIONS
 Puget Island Site, July 31, 1988

<u>Crest Azimuth (deg)</u>	<u>Transport Azimuth (deg)</u>
1	91 (east)
3	90 (east)
350	80 (east)
0	90 (east)
356	86 (east)
4	91 (east)
14	104 (east)
359	89 (east)
355	85 (east)

Selective transport of the fines leaves concentrations of coarse grains (dune crests). Dune troughs are sheltered from the wind and thus host the finer grain sizes.

Wind Generated Water Waves

Wind generated water waves can be predicted using established theory and empirical relationships (USACE, 1984). The dominant easterly winds (tables XVII and XVIII) that occur from the early Fall (August) to early Spring (March), have a mean velocity of 3.7 m/s. The effective wind stress is derived using the empirical expression presented in Equation (3) (USACE, 1984):

$$U_A = 0.71 U^{1.23} \quad (3)$$

where: U_A = wind shear stress velocity

U = wind velocity (m/s)

The above expression can be used in Equations (4) and (5) with a known shallow water depth (constant in theory) and a fetch distance to estimate significant wave height and period.

$$[gH/U^2] = 0.283 \tanh[0.530 (gd/U^2)^{3/4}] * \tanh\{[.00565 (gF/U^2)^{1/2}] / \tanh[.530 (gd/U^2)^{3/4}]\} \quad (4)$$

$$[gT/U] = 7.54 \tanh[.833 (gd/U^2)^{3/8}] \tanh\{[.0379 (gF/U^2)^{1/3}] / \tanh[.833 (gd/U^2)^{3/8}]\} \quad (5)$$

Southeasterly winds at the Puget Island site blow right off the island and thus are assumed to have negligible effect on the generation of water waves at the site. The fetch from the Northwest at the Puget Island site is approximately 1.6 kilometers and an average depth of 25 to 30 feet. The predicted significant wave height (wave height that is greater than 2/3 all waves) is 7 cm and has a period of 1.04 seconds. Ofuya(1970) used wind wave data to estimate the annual energy delivered to a shoreline in ft.lbs/ft of shoreline with Equation (6):

$$W_w = (10 * [(H_s^2 T_s)_n (T_d)_n]_q) / (DY * 24) \quad (6)$$

where: $q = 1, 2, \dots, q$ represents the wind directions
N, NNE, NE, etc.

$n = 1, 2, \dots, n$ represents the wind speed
class, i.e. 1 mph (mile per hour), 2
mph, etc. at the given site.

H_s = significant wave height

T_x = significant wave period

DY = number of days this wind occurs

W_w = energy prorated (work done) to the shore
per hour.

For the Puget site, the above equation is used
with the following variables:

$$q = 1$$

$$n = 1$$

$$H_s = 0.23 \text{ ft } (.07\text{m})$$

$$T_s = 1.04 \text{ sec}$$

$$T_d = 86,400\text{sec } (24 \text{ hrs})$$

$$\text{DY} = 155 \text{ days}$$

Thus $W_w = 47,534 / (155 * 24) = 12.8 \text{ ft.lbs/ft of shoreline or}$
56.9 Newton-meters/meter. This derivation used a DY value
of five months, a conservative value based on the wind data
presented in Table XVII.

Assuming the following criterion:

$$U \text{ (wind velocity)} = 3.7 \text{ m/s}$$

$$d \text{ (depth)} = 9.1 \text{ m}$$

$$F \text{ (fetch)} = 1.6 \text{ km}$$

$$H_s \text{ (sig. wave height)} = .07 \text{ m}$$

$$T_s \text{ (sig. wave period)} = 1.04 \text{ sec}$$

and using Equation (7) for energy flux, P_{lb} (USACE, 1984):

$$P_{ls} = ((pg)/16) H_{sb}^2 C_{gb} \sin(2\alpha_b) \quad (7)$$

where: C_{gb} = wave speed = 0.62 m/s

$$H_{sb} = \text{sig. breaking wave height} = 0.07 \text{ m}$$

$$\alpha_b = \text{wave incidence} = 10^\circ$$

$$P_{ls} = 6.34 \times 10^{-4}$$

Using the empirical expression (8), derived from the data of Bruno and others (1981, IN: USACE, 1984):

$$Q \text{ (m}^3\text{/yr)} = 1290 \text{ (m}^3\text{-s/N-yr)} P_{ls} \text{ (J/m-s)} \quad (8)$$

$$Q = 0.82 \text{ m}^3\text{/yr} = \text{annual longshore transport flux}$$

This derivation suggests that longshore transport due to wind waves at the Puget Island site is negligible.

Effect of Wind on Beach Morphology

Wind is the secondary eroding agent (next to water actions) of beach scarps. The rate of work done by the wind directly control the scarp's slope when it is not exposed to water. Water actions cut into the upper beach creating a beach scarp and moving sediment out onto the beach face, leaving a near vertical incision on the beach. Wind actions will rapidly modify this vertical scarp by blasting the scarp's face and sending grain flows streaming down the scarp to coalesce into "micro-bajadas" or miniature alluvial fan forms on the beach face, illustrated in Figure 70. The rapid work of wind was illustrated by a simple experiment in which a vertical cut was made into a beach well above high high water (thus precluding any water actions from affecting the cut). same site two days later and Note the distinct "micro-hoodoo" type pillars of sand that form and the coalescing fans at the slope's base. The



Figure 70. Eolian slope, beach scarp. Wind build distinctive fan like deposits which coalesce to form "micro-bajadas", such as ones at bottom of the photograph, forming at most recent beach scarp. Wallace Island site, June 24, 1988.

experimental scarp was surveyed immediately after it was cut and again in two days, the result is presented in Figure 71. Fan deposits rapidly developed at the scarp toe. Rapid slope development occurs at a the beach scarp when exposed to wind actions. The distinctive dune above the artificial beach scarp (Figure 71) is a characteristic eolian feature on the shorelines that hosted large beach

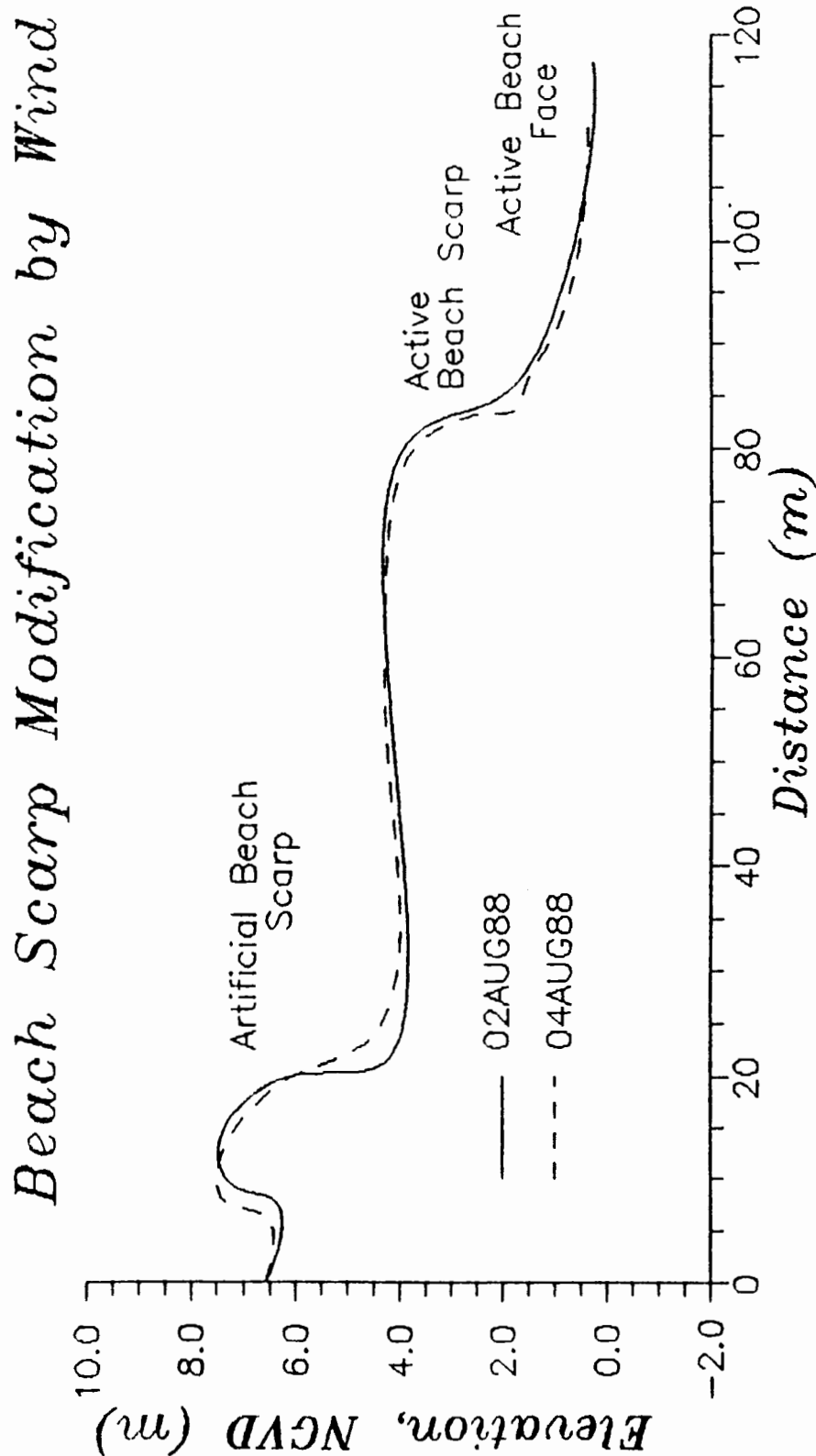


Figure 71. Puget Island profile 4. After 1988 nourishment to examine the changes at a large beach scarp due to wind, between August 2 and August 4.

scarps. This experiment suggests that the vertical slope of west facing beach scarps along the Columbia is a shore lived phenomena without repeated exposure to water actions.

Background River Hydraulics

A current trend in coastal, estuarine, and fluvial studies is mathematical model simulations of the hydraulic system. The present state of mathematical models is such that they must be used with care in evaluating and predicting a system. This is especially true in a tidal environment of flow reversals, as shown by Roovers and others (1981) in an analysis of sedimentation in an estuary/harbor along the coast of Belgium. The region exhibits high current velocities of up to approximately 1.50 m/s during spring tides. The sediment is fine sand and silt. In the Columbia River Estuary the conditions have some similarity. Material transport in these types of systems is considerable and morphological instability appears quickly when changes occur in the hydraulic regime (Roovers and others, 1981). Calculation of sediment transport by currents is prone to considerable variance from the real system, especially when tides come into play, where calculations are very sensitive to minor changes or inaccuracies (Roovers and others, 1981). The five cm/s error in the analysis of Roovers and others (1981) can result in a complete reversal of the erosion and

sedimentation pattern. This can be critical in analysis when the flood (upstream flow) stream is 1.0 m/s and the ebb (downstream flow) stream 0.9 m/s, the difference being only 10 cm/s. Transport in tidal environments is attributed to the "differential" or difference between the two quantities, flood and ebb flows.

Modeling has been done in the Columbia Estuary and the Price Island-Puget Island regions, using a two dimensional vertically integrated numerical model RMA-2 (TABS-2) for open-channel flow and sedimentation (Sedimentation Section, Portland District, USACE, 1986-1988). This model has been used by the Portland District of the Corps of Engineers in evaluating hydraulic patterns with and without structural controls such as pile dikes and submerged groins. The model is used in this study to estimate channel current velocities, for a prototype discharge and tide. Using prototype data from June 1986, the model predicted a maximum flood current of about 0.61 m/s (2 ft/s) and a maximum ebb current of about 1.22 m/s (4 ft/s). Figure 72 plots water elevation and velocities (mid channel and near Puget boundary) predicted by the model in the main channel of the Columbia adjacent to the Puget Island site using prototype data from June 1986 (discharge of about 8,500 m³). The lag is a function of the river's changing surface profile. When a equilibrium of the currents upstream and downstream of the site is reached

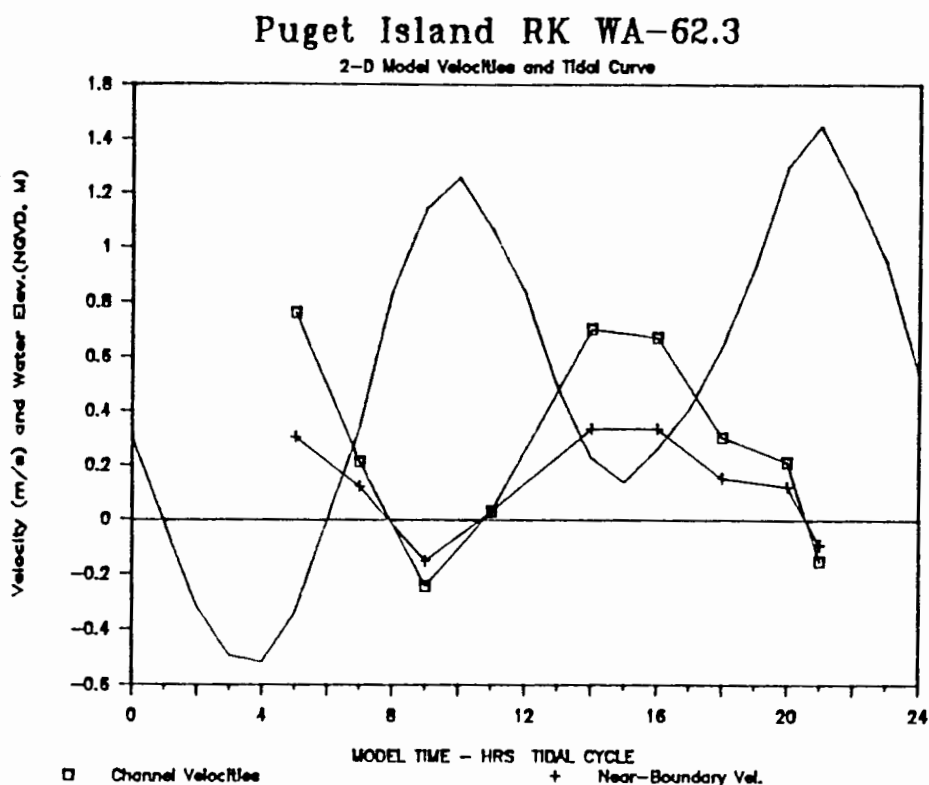


Figure 72. Model results of ebb flows. Plot of tidal curve, mid-channel, and near-boundary vertically integrated velocities at the Puget site, as predicted by the two dimensional model RMA-2.

then slack water will be obtained. Because the model runs were based on one set of daily current data, the true velocities could vary significantly. Nearshore surface velocities done provide estimates of currents in shallow water. The model can supply approximate conditions and responses in the channel, but becomes much less reliable in the shallow near shore area where processes other than tidal and freshwater currents become the controlling

factors. For a more complete discussion of model results, refer to Eriksen (1989).

SHIPS

The ships examined in the study cover a variety of vessel types, presented in Table XVIII.

The total number of ships drafting 6 meters or more moving transiting the lower Columbia is between 3,000 and 3,700.

Predicting Ship Wave Height

Several empirical methods have been published to predict secondary ship wave size (Saunders, 1975; Sorensen and Weggell, 1984). The solutions for ship wave predictions presented by Saunders (1975) and Sorensen and Weggel (1984) and Barrass's (1979) solution for ship squat to compare with measured wave heights and drawdowns, respectively, made in this study (Appendix C). Squat is the lowering of the water surface adjacent to a ship relative to the existing water surface, bringing the ship closer to the channel bed. Drawdown is the lowering of the water surface along the shore as a ship moves by. It is assumed that ship squat is the driving mechanism instigating drawdown along the shoreline, thus it should be of a greater magnitude than drawdown.

Equations (9 - 14) present the set of derivations presented by Sorensen and Weggell (1984) based on field

TABLE XVIII
SHIP PASSAGES

<u>Ship Type</u>	<u>Number of Passages*</u>
o Bulk Carriers	10
o Container Vessels	2
o Tankers	3
o Car Carriers	1
o Naval frigates	5
o Naval destroyers	1
o Naval supply ships	2

*Note: Observed passages only for this study and are not representative of total shipping on the lower Columbia River. Only some of these ship events were also analyzed for sediment transport.

data collected by Sorensen (1973) and further calibrated using laboratory data of Das (1969) by Sorensen and Weggell (1984). Variables were converted into dimensionless units using a denominator of volume (L^3 ; L =length units); the ship's displacement.

H = ship generated wave height (L)

d = water depth (L)

x = distance to sailing line (L)

V = ship velocity (L/T)

SD = ship displacement (L^3)

SL = ship length (L)

SB = ship beam (L)

SS = ship draft (L)

L = length units

T = time units

Dimensionless Variables as defined by Sorensen and Weggell (1984) are listed below:

$$\begin{aligned}
 F &= V/(gd)^{0.5} &&= \text{Froude number} \\
 H^* &= H/SD^{0.33} &&= \text{dimensionless wave height} \\
 x^* &= x/SD^{0.33} &&= \text{dimensionless distance from sailing line} \\
 d^* &= d/SD^{0.33} &&= \text{dimensionless depth} \\
 SL^* &= SL/SD^{0.33} &&= \text{dimensionless ship length} \\
 SB^* &= SB/SD^{0.33} &&= \text{dimensionless ship beam} \\
 SS^* &= SS/SD^{0.33} &&= \text{dimensionless ship draft}
 \end{aligned}$$

Equation (9) is the general expression to predict ship wave height is (Sorensen and Weggell, 1984):

$$H^* = \alpha x^{*n} \quad (9)$$

where $n = \beta (d^*)^\delta$

$$\beta = -0.225F^{-0.699} \quad 0.20 \text{ .LE. } (F) \text{ .LE. } 0.55$$

$$\beta = -0.3420.55 \text{ .LE. } (F) \text{ .LE. } 0.80$$

$$\delta = -0.118F^{-0.356} \quad 0.20 \text{ .LE. } (F) \text{ .LE. } 0.55$$

$$\delta = -0.1460.55 \text{ .LE. } (F) \text{ .LE. } 0.80$$

$$\log \alpha = a + b(\log(d^*)) + c(\log^2(d^*)) \quad (10)$$

$$a = -0.6F$$

$$b = 0.75F^{-1.125}$$

$$c = 2.653F^{-1.95}$$

The final calculated value of (H^*) was corrected (Sorensen and Weggell, 1984) to measured model values (Das, 1969)

using the following linear equations dependent on the model hull configuration:

Box Hull:

$$H^*_{\text{mea}} = 2.427H^*_{\text{calc}} - 0.0728 \quad (11)$$

Cruiser (Broad beam):

$$H^*_{\text{mea}} = 3.158H^*_{\text{calc}} - 0.1105 \quad (12)$$

Mariner (most streamlined):

$$H^*_{\text{mea}} = 0.835H^*_{\text{calc}} - 0.0225 \quad (13)$$

The derivation for ship wave height presented by Saunders (1975) is presented in Equation (14):

$$H = kw[(B/LE) * (V^2/2g)] \quad (14)$$

where: kw = coefficient (used 1.0)

SB = ship beam

LE = distance from bow to midbody

V = ship velocity

g = acceleration due to gravity

Terms for Table XIX:

H1 = wave height predicted without linear correction (Sorensen & Weggell, 1984)

H2 = wave height predicted (Saunders, 1975)

H3 = measured wave height , m = meters, others defined above

The results of these ship wave prediction calculations are presented in Figure 73. Observed drawdown sometimes (though uncommon) exceeded predicted drawdown

TABLE XIX

CALCULATED VALUES OF SECONDARY SHIP WAVE HEIGHT

<u>Ship</u>	<u>SD</u>	<u>F</u>	<u>n</u>	<u>α</u>	<u>H*</u>	<u>H1</u>	<u>H2</u>	<u>H3</u>	<u>Hull</u>
Ocean Beauty	16636	.46	-.43	.064	.024	.61	.34	.27	C
Chevron Oregon	37602	.27	-.68	.015	.004	.13	.13	.17	C
Magnolia	30127	.37	-.53	.040	.013	.41	.24	.38	C
Kee Lung	22612	.41	-.41	.050	.018	.49	.30	.15	C
Luna II	33381	.37	-.53	.042	.014	.45	.26	.31	C
Lake River	38815	.42	-.49	.064	.024	.81	.30	.16	C
Leandros	34446	.36	-.51	.039	.014	.45	.22	.15	C
European Highway	12437	.35	-.52	.025	.007	.17	.26	.30	C
Coast Range	27685	.38	-.52	.042	.014	.42	.25	.11	C
Ocean Jade	28950	.28	-.65	.015	.004	.12	.14	.28	C
Verrazano Bridge ¹	18176	.38	-.50	.037	.012	.31	.21	.19	C
Verrazano Bridge ²	31638	.40	-.50	.052	.018	.58	.23	.61	C
Indah Fuji	16714	.40	-.48	.043	.014	.37	.30	.19	C
USN Chandler	6210	.38	-.48	.029	.008	.15	.17	.21	M
USN Ford	2750	.42	-.42	.038	.011	.16	.21	.42	M
USN Thach	2750	.37	-.46	.024	.006	.09	.17	.08	M
USN Gray ¹	3011	.41	-.43	.035	.010	.15	.22	.43	M
USN Gray ²	3011	.34	-.49	.018	.004	.06	.15	.36	M
USN Ramsey	2640	.38	-.45	.027	.007	.10	.27	.38	M
USCG Boutwell	3050	.42	-.43	.038	.011	.16	.24	.34	M
USCG Iris	935	.31	-.49	.012	.002	.02	.23	.23	C

¹ = inbound ² = outbound

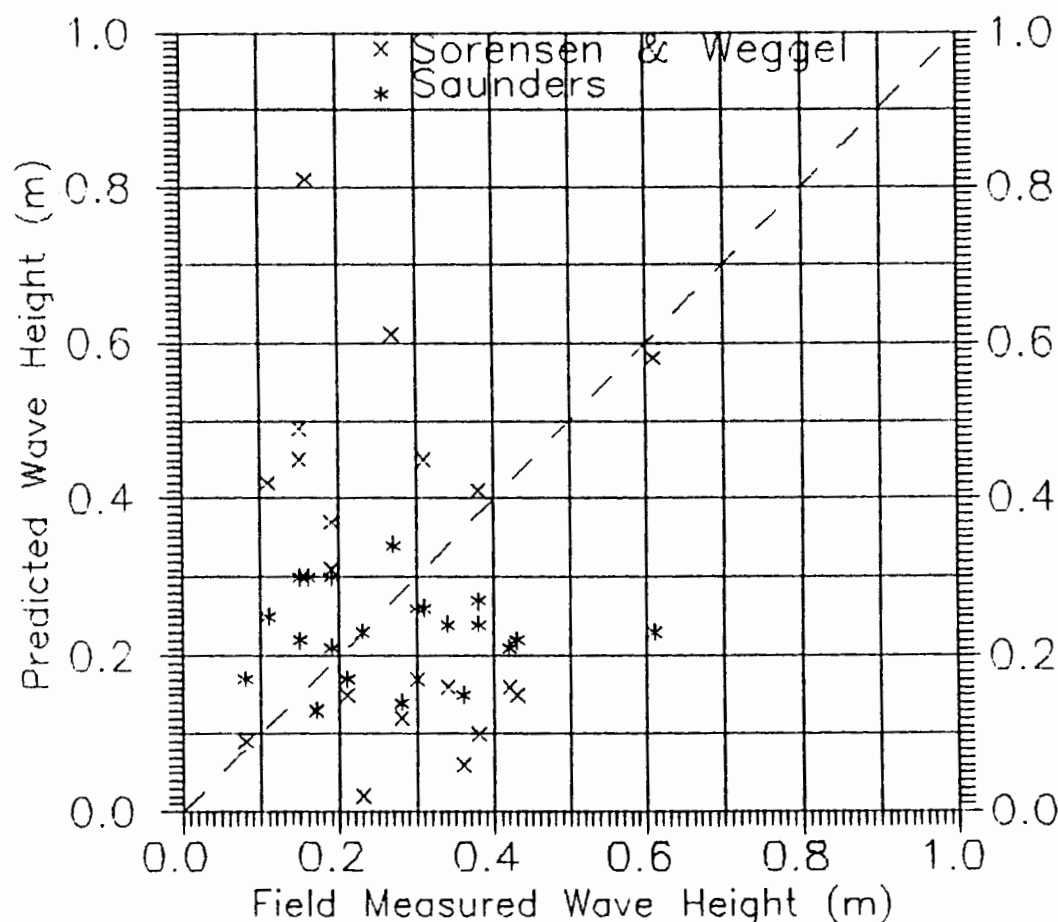


Figure 73. Predicted versus measured ship wave heights.

which should always have been greater than drawdown at the shore.

Ships transiting the lower Columbia River often have draft to depths approaching the maintained channel depth. The ratio of ship cross-sectional areas to channel cross-sectional area at the Puget Island site range from 0.09 to 4.50 (blockage factor). Figure 74 is a scale diagram of the bulk carrier "Magnolia" moving through the Columbia channel adjacent to the Puget Island site and illustrates

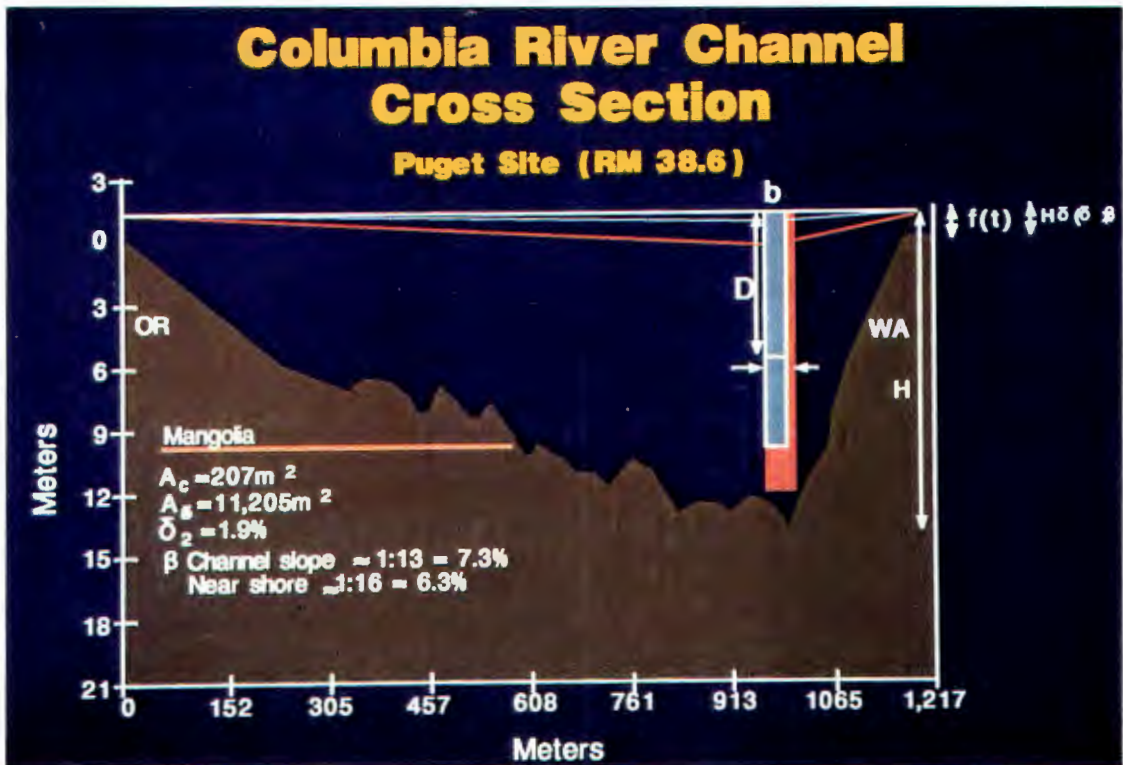


Figure 74. Channel cross-section with ship. Adjacent to Puget Island site with submerged hull of "Magnolia" presented in light blue. The orange rectangle represents the hulls of several of the largest ships observed in the study. Lines associated with drawdowns of each of these ships. Vertical exaggeration is 1:32.

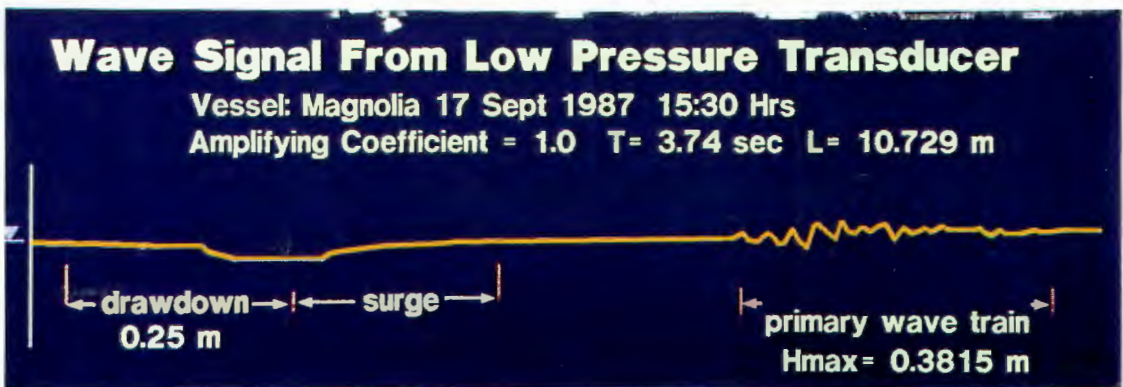


Figure 75. Ship wave record. Ship "Magnolia". Transducer in 1.5 meters of water, ship moving at 12 knots relative to the shore, L = wavelength.

the size ratio of the ships to the navigation channel. The hull outline behind Magnolia's (Figure 74) shows how big some of the ships transiting the lower Columbia get. Figure 75 presents the wave created by the Magnolia, as recorded at the Puget Island site. Figure 76 presents the wave generated by the container vessel Verrazano Bridge. The sequence of events or waves that occur as a ship moves past a site are presented in Figure 77.

The interaction between ship waves and the shore can often be dramatic, as illustrated in Figures 78, 79, 80, and 81, which show the attack of a plunging secondary ship wave near highest high tide at Puget profile PU-9. Appendix C presents other visual examples of ship waves along some of study sites.

Ship wave records (Appendix C) for merchant ships are summarized in Table XX.

Previous work examining the impact of ships waves on shoreline erosion used the analogy that work expended on a shore bank would be directly proportional to the banks erosion; erosion is a function of the work done (Ofuya, 1970). Calculating the rate in which ship waves deliver energy to the shore could allow one to evaluate the erosion along a particular bank. Equation (15) was utilized to calculate the energy in the secondary wave train (Ippen, 1966; Ofuya, 1970):

$$W_s = \frac{20}{S_{\max}} H_m^2 T_m Q_s \quad (15)$$

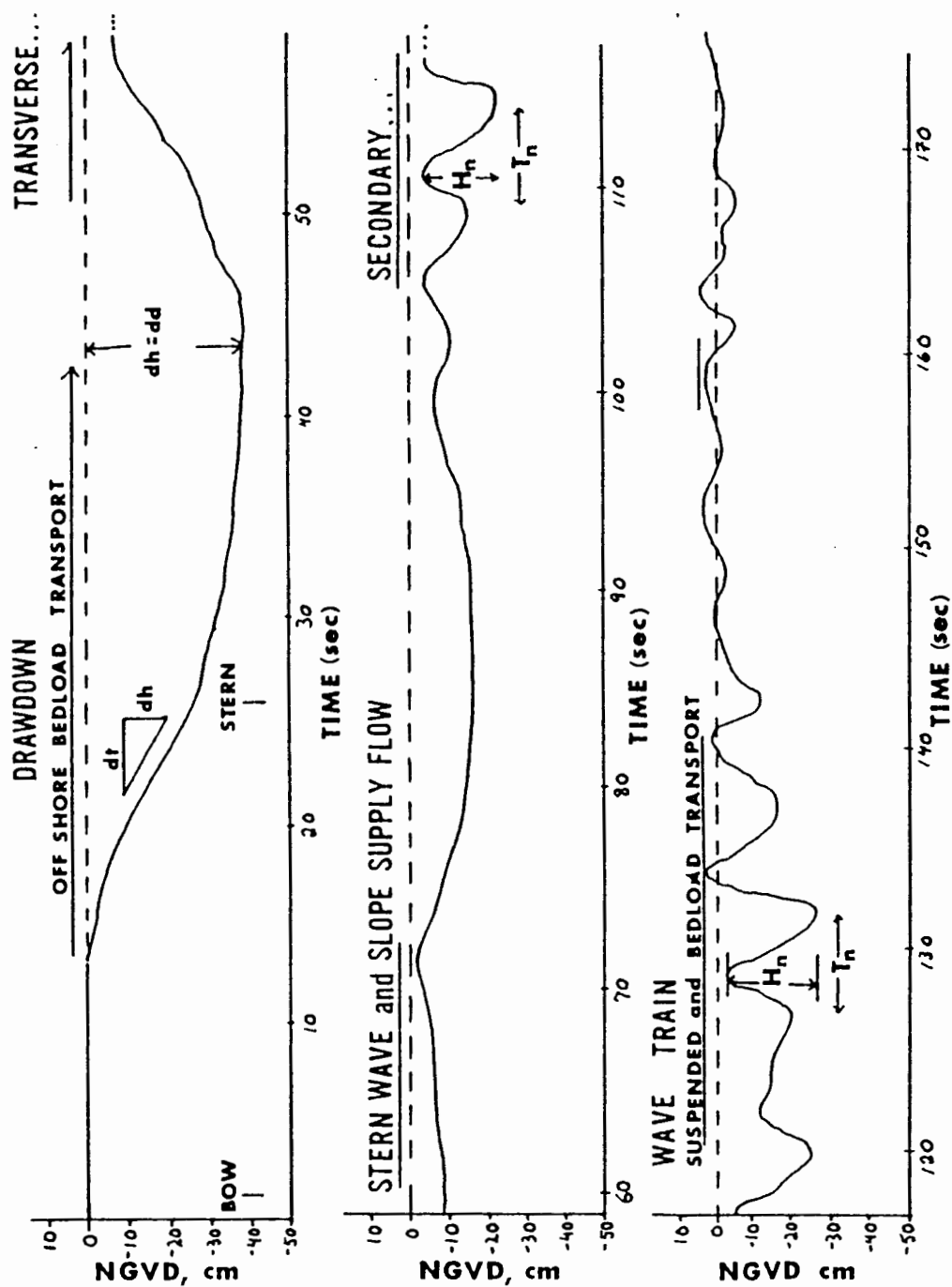


Figure 76. Ship wave. Container ship "Verazzano Bridge", 13JUN88.

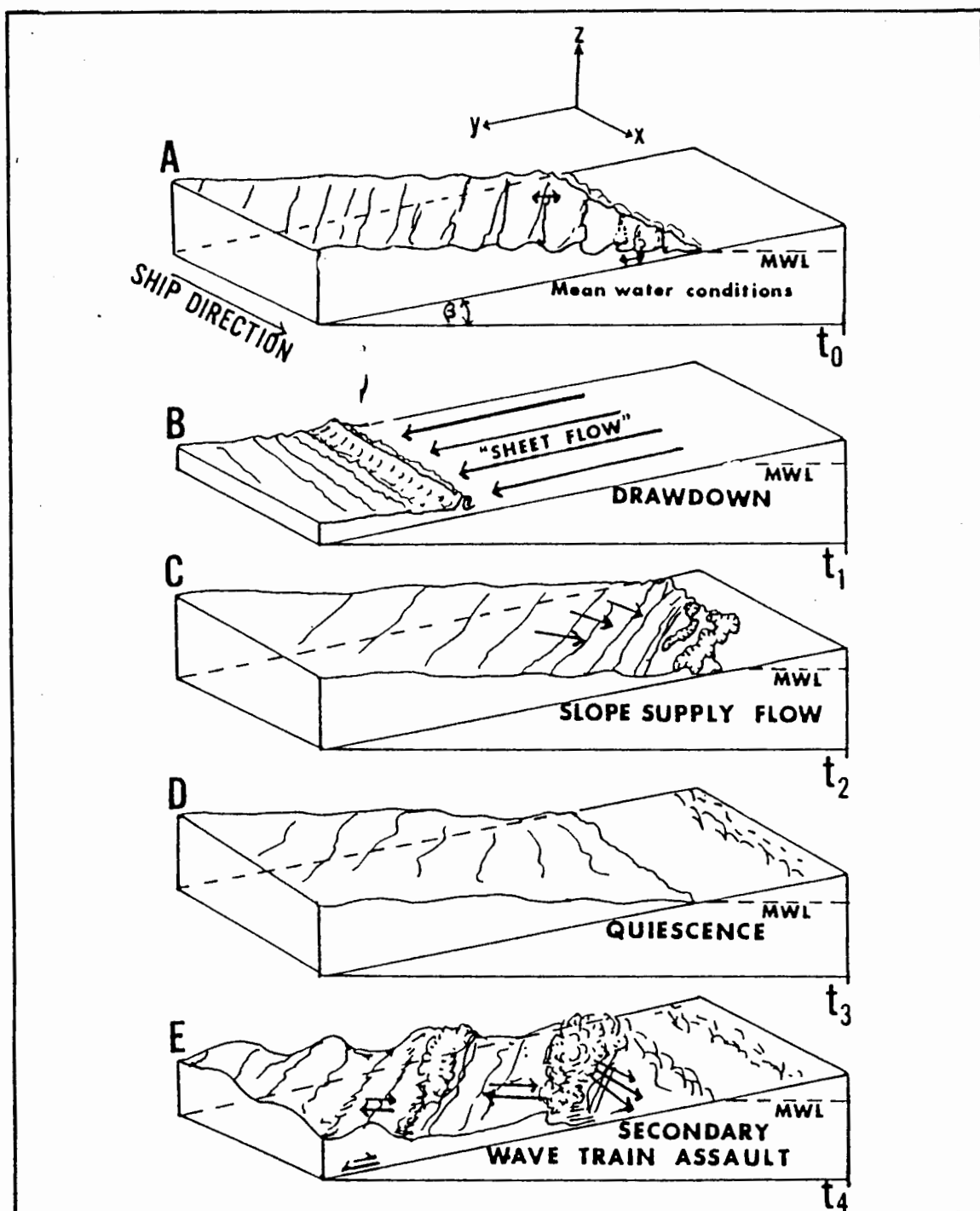


Figure 77. Observed sequence of ship waves. Observed along shores of lower Columbia River.



Figure 78. Plunging breaker (ship wave).
Riverward of large beach scarp cut into Puget
Island nourishment, 14JUL88.



Figure 79. Wave run-up after breaking. Note
turbulence and spray at base of beach scarp.



Figure 80. Wave run-up. Continues with each successive wave.



Figure 81. Beach scarp formation. At end of event we see a distinct scarp has formed at base of the scarp. Puget profile 9, 14JUN88.

TABLE XX

WAVE DESCRIPTION, MERCHANT SHIP PASSAGES

<u>Parameters</u>	<u>Range of Values Observed</u>
mean ship draft	4 - 12m*
ship length.	160.0 - 264.5m**
ship beam...	23.4 - 32.2m**
ship displacement	12,437 - 61,161 tonnes**
V_s	5.2 - 8.0m/s
dd.....	27 - 57cm
$H_{\max(\text{mea})}$...	8.0 - 38.1cm
T_{\max}	2.5 - 4.5sec
α	0° - 21°
bf.....	.009 - .045
β	1:30.0 - 1:13.0
H_b13 - .47m
d_b11 - .44m
E_{mq}	22 - 539 W/m

* mean drafts as reported from CRPA (1987-88)

** ship dimensions from Lloyd's (1987)

where:

V_s = ship velocity

dd = drawdown; E_{mq} = mean wave energy in Watts/meter

β = beach slope; H_b = height of breaking wave

bf = blockage factor; d_b = depth at breaker line

T_{\max} = max. meas. period

$H_{\max(\text{mea})}$ = max. measured wave height

α = angle of incident wave on shoreline

where:

W_s = ship wave energy

S_{\max} = slope of average maximum power versus energy
curve for ship waves 1/sec.
 $= 0.038 - (5.05)10^{-6} X_s$

where x_s is the distance from sailing line, $0 < x < 5000$
(feet); for all values of V_s (ship velocity).

H_{\max} = average maximum wave height

T_{\max} = average maximum wave period

Q_s = rate of ships passing per hour

Based on the average secondary wave trains of fourteen
observed merchant ships:

W_t = 241.7 [(ft lbs/hr)/ft shoreline]
= 1,075 [(N m/hr)/m shoreline]
= 0.3 [Watts/m shoreline]

where:

S_{\max} = 0.09 sec⁻¹

$$E = \sum_1^n H_n^2 T_n^2 = 0.93 \text{ m}^2 \text{sec}^2$$

Q_s = 0.42 hr⁻¹

This estimated average work done by secondary ship waves
lies within the domain of values derived in Ofuya's (1970)
study of navigation channels. The value presented does not
account for energy imparted to the shore by the drawdown
and transversal stern waves.

SEDIMENT TRANSPORT

Process Delineation and Transport Prediction

The first step in evaluating sediment transport is to define the hydraulic conditions that occur in the study region and which will instigate sediment motion. Once hydraulic conditions are distinguished, the likely range (magnitude) of these is estimated. The processes can then be analyzed by applying established theoretical and empirical relationships to determine the possible extent of sediment transport. Using these hydraulic "transport threshold" relationships, projections can be made of the hydraulic actions likely to have the most impact and those likely to have little or no impact. These projections will be compared to actual field measurements. Finally boundary conditions will be established for a descriptive model of the system.

The threshold of particle movement under a unidirectional current can be predicted using criteria presented by several authors (Shields, 1936; Hjulstrom, 1939; Yalin, 1972; Miller and others, 1977). Table XXII presents velocities needed to create sufficient shear stress to mobilize sediment grains (in Macdonald, 1983), as based on horizontal drag forces and critical drag forces due to eddies in the flow (Goncharov, 1938).

TABLE XXI
CRITICAL UNIDIRECTIONAL FLOW VELOCITIES

Average Particle

<u>diameter (mm)</u>	<u>Velocity (m/s)</u>
0.10	0.27
0.25	0.31
0.50	0.36
1.00	0.45
2.50	0.65
5.00	0.85
10.00	1.00

Shields' parameter (Shields, 1936) has been a commonly used measure of sediment motion in fluvial hydraulics. Shield's parameter is a ratio of the driving (shear forces) to the stabilizing (gravity forces). If the forces acting on a sediment grain are examined instantaneously, then Shield's approach is also valid for oscillatory flow (Madsen and Grant, 1975).

Effect of Tidal/River Currents

Currents driven by the tide and river discharge are modeled as unidirectional flows. The Hjulstrom curve presented in Figure 81 can be used to evaluate the approximate current necessary to move standard quartz grains (specific gravity of 2.65). Velocities at the Puget Island site were evaluated using a surface floater.

The surface velocity of a river by theory is greater than that found at the bed (Bagnold, 1966; Streeter and Wylie, 1979), thus it is assumed near bed velocities would be below those found at the surface.

Peak surface velocities observed during maximum ebb current on June 8, 1988 (month of maximum discharge for Columbia in 1988) were about 35 cm/sec where depth was 138 cm; up to 21 cm/sec where depth was 95 cm; and 19 cm/sec where depth was 70 cm. These surface velocities would generate the shear sufficient to instigate motion, but are low enough that near-bed velocities would have little impact. Hydraulic studies and Price meter data collected by the Portland District of the U.S. Army Corps of Engineers in the lower Columbia suggest that the near bed velocities associated with the above surface velocities would be found to fall below the needed threshold velocity of about 15-20 cm/sec. In depths less than 1.5 meters, tidal and river currents have a minimal potential for sediment transport. Further evidence for this is found in sedimentary structures. In depths of 1.5 meters or greater, asymmetrical current ripples were often observed forming in the direction of flow. These are very distinct from the smaller oscillatory wave ripples found in depths less than 1.5 meters that form from wind waves.

Sediment volumes moved during diurnal ebb currents must be evaluated to make conclusions on the relative

importance of each major sediment transport process. An array of three sediment traps were aligned normal to the shoreline to sample peak ebb flow transport during a time in which no ships passed the site. The traps were in the water for 10 minutes on June 14, 1988. The surface velocity of the river was 27.5 cm/sec at the deepest sample trap location. Measured transport increased with distance from the shoreline. Each of the trap arrays suggested all sediment transport occurred as bedload. To extrapolate this measured flux to an annual rate, it was assumed that flow conditions necessary to generate the conditions measured exist for 6 hours per day for 365 days a year. Such conditions probably rarely exceed 6 hours per day (USACE, 1988). Table XXIII presented the measured fluxes at the Puget Island site.

Using the values in Table XXIII, a bed width of 11 meters was used to extrapolate annual flux, derived using the existing beach slope, θ , and the zone from a depth of 0.9 m to 1.5 m.

The estimate of sediment transport rate was calculated in the following method, where a nearshore cell of active transport was derived based on recorded data and observations:

$$\theta = 3^{\circ}$$

$$(2.0/\tan \theta) - (0.9/\tan \theta) = 21 \text{ meters}$$

$$(.006 \text{ kg/m}^3 \cdot \text{min}) (60 \text{ min/hr} \cdot 8 \text{ hr/day} \cdot 365 \text{ day/year})$$

TABLE XXII

RIVER-TIDAL SEDIMENT TRANSPORT

During Ebb Flow, 11:10-11:22 14JUN88

45 minutes after low low tide

NGVD = 0.57m

Surface water velocity = 27.5 cm/s in depth of 122cm

Estimate of sediment flux

<u>Depth</u>	<u>Sediment Flux</u>
0.73m	0.000 kg/m*min
0.94m	0.003 kg/m*min
1.19m	0.006 kg/m*min

$$= 788.4 \text{ kg}/(\text{yr} \cdot \text{unit length(m)}) * 21 \text{ m}$$

$$= 16,556 \text{ kg/yr}$$

$$= 11.8 \text{ m}^3/\text{yr}$$

A volume of 11.8 cubic meters per year was extrapolated using the simple, static conditions represented by those measured for a one year period. No dynamic changes were accounted for in this derivation. The boundaries of the cell of sediment transport were based on the depth of initial sand movement as measured by trap and the deepwater edge of the shallow water zone defined in this study. The river discharge during this sampling was above the annual mean for 1988, but almost one half that during May of 1987. This is a source of potential error, for times of high discharge correspond to times of greatest sediment transport. Anomalous high discharges, such as flood events

can account for more than 80 percent of annual sediment transport in rivers (Dyer, 1986). Even though these anomalous events have been dampened by human modifications, flood events greater than 300,000 cubic feet per second ($8495 \text{ m}^3/\text{s}$), begin to instigate the majority of bedload transport in the lower Columbia River (Beeman, 1985a, b; USACE, 1986).

Effect of Ship Drawdown Wave

Drawdown from ship waves can be used to estimate the magnitude of sheet (plane of water moving downslope) flow down the shore face. Equation (16) was used to estimate maximum near-bed velocities during the drawdown:

$$V_{DD} = (DD_{\text{mea}}/\sin \beta)/t_{DD} \quad [L/T] \quad (16)$$

where:

V_{DD} = velocity of water moving offshore during drawdown event

DD_{mea} = measured drawdown (cm)

β = shore slope (on which DD occurs)

t_{DD} = time of drawdown event

The velocity of water moving down the beach, V_{DD} , can be compared to threshold conditions, or bed shear, was significant enough to move the sand grains, simply by plotting on Hjulstrom's curve. Drawdown velocities were found to range from 0.0 to 70 cm/sec, thus at times they

surpass the critical (point of movement) sediment threshold velocity, as suggested by observations and video records.

Predictions of near-bed velocities can be calculated using linear wave theory, treating the drawdown event as a large period wave. Even a small drawdown of 8 cm and period of 22.4 seconds at a depth of 1.5 meters on a 1:10 slope there is a near-bed orbital velocity, u_o , of 24 cm/s; a velocity sufficient to begin to move some of the sand. It is apparent that the long period drawdown wave generates orbital velocities which can instigate sediment motion in relatively deep water, as presented in Table XXIII.

The passage of a ship can generate a surge (commonly associated with the transverse stern wave) that acts as a turbulent bore front and is often visually observed to entrain sand. This bore moves with a celerity (wave form velocity) far in excess of orbital velocities. Transverse ship waves have a celerity equal to the ship's velocity in deepwater.

Effect of Secondary Ship Waves

Linear wave theory suggests that the secondary waves generated by ships can generate near-bed orbital velocities well in excess of the threshold conditions of the Columbia River sand. Table XXIV presents an example linear wave prediction based on the maximum secondary wave, H_{\max} of the ship Veranzano Bridge (13JUN88).

TABLE XXIII

PREDICTED THRESHOLD VELOCITIES AND DEPTHS

Lower Columbia River Sand, $D_{50} = 0.3\text{mm}$
 Linear Wave Theory, Drawdown Wave Range

Wave Period, T <u>(sec)</u>	Wave Height <u>(cm)</u>	Depth <u>(cm)</u>	Threshold orbital velocity <u>(cm/s)</u>
20	5	8.1	27.5
20	10	32.4	27.5
20	15	72.7	27.5
20	20	128.8	27.5
20	25	200.3	27.5
20	30	286.7	27.5
20	35	387.6	27.5
20	40	502.3	27.5
20	45	630.1	27.5
<u>20</u>	<u>50</u>	<u>770.4</u>	<u>27.5</u>
40	10	20.5	34.6
40	15	46.0	34.6
40	20	81.7	34.6
40	25	127.6	34.6
40	30	183.6	34.6
40	35	249.6	34.6
40	40	325.6	34.6
40	45	411.5	34.6
<u>40</u>	<u>50</u>	<u>507.2</u>	<u>34.6</u>
60	10	15.6	39.6
60	15	35.1	39.6

TABLE XXIII
PREDICTED THRESHOLD VELOCITIES AND DEPTHS
(Continued)

Lower Columbia River Sand, $D_{50} = 0.3\text{mm}$
Linear Wave Theory, Drawdown Wave Range

Wave Period, T <u>(sec)</u>	Wave Height <u>(cm)</u>	Depth <u>(cm)</u>	Threshold orbital velocity <u>(cm/s)</u>
60	20	62.4	39.6
60	25	97.5	39.6
60	30	140.4	39.6
60	35	191.0	39.6
60	40	249.4	39.6
60	45	315.4	39.6
<u>60</u>	<u>50</u>	<u>389.2</u>	<u>39.6</u>

TABLE XXIV
LINEAR WAVE PREDICTIONS

Given

H_{\max} (measured)	= 42cm
T_{\max}	= 4.6sec
α (wave incidence)	= 10°
d_{mea} (depth measured)	= 1.5m
β (shore slope)	= 0.10

Calculated

H_0 (deep water wave height)	= 41cm
T_0 (deep water wave period)	= 4.6sec
L_0	= 33m
α	= 20.2°

TABLE XXIV
 LINEAR WAVE PREDICTIONS
 (Continued)

C	= 7.2 m/s
H _b (breaker height)	= 54cm
d _b (breaker depth)	= 43cm
L _b (wavelength at breaking)	= 9.3m
α	= 5.6°
C	= 1.98 m/s
u _o (orbital velocity near bed at breaking)	= 163 cm/s
u _o (at d=3.0m)	= 87 cm/s
u _o (at d=6.1m)	= 58 cm/s
u _o (at d=9.1m)	= 38 cm/s

(USACE, 1985)

Sediment threshold predictions under waves were also made using a program modified from one written by Komar and Miller (1975). Table XXV presents program output using the mean grain density, the mean grain size, and the range of wave sizes observed at the Puget Island study site.

Sediment transport by ship waves measured at the Puget Island site is presented in Appendix D.

Table XXV illustrates that higher period waves need a higher near-bed orbital velocity to reach the grains' threshold of motion, but that for the same depth water, a higher period wave generates a higher near-bed velocity.

TABLE XXV

PREDICTED THRESHOLD VELOCITIES AND
 DEPTHS FOR LOWER COLUMBIA RIVER SAND

grain density = 2.6g/cm^3 , $D_{50} = 0.3\text{mm}$
 Linear Wave Theory, Secondary Wave Range

Wave Period, T <u>(sec)</u>	Wave Height <u>(cm)</u>	Depth <u>(cm)</u>	Threshold orbital velocity <u>(cm/s)</u>
3.0	10	86.9	14.6
3.0	15	154.2	14.6
3.0	20	212.5	14.6
3.0	25	263.1	14.6
3.0	30	306.1	14.6
3.0	35	343.0	14.6
3.0	40	375.1	14.6
<u>3.0</u>	<u>45</u>	<u>403.3</u>	<u>14.6</u>
3.5	10	85.2	15.4
3.5	15	158.0	15.4
3.5	20	230.8	15.4
3.5	25	294.5	15.4
3.5	30	350.8	15.4
3.5	40	400.1	15.4
3.5	45	443.4	15.4
<u>3.5</u>	<u>50</u>	<u>481.9</u>	<u>15.4</u>
4.0	10	82.2	16.1
4.0	15	159.7	16.1
4.0	20	237.2	16.1
4.0	25	317.4	16.1
4.0	30	386.3	16.1

TABLE XXV

PREDICTED THRESHOLD VELOCITIES AND
 DEPTHS FOR LOWER COLUMBIA RIVER SAND
 (Continued)

grain density = 2.6g/cm^3 , $D_{50} = 0.3\text{mm}$
 Linear Wave Theory, Secondary Wave Range

Wave Period, T <u>(sec)</u>	Wave Height <u>(cm)</u>	Depth <u>(cm)</u>	Threshold orbital velocity <u>(cm/s)</u>
4.0	35	448.3	16.1
4.0	40	503.8	16.1
4.0	45	553.5	16.1
<u>4.0</u>	<u>50</u>	<u>598.3</u>	<u>16.1</u>
4.5	10	78.8	16.7
4.5	15	158.0	16.7
4.5	20	244.6	16.7
4.5	25	335.4	16.7
4.5	30	413.5	16.7
4.5	35	487.5	16.7
4.5	40	555.2	16.7
4.5	45	616.8	16.7
4.5	50	672.8	16.7

Table XXV also shows us that higher period waves begin to "feel" the bottom in deeper water than lower period waves, given the same wave height. These predictions of the maximum depths of motion help to establish boundary limits when constructing a model of sediment transport in the nearshore zone by waves. Using the wave parameters of $T_{\max} =$

3.76 and $H_{\max} = 25\text{cm}$ for the observations of this study, the maximum depth at which grains begin to move is approximately three meters. Thus, the 3 meter depth could be modeled as the boundary at which sediment flux is zero.

Equation (17) defines the threshold condition for sand motion:

$$\begin{aligned} u_{\max(-d)} &= [8 (\delta_s/\delta - 1) g D_{50}]^{0.5} \\ &= [8 ((2.65/1.026) - 1) (9.81) (.0003)]^{0.5} \\ &= 19.3 \text{ cm/sec} \end{aligned} \quad (17)$$

Thus, for the mean grain size of the lower Columbia River sands in the Puget Island region, a near-bed velocity of 19.3 cm/sec is necessary to move the sand, a velocity close to those presented by Hjulstrom's curve.

Figure 82 presents a graph of sediment threshold prediction using small amplitude wave theory. The maximum depth of sediment motion is plotted as a function of wave heights (in the domain of values observed) and wavelengths in Figure 82.

The maximum depth of sediment (of mean grain size, D_{50}) entrainment under the actions of water waves of the range observed at the Puget Island site, with a period of 3.5 seconds, wavelengths between 7 and 21 meters and wave heights between 10 and 60cm range from about 0.5m to 6m. The most common waves had heights between 0.2 and 0.3 meters and wavelengths between 7 and 11 meters, which begin to move sediment in depths less than 2 meters. Using the

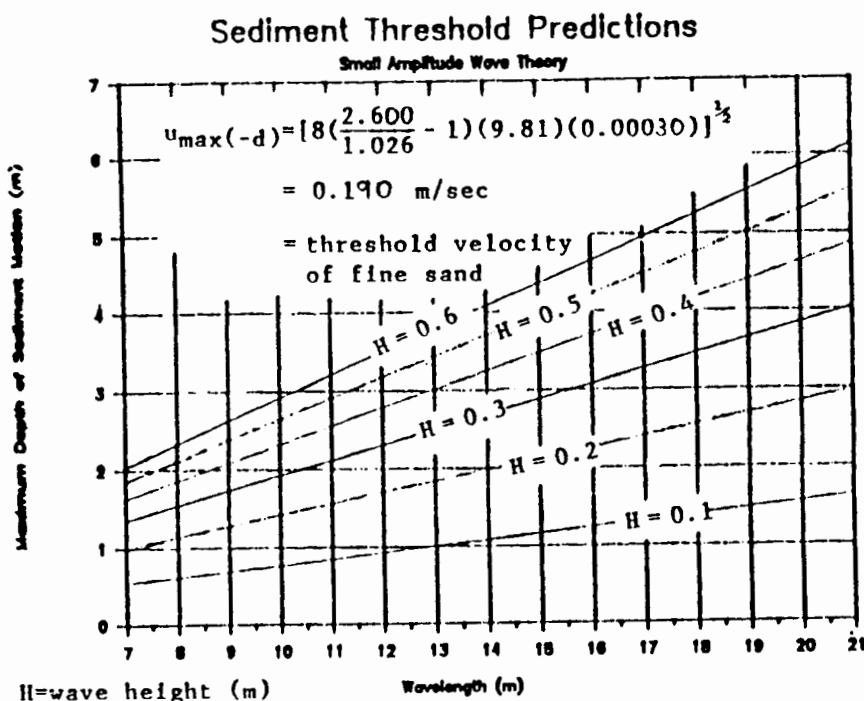


Figure 82. Estimating sediment motion. Effect of water waves using small amplitude linear wave theory (USACE, 1984).

mean observed wave height of 25 cm and wavelengths of about 14 m, sediment motion can be at a maximum water depth of 2 meters. These estimates offer a means to establish a riverward boundary condition of sediment motion for a near-shore shallow water sediment transport model.

The presence of sand in the sediment traps showed consistently that wave orbital velocities were sufficient to move sand. Point sampling with a array of sediment traps measured cumulative sediment flux for some time, t , at 2 depths for transport; parallel to the shoreline (longshore component) and perpendicular to the shoreline

(on and offshore components). Table XXVI presents an example of transport measured for a upstream passage (Magnolia, 17SEPT87). Note that at depths of 48 cm, outside the breaker zone, sand moves both on- and off-shore, but that the offshore component of transport exceeds that moving onshore. This is consistent with most of the ship wave sediment transport observed, suggesting a net erosion of the beach face.

Longshore Currents by Secondary Ship Waves

Longshore currents are those that move parallel to a shoreline and which are for significant sand transport in many coastal settings (Komar, 1976). At the Puget Island site longshore currents generated by ship waves, such as that observed during the passage of the ship Magnolia on September 17, 1987 (Table XXVI), can result in the most sediment moved at a single point in the nearshore zone, but because longshore currents are limited to a relatively narrow zone of about 5-10 meters perpendicular to the shoreline, they may not move the most sediment in a beach cell (section of beach). It was clear from reviewing of aerial imagery of the Puget Island site over the last fifty years, during which time the accretionary lobe developed north of the site, that longshore currents, either by: ebb flows, wind waves (little evidence), or ship waves or a

TABLE XXVI

SEDIMENT TRANSPORT DATA COLLECTED BY
SHALLOW WATER SEDIMENT TRAP ARRAY FOR THE
UPSTREAM PASSAGE OF THE BULK CARRIER, MAGNOLIA, 17SEPT87

Longshore transport was zero in the downstream
Direction, LONG = upstream longshore transport
ON=onshore OFF=offshore

Water Depth (cm)	Sample Depth (cm)	Sediment Transport Dry Weight in Grams			Mean Settling Velocity (cm/s)		
		ON	OFF	LONG	ON	OFF	LONG
20	Bed	5.1	31.4	186.0	3.2	3.6	3.3
20	9.5	1.0	13.9	117.7	3.0	3.2	3.2
20	17.1	0.1	4.4	74.5	2.9	3.2	3.5
48	Bed	26.1	36.0	-	3.9	3.5	-
48	9.5	4.0	5.4	-	3.2	3.2	-
48	17.1	1.8	3.0	-	3.2	3.2	-

combination are responsible for significant sediment transport.

Longshore currents generated by waves on a beach have been extensively investigated by several researchers: Longuet-Higgins, 1970a, 1971; Longuet-Higgins and Steward, 1962, 1964; Komar, 1975, 1979; Komar and Inman, 1970; Galvin, 1972b; Galvin and Eagleson, 1965. The research of these authors and others has resulted in the derivation of analytical and empirical solutions for estimating longshore currents.

The most important variable controlling longshore currents for a given set of wave heights and period is the

angle of incidence at which the wave fronts attack the shoreline (oblique-wave approach). The longshore current is produced by wave set-up, edge waves, and oblique-wave approach. An empirical derivation of longshore current was presented by Komar and Inman (1970) in Equation (18):

$$v_1 = 2.7 u_m \sin \theta_B \cos \theta_B \quad (18)$$

Equation (18) gives a maximum longshore velocity, v_1 , at $\theta_B = 45$ degrees.

where: u_{max} = maximum orbital velocity at breaking point
 $= [(2E_B)/H_B]^{0.5}$ (19)

H_B = wave height at breaking

E_B = wave energy at breaking

θ_B = wave incidence at breaking

Komar (1975) presented Equation (20) in which longshore velocity can be derived based only on the breaking wave height and wave incidence at breaking:

$$v_1 = 1.17 (gH_B)^{0.5} \sin \theta_B \cos \theta_B \quad (20)$$

Figure 83 presents a plot of the estimated longshore current derived using Equation (20); with a range of wave heights and incident angles. The domain of values observed at the Puget Island site include: wave heights from 10 to 50 cm and incident angles from 0 to 21 degrees. Waves with an incidence of 10 or more degrees that surpass the sediment threshold velocity and would be expected to move sand. Sediment trap data and visual observation showed that increased incidence of the waves increased the shore

Empirical Estimate of Longshore Current Velocity

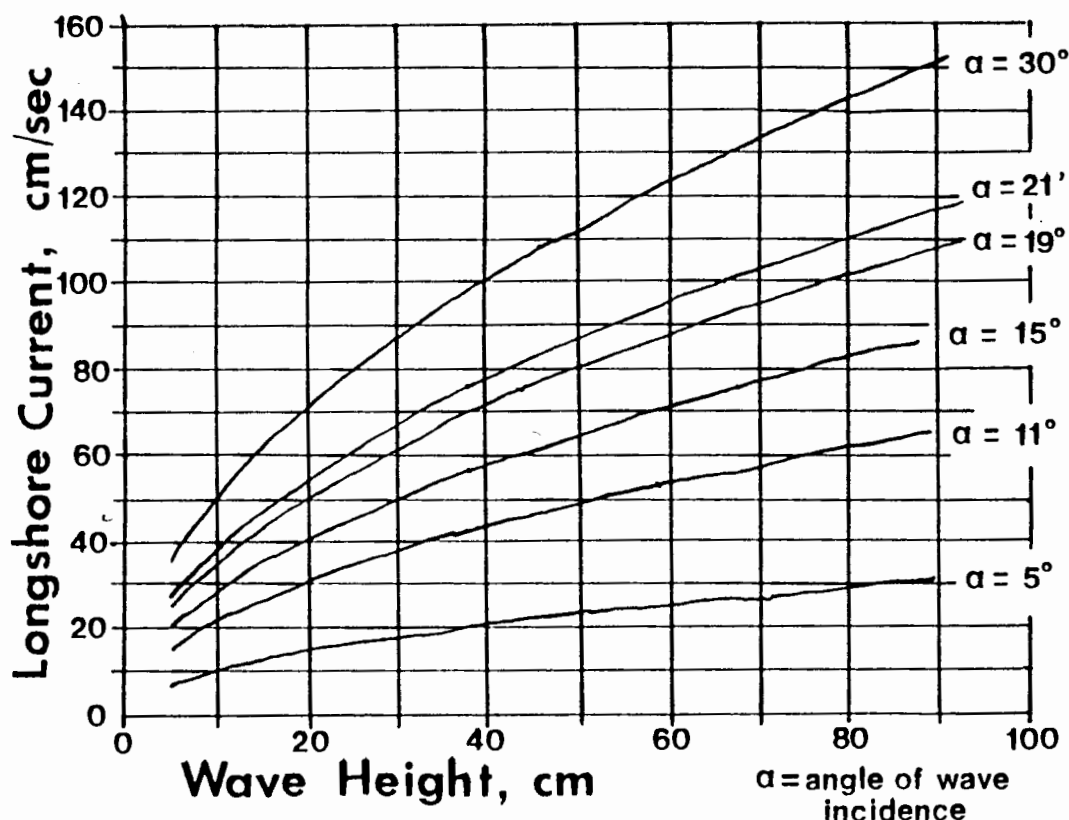


Figure 83. Predicted longshore current velocities, as estimated by Equation (20) (Komar, 1975).

transport. Waves with an incidence of 5 degrees or less had little to no longshore transport component as measured by trap.

Muir Wood and Fleming (1981, p.122) present a method to calculate the longshore velocity distribution in the surf zone. A short BASIC program was written using the technique and Figure 84 graphs the results after entering representative ship wave data into the program. Figure 84

Theoretical Longshore Current Velocity Profile

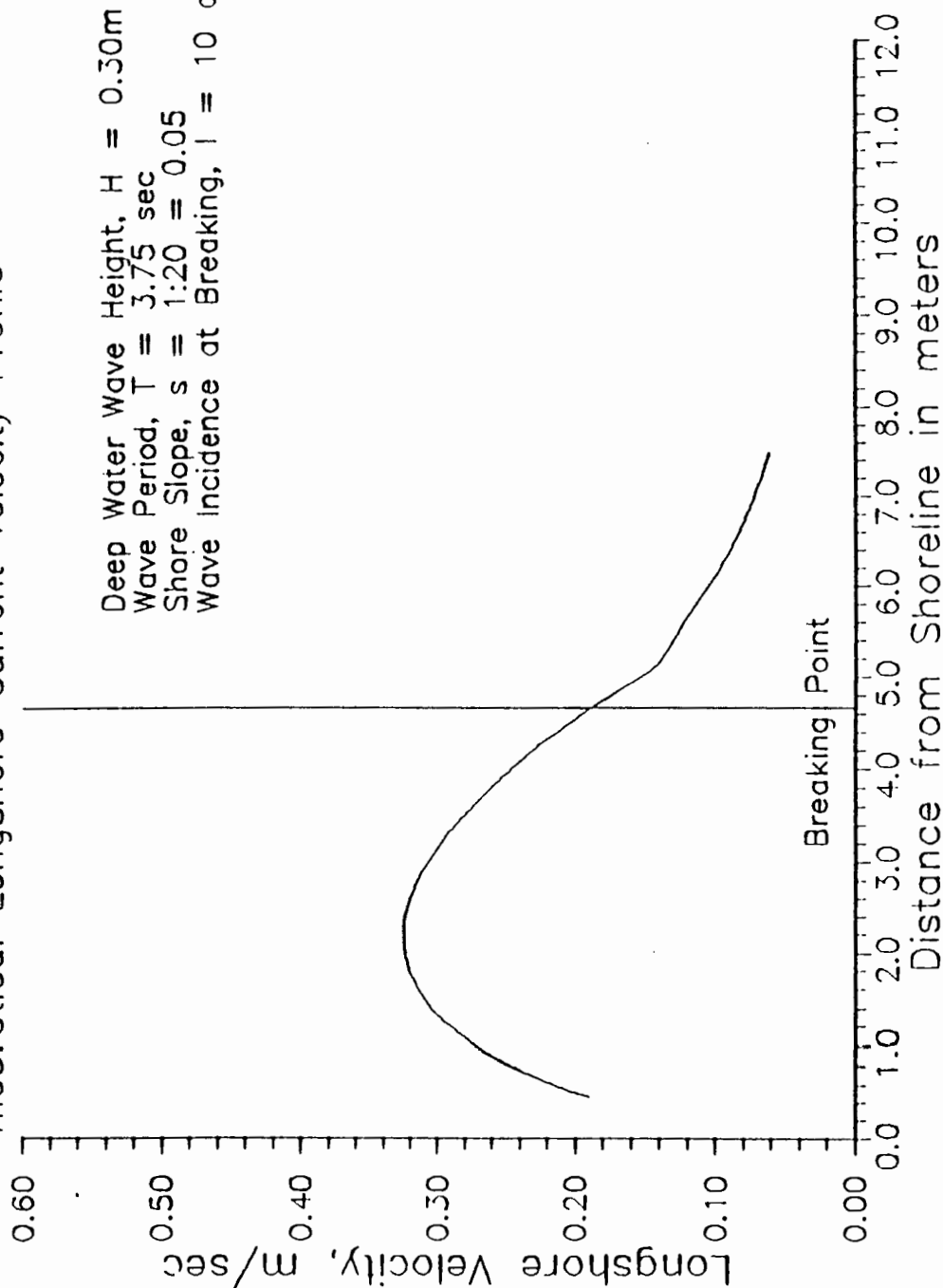


Figure 84. Predicted longshore current distribution through the surf zone. Using BASIC program based on analytical solution presented by MuirWood and Fleming (1981).

illustrates the range of longshore current velocity through the surf zone and the zone in which sediment transport is most likely to occur. Using data representative of observations at the Puget Island site, this analytical solution (Muir Wood and Fleming, 1981) produced velocities great enough that transport would be expected for incident wave angles of 8 degrees or more in the surf zone. These derivations allow limits or boundaries to be estimated for a zone or corridor of longshore sediment transport.

Field Sampling

The results of the sediment trap array system show distinct components of sediment transport in shallow water zones along the lower Columbia River (Appendix D).

The processes instigating sediment transport in the near-shore zone during the passage of a large vessel in the Columbia are illustrated in Figure 85, a time-sequential cartoon of the processes. This set of processes move as a group along the river bank at approximately the same velocity as the ship. The processes are similar to the sequence listed in the Table IV. To better understand this set of processes, they are examined as individual actions, and then modeled by using existing theory of analogous processes common in the coastal environment. The primary difference between ship waves and those waves that have been studied in theory and coastal environments is the time

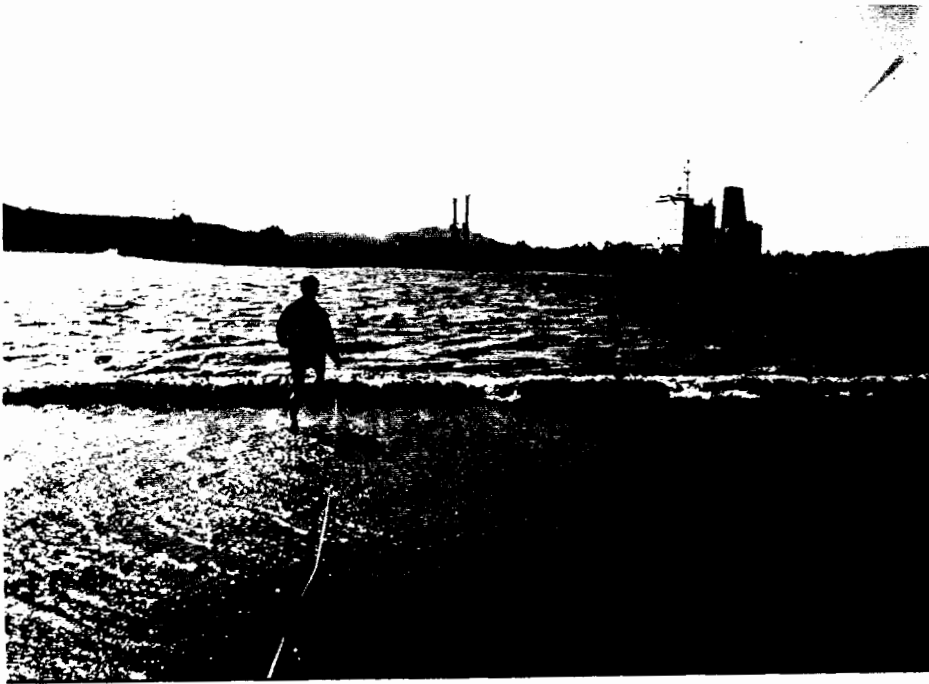


Figure 85. Ship drawdown wave. Sheet flow off the shore slope. Bulk carrier "Coast Range."

dimension and the distribution of wave forms in the set of waves. Wave sets for a given time period in theoretical and natural settings tend to be modeled as a group of individuals with similar dimensions, whereas ship waves are a set of distinctly different waves. Separating the ship waves out into distinct subsets, evaluation by analogy provides a means of analyzing the interaction between ship waves and a shore slope.

The distinct subsets of ship waves observed at the study sites are as follows:

The first action that occurs on the shore is the drawdown wave, a rapid removal of water off the shore when

the ship is approximately normal to the shoreline. As a ship "pulls" itself through the water with its screw (propeller), similar to a screw driven into wood, the ship pushes up a mound of water in front of its bow. This bow wave increases in size as the ship increases its speed (Constantine, 1960, 1961) and the water surface around the ship drops relative to the surrounding mean water level, bringing the ship closer to the bed of the channel. The phenomenon in which the ship's keel approaches the channel bed with increasing speeds is called "ship squat" and is believed to be the driving mechanism behind the drawdown that occurs at the shoreline. The depression in the water surface around the ship creates a head differential with the surrounding water and thus water moves toward that low. The greater the ship squat and the closer to shore the ship, the greater the drawdown wave will be. One of the most detailed analyses and empirical solutions of ship squat was done by Barrass (1979). Barrass's method was used to predict squat for the observed ships during this study. Barrass (1979) found that squat is primarily a function of speed, but is also dependent on channel cross-sectional area and mid-ship cross-sectional area of the ship. Figure 3-67 shows the drawdown for the bulk carrier "Coast Range." The drawdown waves had periods of approximately 40-60 seconds and were followed by replacement of the displaced water back onto the shore.

The surge or transverse stern wave that replaced the water back onto the beach face move diagonally up the beach face, in the direction of ship passage. This contrasts with drawdown which moves water directly down-slope. After the transverse stern wave, the water level returns to near mean conditions, "quiescence" in this study.

The last wave event is often the most obvious, the secondary wave train of the ship. This group of waves had an incidence from 0 to 21 degrees upon the shoreline. The secondary wave train most often broke as plunging breakers. Sediment trap data and visual observation showed that the greater the incident angle of these waves, the greater the longshore transport. The angle of incidence is controlled by the shoreline configuration and offshore bathymetry. The river channel nearshore morphology directly controls the manner in which waves refract and thus wave incidence along the shoreline. Figures 86 and 87 illustrate the assault of a plunging secondary ship breaking wave at Puget Island and associated sediment plumes. The sediment plumes are portions of the bed that have been brought into suspension by water particles accelerating under the wave. As the sediment is lifted up into the wave, the faster moving water particles can continue the sediment plume's upward motion. Water mass has a net movement shoreward in shallow water and the breaking wave cascades much of this water momentum toward the shore, carrying the sediment



Figure 86. Plunging ship wave. Breaking height of wave is approximately 32 cm, 04AUG88.

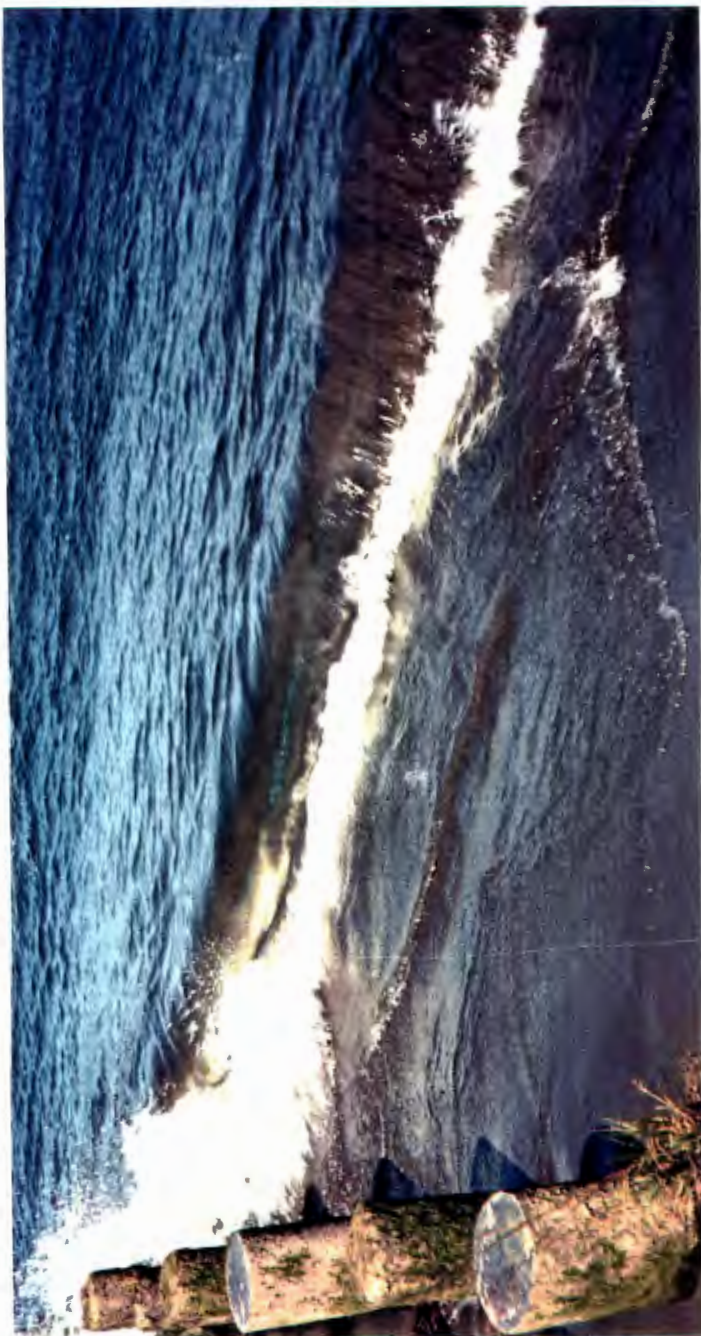


Figure 87. Wave breaking in the plunging form, characteristic of most secondary ship waves observed, but spilling, surging, and collapsing breakers were observed. Note "jet" of water in plunging tongue of the wave. Under the assault of a regular train of waves, the jet scours a longshore trough and a longshore bar develops riverward of the plunge line. Most sediment suspension occurs in close to the breaking line.

plume with it. The plunging mass of water scours into the bed, moving more sediment which is subsequently deposited in the lower energy zone just riverward of the plunge line.

The water mass moved up the shore after the wave breaks retreats off the shore, carrying sediment with it in a sheet flow action similar to the ship's drawdown.

Sediment flux through the water column at a point was determined using sediment trap data. Each individual trap sediment sample in an array was normalized to mass per unit width and plotted versus the mid-trap elevation above the bed. The three points of each array were then fitted with a exponential line of best fit. This method was chosen because on established sediment distributions above a boundary (Einstein, 1972; Bagnold, 1966; King, 1972). The area under best fit curve was than used to estimate the total sediment quantity moving over a unit width of bed during the event in the measured direction. That sediment quantity moving at that point was then compared with the quantities moving at other measured points. The net motion and distribution of transport in the nearshore zone was used to extrapolate the volume of sand moved along, on, or off the shore.

Figure 88 shows the results of measuring sediment transport during the passage of the bulk carrier "Leandros." The curves show a significant longshore transport component at the point closest to the shoreline,

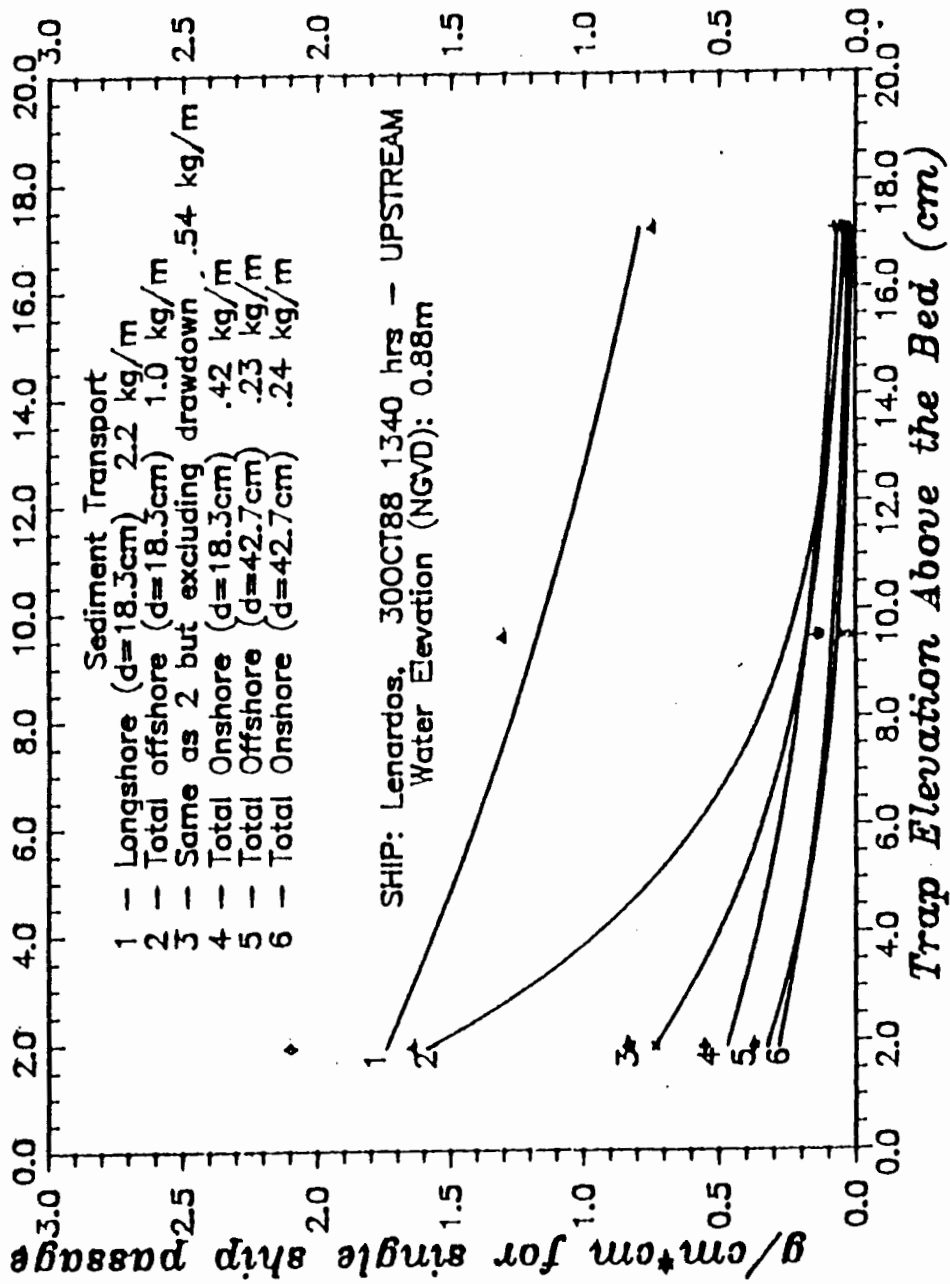


Figure 88. Shallow water sediment transport by the ship waves of "Lenardos." 30OCT87.

in the surf zone. Offshore transport of sand in the surf zone exceeded onshore transport and the drawdown event moved 44% of the total quantity measured offshore. In deeper water where the on-and off-shore components would be expected to be similar due to the oscillatory currents on a wave, it is seen that the two measured quantities are similar.

Figure 89 displays the sediment transport during passage of the bulk carrier "Coast Range." For "Coast Range" offshore transport exceeded onshore transport just outside the surf zone (in a depth of 34 cm). The drawdown event for "Coast Range" was minor, accounting for only 5% of the offshore transport.

Figure 90 presents the results from a large wave trained generated by the U.S. Naval ship "Gray" (#1054). At a depth of 44 cm the waves created an offshore sediment transport of 62.1 kg/m per event and an onshore transport of 24.0 kg/m per event. The ship "Gray" resulted in a net offshore removal of sand of 38.1 kg/m during the event. This data suggests that the high velocity of the Gray, 15.7 knots and resulting H_{\max} of 43 cm in 2 meters of water instigated sediment flux far in excess of most sediment transport rates instigated during the passage of observed merchant vessels. The "Gray" did not create a large drawdown because of its small size compared to merchant vessels.

Coast Range, 09JUN88 13:07 UPSTREAM

Water Elevation (NGVD) = 0.80m

Ebb flow = 0.0-0.1 m/sec

- 1 - offshore flux, $d=.34m$, $q=8.62$ kg/m per min
 - 2 - onshore flux, $d=.37m$, $q=6.71$ kg/m per min
 - 3 - drawdown (offshore) flux, $q=.44$ kg/m per min
- offshore flux, $d=.70m$, $q=.22$ kg/m per minute
 onshore flux, $d=.76m$, $q=.33$ kg/m per minute
 offshore flux, $d=.98m$, $q=.11$ kg/m per minute
 where q = sediment flux and d = water depth

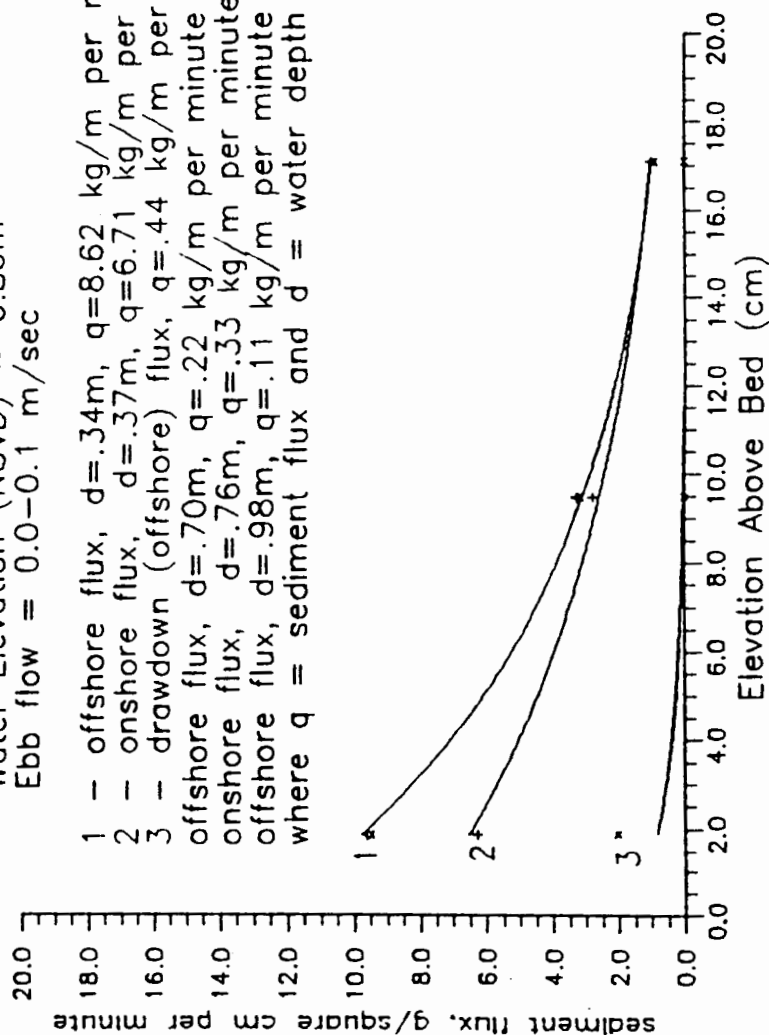


Figure 89. Shallow water sediment transport by the ship waves of "Coast Range." 09JUN88.

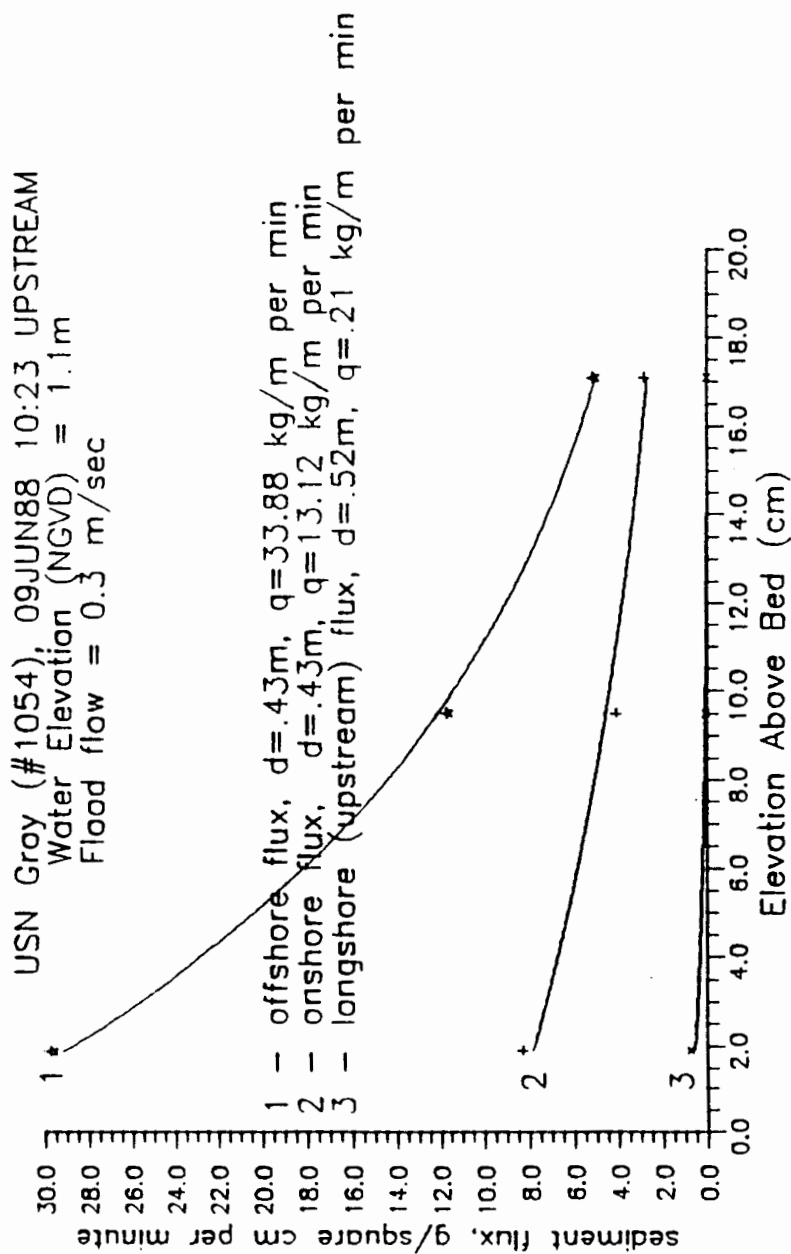


Figure 90. Shallow water sediment transport by the ship waves of the "U.S. Gray". 09JUN88.

Merchant vessels observed had a mean velocity of 12.5 knots, ranging from 10.0 to 14.6 knots (14 ships) and a mean wave height of 21 cm. The naval vessels observed transiting the lower Columbia for the 1988 Rose Festival in Portland, Oregon, had a mean velocity of 14.2 knots and a mean wave height of 29.7 cm. Because the naval vessels are an anomaly, with about a dozen ships transiting the lower Columbia during a 2 to 3 day period twice year (in and outbound passages during the Portland, Oregon Rose Festival in June), the actions of their waves were not used to extrapolate annual transport rates. The erosion caused by the naval ship waves did show what can occur when ships move at higher velocities, as evidenced by the work of Ofuya (1970) and Sorensen and Weggell (1984). Both primary and secondary ship wave heights are proportional to velocity squared (Barrass, 1979; Sorensen and Weggell, 1984; respectively).

The range in magnitude of sediment transport caused by the waves generated by merchant ships are presented in Table XXVII.

Sediment transport distribution across the beach face (perpendicular to the shoreline) was measured for the ship "Coast Range," and found to vary greatly for the points sampled. Figure 91 displays the sediment flux distribution based on the points sampled during the passage of "Coast Range." Sediment flux increases approaching the breaker

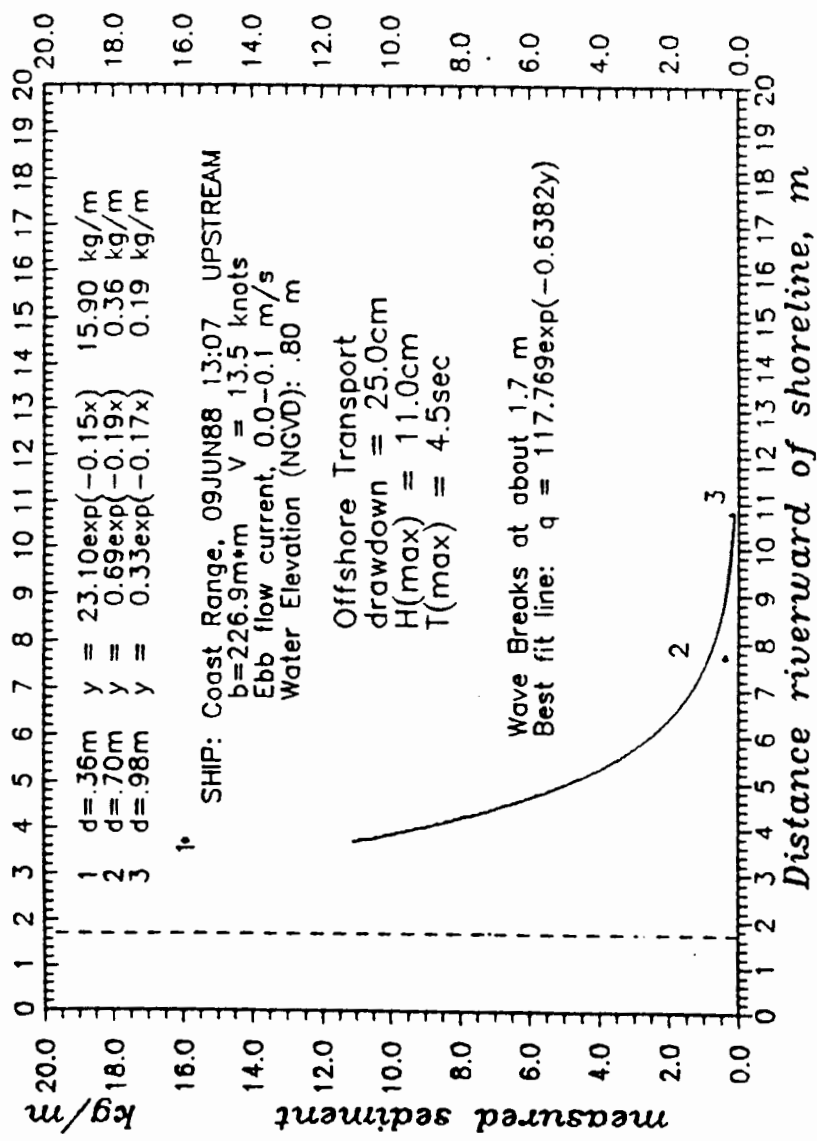


Figure 91. Sediment flux distribution normal to the shoreline for the ship "Coast Range." 09JUN88.

TABLE XXVII
SHALLOW WATER SEDIMENT TRANSPORT BY
MERCHANT SHIP WAVES

	Minimum $q_{\text{mea}} \text{ (kg/m)}$	Maximum $q_{\text{mea}} \text{ (kg/m)}$	Net flux $\text{(m}^3\text{)}$
depth	.18m	.33m	
Onshore	= .42	= 12.5	23,397
<hr/>			
depth	.18m	.33m	
Offshore	= 1.0	= 15.9	29,761
<hr/>			
depth	-	.10m	
Longshore	= 0.0	= 18.2	
<hr/>			

zone. This observation is supported by the work by the Beach Erosion Board (1933; in: King, 1972), that showed an increase in sediment flux and suspension in proximity to the surf zone during ocean wave assault (Figure 92). Using the analogy to previous work (King, 1972) and shallow water sediment trap data, it is suggested that most sand transport by ship waves in the lower Columbia will occur in proximity to the surf zone.

To model sediment transport in the shallow water near-shore zone, sediment trap data was extrapolated in the following manner.

The measured points in the water column were fit with an exponential line of best-fit based on exponential current and sediment transport distributions above a boundary (Bagnold, 1966; Kraus, 1987; King, 1972). This

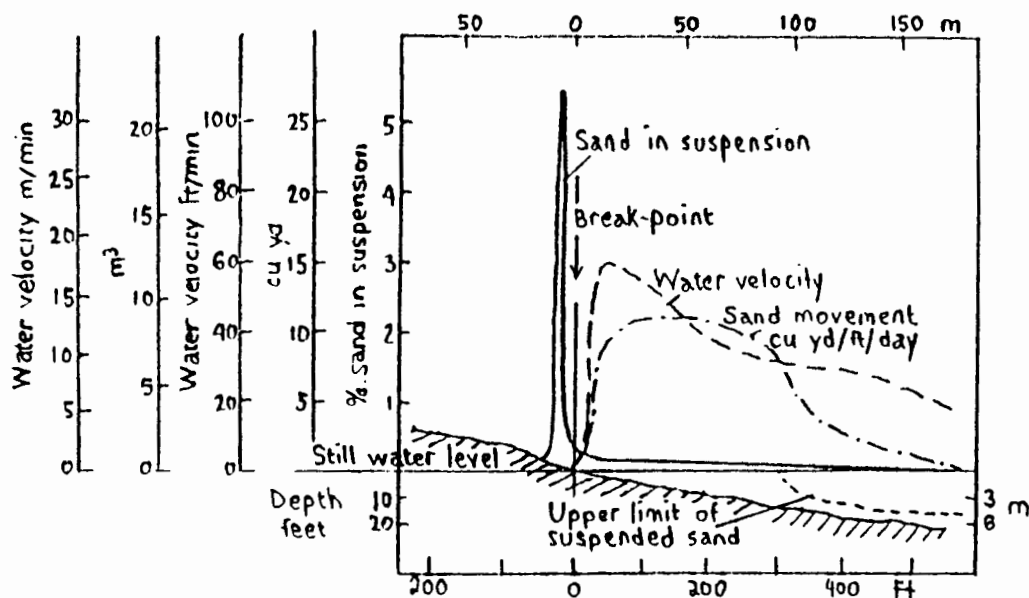


FIGURE (King, 1972, p. 251)

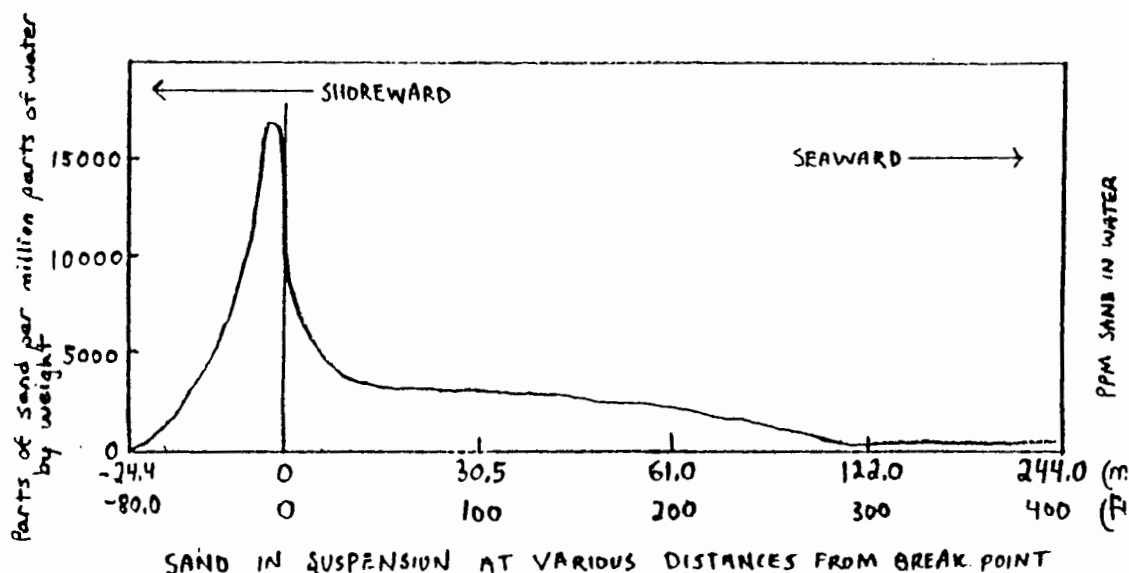


Figure 92. Results of studies by the Beach Erosion Board, 1933 (in: King, 1972, p. 251). Near the wave breaking point, sand is moved in suspension in concentrations of 17,000 ppm (mg/l) by weight. Moving 7.6 meters seaward, this concentration dropped to only 4,000 ppm and at 84 meters it has fallen to 1,000 ppm.

plot was then integrated using the bed and water surface as boundary limits to give an estimate of the total sediment flux at that point. Equation (21) presents the simple integration to determine sediment flux during a single event.

$$q_{\text{mea}} = \frac{\int_0^h k_1 * \exp(-k_2 z) dz}{10} \quad [\text{kg/m} * d_{\text{cm}}] \quad (21)$$

where: h = water depth

q = sediment flux

k_n = constants of integration

z = elevation above the bed

To derive the estimated annual sediment transport rate from the net sediment transport on- or offshore as derived from Equation (21), the quantity was extrapolated for the total number of events during the year, the entire length of the Puget Island beach cell, and divided by the sediment's bulk density. Equation (22) used the annual number of ship passages, the sediment bulk density, and the shore dimensions of the sediment cell in question:

$$M_{\text{mea-max}} [\text{m}^3/\text{yr}] = \frac{q_{(\text{mea-max})} [\text{kg/m}]}{1,400 [\text{kg/m}^3]} * Xb_n [\text{m}] * Q_s \quad (22)$$

where: q = sediment flux

X_b = beach cell length

Q_s = rate of ship passage

M = total estimate of annual sediment flux

Sediment trap data reveals that drawdown only transports sediment along the bed (none in suspension), but can account for about half of the sediment mass moved offshore during the entire set of ship waves.

The relative importance of a ship's displacement within a confined channel can be mathematically represented in the blockage factor, bf . Blockage factor is a measure of the ship hull cross-sectional area's percentage of total channel cross-sectional area (the ship's mid-sectional cross-sectional area divided by the channel cross-sectional area). Brebner and others (1966) suggested that if $bf > 1-2\%$ for ships moving at or above an established velocity then the ship drawdown or removal of water off the beach may become the dominant erosive agent. For most merchant ships drafting 6 m and more in the Columbia, the blockage factor ranges from 0.9-4.5% (Abbe, 1988b). Ships observed with blockage factors of .009 caused only slight drawdowns moving at the same or greater velocities (naval frigates) as larger merchant ships with blockage factors of 0.02 or more.

Trap data showed a general trend toward a net offshore sediment flux in water less than 1m in depth. Longshore transport can far exceed onshore and offshore transport components, but was heavily dependent on the wave incidence and shore morphology. When wave incidence became negligible, the longshore transport likewise became

negligible. Field data showed that all longshore transport during ship passage occurs in the direction of ship motion.

A simple geometric model to illustrate hypothetical sediment transport during ship wave assault is presented in Figure 93. The model is based on the sediment flux samples measured by the traps and boundary conditions established from wave parameters and theory. The maximum measured flux, q_{mea} , is used as the maximum flux, q_{max} , along the beach, an estimate that is most likely below the real maximum flux, q_{rmax} . Sediment flux down beach slope gradient is greatly simplified in the model as a set of linear functions increasing to some point near the breaker zone and decreasing seaward of some peak position and

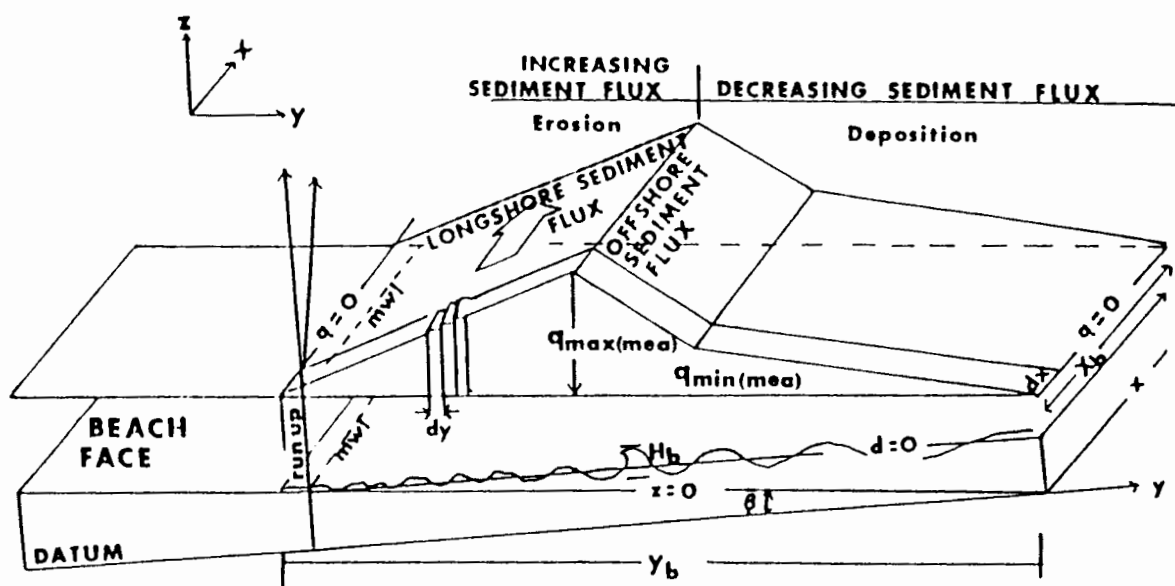


Figure 93. Simple linear model illustrating ship wave sediment transport in shallow water as measured by shallow trap array.

representing the erosion/deposition on the beach face. The model assumptions include:

no net sediment motion preceding the measured ship wave assault; sediment trap data is representative of the real world system;

the maximum measured sediment flux is close to the real maximum flux for some beach cell, but probably is less than the actual peak flux, q_{rmax} (thus a conservative measure);

the beach is smooth and continuous for the entire cell; the change in water level up and down the beach does not alter the processes that occur, just where they will occur;

the shoreline and bathymetry of the beach cell is linear, thus neglecting wave refraction and localized current amplification or dampening; the data is representative of all ships drafting more than 5.8 meters;

and that the measured sediment transport direction is representative.

The boundary conditions are established using the maximum depth of critical velocities generated by passing waves and the maximum runup onto the beach by these waves.

The offshore sediment flux can be compared to the actual sediment volume changes at the study beach. The total changes in sediment storage along the shore of the study beach to a minimum elevation of approximately -1.0 NGVD (low low water) were computed using 2-D computerized cell changes (Birkemeier, 1988) of field surveys (Abbe, 1989). After the 1987 nourishment at the Puget site, from July 31, 1987 to June 7, 1988 the loss of sand was 26,197 m^3 (Abbe, 1989), about twenty seven percent of the 97,903

m³ quantity placed at the site during the July 24-29, 1987 nourishment.

The maximum net (ABS[offshore-onshore]) sediment flux component of the trap data suggests that for 3,600 merchant ships (in- and outbound traffic) with drafts of 6 meters or more moving past the Puget Island Site, the generated waves (acting on a smooth beach face) can account for the transport of a minimum sand volume of 1,086 m³ to a maximum of 6,364 m³ moved offshore in shallow water. The average duration during which the actions of merchant ship waves act the shoreline is 176 seconds, thus the maximum measured offshore sediment flux is 1.2 kg/m per minute. Because of the exponential distribution of sediment transport through the surf zone, I believe the maximum estimate is well below the actual offshore transport occurring in the surf zone. By examining sediment transport caused by the waves of naval ships, I believe a more representative upper limit of sediment flux out of the beach cell can be estimated. Assuming the impact of the waves generated by a passing naval frigate is representative of all deep draft ship waves during a year, the estimated maximum net transport (using the maximum measured transport during passage of the "US Gray") comes to 73,478 m³ per year offshore; a value that exceeds the eroded 26,197 m³ volume of sand at the Puget Island site by 2.8 times. The average duration of naval ship wave actions on a shore was 63 seconds. The "US

Gray" caused a flux of 59.1 kg/m per minute offshore and 22.9 kg/m per minute onshore; a maximum net offshore sediment flux of 36.2 kg/m per minute. These calculations offer a range of sediment transport that encompasses the measured volume of sand that eroded from the Puget Island beach cell.

The model and extrapolations of sediment transport based on measured values suggests erosion transgresses up the beach face and deposition occurs on the lower beach in shallow water depths offshore. The effect is a lowering of beach slope. Profiling showed erosion of the upper beach, deposition in the shallow water depths of the lower beach and an overall lowering of the beach slope.

The net longshore sediment transport component generated by ship waves over time is downstream because of the significant increase in ship drafts on the outbound (downstream) passages, as presented in Figure 94. It is a conclusion that there is a definite longshore and offshore transport of sand in the shallow near shore zone at the Puget Island site.

SEDIMENT CHARACTER

The sand of the Puget Island Reach was analyzed for grain size distributions by mechanical sieving and settling tube. Settling tube analysis most accurately presents the settling velocity distributions of the grain populations,

Comparison of Vessel Draft In and Out of the Columbia River
1984

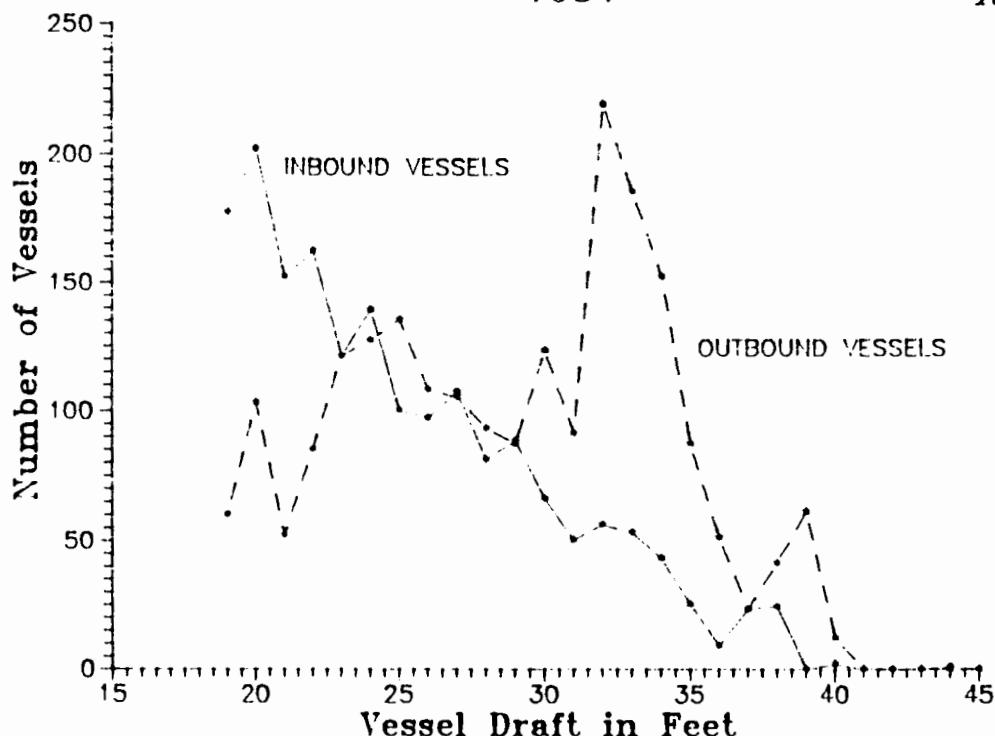


Figure 94. Ship passages in the lower Columbia River.

with size estimation made after calibrating the tube. Calibration results for Columbia River sands of the Puget Island region appear in Figure 95 (calibration curves). In the Puget Island Reach of the Lower Columbia the sediment particles are primarily fine and medium sand (0.25 - 0.50 mm), angular and with an approximate density of 2.60 g/cm³.

SETTLING TUBE CALIBRATION
COLUMBIA RIVER SEDIMENTS AND GLASS BEADS

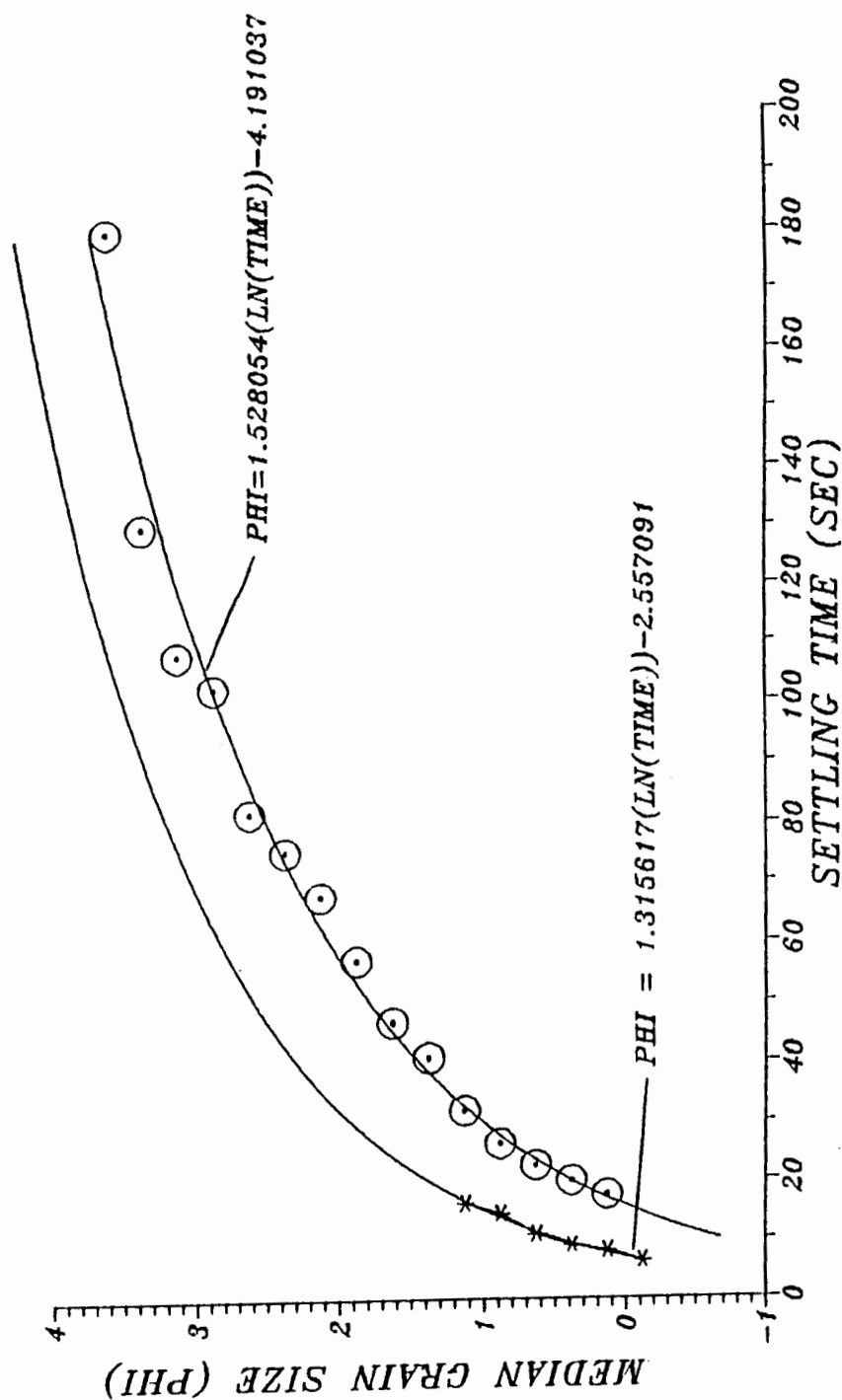


Figure 95. Calibration curves, Puget Island sand.

Sediment Density

The density of common sands is presented in Table XXVIII (USACE, 1984, table 4-2). Table XXIX lists the dry and wet densities and porosities of sand populations along on the Puget Island site (RK 62) and the Gull Island site (RK 88). Knowledge of the density of the shore sands is necessary when a model is constructed to extrapolate volumes of sand moved along the beach. The value of $1,400 \text{ kg/m}^3$ will be used as the representative bulk density for Puget Island sand.

Sediment Size Distribution

The Lower Columbia River sediment is angular plagioclase rich fine to medium sized sand (Figure 96 and Appendix E). The small grain size and relatively low density of the Columbia sand examined indicates that this sediment is easily moved, as based on Shields, Yalin's, or Hjulstrom's sediment motion threshold curves (Shields, 1936; Yalin, 1972; Sundborg and Norrman, 1968; respectively). Sand samples from beach scarp faces eroding into original disposal sites were used to represent the sand making up the shore upon which all physical processes will subsequently interact.

The graphical statistics of sand at the Puget Island site (Folk and Ward, 1957) are presented in Table XXX.

TABLE XXVIII
SEDIMENT DENSITIES

Specific Gravity (dimensionless)

Quartz	2.65
Calcite	2.72
Heavy Minerals	>2.87 (commonly 2.87-3.33)

<u>Sand</u>	Unit Weight kg/m^3	
	<u>Dry</u>	<u>Saturated</u>
Uniform sand		
loose	1442	1890
dense	1746	2082
Mixed sand		
loose	1586	1986
dense	1858	2163
Clay		
stiff glacial	-	2066
soft, very organic	-	1426

(from Terzaghi and Peck, 1967: in USACE, 1984)

TABLE XXIX
PUGET ISLAND SAND CHARACTERISTICS

Examined for grain density, bulk
densities, and porosity

<u>Sand</u>	<u>Dry loose unit weight, kg/m³</u>	<u>Average Sp. Gravity</u>
PUGET ISLAND		
Channel Dredge porosity = 0.46	1390	2.60
Beach Face porosity = 0.46	1410	2.59
Dune Crest (eolian) porosity = 0.44	1450	2.57
Dune Trough (") porosity = 0.45	1400	2.53
GULL ISLAND		
Active beach face porosity = 0.48	1360	2.64
porosity = 0.42	1380	2.39
MEAN OF SAMPLES (excluding dune sand)		
mean porosity = 0.46	1385	2.56

Sieved Versus Settling Tube Grain Size Analysis

Calibration of the settling tube was compared to the sieve analyses. There is a difference between the two types of analyses, with the settling tube giving a finer distribution than the sieved distribution. The settling tube also suggested a more normal distribution with a slightly positive skew (Φ), not distinguishing a slightly bimodal character of the sediment population which was

TABLE XXX
GRAPHICAL STATISTICS OF COLUMBIA RIVER SANDS
Price, Puget, and Gull Islands, 1987-88.
(All numbers are in phi)

<u>Sample</u>	Standard				
	<u>mean</u>	<u>median</u>	<u>dev.</u>	<u>skew.</u>	<u>kurt.</u>
Scarp face	1.69	1.73	0.44	-0.08	0.88
Beach face	1.87	1.88	0.36	-0.03	0.95
Beach Berm face	1.73	1.76	0.51	-0.06	1.42
Eolian Dune Crest	0.53	0.35	0.69	0.26	0.59
Trough	1.89	1.88	0.44	0.02	1.01

observed in sieve analysis. The interpolated grain size distribution from sieve analysis was compared to a whole sample settling tube size distribution for the two samples and is presented in Figure 96 (grain size curves A-D). Table XXXI presents the graphical statistics for each of these populations.

The distribution of sample grain settling velocities was accurately obtained from the settling tube system. Grains trapped with the bedload sampler (of the shallow water trap arrays) showed higher settling velocities than the sand moved in suspension, as presented in Table XXVI giving data for the passage of the ship "Magnolia". Figure 97 presents a cumulative percent graph of the settling velocities of a representative beach sample.

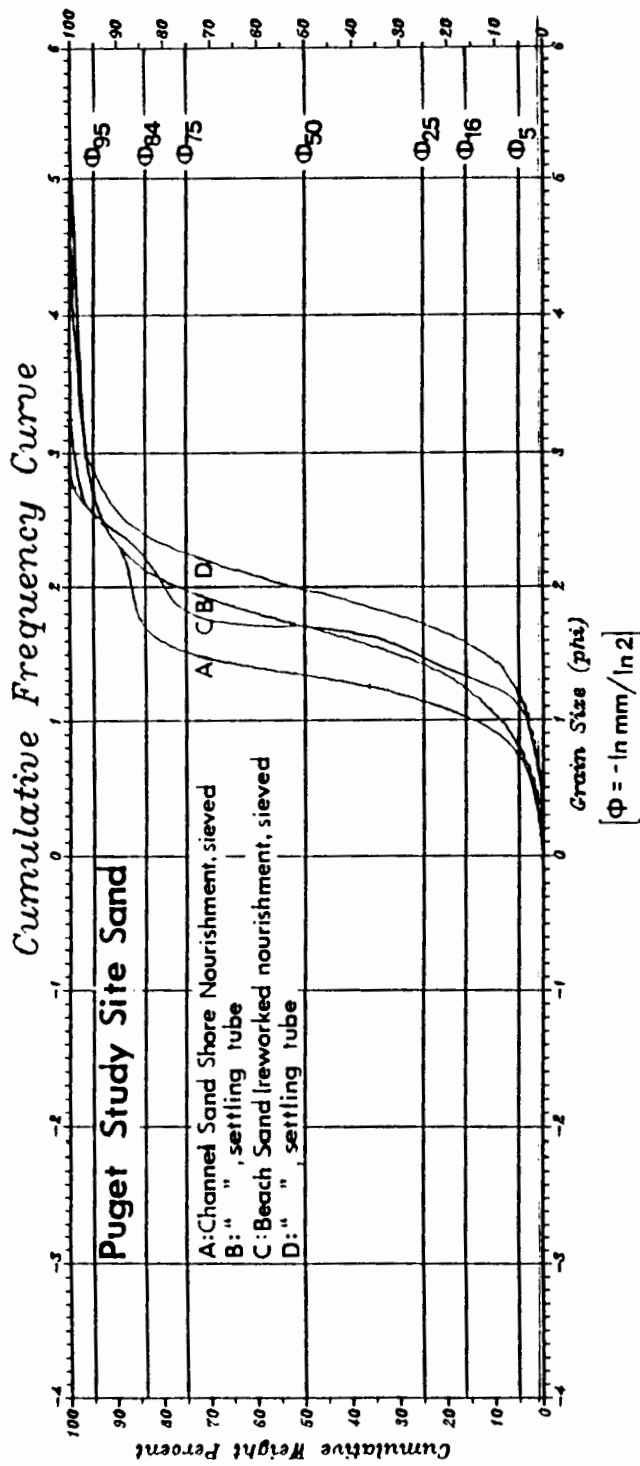


Figure 96. Sediment size distribution curves. For study site sands, using both sieving and settling tube analysis.

TABLE XXXI
GRAIN SIZE STATISTICS
SAMPLES

	<u>A</u>	<u>B</u>	<u>C</u>	<u>D</u>
Mean	1.36	1.69	1.75	1.99
Std. Dev.	0.48	0.52	0.46	0.46
Sorting	well	moderate	well	well
Skewness	0.183 positive	0.005 normal	0.180 positive	0.063 normal
Kurtosis	1.725	1.390	1.685	1.250
peakedness	leptokurtic	leptokurtic	very lepto.	lepto.

Petrography

All sediment samples examined for petrography were derived from dominantly volcanic terrain. This is characteristic for drainage basins west of the Cascades in the Pacific northwest. Samples also include mineral and rock fragments with a crystalline provenance terrain, such as the eastern drainage of the Columbia River. Such crystalline grains include: monocrystalline quartz, schistose rock fragments, potassium feldspar, muscovite, biotite (also found in Cascade dacites and andesites), garnet, spinel, and monazite. These crystalline grains are rare, not occurring with the abundance of the volcanic plagioclase and rock fragments likely derived from the Cascades. Figure 98 presents pie charts illustrating the abundance of primary rock fragments, minerals, and heavy minerals in the lower Columbia River sands.

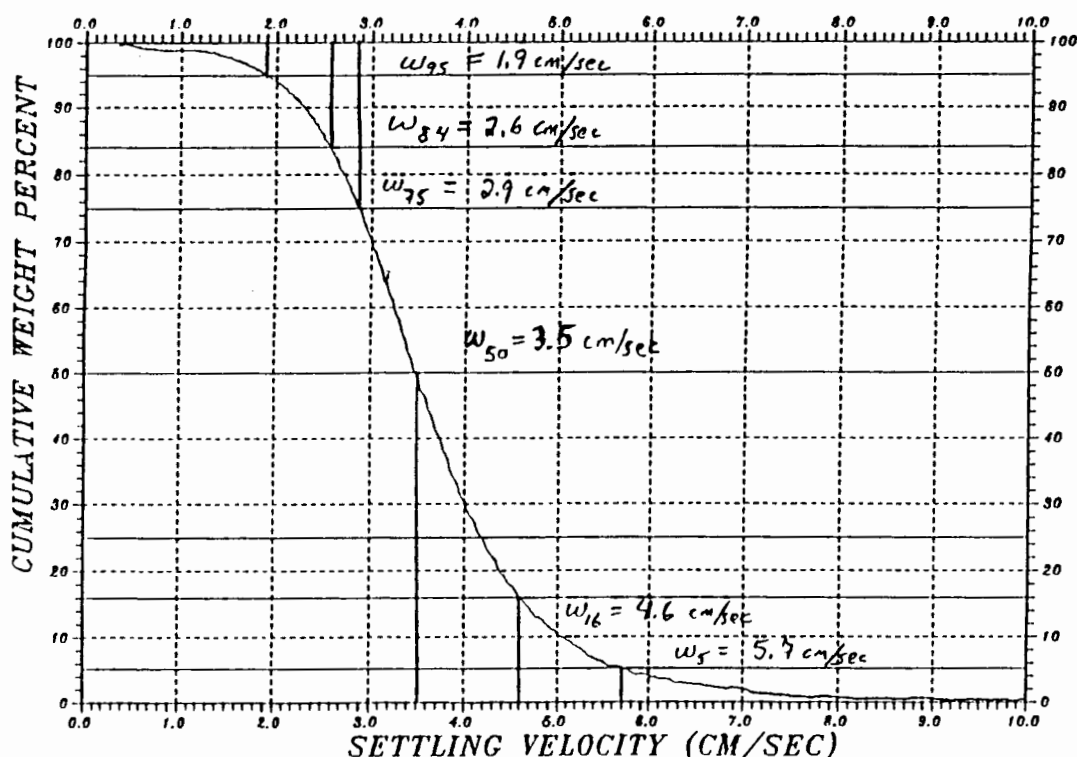
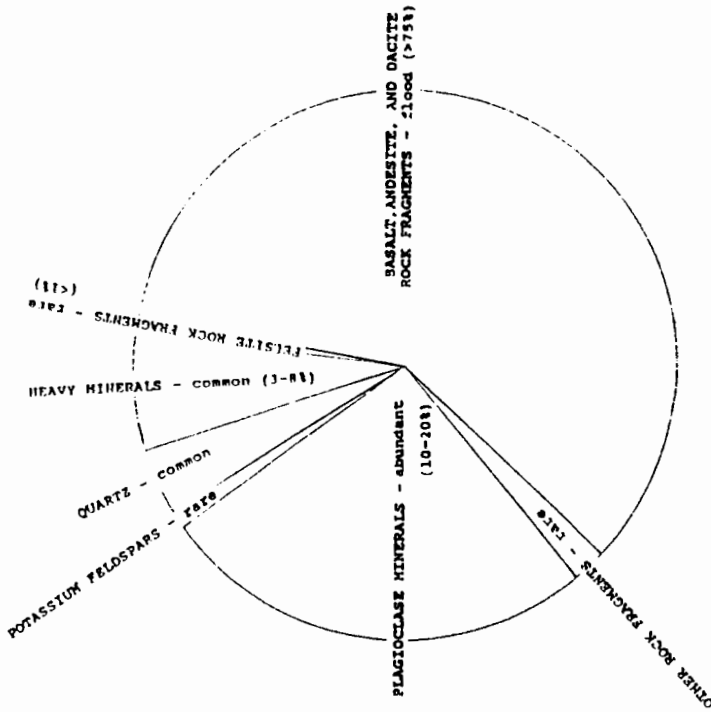


Figure 97. Settling velocities, Puget Island sand. Beach face sample, June 1988.

Grain mounts made of several size fractions were used to determine any relationship between petrography and grain size in the sand population. Two distinct mineral groups were examined, plagioclase and opaque (heavy) minerals. The general hypothesis is that no variation in the percentage of plagioclase with grain size would exist because the characteristically ubiquitous distribution of plagioclase in sediments derived from a volcanic source terrain. Heavy mineral percentages average 10% of the total number of grains and are generally found to increase with finer size fractions as found in other estuarine and

PERCENT COMPOSITION OF THE 18-125 MESH SIZE SANDS.

PRICE ISLAND WASHINGTON
Based on 500 points, 21JUN67



APPROXIMATE PERCENT HEAVY MINERALS OF PRICE ISLAND SAND

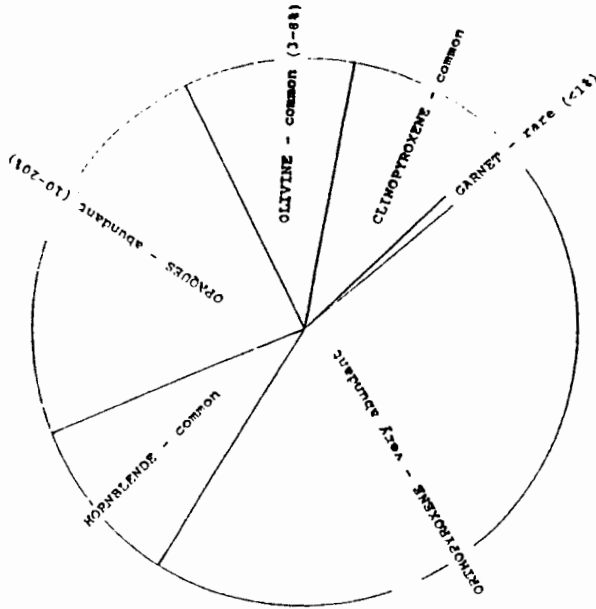


Figure 98. Petrography of lower Columbia sand. Price Island, Washington.

coastal sands (Peterson and others, 1985). Table XXXII presents a simple linear regression and student's t test of significance of the plagioclase content in five size fractions of a one Puget Island site sand. Table XXXIII presents an identical analysis of the opaque content.

The student's t test at the 10% level for the plagioclase-size correlation revealed that the correlation was not significantly different from zero and there is no significant correlation. The same test on the opaque-size correlation revealed a significant difference from zero to the 2.5% level, there is a correlation between increasing opaque percentages with decreasing size fractions.

Figure 99 illustrates the relationship between the percent composition of some of the major minerals and rock fragments found in different grain size ranges. A variety of distinct sedimentary features observed were enhanced by the assemblage of minerals and rock fragments found in the lower Columbia River sand. Hydraulic and aeolian actions segregate the rock and mineral assemblage to form structures that can be preserved in the shore/beach stratigraphy, offering clues in deducing the dominant processes of a sedimentary environment.

TABLE XXXII

LINEAR REGRESSION: PLAGIOCLASE AND GRAIN SIZE

Linear regression and student t test of the percentage of plagioclase in varying size fractions of a Puget Island sample of modern Columbia River channel sand.

n	x_n (phi)	y_n (%)	x^2	xy	y^2
1	-0.50	31.58	0.25	-15.79	997.30
2	0.88	27.33	0.77	24.05	746.93
3	1.88	26.33	3.53	49.50	693.27
4	2.88	32.00	8.29	92.16	1024.00
5	<u>3.88</u>	<u>19.33</u>	<u>15.05</u>	<u>75.00</u>	<u>373.65</u>
$\Sigma_{i=1}^n = 9.02$		136.57	27.89	224.92	3835.15

$$\begin{aligned}
 &_0 = 30.64 \quad \beta_1 = -1.846 \quad y = 30.64 - 1.846 x \\
 S &= 65.30 \quad \Gamma = 1 - (SSE/SST) \quad SST = \Sigma y^2 - (\Sigma y)^2/n = 104.88 \\
 &= \text{correlation}(r) = 0.38 \\
 &1.638 \text{ for } 10\% \text{ level} \\
 &\text{calculated } t = (\Gamma(n-2)^{0.5}) / (1-\Gamma^2)^{0.5} = 0.711
 \end{aligned}$$

thus correlation is not significantly different than zero.

TABLE XXXIII

LINEAR REGRESSION: OPAQUE MINERALS AND GRAIN SIZE

Linear regression and student t test of the percentage of opaque minerals in varying size fractions of a Puget Island sample of modern Columbia River channel sand.

n	x_n (phi)	y_n (%)	x^2	xy	y^2
1	-0.50	13.16	0.25	- 6.58	173.18
2	0.88	16.67	0.77	14.67	277.89
3	1.88	41.67	3.53	78.34	1736.39
4	2.88	29.67	8.29	85.45	880.31
5	<u>3.88</u>	<u>59.00</u>	<u>15.05</u>	<u>228.92</u>	<u>3481.00</u>
$\Sigma_{i=1}^n = 9.02$		160.17	27.89	400.80	6528.77

$$\begin{aligned} \beta_0 &= 142.83 & \beta_1 &= 9.61 & y &= 142.83 + 9.61 x \\ \text{SSE} &= 114.22 & \Gamma &= 1 - (\text{SSE}/\text{SST}) & \text{SST} &= \Sigma y^2 - (\Sigma y)^2/n = 1417.89 \\ \Gamma &= \text{correlation}(r) = 0.92 \\ t &= 1.638 \text{ for } 10\% \text{ level, } 2.353 \text{ for } 5\%, 3.182 \text{ for } 2.5\% \\ &\text{calculated } t = (\Gamma(n-2)^{0.5}) / (1-\Gamma^2)^{0.5} = 4.06 \end{aligned}$$

thus correlation is significantly different than zero.

Petrography of Columbia River Sand

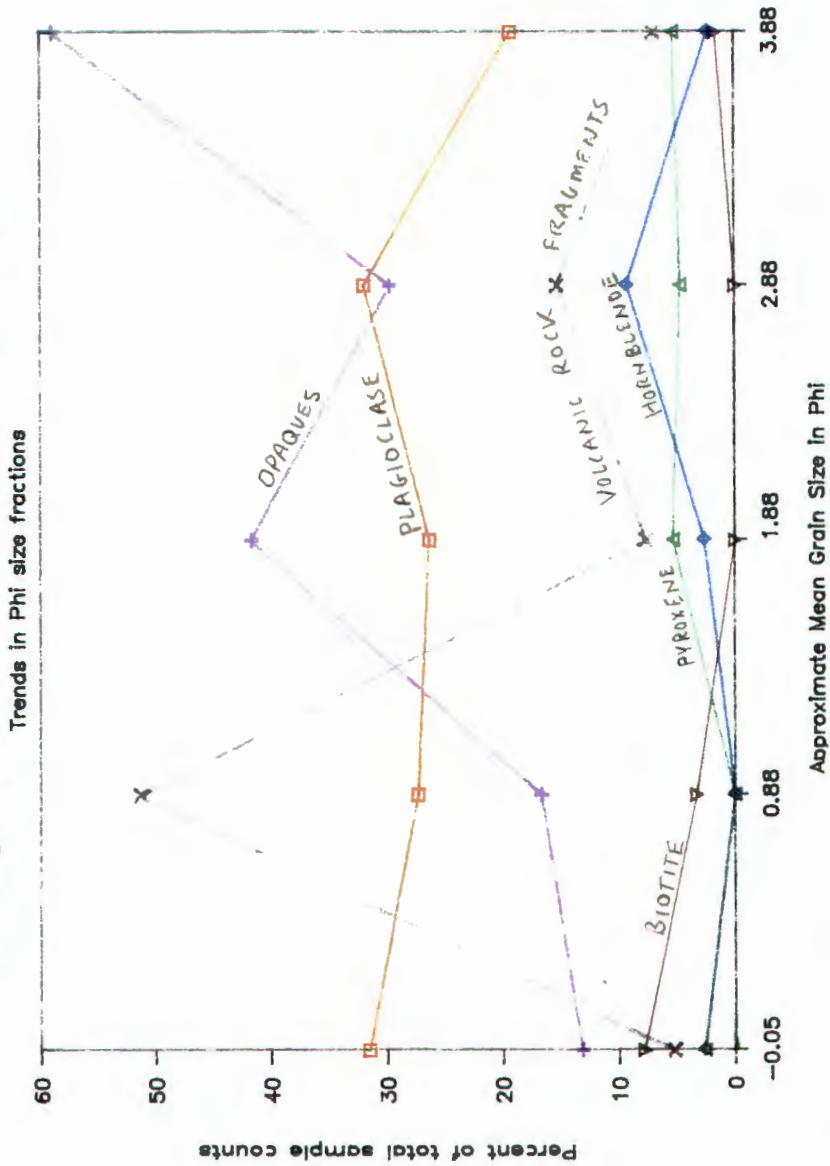


Figure 99. Relationship between grain size and petrography in lower Columbia sand. Phi sizes represent intermediate grain axis length.

CONCLUSION

The shore slopes of the lower Columbia River reflect a variety of physical processes. Ship waves play an important role in the transport of sediments in the shallow water regions of shore slopes in proximity to the navigation channel. Theoretical derivations and data collected in the field suggest that ship wave generated currents instigate sediment movement.

SHORE EROSION

The results of examining historic aerial photographs and map records showed that Price Island and Puget Island have traditionally experienced erosion. Gull Island has experienced a accretion with time due to dredge disposals.

Profiling of three study sites shows a considerable variation in the rates of erosion along beach nourishments of the Puget Island Region of the lower Columbia River.

Hypothetically, the most rapid loss of sand is expected immediately after nourishment since that is the period in which the artificial deposit is most unstable. But this could not be substantiated by this study and can be misleading in the case of shore notches which can exhibit high erosion rates well after emplacement of the nourishment. Profiling revealed that the shore notch

exhibits a much higher rate of erosion than any other locality along a site.

Two sites, Price Island and Puget Island both displayed local zones of very high erosion as well as apparently stable beach slopes. The Gull site showed some erosion after nourishment, but in general remained a stable site. The total estimates of sand lost in the shallow water nearshore zone are presented in Table XXXIV.

TABLE XXXIV
STUDY SITE EROSION

<u>1988 Site</u>	July 1987 - July
	<u>Volume Lost (m³)</u>
Price Island, WA	27,729
Puget Island, WA	26,197
Gull Island, OR	4,266

GEOMORPHIC OBSERVATION AND DEVELOPMENT

A variety of distinct and characteristic geomorphic forms of an active sandy shoreline have been described. The shore forms and sedimentary structures presented in this study show that sand is reworked by several physical processes that include; wind, wind generated water waves, tidal fluctuations, and ship waves.

Beach scarps are strong evidence of continued wave action and unstable beach slopes. Beach scarps suggest

active sediment contribution to the beach face. On a smooth beach face at the northwest end of Puget Island, Washington, sediment transport analyses showed a net offshore flux. Wave generated features were the most common structures observed on the shore surface and trench stratigraphy. The lack of some structures, such as ripples not being preserved in beach stratigraphy is the result of ship wave actions.

The shore notch is composed of two components: an erosive scarp in the upper beach and an accreting lobe on the lower beach face. The shore notch is attributed to ship wave actions. The shore notch was shown to be a zone of accelerated erosion in which sand is transferred from the upper beach nourishment to the beach face. Sediment character across the shore notch shows a distinct grain coarsening toward the notch.

SEDIMENT TRANSPORT

Observations of sedimentary structures at the study sites and sediment trap data from the Puget Island site show that wind instigates sediment entrainment in both the subaerial and shallow subaqueous environments. This sediment entrainment appears to account only for a small portion of total sediment transport. Wind and water wave actions are responsible for the retreat of beach scarps. Wind generated water waves create ripple bedforms in

shallow water, but apparently cause very little net sand transport. During peak freshwater currents, sediments begin to move in shallow water depths of 50 cm and more, with increasing flux in deeper water. Sediment transport by ebb currents is not important in water depths less than two meters along the Puget Island site.

SHIP WAVES

Ship waves are a set of waves that vary greatly in size and period. This study has used established theory regarding the drawdown wave (long period) and the maximum secondary wave (short period) to show that both types of waves are capable of moving sand in shallow water regions. The direction in which sand particles move on the beach surface can also be predicted by calculating the near-bed shear velocities vectors.

Local land owners along the river remarked upon the impact of ship generated waves on the shore. Resident observations have been noted in reports on analogous systems in North America and Europe. Ship wave observations made along the lower Columbia River are similar to those in other works (Ofuya, 1970; Sorensen, 1973; Sorensen and Weggel, 1984; Span and others, 1981; Balanin and others, 1981).

A significant difference in draft between ships moving downstream and those moving upstream could not be

established. Downstream passage of deep draft ships should instigate greater sediment transport than upstream passage, because of the increased displacement of outbound ships. Data suggests no significant difference between downstream ship velocities versus upstream velocities. Holding velocity constant the most critical variables become ship draft and channel cross-sectional area. Because most deep draft ships time their outbound passages to coincide with high water elevations, the increased channel cross-sectional area will dampen the effect of increased ship draft, thus it is possible that the increased draft of outbound ships may would not cause a substantial increase in the size of waves generated by the same ship on its inbound passage. But geomorphic observations show the net longshore sediment transport is downstream, suggesting that outbound ships have a greater impact than inbound ships. The other explanation of the downstream longshore sediment transport is that ebb currents have a greater impact than observed in this study, such as during anomalous storm events, high flow releases, and/or spring tides.

Sediment Transport by Ship Induced Water Motions

Ship waves deliver energy to the shore in the form of several distinct water motions. These hydraulics are responsible for a part of the sediment transport along the shore slope. The magnitude of each wave set dictates the

manner in which sediment transport occurs. The problem of examining ship wave processes in a channel such as the lower Columbia River involves a complicated set of processes. A simple model was delineated and applied to sediment transport on a smooth beach face at the Puget Island study site. The illustrates the movement of sand and resulting changes in a beach form. Over time the upper beach undergoes degradation, the lower beach experiences aggradation, and net longshore drift results in accretionary lobes of sand, as observed at the north end of the Puget site. This model (3,600 ship passages) estimated an offshore sediment flux between $1,028 \text{ m}^3$ to $6,364 \text{ m}^3$ for the Puget Island site, 4 to 24 percent of the surveyed sediment volume that eroded. Using the sediment transport caused by the waves of naval ships, an upper limit of offshore sediment flux was derived using the same method to be $73,478 \text{ m}^3$, 2.8 times the $26,197 \text{ m}^3$ that eroded from the site.

The model was based on measured sediment flux at points on the beach face. These point samples give a limited distribution of flux through the surf zone that is unlikely to record the peak flux actually occurring. Because sediment flux through the surf zone is interpreted to have an exponential distribution perpendicular to the shoreline, the change in flux over a relatively small distance near the line of wave breaking can be dramatic.

Thus the maximum measured flux is unlikely to represent the maximum point flux, as illustrated in Figure 100. The maximum measured flux must be less than or equal to the true maximum flux, as seen in Figure 100. It is concluded that the maximum error, up to several orders of magnitude, is introduced in the field sampling method of measuring flux only at single points.

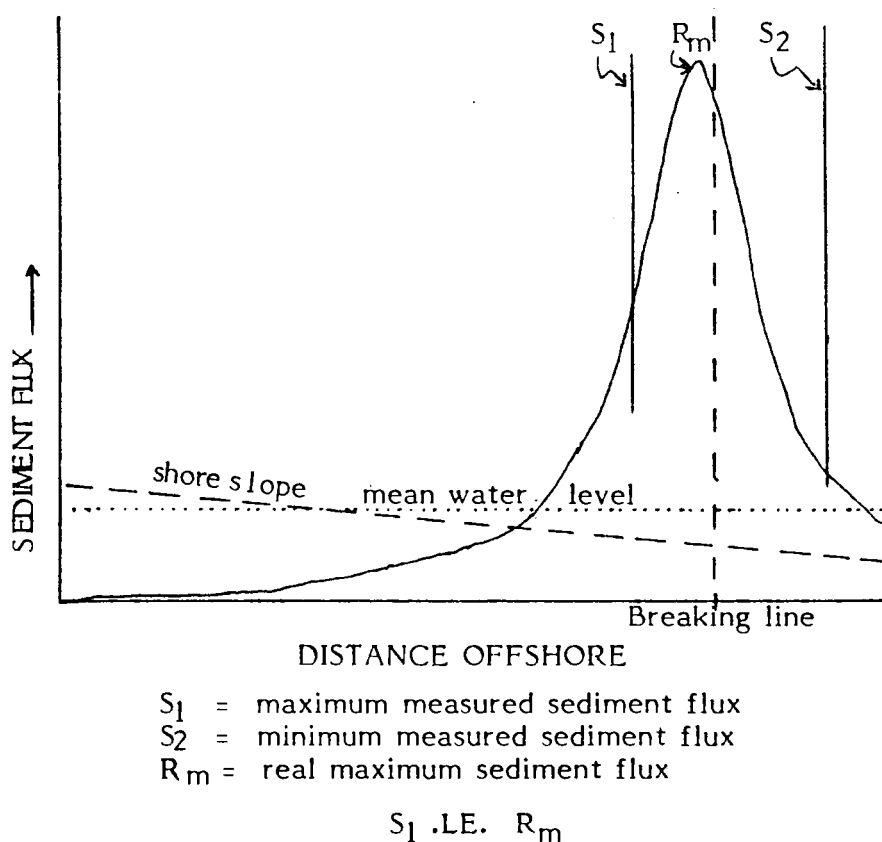
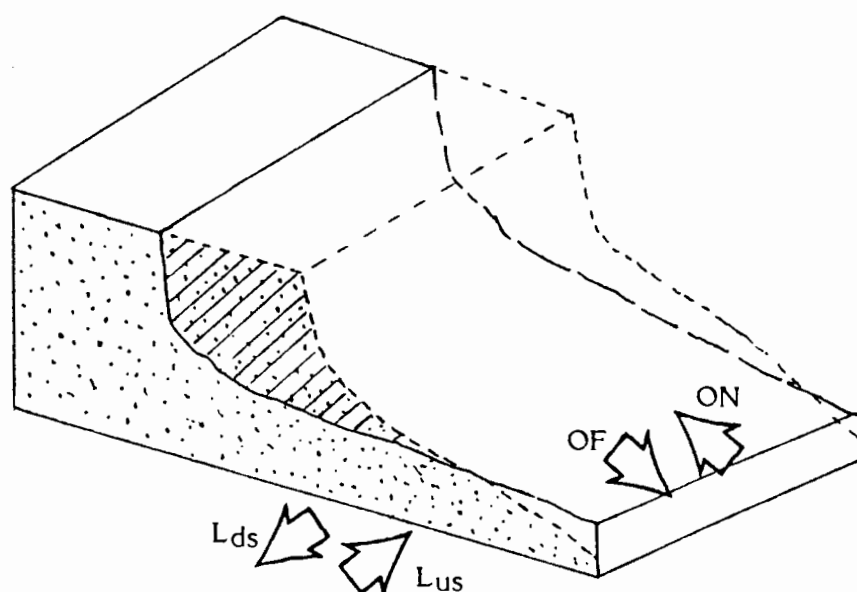


Figure 100. Surf zone sediment flux distribution. Interpretation of true flux distribution through the surf zone and measured points.

MASS BALANCE OF MEASURED VALUES AND SOURCES FOR ERROR

The difference between sediment moving into and out of a beach cell provides a measure of accuracy of sediment transport measurements and extrapolations, based on the conservation of mass. A mass balance, as schematically presented in Figure 101, was done using measures of sediment transport on the shore slope, in the shallow water intertidal region. Particular factors introducing error in the mass balance equation and used to resolve mass discrepancy of sediment transported along the shore. I suggest that the largest source of error is the maximum value of measured sediment offshore flux by trap used to represent maximum point flux. It has been presented that offshore flux dramatically increases through the surf zone and decreases rapidly beyond the breaking line in this study and other investigations (Kraus, 1987; King, 1972; Hallimeier, 1982).

Because of peaked distribution of sediment flux in the surf zone, measuring the point of maximum flux is nearly impossible without a continuous sampling regime through the surf zone. Accurate wave predictions can enable the best positioning of limited number of samplers. Using the point sampling regime established in this study, it was unlikely to sample the true peak flux. The value of flux used in the sediment transport extrapolations



= Original sand disposal (shore nourishment)



= Sand volume eroded after time t



= Sediment transport

OF = offshore transport; ship waves, wind waves, gravity

ON = onshore transport; ship waves, wind waves

L_{ds} = longshore transport; ship waves, wind waves, ebb currents

L_{us} = longshore transport; ship waves, wind waves, flood tide currents

Ideal mass balance: mass into beach cell = mass out of beach cell

Figure 101. Mass Balance. Schematic illustration of mass balance in near-shore beach cell, such as the Puget Island site.

presented are assumed to underestimate peak flux, probably by several order of magnitudes.

An annual ebb current sediment transport rate along the shore was calculated to be approximately 12 cubic meters.

Using the maximum measured longshore transport measured for the ship passages observed of 18.2 kg/m in the upstream direction and a zone of transport perpendicular to the shoreline of 5 meters, and 1,500 (one way) ship passages per year reveals an annual transport volume of 98 cubic meters. Because ships also move in the opposite direction, there is a transport component that would negate part or all the extrapolated value of 98 cubic meters per year. Based on theoretical derivation of ship waves (Havelock, 1931; Saunders, 1975; Sorensen and Weggel, 1984; Johnson, 1968; Constantine, 1961; and others) and field observations (Ofuya, 1970; Brebner and others, 1966; Sorensen, 1973) identical ships with the same displacement moving at increasing velocities will cause an increase in wave height proportional to ship velocity squared; for ships moving at the same velocity but with increased displacement, the relationship to wave height is less clear, but wave height does increase. Barrass (1979) presented ship squat (ship draft relative to the bed, not the water surface) to be a linear function of the blockage factor; the blockage factor is the ship's cross sectional

area relative to the channel cross sectional area. It is assumed from the observations made during this study and the Columbia River Pilots, there is no consistent difference in the velocity of upstream and downstream ships in the lower Columbia River navigation channel. But it is clear that a dramatic difference exists between the displacements of ships moving upstream and downstream in the lower Columbia (USACE, Waterborne Commerce, 1970-1986; Columbia River Pilots, 1987-1988). The lower Columbia navigation system exports 4 to 6 times the tonnage that is imported (main exports are bulk commodities: grain and timber). It can be deducted from higher export tonnages and assuming equivalent ship velocities, that will be a net downstream longshore sediment flux. The records of this study did not substantiate that outbound moving ships move more sediment along the shore than inbound moving ships. But a export tonnage of 4 times the import tonnage and a proportional increase in the impact of ship waves, the resulting downstream longshore sediment flux would be about $74 \text{ m}^3/\text{year}$.

Equation (23) presents the mass balance solution of sediment into and out of the Puget Island site:

$$Q_t = L_{ds} - L_{us} + L_{de} - L_{uf} + L_w - On_s + Of_s - On_w + Of_w \quad (23)$$

Q_t = Total sediment removed from site

L_{ds} = Downstream longshore transport by ship
waves

L_{us} = Upstream longshore transport by ship waves

L_{de} = Downstream longshore transport by ebb current

L_{uf} = Upstream longshore transport by flood current

L_w = Longshore transport by wind generated water waves (net upstream)

On_s = On-shore transport by ship waves

Of_s = Off-shore transport by ship waves

On_w = On-shore transport by wind generated water waves

Of_w = Off-shore transport by wind generated water waves

The values of each of factors (cubic meters):

$$Q_t = 26,197$$

$$L_{ds} = 98$$

$$L_{us} = 24$$

$$L_{de} = 12$$

$$L_{uf} = 0$$

$$L_w = 1$$

$$On_s = 23,397$$

$$Of_s = 29,761$$

$$On_w = 0$$

$$Of_w = 0$$

$$(On_w > Of_w)$$

Merchant ship wave derivation (cubic meters of sand):

$$26,197 = 98 - 24 + 12 - 0 + 1 - 23,397 + 29,761 - 0 + 0$$

$$26,197 = -6,451$$

Naval ship wave derivation (cubic meters of sand):

$$26,197 = 98 - 24 + 12 - 0 + 1 - 119,764 + 46,286 - 0 + 0$$

$$26,197 = -73,391$$

$$\text{Error} = -47,194$$

No sediment mass was ever observed to be moved off- or on-shore by wind waves (on_w off_w), but a conservative estimate was calculated using the same proportions found between longshore transport and on- offshore transport by ship waves.

The discrepancy between the total volume eroded from the Puget Site beach and the amount moved from the site by the dominant physical factors can be only postulated by considering the most reasonable sources of error. Because offshore transport by ship waves accounted for the vast majority of observed sediment transport, it is concluded that under mean weather and river flow conditions such as those observed, it is ship waves that instigate the vast majority of sediment transport. This conclusion is based on the fact that even though ship waves occur as an anomalous event, the energy to they deliver to the shore usually exceeds the threshold conditions for transport of the bed material whereas other processes observed such as wind and ebb currents do not sufficiently surpass threshold conditions to cause appreciable sand transport. It is the instantaneous energy (in the form of a shear force) that will determine the importance of a process in sediment

transport. Even if the cumulative energy delivered to the shore by wind generated water waves or tidal currents exceeded the cumulative ship wave energy, if the instantaneous energy supplied by these processes cannot surpass the threshold conditions of the sediment, the processes are secondary to ship waves. The error in the mass balance is probably not an unaccounted process, but rather an error in representative measure of maximum sediment transport by ship waves.

The other plausible source of error comes from the impact of anomalous storm, spring tide, or high flow release events. A storm generating waves similar size in to ship generated waves could in one day (twenty-four hours) do as much (more given concentration of energy in small period of time) sediment transport as about 480 ships (a two month period). Further observations during times of high river discharge and storm events are needed to evaluate the importance of these events in near-shore shallow water sediment transport.

SEDIMENT CHARACTER

The sediments of the Columbia River channel in the Puget Island study region are primarily composed of a well sorted fine to medium subrounded to angular volcanoclastic sand. Some of the muscovite population seen in the lower Columbia sands may be recycled mica of the regional

sedimentary formations such as the Astoria, not necessarily the exclusive product of the Columbia River's present-day eastern plutonic drainage terrains.

Settling tube analysis suggests that the sand populations behave unimodally in their settling velocities. The anomalous grains in the population exhibit distinct preference on the beach, such as pumice swash at high water lines, heavy mineral banding along high water berms. Thus certain sediments can act as excellent markers on the beach face for the interpretation of different hydraulic regimes.

FUTURE WORK

Much of the work done in this study has brought to bear questions concerning the lower Columbia River's shore response to the primary physical processes of tidal currents, wind, and ship waves.

Suggestions concerning the nearshore sediment trap array and elaborating on a sediment flux model include:

Sample at more locations in a line perpendicular to the shoreline to define a function more descriptive of sediment transport in a unit cell of beach.

Account for wave refraction, changing wave incidence along a unit beach or use a step function model that splits up site into cells based on changes in wave characteristics.

Examine transport in deeper water, the channel slopes in depths between 2 to 8 meters.

Better estimate ship distance from shoreline.

REFERENCES

- Abbe, T., 1988a, Report on the Geology and Geomorphology of Price Island, WA, In: US Army Corps of Engineers Portland District, Price Island Erosion Control Study, Reconnaissance Report, September 1988, Portland, OR.
- Abbe, T., 1988b, Ship wave theory and shallow water sediment transport in the Lower Columbia River, U.S.A. [abs.], Pacific Northwest American Geophysical Union 35th Annual Meeting Abstracts, Victoria, Canada.
- Abbe, T., 1989, Wave energy and resulting sand transport on the shore slopes of the Lower Columbia River, WA and OR, In: Coastal Zone 89 Proceedings, paper 226, American Society of Civil Engineers, Charleston, SC.
- Abbe, T., Johnson, A. J., Thoms, R. E., and Eriksen, K., 1988, Nearshore sand transport by wave energy on the shore slopes of the Columbia River, the Puget Island Reach, Oregon and Washington [abs.], Oregon Academy of Sciences 1988, Portland State University, Portland, OR.
- Abbe, T., and Phan, T., 1987, A preliminary report on the design and implementation of a sediment transport study on the shore slopes of the Columbia River in the Puget Island Reach, Oregon and Washington [abs.], Pacific Northwest Region of the American Geophysical Union 34th Annual Meeting Abstracts, Olympia, WA.
- Abou-Seida, M.M., 1965, Bedload function due to wave action, Hydraulic Engineering Laboratory, Wave Research Projects, University of California, Institute of Engineering Research Technical Report HEL-2-11, Berkeley, CA.
- Airy, G.B., 1845, On tides and waves: Encyclopedia Metropolitana, v.5, pp. 241-396.
- Allen, J.E., 1987, Cataclysms on the Columbia, Timber Press, Portland, OR, 211 p.

- Allen, P.A., 1981, Wave-generated structures in the Devonian lacustrine sediments of south-east Shetland and ancient wave conditions, *Sedimentology*, v.28, pp. 369-379.
- Anderson, L., 1985, The development of modern Columbia River navigation, *Bulletin of the Permanent International Association of Navigation Congresses*, no.51, pp. 37-43.
- Ando, M. and Balazas, E.I., 1979, Geodetic evidence for a seismic subduction of the Juan de Fuca plate, *Journal of Geophysical Research*, v.84, pp. 3023-3028.
- Araya-Vergara, J.F., 1986, Toward a classification of beach profiles, *Journal of Coastal Research*, v.2, pp. 159-165.
- Bagnold, R.A., 1946, Motion of waves in shallow water; interactions between waves and sand bottom, *Proceedings of the Royal Society, (London)*, series A, 187:1-15.
- Bagnold, R.A., 1963, Beach and Nearshore Processes, IN: Thorne, C.R., MacArthur, R.C., and Bradley, J.B.[eds.], 1988, *The Physics of Sediment Transport by Wind and Water*, American Society of Civil Engineers, NY, NY, pp. 188-230: Article originally published in: Hill, M.N.[ed.], 1963, *The earth beneath the Sea*, vol. 3 of "The Sea--Ideas and Observations on Progress in the Study of the Seas, Wiley-Interscience, London, pp.507-553.
- Bagnold, R.A., 1966, An approach to the sediment transport problem from general physics, *U.S. Geological Professional Paper 422-I*, Washington, D.C., 37 p.
- Bagnold, R.A., 1983, The nature and correlation of random distributions, *Proceedings of the Royal Society of London, Series A*, v.388, pp. 273-291.
- Bagnold, R.A., and Barndorff-Nielsen, O. E., 1980, The pattern of natural size distributions, *Sedimentology*, v.27, pp. 199-207.
- Balanin, V., Bykov, L., Zernov, D., Metelytsina, G., and Natalchishin, G., 1981, Means of protecting waterway slopes and beds from streams and waves, including ship effect, *Inland & Maritime Waterways & Ports, Section I Inland Waterways & Ports*, vol.1, 25th International Navigation Congress, Edinburgh, pp.167-182.

- Barrass, C.B., 1979, A unified approach to "squat" calculations for ships, Permanent International Association of Navigation Congresses, v.1, pp. 3-10.
- Bascom, W.N., 1951, The relationship between sand size and beach face slope, Transactions of the American Geophysical Union, v.32, pp.866-874.
- Beeman, O., 1985a, Studies to control shoaling of the navigation channel, Lower Columbia River, unpublished report to Portland District Operations Branch of U.S. Army Corps of Engineers, Portland, OR.
- Beeman, O., 1985b, Channel optimization - the Columbia River deep draft navigation project, Permanent International Association of Navigation Congresses Bulletin, no.51, pp.44-51.
- Bekendam, A.J., Blok, P.M, de Boer, W., Bos, M., Brolsma, J.U., van der Burg, J., Deelen, C., van Doorn, J.T.M., Filarski, R., Havinga, H., Heinen, H.G., Koeman, J.W., Leemans, J.A.A.M., Rem, A., Schulffel, H., van Schuylenburg, M., Steentjes, J.B.W., Verney, H.J., Veldhuyzen, W., de Vries, W., Wels, H., van der Weijde, R., [Brolsma, J.U.(Coordinator)], 1988, Six-Barge Pushtow Trials, Bulletin of the Permanent International Association of Navigation Congresses, no.62, pp. 21-84.
- Bidde, D.D., 1968, Ship waves in shoaling water, Hydraulic Engineering Laboratory College of Engineering, University of California, Berkeley, CA, 32 pp.
- Birkemeier, W.A., 1988, The interactive survey reduction program (ISRP), version 1.25, Feb. 1986, U.S. Army Waterways Experiment Station, Vicksburg, MI.
- Blatt, H., Middleton, G., and Murray, R., 1980, Origin of Sedimentary Rocks, 2nd Ed., Prentice-Hall, Inc., Englewood Cliffs, NJ.
- Borgeld, J.C. and others, 1978, A geological investigation of sedimentary environments at sites E, G, and H, near the mouth of the Columbia River, University of Washington Department of Oceanography, Seattle, WA; In: Gordon, M. (chairs), 1980, A literature survey of the Columbia River Estuary, v.II, Annotated Bibliography, Columbia River Estuary Data Development Program, Pacific Northwest River Basins Commission, Vancouver, WA.

- Brebner, A., Helwig, P.C., and Carruthers, J., 1966, Waves produced by ocean-going vessels: a laboratory and field study, IN: 10th conference on Coastal Engineering, chapter 28, Tokyo, Japan, pp. 455-465.
- Brenninkmeyer, B.M., 1975, Frequency of sand movement in surf zone; Proc. 14th conf. on coast. eng., pp.812-827.
- Chelton, D.B. and Davies, R.E., 1982, Monthly mean sea-level variability along the west coast of North America, Journal of Physical Oceanography, v.12, pp.757-784.
- Clemens, K.E. and Komar, P.D., 1988, Oregon Beach-sand compositions produced by the mixing of sediments under a transgressing sea, Journal of Sedimentary Petrology, v.58, no.3, pp. 519-529.
- CRPA (Columbia River Pilots Association), 1987-1988, Data on Vessel Drafts (unpubl.), Columbia River Pilots Association, Portland, OR.
- Constantine, T., 1960, On the movement of ships in restricted waterways, Journal of Fluid Mechanics, v.9, pp. 247-257.
- Constantine, T., 1961, The behavior of ships moving in restricted waterways, Institution of Civil Engineers, Proceedings, v.19, London, pp. 549-562.
- Cook, D.O. and Gorsline, D.S., 1972, Field observations of sand transport by shoaling waves, Marine Geology, v.13, pp. 31-55.
- Crowson, R.A., Birkemeier, W.A., Klein, H.M., and Miller, H.C., 1988, Superduck nearshore processes experiment: summary of studies, CERC Field Research Facility, CERC (Coastal Engineering Research Center), U.S. Army Waterways Experiment Station, Technical Report CERC-88-12, Vicksburg, MI.
- CRWMG (Columbia River Water Management Group, 1988, Columbia River Water Management Report for Water Year 1987, Mark Maher [Chairman], Bonneville Power Administration, Portland, OR.
- Curry, J.R., 1965, Late Quaternary history, continental shelves of the United States, IN: The Quaternary of the United States, Wright, H.E. and Frey, D.G., Princeton University Press, pp.723-735.

- Das, M.M., 1969, Relative effects of waves generated by large ships and small boats in restricted waterways, Technical Report HEL 12-9, Hydraulic Engineering laboratory, University of California, 112 pp.
- Davies, A.G., 1985, Field Observations of the Threshold of Sediment Motion by Wave Action, *Sedimentology*, v.32, p.685-704.
- DeRaaf, J.F.M., Boersma, J.R., and Van Gelder, A., Wave generated structures and sequences from a shallow marine succession, Lower Carboniferous, County Cork, Ireland, *Sedimentology*, v.24, no.4, pp. 451-485.
- Dyer, K.R., 1986, Coastal and Estuarine Sediment Dynamics, John Wiley and Sons, 342 pp.
- Dunne, T. and Leopold, L.B., 1978, Water in Environmental Planning, W. H. Freeman and Co., New York.
- Eagleson, P.S. and Dean, R.G., 1966, Small amplitude wave theory, In: Ippen, A.T.(Ed.), *Estuary and Coastline Hydrodynamics*, McGraw-Hill Book Co., Inc., New York, pp. 1-92.
- Einstein, H.A., 1972, A basic description of sediment transport on beaches, IN: Meyer, R.E.(ed.), 1972, *Waves on beaches and resulting sediment transport*, Academic Press, New York.
- ENR (Engineering News-Record), 1987, McGraw-Hill, Inc., September 3, p.14.
- Eriksen, K.W., 1988, personal communication, research on dredging activities in the Lower Columbia River (unpubl.), MIR (Maintenance Improvement Review, Hydraulics and Hydrology Branch, Portland District, U.S. Army Corps of Engineers.
- Eriksen, K.W., 1989, Columbia River - Puget Island Reach Hydraulic and Sedimentation Analysis, U.S. Army Corps of Engineers Portland District, CENPP-EN-HY memorandum for files (unpubl.), 13MAR1989.
- Farr, L. and Abbe, T., 1987, Sand Dispersal on a Puget Island Beach Along the Columbia River: An Investigation of Quantitative Methods, final research project for G474, Geomorphic Processes, Prof. L. Palmer, Portland State University Geology, Portland, OR, 23 pp.(unpubl.).

- Folk, R.L. and Ward, W.C., 1957, Brazos River Bar: A study in the significance of grain size parameters, *Journal of Sedimentary Petrology*, v.27, pp.3-27.
- Fuehrer, M., Romisch, K., and Engelke, G., 1981, Criteria for dimensioning the bottom and slope protections and for applying the new methods of protecting navigation canals, *Inland & Maritime Waterways & Ports, Section II Maritime Ports and Seaways*, v.5, 25th International Navigation Congress, Edinburgh, pp. 29-40.
- Galvin, C.J., Jr., 1969, Breaker travel and choice of design wave height, *Journal of the Waterways and Harbors Division, American Society of Civil Engineers*, WW2, v.95, paper 6569.
- Galvin, C.J., 1972a, Wave breaking in shallow water, In: *Waves on Beaches and Resulting Sediment Transport*, Academic Press.
- Galvin, C.J., 1972b, A gross longshore transport rate formula, *Proceeding of the 13th Coastal Engineering Conference*, Vancouver, B.C., Canada, July.
- Galvin, C.J., Jr. and Eagleson, P.S., 1965, Experimental study of longshore currents on a plane beach, TM-10, U.S. Army Corps of Engineers, Coastal Engineering Research Center, Washington D.C.
- Gomez, B. and Church, M., 1989, An assessment of bed load sediment transport formulae for gravel bed rivers, *Water Resources Research*, v.25, no.6, pp.1161-1186.
- Goncharov, V.N., 1938, Movement of Sediments in a Steady Stream, ONTI, Moscow.
- Gordon, M. (chairman), 1980, A literature survey of the Columbia River Estuary, v.II, Annotated Bibliography, Columbia River Estuary Data Development Program, Pacific Northwest River Basins Commission, Vancouver, WA.
- Graf, W.H., 1971, *Hydraulics of Sediment Transport*, McGraw-Hill Book Co., 513 pp.
- Guilloton, R.S., 1960, The Waves Generated by a Moving Body, *The Royal Institution of Naval Architects, Quarterly Transactions*, v.102, no.2, pp. 157-173.

- Hails, J. and Carr, A. [Eds.], 1975, Nearshore Sediment Dynamics and Sedimentation, An Interdisciplinary Review, John Wiley and Sons, London.
- Hallermeir, R.J., 1982, Bedload and wave thrust computations of alongshore sand transport, Journal of Geophysical Research, v.87, no.C8, pp.5741-5751.
- Hartmann, D., 1988, The goodness-of-fit to ideal Gauss and Rosin distributions: a new grain-size parameter - Discussion, Journal of Sedimentary Petrology, v.58, no.5, 913-917.
- Hay, D., 1968, Ship waves in navigable waterways, Proceeding of 11th conference on Coastal Engineering, chapter 95, London, England, pp. 1472-1487.
- Havelock, T.H., 1931, Ship waves: the calculation of wave profiles, Proceedings of the Royal Society, Section A, pp. 1-13.
- Heller, P.L., Tabor, R.W., and Suczek, C.A., 1987, Paleographic evolution of the United States Pacific Northwest during Paleogene time, Canadian Journal of Earth Science, v.24, pp. 1652-1667.
- Hertzberg, R., 1954, Wave-wash control on Mississippi River levees, Proceedings of the American Society of Civil Engineers, v.119, pp. 628-638.
- Hjulstrom, F., 1939, Transportation of detritus by moving water, IN: Trask, P.D.(Ed.), Recent Marine Sediments A Symposium, The American Association of Petroleum Geologists, Dover Publications, London.
- Horikawa, K. and Watanabe, A., 1967, A study on sand movement due to wave action, Coast. Eng. in Japan, 10, 39-57.
- Howd, P.A., and Holman, R.A., 1987, A Simple Model of Beach Shore Response to Long Period Waves, Marine Geology, v.78, p.11-22.
- Hubbell, D.W., Stevens, H.H., Skinner, J.V., and Beverage, J.P., 1986, Characteristics and use of Helley-Smith type bedload samplers, U.S. Geological Survey open file report OF86-415W.
- Hubbell, D.W., Laenen, J.M. and McKenzie S.W., 1983, Characteristics of Columbia River Sediment Following the Eruption of Mount St. Helens on May 18, 1980, USGS Circular 850-J.

- Ingle, J.C., 1966, The movement of beach sand, Elsevier, NY, 221 pp.
- Inman, D.L., 1952, Measures for describing the size distribution of sediments, Journal of Sedimentary Petrology, v.22, no.3, pp. 125-145.
- Ikeda, S., 1982, Lateral bed loads transport on side slopes, Technical Notes, Journal of the Hydraulics Division, American Society of Civil Engineers, v.108, no. HY11, pp.1369-1373.
- Ippen, A.T., ed., 1966, Estuary and Coastline Hydrodynamics, McGraw-Hill Book Company.
- Ippen, A.T. and Eagleson, P.S., 1955, A study of sediment sorting by waves shoaling on a plane beach, U.S.Army Corps of Engineers, Beach Erosion Tech. Memo no.63, 83pp.
- Jane's, 1987-88, Jane's Fighting Ships 1987-88, Jane's Publishing Company, Ltd., London, UK, pp. 696-808.
- Jay, D., 1984, Circulatory Processes in the Columbia River Estuary, Final CREDDP Report (Columbia River Estuary Data Development Program), CREST (Columbia River Estuary Study Taskforce), Astoria, OR, 169 pp.
- Johnson, J.W., 1956, Dynamics of Nearshore Sediment Movement, Bulletin of the American Society of Petroleum Geology, 40, no.9, pp. 2211-32.
- Johnson, J.W., 1958, Ship waves in navigation channels, IN: 6th Conference on Coastal Engineering, chapter 40, ASCE, pp. 666-690.
- Johnson, J.W., 1968, Ship waves in shoaling waters, Proceedings of 11th conference on Coastal Engineering, chapter 96, London, England, pp. 1488-1498.
- Katori, S., 1982, Measurement of sediment transport by streamer trap, Report of the 6th Cooperative Field Investigation, Nearshore Environment Research Center, Report no. 16, TR-82-2, pp. 138-141. (in Japanese).
- Katori, S., 1983, Measurement of sediment transport by streamer trap, Report of the 7th Cooperative Field Investigation, Nearshore Environment Research Center, Report No. 17, TR-82-1, pp. 110-117. (in Japanese).

- Kelley, J.C. and Whetten, J.T., 1969, Quantitative Statistical Analyses of Columbia Sediment Samples, *Journal of Sedimentary Petrology*, v.39, no.3, pp. 1167-1173.
- King, C.A.M., 1972, *Beaches and Coasts*, Edward Arnold, Ltd., London, (pp. 43-191; pp. 215-381).
- Knebel, H.J., Kelley, J.C., and Whetton, J.T., 1968, Clay minerals of the Columbia River: a qualitative, quantitative, and statistical evaluation, *Journal of Sedimentary Petrology*, v.38, pp. 600-611.
- Komar, P.D., 1971, Mechanics of Sand Transport on Beaches, *Journal Geophysical Research*, v.76, no.3, 716-721.
- Komar, P.D., 1975, Nearshore currents: generation by obliquely incident waves and longshore variations in breaker height, In: Hails, J. and Carr, A. [Eds.], 1975, *Nearshore Sediment Dynamics and Sedimentation, An Interdisciplinary Review*, John Wiley and Sons, London.
- Komar, P.D., 1976, *Beach processes and sedimentation*, Prentice-Hall, Inc., Englewood Cliffs, NJ.
- Komar, P.D., 1979, Beach-slope dependence of longshore currents, *Journal of the Waterway, Port, Coastal, and Ocean Division, Proceedings of the American Society of Civil Engineers*, v.105, no.WW4, pp. 460-464.
- Komar, P.D., 1987a, Selective grain entrainment by a current from a bed of mixed sizes: a reanalysis, *Journal of Sedimentary Petrology*, v.57, no.2, pp. 203-211.
- Komar, P.D., 1987b, Selective gravel entrainment and the empirical evaluation of flow competence, *Sedimentology*, v.34, pp. 1165-1176.
- Komar, P.D. and Clemens, K.E., 1986, The relationship between a grain's settling velocity and threshold of motion under unidirectional currents, *Journal of Sedimentary Petrology*, v.56, no.2, pp.258-266.
- Komar, P.D. and Cui, B., 1984, The analysis of grain-size measurements by sieving and settling-tube techniques, *Journal of Sedimentary Petrology*, v.54, no.2, pp. 603-614.

- Komar, P.D. and Gaughan, M.K., 1973a, Airy Wave Theory and Breaker Height Prediction, In: 13th Proceedings on Coastal Engineering.
- Komar, P.D. and Inman, D.L., 1970, Longshore sand transport on beaches, *Journal of Geophysical Research*, v.75, no.30, pp. 5914-5927.
- Komar, P.D. and Miller, M.C., 1973, The threshold of sediment movement under oscillatory water waves, *Journal of Sedimentary Petrology*, v.43, pp.1101-1.
- Komar, P.D. and Miller, M.C., 1975, Reply: On the comparison between the threshold of sediment motion under waves and unidirectional currents with a discussion of the practical evaluation of the threshold: a discussion, *Journal of Sedimentary Petrology*, v.45, pp. 362-367.
- Komar, P.D. and Wang, C., 1984b, Processes of selective grain transport and the formation of placers on beaches, *Journal of Geology*, v.92, pp. 637-655.
- Kraft, J.C., 1971, Sedimentary environment facies patterns and geologic history of a Holocene marine transgression, *Geologic Society of America Bulletin*, v.82, pp. 2131-2158.
- Kraus, N.C., 1987, Application of portable traps for obtaining point measurements of sediment transport rates in the surf zone, *Journal of Coastal Research*, v.3, pp. 139-152.
- Kraus, N.C. and Dean, J.L., 1987, Longshore sediment transport rate distributions measured by trap, *Coastal Sediments '87*, WW Division, ASCE, New Orleans, LA.
- Kraus, N.C. and Nakashima, L., 1986, Field Method for determining rapidly the weight of wet sand samples, *Journal of Sedimentary Petrology*, v.56, no. 4, pp.550-551.
- Longuit-Higgins, M.S., 1970, Longshore Currents generated by obliquely incident sea waves, *Journal of Geophysical Research*, v.75, no.33, pp. 6788-6801.
- Longuit-Higgins, M.S., 1971, Recent progress in the study of longshore currents, In: *Waves on Beaches and Resulting Sediment Transport*, Academic Press, New York.

- Longuit-Higgins, M.S. and Steward, R.W., 1962, Radiation stress and mass transport in gravity waves with application to surf beats, *Journal of Fluid Mechanics*, v.13, pp. 481-504.
- Longuit-Higgins, M.S. and Steward, R.W., 1964, Radiation stress in water waves; a physical discussion with applications, *Deep Sea Research*, v.11, no.4, pp. 529-563.
- Lowry, W.D. and Baldwin, E.M., 1952, Late Cenozoic Geology of the Lower Columbia River valley, Oregon and Washington, *Geological Society of America Bulletin*, v.63, pp. 1-24.
- Lutz, G.A., Hubbell, D.W., and Stevens, H.H. Jr., 1975, Discharge and flow distribution, Columbia River Estuary, U.S. Geological Survey Professional Paper 433-P, Washington D.C., 31 pp.
- Lloyds (Lloyd's Register of Shipping), 1987, Register of Ships 1987-1988 (3 Volumes), Lloyd's Register of Shipping, London, UK.
- Macdonald, E.H., 1983, Alluvial Mining The geology, technology, and economics of placers, Chapman and Hall, New York, 508pp.
- Madsen, O.S. and Grant, W.D., 1975, The threshold of sediment movement under oscillatory waves: a discussion, *Journal of Sedimentary Petrology*, v.45, pp. 360-361.
- Manohar, M., 1955, Mechanics of Bottom Sediment Movement Due to Wave Action, U.S. Army Corps of Engineers. Beach Erosion Board, Technical Memorandum no.75, 121p.
- Mcdonald, E.H., 1983, Alluvial Mining, University Press, Cambridge, Chapman and Hall, NY, NY.
- McKee, B., 1972, Cascadia, McGraw-Hill, Inc. New York.
- Merchants Exchange, 1987-1988, Merchants Exchange Daily Ship Log (unpubl.), Merchants Exchange, Portland, OR.
- Meyer, R.E.[Ed.], 1972, Waves on Beaches and Resulting Sediment Transport, Academic Presses, New York.
- Michell, J.H., 1893, On the highest waves in water, *Philosophical Magazine*, 5th series, v.36, pp. 430-437.

- Middleton, G.V. and Southard, J.B., 1978, Mechanics of Sediment Transport, Society of Economic Paleontologists and Mineralogists, Tulsa, OK.
- Miller, M.C., McCave, I.N., and Komar, P.D., 1977, Threshold of sediment motion under unidirectional currents, Sedimentology, v.24, pp.507-527.
- Muir Wood, A.M. and Fleming, C.A., 1981, Coastal Hydraulics 2nd Ed., Halsted Press, John Wiley & Sons, New York, 280 pp.
- Newman, J.N., 1970, Recent Research on Ship Waves, pp.519-545; IN: Plesset, M.S., Yao-Tso Wu, T., and Doroff, S.W. (Eds.), Eighth Symposium Naval Hydrodynamics (Rome, Italy), Office of Naval Research, Department of Navy (U.S.A.), ACR-179.
- Newton, R.S., 1968, Internal Structure of Wave-formed ripple marks in the nearshore zone, Sedimentology, v-11, pp.272-292.
- NOAA, 1913, Columbia River Harrington Point to Grims Island 1:40,000 Plate, Soundings in feet, (National Oceanic and Atmospheric Administration), U.S. Department of Commerce, Washington D.C.
- NOAA, 1985, Columbia River Harrington Point to Crims Island 1:40,000 Plate, Soundings in feet, (National Oceanic and Atmospheric Administration, U.S. Department of Commerce, Washington, D.C..
- Ofuya, A.O., 1970, Shore Erosion-Ship and Wind Waves, St. Claire, Detroit and St. Lawrence Rivers, Department of Public Works of Canada. Design Branch Report No.21, Marine Engineering Division.
- Oregonian, 1987-1988, Port Calendar, (various dates), Oregonian Newspaper Business Section, Portland, OR.
- Oswalt, N.R., Mellema, W.J., and Perry, E.B., 1981, Riverbank Erosion, Evaluation, Prevention and Control, Inland & Maritime Waterways & Ports, Section II Maritime Ports and Seaways, v.5, 25th International Navigation Congress, Edinburgh, pp.155-161.
- Palmer, L.A., 1987, Personal Communication, Asst. Professor, Portland State University, Portland, OR.

- Peterson, C.D., Komar, P.D., and Scheidegger, 1985, Distribution, Geometry, and Origin of heavy mineral placer deposits on Oregon beaches, *Journal of Sedimentary Petrology*, v.56, no.1, pp.67-77.
- PIANC (Permanent International Association of Navigation Congresses), 1987, Guidelines for the design and construction of flexible revetments incorporating geotextiles for inland waterways, Report of Working Group 4 of the Permanent Technical Committee I, Supplement to Bulletin No.57, Brussels, Belgium.
- Port of Portland, 1986, Guide to Navigation on the Lower Columbia.
- Reading, H.G. [Ed.], 1978, *Sedimentary Environments and Facies*, Elsevier, New York.
- Reed, W.E., Fever, R.L., and Moir, G.J., 1975, Depositional environment interpretation from settling-velocity (Ψ) distributions, *Geological Society of America Bulletin*, v.86, pp. 1321-1328.
- Robinson, L.S., 1897, Mechanical Propulsion on Canals, The Institution of Mechanical Engineers, Proceedings, Parts 1-2, Westminster, UK, pp. 148-167 and plates.
- Roovers, P.P.L., Kerchkaert, P., Burgers, A., Noordam, A., and De Candt, P., 1981, Beach protection as part of the harbour extension at Zeebrugge, Belgium, *Inland & Maritime Waterways & Ports, Section II Maritime Ports and Seaway*, v.5, 25th International Navigation Congresses, Edinburgh, pp. 755-768.
- Russell, J.S., 1834, Notice of the reduction of an anomalous fact in hydrodynamics, and of a new law of the resistance of fluids to the motion of floating bodies, Report of the 4th Meeting of the British Association for the Advancement of Science, John Murray, London, 1835, pp. 531-534.
- Russell, J.S., 1835, On the solid of least resistance, Report of the 5th Meeting of the British Association for the Advancement of Science, John Murray, London, 1836, pp. 107-108.
- Saunders, H.E., 1975, *Hydrodynamics in Ship Design*, vol.2, New York Society of Naval Architects and Marine Engineers.

- Savage, R.P., 1953, Laboratory study of wave energy losses by bottom friction and percolation, Beach Erosion Board, Technical Memorandum 31, 25 p.
- Schleyer, R., 1988, The goodness-of-fit to ideal Gauss and Rosin distributions: A new grain-size parameter - Reply, Journal of Sedimentary Petrology, v.58, no.5, pp. 917-918.
- Scholle, P.A. and Spearing, D.(Eds.), 1982, Sandstone Depositional Environments, American Association Petroleum Geologists, Tulsa, OK, 410 pp.
- Sherwood, C.R., Creager, J.S. (Principal Investigator), Roy, E.H., Gelfenbaum, G., and Dempsey, T., 1984, Sedimentary processes and environments in the Columbia River Estuary, Final CREDDP Report (Columbia River Estuary Data Development Program), CREST (Columbia River Estuary Study Taskforce), Astoria, OR., 318 p.
- Shepard, F.P., 1963, Submarine Geology (2nd ed.), New York, Harper and Row.
- Shields, A., 1936, "Anwendung der Aehnlichkeitsmechanik und Turbulenz forschung auf die Geschiebewegung, IN: Ott, W.P. & van Uchelen, J.C. (translators), California Institute of Technology, W.M. Keck laboratory of Hydraulics and Water Resources, Report No.167.
- Simons, D.B. and Şentürk, F., 1976, Sediment Transport Technology, Water Resources Publications, Fort Collins, CO.
- Sorensen, R.M., 1967, Investigation of Ship-Generated Waves, Journal of the Waterways and Harbors Division, ASCE, WW2, pp.85-99.
- Sorensen, R.M., 1973, Water waves produced by ships, Journal of the Waterways, Harbors, and Coastal Engineering Division, WW2, ASCE, pp. 245-256.
- Sorensen, R.M. and Weggel, J.R., 1984, Development of ship wave design information, chapter 216, Coastal Engineering Conference, ASCE.

- Span, H.J.Th., Altink, H., Barends, F.J., Biemond, C., Biesheuvel, G.J., Huis in't Veld, J.C., Thanbet, R., Tutuarima, W.H., and Woestenenk, A.J., 1981, A review of relevant hydraulic phenomena and recent developments in research, design and construction of protective works, Inland & Maritime Waterways & Ports, Section II Maritime Ports and Seaways, v.5, 25th International Navigation Congress, Edinburgh, pp. 112-118.
- Sundborg, Å. and Norrman, J., 1963, Gūta Älv-Hydrologi och Morfologi, Med Särakild Hänsyn till-Erosionsprocesserna, Sveriges Geologiska Undersökning, Avhandlingar och Uppersatser, I4=0, ser. Ca., NR 43, Stockholm (in Swedish).
- State of Maryland, 1949, Shore Erosion in Tidewater Maryland, reprint from Bulletin 6.
- State of Maryland, 1981, The role of boat wakes in shore erosion in Anne Arundel County, Maryland, Maryland Coast Report no. 5.
- State of Oregon, 1966-1984, Water Well Reports, Water Resources Department, Salem, OR.
- State of Washington, 1973-1984, Water Well Reports, Department of Ecology, Olympia, WA.
- State of Washington, 1985, Contract Provisions for Construction of SR 409 MP 3.32 to MP 2.65 PUGET ISLAND BRIDGE 409/10, Wahkiakum County, Department of Transportation, Olympia, WA.
- Streeter, V.L. and Wylie, E.B., 1979, Fluid Mechanics, McGraw-Hill, Inc., pp.562.
- Terzaghi, K. and Peck, R.B., 1967, Soil Mechanics in Engineering Practice, John Wiley and Sons, New York.
- Thomson, W.(Lord Kelvin), 1887, On Ship Waves, Proceedings, Institute of Mechanical Engineers, Edinburgh, Great Britain, pp.409-433 and plates.
- Thorne, C.R., MacArthur, R.C., and Bradley J.B., 1988, The Physics of Sediment Transport by Wind and Water, A Collection of Hallmark Papers by R.A. Bagnold, American Society of Civil Engineers, New York, 359 pp.

- Thornton, E.B., 1973, Distribution of sediment transport across surf zone, Proc. 13th conf. on coast Engineering, pp.1049-68.
- Tolan, T.L., Reidel, S.P., Beeson, M.H., Anderson, J.L., Fecht, K.R., and Swanson, D.A., 1987, Columbia River Basalt Group (CRBG): New Estimates of its Extent and Volume [abs. and poster], Abstracts of the 34th Annual Meeting of the Pacific Northwest Region of the American Geophysical Union, Olympia, WA.
- Trask, P.D., 1939, Recent Marine Sediments A Symposium, The American Association of Petroleum Geologists, Dover Publications, London.
- USACE (U.S. Army Corps of Engineers), 1960, Lower Columbia River Bank Protection, Oregon and Washington, General Design Memorandum, plates 6,7,8, Engineering Division, Portland District, Portland, OR.
- USACE (U.S. Army Corps of Engineers), 1961, Sedimentation Investigation Lower Columbia and Lower Willamette Rivers July 1959-August 1960, Portland District, Portland, OR.
- USACE (U.S. Army Corps of Engineers), 1970-1986, Waterborne Commerce of the United States, Part 4: Waterways and Harbors Pacific Coast, Alaska, Hawaii, Water Resources Support Center, Fort Belvoir, VA.
- USACE (U.S. Army Corps of Engineers), 1984, Shore Protection Manual, v.I, U.S. Army Coastal Engineering Research Center, Vicksburg, MI.
- USACE (U.S. Army Corps of Engineers), 1985, Computer Program: Sinewaves (MACE-11) Linear Wave Theory Predictions, CERC Technical Note, CETN-I-32, Coastal Engineering Research Center), Burke, C.E., 7 p.
- USACE (U.S. Army Corps of Engineers), 1986, Investigation of bank erosion at Sauvie Island, OR, Planning Division Technical Report, Portland District, Portland, OR.
- USACE (U.S. Army Corps of Engineers), 1987, Environmental Engineering for Deep Draft Navigation Projects, EM 1110-2-1202, Engineer Manual.
- USACE (U.S. Army Corps of Engineers), 1988a, Prediction of eroded versus accreted beaches, CERC Technical Note, CERC (Coastal Engineering Research Center), 7 p., Kraus, N. C. and Gingerich, K. J.

- USACE (U.S. Army Corps of Engineers), 1988b, Maintenance Improvement Review Long Range Operational Plan, Lower Columbia River Dredging River Miles 32 to 48, Portland District, Portland, OR.
- USACE (U.S. Army Corps of Engineers), 1988c, Dredging records, Navigation Branch, Operations Division, Portland District Office, Portland, Oregon, (unpubl.).
- USACE (U.S. Army Corps of Engineers), 1988d, Flood analysis of the lower Columbia, Hydrology Section (Hydrologic and River Engineering section), Portland District, Portland, Oregon.
- USACE (U.S. Army Corps of Engineers), 1989, Maintenance Improvement Review Long Range Operational Plan, Lower Columbia River Dredging River Miles 32 to 48, Portland District, Portland, OR.
- USDI (U.S. Department of the Interior), 1947, The Columbia River, Prepared by Bureau of Reclamation, Michael W. Straus (Commissioner), R.J. Newell (Director, Region I).
- USSCS (U.S. Soil Conservation Service), 1986a, Soil Survey of Columbia County, Oregon, U.S. Department of Agriculture, Washington, D.C., 197 pp.
- USSCS (U.S. Soil Conservation Service), 1986b, Soil Survey of Grays Harbor County Area, Pacific County, and Wahkiakum County, Washington, U.S. Department of Agriculture, Washington, D.C., 296 pp.
- Vanoni, V.A., 1975, Sedimentation Engineering, American Society of Civil Engineers, New York, New York.
- Visher, G.S., 1969, Grain size distributions and depositional processes, Journal of Sedimentary Petrology, v.39, no.3, pp. 1074-1100.
- Walpole, R.E. and Myers, R.H., 1985, Probability and Statistics for Engineers and Scientists, third ed., Macmillan Publishing Company, New York.
- Walsh, T.J., 1987, Geologic Map of the Astoria and Ilwaco Quadrangles, Washington and Oregon, WA State Department of Natural Resources.
- Waugh, R.G., 1971, Water depths required for ship navigation, Journal of Waterways, Harbors, and Coastal Engineering Division, WW3, ASCE, pp. 455-473.

- West, D.O., 1987, Nature of shallow Cascadia Subduction Zone Paleoseismicity inferred from characteristics of Oregon-Washington coastline uplift [abs. and poster], Abstracts of the 34th Annual Meeting of the Pacific Northwest Region of the American Geophysical Union, Olympia, WA.
- Whetton, J.T., Kelley, J.C., and Hanson, L.G., 1969, Characteristics of Columbia River sediment and sediment transport, Journal of Sedimentary Petrology, vol.39, no.3, pp. 1149-1166.
- Yalin, M.S., 1972, Mechanics of Sediment Transport, Pergamon Press, New York.

APPENDIX A

SHORE PROFILES

This appendix presents study site profiles recorded during this study and the computer data files. Profiling is presented first for Price Island, then Puget Island, and finally Gull Island.

Price Island Study Site RK WA-55 Profile Data Base (ISRP)
DATA is in FEET

PR 1	81880629	1141	13	-420	PRICELINE1	0	845	25	795	50	700	75	610		
PR 1	82	100	520	150	380	200	240	225	160	250	60	261	10	275	-60
PR 1	83	291	-190	309	-420										
PR 2	81880629	1115	15	-200	PRICELINE2	0	939	25	950	50	930	75	930		
PR 2	82	93	910	95	790	95	650	99	570	112	360	120	290	145	170
PR 2	83	170	60	195	-20	220	-110	245	-200						
PR 3	81880629	1052	17	-370	PRICELINE3	0	873	25	850	50	840	75	860		
PR 3	82	100	790	113	700	114	690	116	610	120	540	139	330	164	210
PR 3	83	174	130	184	50	199	-30	224	-120	249	-240	268	-370		
PR 4	81880629	1030	17	-490	PRICELINE4	0	1270	10	1190	20	1120	28	730		
PR 4	82	34	790	50	732	51	460	55	370	65	170	76	60	101	30
PR 4	83	126	-40	151	-90	201	-210	226	-280	251	-360	279	-490		
PR 1	51870820	1332	13	-65	PRICELINE1	0	845	25	765	50	755	75	705		
PR 1	52	100	625	125	545	150	465	175	395	200	315	210	275	235	175
PR 1	53	260	55	280	-65										
PR 2	51870820	1323	12	-110	PRICELINE2	0	939	25	900	50	890	75	870		
PR 2	52	100	860	125	830	150	740	175	700	200	440	225	240	250	50
PR 2	53	275	-110												
PR 3	51870820	1306	13	-180	PRICELINE3	0	873	25	800	50	790	75	820		
PR 3	52	100	720	125	660	150	580	162	550	175	390	200	180	203	140
PR 3	53	228	-70	240	-180										
PR 4	51870820	1249	16	-220	PRICELINE4	0	1270	10	1190	20	1120	28	730		
PR 4	52	34	790	50	732	75	690	100	680	125	620	150	510	175	360
PR 4	53	200	220	221	90	225	70	250	-80	275	-220				
PR 1	61870909	1205	15	-510	PRICELINE1	0	845	25	760	50	760	75	720		
PR 1	62	100	640	125	540	150	460	175	380	200	310	225	230	250	140
PR 1	63	275	40	294	-120	319	-310	322	-510						
PR 2	61870909	1156	15	-500	PRICELINE2	0	939	25	900	50	880	75	860		
PR 2	62	100	840	115	840	125	820	150	730	171	710	182	0	207	320
PR 2	63	232	140	257	0	293	-200	333	-500						
PR 3	61870909	1144	14	-720	PRICELINE3	0	873	25	820	50	800	75	830		
PR 3	62	100	740	125	660	150	590	161	550	166	460	184	290	209	130
PR 3	63	234	-30	289	-280	314	-720								
PR 4	61870909	1142	18	-760	PRICELINE4	0	1270	10	1190	20	1120	28	730		
PR 4	62	34	790	50	732	75	680	100	670	125	620	150	480	175	330
PR 4	63	200	190	225	20	250	-130	275	-240	305	-390	330	-550	342	-760
PR 1	71871003	1320	12	-140	PRICELINE1	0	845	25	760	50	750	75	710		
PR 1	72	100	630	125	530	150	440	175	370	181	350	241	170	281	20
PR 1	73	301	-140												
PR 2	71871003	1340	13	-170	PRICELINE2	0	939	25	900	50	880	75	860		
PR 2	72	100	850	125	820	150	740	166	690	179	510	202	280	227	130

ISRP = Interactive Survey Reduction Program
(Birkemeier, 1988)

PR 2	73	252	-10	277	-170														
PR 3	71871003	1350	15	-420	PRICELINE3	0	873	25	810	50	790	75	740						
PR 3	72	100	650	125	580	147	520	150	510	154	480	157	420	169	270				
PR 3	73	194	80	219	-80	244	-270	253	-420										
PR 4	71871003	1400	17	-410	PRICELINE4	0	1270	10	1190	20	1120	28	730						
PR 4	72	34	790	50	732	75	690	100	680	125	620	134	560	150	460				
PR 4	73	175	320	200	260	210	80	235	-170	260	-310	281	-410						
PR 3	41870727	1115	15	-607	PRICELINE3	0	873	25	843	50	833	75	863						
PR 3	42	100	763	125	693	150	603	175	593	181	563	200	293	225	113				
PR 3	43	250	-117	270	-357	275	-437	286	-607										
PR 4	41870727	1100	20	-678	PRICELINE4	0	1270	10	1190	20	1120	28	730						
PR 4	42	34	790	50	732	75	722	100	682	125	652	145	562	150	542				
PR 4	43	175	412	200	282	225	152	250	32	275	-108	300	-278	323	-458				
PR 4	44	325	-498	343	-678														
PR 2	21870623	1120	13	899	PRICELINE2	0	939	25	949	50	939	75	919						
PR 2	22	100	899	125	889	150	819	175	779	200	699	225	599	250	479				
PR 2	23	275	279	290	89														
PR 3	21870623	1110	12	-37	PRICELINE3	0	873	25	853	50	833	75	873						
PR 3	22	100	783	125	693	150	623	175	573	200	563	225	243	250	-27				
PR 3	23	252	-37																
PR 4	21870623	1015	16	-248	PRICELINE4	0	1270	10	1190	20	1120	28	730						
PR 4	22	34	790	50	732	75	722	100	692	125	672	150	542	175	462				
PR 4	23	200	372	225	272	250	152	275	-18	300	-248								
PR 1	31870702	1035	13	-35	PRICELINE1	0	845	25	765	50	755	75	725						
PR 1	32	100	635	125	575	150	505	175	435	200	355	225	275	250	175				
PR 1	33	275	45	284	-35														
PR 2	31870702	1020	14	699	PRICELINE2	0	939	25	909	50	899	75	879						
PR 2	32	100	859	125	839	150	739	175	669	200	599	225	529	233	469				
PR 2	33	234	389	250	269	275	69												
PR 3	31870702	1012	12	-37	PRICELINE3	0	873	25	833	50	813	75	793						
PR 3	32	100	833	125	743	150	653	175	583	200	543	201	393	225	183				
PR 3	33	249	-37																
PR 4	31870702	931	16	-78	PRICELINE4	0	1270	10	1190	20	1120	28	730						
PR 4	32	34	790	50	732	75	692	100	652	125	642	150	542	175	432				
PR 4	33	200	332	225	202	250	92	275	-48	279	-78								
PR 1	41870727	1150	16	-495	PRICELINE1	0	845	25	765	50	745	75	705						
PR 1	42	90	665	100	625	125	555	150	475	175	405	200	335	225	275				
PR 1	43	250	155	275	5	300	-175	309	-285	320	-495								
PR 2	41870727	1130	17	-421	PRICELINE2	0	939	25	949	50	919	75	909						
PR 2	42	100	879	125	859	150	779	175	709	181	639	200	569	225	329				
PR 2	43	250	149	275	-31	300	-221	317	-341	325	-421	337	-351						

Puget Island Study Site RK WA-62 Profile Data Base (ISRP)
 Data entry= x z x z x z

where x=horizontal coordinate, 0 decimal places in FEET
 z=vertical coordinate, 2 decimal places in FEET

PU 0	11880802	1120	30	-250	PUGETLINE 1W	0	1880	28	1850	53	1740	78	1570
PU 0	12	103	1280	108	1330	124	1840	144	1340	146	1160	166	1060
PU 0	13	196	760	199	760	224	590	234	550	259	490	309	440
PU 0	14	409	350	459	300	509	260	559	210	595	120	611	20
PU 0	15	711	-40	761	-90	771	-120	821	-210	846	-250		
PU 1	11880321	954	22	-143	PUGETLINE 1W	0	1880	34	1820	64	1850	82	1900
PU 1	12	97	1940	107	1880	120	1650	124	1390	131	650	141	538
PU 1	13	191	510	216	492	257	432	308	311	333	138	342	188
PU 1	14	383	-15	409	-67	434	-97	459	-143				
PU 1	21880607	1050	11	271	PUGETLINE 1W	0	1880	34	1820	64	1850	94	2070
PU 1	22	109	1750	121	1410	125	751	175	641	225	541	275	441
PU 1	31880617	1116	25	-115	PUGETLINE 1W	0	1880	34	1820	64	1850	69	1980
PU 1	32	84	2030	114	1660	125	1335	129	985	134	745	140	745
PU 1	33	165	755	183	755	189	705	214	675	264	595	314	465
PU 1	34	364	295	374	265	389	165	399	75	414	-15	426	-65
PU 1	41880804	1019	13	055	PUGETLINE 1W	0	1880	34	1820	38	1960	88	1790
PU 1	42	113	1845	134	625	145	665	170	675	220	435	282	385
PU 1	43	343	105	368	55								
PU 2	21880802	1452	21	-240	PUGETLINE 2	0	2110	20	1810	28	2210	45	2140
PU 2	22	70	1670	98	1130	123	980	142	940	167	1070	180	1230
PU 2	23	216	490	231	350	256	210	281	110	321	-50	338	-40
PU 2	24	369	-50	394	-80	408	-240						
PU 3	11870731	0950	13	-140	PUGETLINE 3	0	2082	12	2100	24	2150	49	2000
PU 3	12	150	1600	165	1000	175	650	177	550	197	350	247	200
PU 3	13	273	060	293	-140								
PU 3	21880321	1021	16	-242	PUGETLINE 3	0	2082	12	2112	24	2262	49	2002
PU 3	22	53	1522	59	542	84	468	109	497	159	442	194	385
PU 3	23	253	246	303	111	341	6	363	-100	388	-242		
PU 3	31880607	1100	10	202	PUGETLINE 3	0	2082	10	2260	20	2302	30	2242
PU 3	32	45	2042	63	602	113	552	163	492	213	392	278	202
PU 3	41880617	1140	19	26	PUGETLINE 3	0	2082	10	2060	21	2070	41	2620
PU 3	42	71	2190	78	1750	81	1200	86	941	91	890	101	803
PU 3	43	176	674	201	641	251	520	301	383	376	183	401	137
PU 3	44	445	-76										
PU 4	11880617	1116	14	-519	PUGETLINE 4	0	2160	22	2210	37	2360	67	2320
PU 4	12	78	1230	88	680	113	605	163	546	213	456	263	319
PU 4	13	363	65	385	-113	410	-259						
PU 4	21880802	1502	11	290	PUGETLINE 4	0	2160	26	2160	31	2370	41	2450
PU 4	22	65	2030	68	1480	193	1400	268	1190	280	630	295	420
PU 4	31880804	1035	13	220	PUGETLINE 4	0	2160	26	2160	31	2420	40	2450
PU 4	32	65	2000	78	1490	178	1460	263	1220	273	870	274	670

ISRP = Interactive Survey Reduction Program
 (Birkemeier, 1988)

PU 4	33	297	440	364	220								
PU 5	11870731	1010	11	-100	PUGETLINE 5	0	2280	20	2250	40	2100	70	2200
PU 5	12	200	2100	215	1500	225	800	227	700	250	400	300	50
PU 5	21880607	1112	9	440	PUGETLINE 5	0	2280	20	2260	40	2220	60	2210
PU 5	22	85	2130	106	760	156	590	206	510	237	440		
PU 5	31880617	1155	11	00	PUGETLINE 5	0	2280	10	2270	78	2180	86	1380
PU 5	32	98	760	148	610	194	530	244	410	294	300	344	150
PU 7	11870723	1057	15	-40	PUGETLINE A	0	1680	10	1700	16	1610	31	1730
PU 7	12	56	1500	67	1260	84	1210	100	800	125	710	150	640
PU 7	13	189	260	214	60	249	-10	269	-40				
PU 7	21870731	1020	18	-520	PUGETLINE A	0	1680	10	1700	16	1610	18	1570
PU 7	22	27	1870	77	1640	127	1450	177	1240	215	1060	227	680
PU 7	23	248	370	298	190	318	110	324	40	342	-260	354	-420
PU 7	31870821	1046	19	-510	PUGETLINE A	0	1680	10	1700	13	1660	16	1610
PU 7	32	28	1780	31	1730	53	1730	128	1410	175	1250	205	1060
PU 7	33	227	460	237	360	287	230	316	-30	336	-170	354	-310
PU 7	34	381	-510										
PU 7	41870911	954	16	-350	PUGETLINE A	0	1680	10	1700	16	1610	26	1810
PU 7	42	31	1730	38	1790	122	1430	172	1260	196	1120	203	960
PU 7	43	216	370	252	200	286	20	322	-150	354	-350		
PU 7	51880120	1017	15	-70	PUGETLINE A	0	1680	10	1700	16	1610	21	1730
PU 7	52	30	1710	70	1640	110	1510	155	1380	157	830	158	720
PU 7	53	180	280	190	110	210	-30	225	-70				
PU 7	61880321	1106	15	-250	PUGETLINE A	0	1680	10	1700	55	1780	85	1600
PU 7	62	105	1480	119	1480	129	650	138	374	148	236	152	140
PU 7	63	202	50	227	-14	277	-146	287	-250				
PU 7	71880607	1123	13	70	PUGETLINE A	0	1680	10	1700	16	1610	31	1730
PU 7	72	70	1600	112	1400	115	570	122	410	130	250	139	230
PU 7	73	214	100	229	70								
PU 7	81880617	1217	14	-200	PUGETLINE A	0	1680	10	1650	25	1610	40	1630
PU 7	82	65	1580	90	1490	104	1380	106	800	109	570	112	480
PU 7	83	207	140	257	20	313	-200						
PU 7	91880804	1139	14		PUGETLINE A	0	1680	10	1650	15	1570	60	1700
PU 7	92	105	1450	150	1470	195	1440	252	1470	266	670	286	490
PU 7	93	386	70	411	10	436	-40						
PU 8	11870723	1256	11	100	PUGETLINE B	0	1600	5	1680	10	1820	29	1500
PU 8	12	42	860	67	740	92	610	117	470	142	380	167	260
PU 8	21870731	1115	18	-510	PUGETLINE B	0	1600	5	1680	10	1820	13	1620
PU 8	22	29	1500	63	1350	113	1350	138	1240	150	790	171	580
PU 8	23	204	300	219	260	250	120	261	-20	281	-280	294	-410
PU 8	31870821	1134	16	-250	PUGETLINE B	0	1600	5	1680	10	1820	14	1620

PU 8	32	29	1500	64	1360	89	1390	100	1370	133	1310	143	1140	158	720
PU 8	33	198	370	236	160	262	60	284	-150	291	-250				
PU 8	41880120	1028	12	40	PUGETLINE B			0	1600	5	1680	10	1820	29	1500
PU 8	42	50	1470	98	1390	118	1370	120	790	140	460	175	210	195	130
PU 8	43	215	40												
PU 8	51880321	1114	20	-303	PUGETLINE B			0	1600	5	1680	10	1820	15	1580
PU 8	52	29	1500	45	1370	65	1340	88	1330	92	650	100	446	101	398
PU 8	53	113	234	120	120	145	76	161	54	186	-23	198	-73	214	-120
PU 8	54	239	-226	254	-303										
PU 8	61880607	1131	13	0	PUGETLINE B			0	1600	5	1680	10	1820	12	1560
PU 8	62	29	1500	72	1280	77	540	84	370	92	180	97	120	122	100
PU 8	63	157	40	172	00										
PU 8	71880617	1000	15	-100	PUGETLINE B			0	1600	5	1680	10	1820	14	1570
PU 8	72	39	1420	64	1330	66	1310	68	680	69	600	72	530	73	490
PU 8	73	93	240	143	100	193	000	253	-200						
PU 8	81880804	1144	12	130	PUGETLINE B			0	1600	5	1680	10	1820	14	1660
PU 8	82	29	1550	119	1480	198	1470	211	860	236	610	258	560	348	290
PU 8	83	398	130												
PU 9	11870723	1308	13	50	PUGETLINE C			0	1480	10	1430	35	1370	39	1370
PU 9	12	48	910	73	730	98	600	123	490	148	430	173	330	193	270
PU 9	13	218	150	241	50										
PU 9	21870821	1206	15	-340	PUGETLINE C			0	1480	10	1430	35	1370	60	1380
PU 9	22	110	1340	150	1370	160	1330	170	1180	179	630	189	480	204	380
PU 9	23	227	160	265	-40	282	-240	303	-340						
PU 9	31880120	1042	13	-40	PUGETLINE C			0	1480	10	1430	35	1370	70	1380
PU 9	32	110	1350	150	1390	151	980	155	700	175	430	195	260	331	170
PU 9	33	351	70	371	-40										
PU 9	41880321	1122	19	-379	PUGETLINE C			0	1480	10	1430	35	1370	70	1360
PU 9	42	100	1310	120	1320	134	1360	137	560	139	480	145	363	146	317
PU 9	43	158	235	169	-41	194	-196	219	-134	244	-169	262	-206	287	-275
PU 9	44	312	-379												
PU 9	51880607	1141	9	60	PUGETLINE C			0	1480	10	1480	80	1400	122	1420
PU 9	52	125	620	131	490	138	240	143	140	155	60				
PU 9	61880617	1246	18	-120	PUGETLINE C			0	1480	10	1480	25	1440	50	1450
PU 9	62	63	1490	88	1430	113	1420	120	1320	123	830	125	650	127	610
PU 9	63	128	550	141	340	161	70	162	50	166	30	216	-30	231	-120
PU 9	71880804	1152	11	-270	PUGETLINE C			0	1480	10	1480	25	1440	31	1390
PU 9	72	91	1380	151	1370	215	1370	227	590	252	350	314	00	339	-270
PU 10	11870723	1322	15	100	PUGETLINE D			0	1490	10	1540	20	1460	31	860
PU 10	12	56	810	64	780	76	540	101	470	126	430	151	410	176	370
PU 10	13	201	320	205	290	230	180	242	100						

PU 10	21870731	1225	13	-660	PUGETLINE D	0	1490	10	1540	60	1470	110	1390
PU 10	22	163	1360	176	570	201	390	251	290	276	220	289	120
PU 10	23	336	-560	367	-660								
PU 10	31870821	1232	14	-270	PUGETLINE D	0	1490	10	1540	85	1410	135	1450
PU 10	32	155	1350	161	1260	172	600	184	470	197	400	241	220
PU 10	33	296	-70	321	-170	326	-270						
PU 10	41870211	1008	15	-370	PUGETLINE D	0	1490	10	1540	70	1435	94	1400
PU 10	42	136	1450	148	1390	160	1250	164	1050	165	570	175	450
PU 10	43	221	200	267	30	303	-210	315	-370				
PU 10	51880120	1054	11	0	PUGETLINE D	0	1490	10	1540	70	1430	133	1460
PU 10	52	150	1370	152	790	172	500	192	320	216	190	236	70
PU 10	61880321	1028	13	-230	PUGETLINE D	0	1490	10	1540	60	1430	100	1450
PU 10	62	146	1320	149	650	153	590	168	370	180	230	193	090
PU 10	63	256	-130	281	-230								
PU 10	71880607	1148	9	-40	PUGETLINE D	0	1490	10	1505	100	1380	133	1430
PU 10	72	139	560	147	410	164	160	172	20	176	-40		
PU 10	81880617	1130	12	670	PUGETLINE D	0	1490	10	1510	114	1350	128	1400
PU 10	82	131	1300	133	670	136	500	138	340	139	290	150	110
PU 10	83	185	-220										
PU 10	91880804	1156	8	-280	PUGETLINE E	0	1490	10	1510	220	1410	234	550
PU 10	92	259	260	284	090	296	-50	316	-280				
PU 11	11870723	1336	12	-378	PUGETLINE E	0	1600	10	1580	17	1500	27	850
PU 11	12	52	740	77	630	102	510	127	450	152	350	168	310
PU 11	13	213	130										
PU 11	21870731	1241	14	-650	PUGETLINE E	0	1600	10	1550	17	1440	42	1460
PU 11	22	142	1460	166	1360	178	740	186	610	198	540	248	150
PU 11	23	319	-270	340	-450	375	-560						
PU 11	31870821	1340	15	-170	PUGETLINE E	0	1600	10	1550	35	1470	85	1470
PU 11	32	125	1500	140	1440	150	1360	166	1280	181	460	191	370
PU 11	33	224	130	241	30	257	-70	269	-170				
PU 11	41880120	1105	11	40	PUGETLINE E	0	1600	10	1550	20	1550	80	1470
PU 11	42	148	1400	154	1310	158	820	198	340	209	240	229	70
PU 11	51880321	11	8	700	PUGETLINE E	0	1600	10	1550	16	1430	76	1420
PU 11	52	131	1480	151	1310	154	1070	159	700				
PU 11	61880607	1227	10	-100	PUGETLINE E	0	1600	10	1550	76	1420	125	1500
PU 11	62	147	1330	159	720	184	420	209	210	223	80	248	-100
PU 11	71880617	1200	12	790	PUGETLINE E	0	1600	10	1540	15	1510	17	1440
PU 11	72	22	1470	47	1460	94	1430	104	1460	126	1500	142	1390
PU 11	73	153	790										
PU 11	81880804	1206	9	-360	PUGETLINE E	0	1600	10	1540	88	1500	90	1550
PU 11	82	243	1560	259	1590	284	1240	302	00	322	-360		

PU 12	11870723	1408	11	200PUGETLINE F	0	2060	10	2040	48	1430	55	620			
PU 12	12	87	670	88	480	113	480	138	410	149	360	174	250	195	200
PU 12	21870731	1315	13	-620PUGETLINE F	0	2060	10	2040	30	1650	55	1560			
PU 12	22	155	1500	189	1490	203	560	220	370	270	120	275	40	306	-120
PU 12	23	320	-520	340	-620										
PU 12	31870821	1412	18	-120PUGETLINE F	0	2060	10	2040	30	1650	60	1520			
PU 12	32	85	1490	110	1510	135	1480	160	1540	170	1520	176	1490	188	1250
PU 12	33	198	670	208	520	232	370	258	180	275	80	291	-20	303	-120
PU 12	41870911	1024	18	-468PUGETLINE F	0	2060	10	2040	30	1650	60	1520			
PU 12	42	96	1480	120	1480	142	1430	171	1400	183	1340	190	1150	199	800
PU 12	43	200	600	212	430	224	340	270	37	294	-258	306	-368	310	-468
PU 12	51880120	1114	12	100PUGETLINE F	0	2060	10	2040	30	1650	60	1520			
PU 12	52	120	1500	171	1510	185	1300	191	840	211	580	231	380	240	290
PU 12	53	260	100												
PU 12	61880321	1225	14	-273PUGETLINE F	0	2060	10	2040	30	1650	50	1520			
PU 12	62	110	1500	170	1520	183	1350	184	1200	190	810	199	650	224	390
PU 12	63	244	230	282	-110	307	-310								
PU 12	71880607	1237	12	-60PUGETLINE F	0	2060	10	2040	30	1650	60	1520			
PU 12	72	110	1500	162	1500	172	1330	182	770	207	480	232	260	245	140
PU 12	73	270	-60												
PU 12	81880617	1407	16	-30PUGETLINE F	0	2060	10	2040	30	1650	48	1520			
PU 12	82	73	1490	98	1500	104	1500	123	1470	141	1550	166	1440	172	1280
PU 12	83	181	790	121	650	216	390	219	330	262	-30				
PU 12	91880804	1310	18	-350PUGETLINE F	0	2060	10	2040	30	1650	60	1520			
PU 12	92	135	1470	153	1570	161	1540	165	1200	176	1200	181	1110	231	1110
PU 12	93	263	1050	288	1240	294	1230	306	500	356	180	378	-100	390	-350
PU 13	11870723	1431	7	360PUGETLINE G	0	1410	10	1450	26	1510	37	1130			
PU 13	12	39	1170	49	590	62	360								
PU 13	21870731	1340	14	-660PUGETLINE G	0	1410	10	1450	35	1470	110	1470			
PU 13	22	170	1530	184	640	185	520	195	410	235	130	245	30	248	20
PU 13	23	259	-130	275	-520	303	-660								
PU 13	31870821	1430	12	-40PUGETLINE G	0	1410	10	1450	35	1470	85	1420			
PU 13	32	115	1460	165	1410	173	1150	182	620	206	340	230	160	255	60
PU 13	33	264	-40												
PU 13	41880120	1125	10	140PUGETLINE G	0	1410	10	1450	35	1470	70	1480			
PU 13	42	138	1510	164	1370	168	870	188	590	211	330	229	140		
PU 13	51880321	1230	17	-284PUGETLINE G	0	1410	10	1450	35	1470	60	1460			
PU 13	52	120	1440	150	1500	164	1430	165	1300	173	790	184	628	187	589
PU 13	53	199	588	201	542	226	292	251	56	269	-126	284	-284		
PU 13	61880607	1235	11	-60PUGETLINE G	0	1410	10	1450	35	1470	135	1510			
PU 13	62	155	1490	164	1030	168	800	181	610	206	340	230	140	247	-60

PU 18	43	140	242	165	-33	180	-205							
PU 18	51880607	1256	9	20	PUGETLINE L	0	1450	10	1430	37	1200	62	1060	
PU 18	52	94	1040	99	750	119	470	141	190	156	20			
PU 19	11870826	1252	14	-460	PUGETLINE M	0	1170	10	1070	20	1100	35	1080	
PU 19	12	50	1160	60	1110	81	820	91	620	106	430	120	300	140 80
PU 19	13	144	0	162	-260	168	-460							
PU 19	21880321	1300	11	-130	PUGETLINE M	0	1170	10	1070	20	1100	50	1160	
PU 19	22	61	1120	67	680	82	470	92	360	107	170	122	20	139 -130
PU 19	31880607	1305	10	-70	PUGETLINE M	0	1170	10	1070	20	1100	50	1150	
PU 19	32	52	830	56	650	71	410	90	120	100	-10	105	-70	
PU 19	41880804	1420			PUGETLINE M	0	1170	10	1070	14	940	64	850	
PU 19	42	84	720	87	570	105	380	125	-30	135	-220			
PU 20	11870826	1217	17	-250	PUGETLINE N	0	1070	10	1070	11	1080	12	810	
PU 20	12	13	750	25	620	31	560	50	470	75	360	110	240	137 60
PU 20	13	139	0	145	40	155	40	158	-30	178	-120	256	-250	
PU 20	21870911	1125	15	-431	PUGETLINE N	0	1070	10	1070	11	1080	12	830	
PU 20	22	22	650	34	570	78	400	104	340	108	280	111	180	234 120
PU 20	23	235	50	262	-31	274	-191	474	-431					
PU 20	31880321	1310	9	-630	PUGETLINE N	0	1070	2	450	3	196	13	22	
PU 20	32	38	-136	75	-274	100	-336	125	-490	139	-630			
PU 21	11870826	1158	14	-250	PUGETLINE O	0	980	10	1000	28	1170	34	690	
PU 21	12	46	490	56	430	81	360	106	280	131	230	141	150	156 20
PU 21	13	206	-130	220	-160	277	-250							
PU 21	21870911	1140	13	-446	PUGETLINE O	0	980	10	1000	28	1170	34	784	
PU 21	22	50	544	87	454	143	334	147	164	171	24	207	-36	219 -66
PU 21	23	363	-296	411	-446									
PU 21	31880321	1314	11	-40	PUGETLINE O	0	980	10	1000	22	980	23	820	
PU 21	32	36	600	49	480	74	420	93	320	143	260	146	70	163 -40
PU 21	41880607	1310	8	70	PUGETLINE O	0	980	10	1000	19	1120	20	830	
PU 21	42	40	560	135	430	153	180	173	70					

Gull Island Study Site RK OR-88.5 Profile Data Base (ISRP)
DATA is in FEET

GU 1	11870728	1100	14	-20	GULL LINEAW	0	1910	10	1890	25	1880	40	830
GU 1	12	65	450	90	180	115	60	140	50	165	20	190	10
GU 1	13	250	0	265	-10	290	-20						
GU 1	21870806	1728	12	-110	GULL LINEAW	0	1910	10	1890	26	1860	42	700
GU 1	22	60	500	86	270	111	-30	136	-60	161	-80	186	-100
GU 1	23	236	-110										
GU 1	31870818	1000	17	-30	GULL LINEAW	0	1910	10	1890	25	1890	41	780
GU 1	32	62	500	82	360	92	240	117	70	142	50	167	20
GU 1	33	217	10	242	0	267	-10	292	-10	317	-20	342	-30
GU 1	41870824	1055	11	40	GULL LN A-W	0	1950	25	1920	43	830	46	770
GU 1	42	56	600	66	520	97	240	107	140	124	100	174	50
GU 1	51870930	1045	10	30	GULL LN A-W	0	1910	10	1900	25	1870	40	780
GU 1	52	53	570	71	370	96	190	121	90	146	40	171	30
GU 1	61880119	1028	7	300	GULL LN A-W	0	1910	10	1890	25	1890	30	1010
GU 1	62	55	640	69	460	86	300						
GU 1	71880622	1021	12	220	GULL LN A-W	0	1910	10	1890	23	1870	24	1550
GU 1	72	34	950	41	830	43	790	57	600	60	550	73	410
GU 1	73	92	220										
GU 2	11870728	1130	11	-300	GULL LN A-W	0	1910	10	1960	32	2120	63	820
GU 2	12	88	430	116	120	141	30	166	-30	191	-90	216	-180
GU 2	21870806	1720	10	-200	GULL LN A-W	0	1910	10	1970	30	2120	70	680
GU 2	22	120	650	220	560	274	420	294	270	316	0	322	-200
GU 2	31870818	1025	15	-210	GULL LN A-W	0	1910	10	1970	30	2120	60	790
GU 2	32	80	660	130	650	187	620	199	550	224	560	249	500
GU 2	33	300	280	310	150	326	-110	328	-210				
GU 2	41870824	1040	18	-340	GULL LN A-W	0	1950	10	1970	30	2140	66	800
GU 2	42	91	700	106	700	116	780	191	630	196	610	201	580
GU 2	43	301	590	309	560	329	470	354	220	360	100	376	-170
GU 2	51870930	1044	9	290	GULL LN A-W	0	1910	10	1970	29	2100	54	820
GU 2	52	79	660	129	600	239	520	254	380	266	290		
GU 2	61880119	1045	15	300	GULL LN A-W	0	1910	10	1960	30	2080	42	1600
GU 2	62	44	1050	69	840	94	690	119	660	144	640	169	630
GU 2	63	219	570	237	490	262	350	282	300				
GU 2	71880622	1030	11	220	GULL LN A-W	0	1910	10	1970	28	2100	35	1720
GU 2	72	58	970	83	820	123	780	173	560	205	370	230	280
GU 3	11870728	1207	9	-240	GULL LINE B	0	2060	10	1972	60	2110	140	1700
GU 3	12	154	880	179	480	208	130	258	-100	279	-240		
GU 3	21870806	1711	14	-190	GULL LINE B	0	2060	10	2050	60	2110	100	1700
GU 3	22	115	1300	125	1170	150	1110	200	930	250	710	300	530
GU 3	23	338	290	353	-90	357	-190						
GU 3	31870818	1046	12	600	GULL LINE B	0	2060	10	2050	55	2150	102	1720

ISRP = Interactive Survey Reduction Program
(Birkemeier, 1988)

GU 3	32	119	1250	144	1130	194	1050	204	870	214	690	252	650	268	640
GU 3	33	270	600												
GU 3	41870824	1110	19	-490	GULL LINE B			0	2060	10	2050	60	2010	100	1700
GU 3	42	102	1650	118	1210	143	1060	218	900	243	830	268	700	268	640
GU 3	43	297	610	322	480	327	440	337	330	358	130	366	10	376	-190
GU 3	44	386	-490												
GU 3	51870930	1057	14	210	GULL LINE B			0	2060	10	2050	60	2030	61	2070
GU 3	52	96	1710	111	1240	186	1030	236	840	261	730	286	710	292	600
GU 3	53	318	440	328	310	338	210								
GU 3	61880119	1050	10	330	GULL LINE B			0	2060	10	2050	60	2010	90	1660
GU 3	62	100	1710	125	1140	185	990	230	830	265	520	290	330		
GU 3	71880622	1043	22	210	GULL LN A-N			0	2060	10	2040	35	1990	48	2000
GU 3	72	53	2040	65	1970	90	1740	101	1710	110	1410	116	1290	131	1120
GU 3	73	156	1090	181	1010	206	920	231	900	241	890	253	810	268	640
GU 3	74	273	580	286	460	292	360	317	210						
GU 4	11870728	1305	10	-420	GULL LINE C			0	2020	10	1950	85	1520	126	1210
GU 4	12	148	1240	159	880	184	470	199	-30	244	-270	259	-420		
GU 4	21870806	1651	13	-210	GULL LINE C			0	2020	10	1960	100	1420	150	1160
GU 4	22	200	1190	270	1200	288	820	300	760	347	610	357	530	373	290
GU 4	23	393	-10	463	-210										
GU 4	31870818	1105	14	-140	GULL LINE C			0	2020	10	1960	100	1430	150	1160
GU 4	32	225	1200	270	1210	288	850	351	600	356	530	371	420	379	340
GU 4	33	397	160	419	-40	426	-140								
GU 4	41870824	1125	15	-430	GULL LINE C			0	2020	10	1960	100	1420	175	1200
GU 4	42	250	1170	270	1210	288	830	313	710	336	680	346	580	358	500
GU 4	43	393	190	403	60	419	-260	426	-430						
GU 4	51870930	1108	16	-90	GULL LINE C			0	2020	10	1960	100	1430	125	1240
GU 4	52	150	1170	200	1190	239	1170	267	1210	280	810	296	720	317	720
GU 4	53	340	520	350	520	375	120	390	-10	393	-90				
GU 4	61880119	1055	10	260	GULL LINE C			0	2020	10	1960	100	1440	160	1180
GU 4	62	260	1220	270	1170	271	1060	296	860	326	530	341	260		
GU 4	71880622	1110	18	220	GULL LINE C			0	2020	10	1970	78	1580	128	1230
GU 4	72	153	1160	178	1200	203	1200	253	1190	271	1200	275	1140	282	1010
GU 4	73	294	900	307	770	312	660	317	600	328	480	342	360	360	220
GU 5	11870728	1323	12	-400	GULL LINE D			0	2060	10	1930	85	1420	135	1180
GU 5	12	142	1270	175	1180	181	1030	219	420	247	40	287	-210	297	-340
GU 5	13	303	-400												
GU 5	21870806	1637	15	-140	GULL LINE D			0	2060	10	1930	72	1510	100	1300
GU 5	22	168	1150	200	1170	250	1180	275	1040	305	750	355	630	400	410
GU 5	23	430	330	463	160	471	-40	476	-140						
GU 5	31870818	1122	16	-150	GULL LINE D			0	2060	10	1930	72	1510	100	1330

GU	5	32	150	1230	205	1160	230	1240	271	1140	306	790	377	560	427	390
GU	5	33	429	410	436	340	462	50	483	-50	487	-150				
GU	5	41870824	1140	16	-470	GULL LINE D			0	2060	10	1930	72	1510	100	1300
GU	5	42	175	1120	200	1130	225	1210	270	1080	305	710	343	630	400	430
GU	5	43	414	370	434	180	457	20	482	240	490	-470				
GU	5	51870930	1109	14	170	GULL LINE D			0	2060	10	1930	72	1510	100	1300
GU	5	52	200	1140	225	1200	275	1050	310	680	331	630	341	630	391	460
GU	5	53	409	350	423	250	438	170								
GU	5	61880119	1102	14	320	GULL LINE D			0	2060	10	1940	60	1570	100	1340
GU	5	62	150	1230	200	1190	225	1250	250	1170	275	1000	300	780	325	690
GU	5	63	348	520	373	360	383	320								
GU	5	71880622	1123	12	120	GULL LINE D			0	2060	10	1930	60	1570	110	1230
GU	5	72	150	1230	200	1180	220	1250	270	1140	322	810	337	660	367	350
GU	5	73	397	120												
GU	6	11870728	1341	11	-270	GULL LINE E			0	2140	10	2040	85	1630	140	1340
GU	6	12	147	1380	193	1120	213	710	243	520	261	90	311	-170	341	-270
GU	6	21870806	1620	11	-150	GULL LINE E			0	2066	10	2140	100	1560	200	1250
GU	6	22	270	1100	297	830	347	600	394	350	420	150	430	50	437	-150
GU	6	31870818	1141	14	-150	GULL LINE E			0	2140	10	2140	100	1560	125	1460
GU	6	32	187	1290	225	1130	258	1190	283	940	298	820	364	570	404	360
GU	6	33	449	50	459	-60	463	-150								
GU	6	41870824	1155	16	-390	GULL LINE E			0	2140	10	2140	100	1560	200	1250
GU	6	42	225	1230	255	1230	297	870	340	750	340	720	358	640	380	530
GU	6	43	397	460	413	360	426	110	446	-200	459	-390				
GU	6	51870930	1120	13	160	GULL LINE E			0	2140	10	2140	100	1560	200	1210
GU	6	52	225	1120	262	1150	287	1030	307	860	357	650	415	410	435	280
GU	6	53	450	220	460	160										
GU	6	61880119	1103	10	430	GULL LINE E			0	2140	10	2140	100	1560	115	1450
GU	6	62	175	1260	200	1190	263	1180	328	760	378	560	418	430		
GU	6	71880622	1142	9	120	GULL LINE E			0	2140	10	2140	100	1560	135	1390
GU	6	72	185	1220	260	1140	375	620	427	260	462	120				
GU	7	11870728	1405	12	-260	GULL LINE F			0	2300	10	2320	85	1640	132	1430
GU	7	12	138	1440	161	1330	167	1130	188	720	213	460	229	240	279	110
GU	7	13	332	-260												
GU	7	21870806	1551	15	-100	GULL LINE F			0	2300	10	2300	100	1640	186	1240
GU	7	22	189	1180	200	1200	217	1150	247	920	422	680	447	610	483	510
GU	7	23	484	500	495	400	515	100	521	-100						
GU	7	31870818	1202	16	-110	GULL LINE F			0	2300	10	2300	100	1640	125	1470
GU	7	32	187	1290	200	1220	260	1190	290	1000	365	720	423	570	426	570
GU	7	33	438	470	444	380	469	50	475	-20	479	-110				
GU	7	41870824	1205	17	-410	GULL LINE F			0	2300	10	2300	100	1640	186	1240

GU 9	51870930	1152	14	130GULL LINE H	0	2060	10	2070	60	1950	160	1250			
GU 9	52	172	1340	200	1210	250	1180	267	1170	292	1190	318	900	338	650
GU 9	53	438	350	463	280	478	130								
GU 9	61880119	1125	13	350GULL LINE H	0	2060	10	2070	60	1950	160	1250			
GU 9	62	172	1340	200	1210	275	1140	300	1120	325	850	350	610	376	500
GU 9	63	401	430	426	350										
GU 9	71880622	1158	13	080GULL LINE H	0	2060	10	2070	60	1950	160	1250			
GU 9	72	172	1340	200	1210	275	1140	305	1100	310	950	360	590	438	290
GU 9	73	463	190	483	080										
GU 10	11870729	1148	12	-230GULL LINE I	0	1450	10	1440	110	1220	160	1120			
GU 10	12	185	1220	210	1010	235	730	260	430	301	170	351	10	401	-120
GU 10	13	451	-230												
GU 10	21870806	1514	13	-40GULL LINE I	0	1450	10	1450	100	1250	150	1100			
GU 10	22	200	1220	300	1230	320	1200	350	730	359	550	383	440	400	410
GU 10	23	461	130	473	-40										
GU 10	31870818	1346	17	-370GULL LINE I	0	1450	10	1450	100	1250	150	1100			
GU 10	32	200	1210	250	1160	297	1250	304	1180	319	1210	341	960	349	770
GU 10	33	367	550	400	420	417	340	445	130	464	-70	470	-370		
GU 10	41870824	1330	17	-210GULL LINE I	0	1450	10	1450	100	1250	150	1100			
GU 10	42	200	1220	275	1190	298	1240	305	1170	320	1200	342	920	348	770
GU 10	43	355	670	362	570	387	440	425	250	464	-10	478	-210		
GU 10	51870930	1153	21	-190GULL LINE I	0	1450	10	1450	100	1250	150	1100			
GU 10	52	200	1210	225	1170	250	1160	275	1210	297	1230	303	1160	309	1170
GU 10	53	316	1190	341	910	345	760	369	560	413	330	438	210	463	120
GU 10	54	488	-40	495	-140	498	-190								
GU 10	61880119	1127	10	320GULL LINE I	0	1450	10	1450	100	1250	150	1100			
GU 10	62	200	1220	330	1220	339	2080	384	620	399	520	419	320		
GU 10	71880622	1230	20	050GULL LINE I	0	1450	10	1450	100	1250	150	1100			
GU 10	72	200	1220	250	1180	295	1240	303	1190	320	1190	328	1100	338	950
GU 10	73	340	850	365	610	379	510	383	590	394	520	408	320	423	290
GU 10	74	434	270	459	050										
GU 11	11870729	1220	13	-260GULL LINE J	0	1160	10	1170	85	1230	205	1230			
GU 11	12	240	970	265	690	290	430	315	290	340	170	350	140	400	-10
GU 11	13	450	-130	500	-240										
GU 11	21870806	1456	14	-50GULL LINE J	0	1160	10	1170	100	1220	211	1210			
GU 11	22	211	1190	300	1190	360	1230	380	620	382	500	384	500	400	390
GU 11	23	435	230	446	60	452	-50								
GU 11	31870818	1359	18	-200GULL LINE J	0	1160	10	1170	100	1220	200	1210			
GU 11	32	211	1180	343	1240	358	1210	363	930	368	730	381	560	386	490
GU 11	33	399	390	405	370	408	380	416	310	449	0	457	-110	468	-200
GU 11	41870824	1345	16	-190GULL LINE J	0	1160	10	1170	100	1220	200	1210			

GU 11	42	210	1170	310	1200	345	1220	362	930	367	770	373	670	388	470
GU 11	43	398	420	405	380	416	290	447	10	466	-190				
GU 11	51870930	1202	9	340	GULL LINE J	0	1160	10	1170	100	1220	200	1210		
GU 11	52	348	1240	371	900	372	770	386	570	410	340				
GU 11	61880119	1140	11	400	GULL LINE J	0	1160	10	1170	100	1220	200	1230		
GU 11	62	225	1180	325	1200	347	1190	348	1010	373	650	378	590	396	400
GU 11	71880622	1227	11	060	GULL LINE J	0	1160	10	1170	100	1220	200	1230		
GU 11	72	210	1210	345	1240	352	945	372	670	389	290	414	120	424	060
GU 12	11870729	1344	12	-290	GULL LINE K	0	1480	10	1520	70	1610	165	1380		
GU 12	12	205	1360	235	1030	275	500	325	230	362	90	412	-50	462	-160
GU 12	13	517	-290												
GU 12	21870806	1437	19	-10	GULL LINE K	0	1480	10	1520	70	1610	95	1690		
GU 12	22	150	1460	200	1350	216	1150	228	1120	229	1170	300	1220	347	1260
GU 12	23	379	590	381	670	383	510	385	480	395	340	400	310	460	90
GU 12	24	468	-10												
GU 12	31870818	1411	19	-200	GULL LINE K	0	1480	10	1520	80	1610	95	1690		
GU 12	32	150	1460	200	1350	225	1100	229	1190	336	1210	346	1250	365	950
GU 12	33	369	740	381	550	384	490	389	470	406	300	458	100	480	-100
GU 12	34	492	-200												
GU 12	41870824	1355	17	-140	GULL LINE K	0	1480	10	1520	80	1610	95	1690		
GU 12	42	150	1460	200	1350	229	1190	279	1220	348	1260	361	1070	369	760
GU 12	43	372	690	379	560	384	520	404	340	463	60	482	-140		
GU 12	51870930	1209	20	-160	GULL LINE K	0	1480	10	1520	70	1610	95	1690		
GU 12	52	150	1460	200	1350	216	1150	229	1170	230	1170	280	1190	305	1190
GU 12	53	324	1230	340	940	341	770	352	570	384	310	409	160	434	30
GU 12	54	459	-130	462	-160										
GU 12	61880119	1200	11	540	GULL LINE K	0	1480	10	1520	70	1610	95	1690		
GU 12	62	150	1460	200	1350	216	1150	229	1190	310	1210	315	870	335	800
GU 12	71880622	1241	16	140	GULL LINE K	0	1480	10	1520	70	1610	95	1690		
GU 12	72	150	1460	200	1350	216	1150	279	1220	304	1200	320	1030	338	750
GU 12	73	344	660	369	470	385	360	410	200	419	140				
GU 13	11870729	1404	16	-300	GULL LINE L	0	1790	10	1820	77	1970	127	1680		
GU 13	12	197	1360	211	1360	226	1180	239	1120	242	930	262	600	278	450
GU 13	13	323	250	363	100	413	-60	463	-190	524	-300				
GU 13	21870808	1403	13	0	GULL LINE L	0	1790	10	1830	77	1980	200	1360		
GU 13	22	230	1230	300	1190	354	1200	384	650	398	580	400	550	406	480
GU 13	23	460	100	466	0										
GU 13	31870818	1422	16	-200	GULL LINE L	0	1790	10	1830	77	1980	200	1360		
GU 13	32	230	1230	330	1200	347	1240	354	1200	359	1070	375	790	399	560
GU 13	33	403	500	433	290	470	0	479	-100	506	-200				
GU 13	41870824	1405	16	-150	GULL LINE L	0	1790	10	1830	77	1980	200	1360		

GU 13	42	230	1230	249	1230	254	1180	280	1200	359	1160	374	800	384	690
GU 13	43	396	540	401	510	418	360	462	50	489	-150				
GU 13	51870930	1212	13	-160	GULL LINE L			0	1790	10	1830	77	1980	200	1360
GU 13	52	230	1230	315	1180	357	1190	373	900	397	590	406	330	430	120
GU 13	53	459	-130	462	-160										
GU 13	61880119	1152	12	430	GULL LINE L			0	1790	10	1830	75	1980	200	1360
GU 13	62	230	1240	330	1210	352	1190	354	1140	355	990	370	770	382	610
GU 13	63	399	430												
GU 13	71880622	1241	13	-006	GULL LINE L			0	1790	10	1830	75	1980	200	1360
GU 13	72	230	1240	330	1210	350	1210	357	1020	384	640	392	530	434	254
GU 13	73	454	144	474	-006										
GU 14	11870729	1427	15	-240	GULL LINE H			0	2120	10	2120	30	2140	130	1600
GU 14	12	200	1300	213	1320	227	1220	230	940	236	810	261	490	326	220
GU 14	13	351	130	401	10	451	-130	515	-240						
GU 14	21870808	1244	14	-260	GULL LINE H			0	2120	10	2130	30	2150	100	1770
GU 14	22	200	1310	214	1330	300	1240	340	1250	378	580	400	500	424	420
GU 14	23	468	220	474	50	488	-260								
GU 14	31870818	1440	16	-200	GULL LINE H			0	2120	10	2130	30	2150	100	1770
GU 14	32	200	1310	216	1330	241	1210	331	1230	343	1240	360	960	368	770
GU 14	33	389	560	424	420	453	280	489	0	505	-200				
GU 14	41870824	1420	14	-80	GULL LINE H			0	2120	10	2130	30	2150	100	1770
GU 14	42	200	1310	300	1230	342	1250	367	790	378	670	387	600	414	490
GU 14	43	433	390	478	120	501	-80								
GU 14	51870930	1230	16	-150	GULL LINE H			0	2120	10	2130	30	2150	100	1770
GU 14	52	200	1310	213	1330	238	1220	263	1180	288	1180	313	1220	345	1200
GU 14	53	366	810	444	300	469	110	494	-50	508	-150				
GU 14	61880119	1204	12	490	GULL LINE H			0	2120	10	2130	30	2150	100	1770
GU 14	62	200	1300	225	1270	300	1230	350	1150	354	1060	379	740	386	550
GU 14	63	406	490												
GU 14	71880622	1304	21	010	GULL LINE H			0	2120	10	2130	30	2150	100	1770
GU 14	72	200	1310	225	1290	275	1180	300	1210	347	1210	355	1040	364	910
GU 14	73	380	740	388	650	394	600	397	600	400	530	419	440	444	320
GU 14	74	458	240	483	110	498	010								
GU 15	11870729	1445	14	-200	GULL LINE H			0	2170	10	2190	35	2220	135	1600
GU 15	12	195	1290	201	1320	209	860	225	610	243	460	293	290	330	180
GU 15	13	380	50	430	-50	483	-200								
GU 15	21870808	1216	14	-120	GULL LINE H			0	2170	10	2270	30	2240	100	1810
GU 15	22	190	1310	200	1300	331	1250	344	1190	368	790	400	660	460	370
GU 15	23	500	170	510	-20	520	-120								
GU 15	31870818	1506	15	-240	GULL LINE H			0	2170	10	2270	30	2240	100	1810
GU 15	32	190	1310	200	1300	275	1180	340	1200	375	720	429	550	432	510

GU 15	33	452	410	482	250	520	-40	535	-240						
GU 15	41870824	1430	13	-80	GULL LINE N	0	2170	10	2270	30	2240	100	1810		
GU 15	42	190	1310	200	1300	300	1190	340	1190	370	760	395	660	457	430
GU 15	43	504	120	522	-80										
GU 15	51870930	1230	15	120	GULL LINE N	0	2170	10	2270	30	2240	100	1810		
GU 15	52	190	1310	200	1300	275	1180	300	1170	350	1210	371	920	383	790
GU 15	53	453	480	482	330	507	180	517	120						
GU 15	61880119	1212	14	490	GULL LINE N	0	2170	10	2190	30	2230	100	1810		
GU 15	62	190	1310	200	1310	250	1180	300	1190	340	1190	347	1040	372	780
GU 15	63	383	690	408	540	418	490								
GU 15	71880622	1301	15	030	GULL LINE N	0	2170	10	2190	30	2230	100	1810		
GU 15	72	190	1310	200	1300	300	1170	325	1200	332	1210	342	1010	352	620
GU 15	73	360	530	438	230	463	120	483	030						
GU 16	11870808	1135	15	-260	GULL LINE O	0	1590	10	1560	100	1370	144	1240		
GU 16	12	165	1299	200	1140	250	1130	290	1120	400	660	450	450	496	180
GU 16	13	504	0	508	-40	513	-160	515	-260						
GU 16	31870818	1516	14	-320	GULL LINE O	0	1590	10	1560	100	1370	144	1240		
GU 16	32	165	1299	265	1120	365	780	456	490	459	440	468	380	475	340
GU 16	33	487	180	513	-120	519	-320								
GU 16	41870824	1440	14	-120	GULL LINE O	0	1590	10	1560	100	1370	144	1240		
GU 16	42	165	1299	200	1140	250	1130	290	1090	365	770	412	590	437	530
GU 16	43	464	350	495	80	510	-120								
GU 16	51870930	1238	15	-340	GULL LINE O	0	1590	10	1560	100	1370	144	1240		
GU 16	52	165	1299	175	1180	250	1140	285	1110	360	810	373	750	443	500
GU 16	53	471	250	496	20	515	-210	518	-340						
GU 16	61880119	1221	15	450	GULL LINE O	0	1590	10	1570	100	1370	144	1240		
GU 16	62	165	1300	200	1140	215	1120	265	1110	290	1090	315	980	340	860
GU 16	63	365	740	388	630	413	490	423	450						
GU 16	71880622	1313	22	-040	GULL LINE O	0	1590	10	1570	100	1370	144	1240		
GU 16	72	165	1300	190	1170	240	1130	286	1110	336	890	351	820	353	790
GU 16	73	357	700	366	570	366	570	372	480	397	370	412	330	418	314
GU 16	74	432	274	460	170	485	020	501	-040						

APPENDIX B

SEDIMENTARY FEATURES

This appendix presents sedimentologic features observed along the shorelines of the lower Columbia River. Common terminology used in shore studies are listed below.

DEFINITION OF SHORE TERMINOLOGY

(Komar, 1986; King, 1972; USACE, 1984)

- Shore: the strip of ground bordering any body of water whether the ground is rock or loose sediment. If it is unconsolidated sediment, then shore becomes synonymous with beach used in its restricted sense.
- Offshore zone: (Bagnold, 1963) area extending from bed contour at which depth admits disturbance of bed sediment by wave motion inward to the contour at which waves begin to break.
- Shoreline: the line of demarcation between the water and the exposed beach.
- Backshore: portion of profile extending landward from the sloping foreshore to the point of development of vegetation or change in physiography.
- Beach face: sloping section of the beach profile below the berm which is normally exposed to the action of wave swash.
- Beach scarp: vertical escarpment notch into beach profile by wave erosion, height is commonly less than a meter, but can be higher.
- Berm: nearly horizontal portion of the beach or backshore formed by the disposition of sediment by receding waves - some beaches may have more than one.
- Breaker zone: portion of the nearshore region at which the waves arriving from offshore reach instability and break. With very simple uniform waves, such as those generated in a wave tank, the zone may be reduced to a breaker line.
- Foreshore: sloping portion of the beach profile lying between a berm crest (or in the absence of

a berm crest, the upper limit of wave swash at high tide) and the low-water mark of the backrush of the wave swash at low tide.

Surf zone: the portion of the nearshore region in which bore-like translation waves occur following wave breaking - the dissipation of wave energy by surface turbulence. This portion extends from the inner breakers shoreward to the swash zone.

Swash zone: portion of the nearshore region in which the beach face is alternately covered by the uprush of the wave swash and exposed by the backwash, the zone of residual wave motion.

STRATIGRAPHIC SECTIONS

Set No. 1 Profile PU11, 29JUL88
Alluvial or "micro-bajada" laminae

laminae thickness (mm)

10	
5	
10	
5	
4	
3	laminae
3	inclined 49° to shore
6	
12	
7	
17	
3	
3	
15	

STATISTICS

mean	=	7.15 mm
median	=	5.0 mm
std. dev.	=	4.83
range	=	14
min.	=	3 mm
max.	=	17 mm

Data recorded from trench in profile PU11, 29JUL88.

SET No. 2

Wave laminae

<u>laminae thickness (mm)</u>	<u>laminae thickness (mm)</u>
5	4
6	3
3	6
5	2
4	10 laminae
8	5 inclined 5° to shore
5	4
10 laminae	6
3 inclined 9° to shore	2
8	5
3	6
6	6
5	3
5	3
8	12
3	7
5	3
3	6
7	4
2	4
8	7
4	3
4	5
4	3
15	2
2	12
3 laminae	5
7 inclined 5° to shore	3
3	10
7	5
4	10
13	5
4	
6	STATISTICS
3	mean = 5.46 mm
7	median= 5.0 mm
5	std. dev.= 2.85
3	Range =13 mm
10	min. = 2 mm
	max. = 15 mm

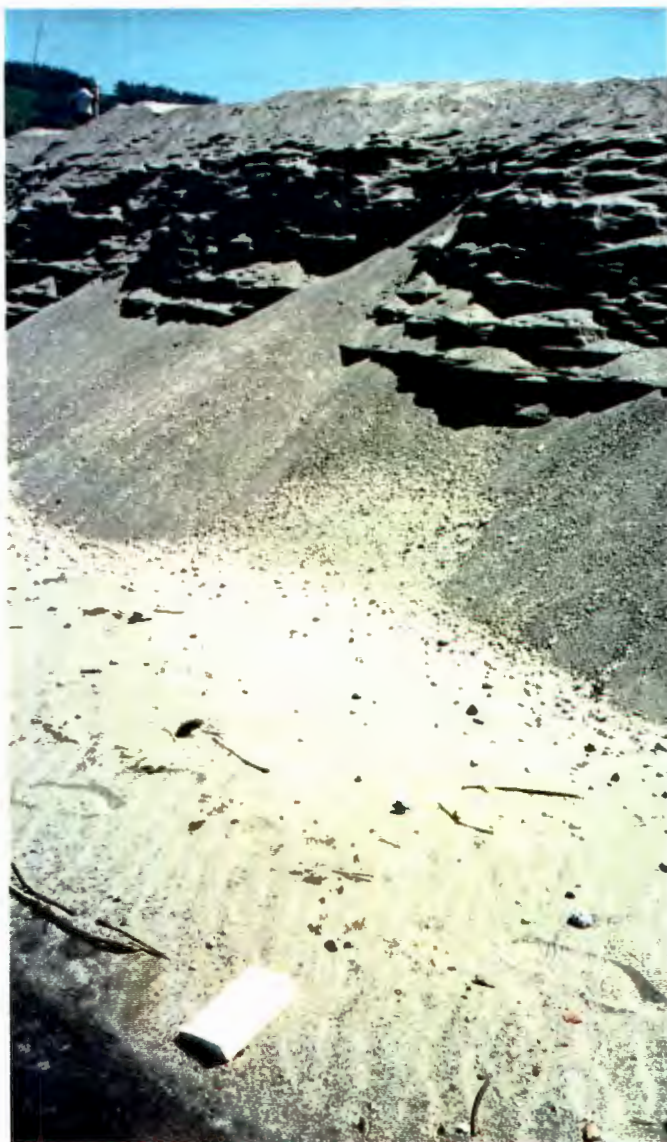
The following photos exhibit shore morphology and sedimentary structures moving from supratidal zone (above highest high water) to water depths of about 50 cm.



Eolian features observed on sandy shore slopes above highest high water in the study region. Dune size decreases shoreward from the crest of the beach scarp.



Eolian dune. Note coarse grained dune crest and finer grained troughs, clearly apparent in grain size distributions. Predominant wind direction is right to left, blowing from the west.



Beach scarp in sand disposal pile. Note distinct fan development and terraces developed by wind erosion. Note accumulation of pumice and dacite cobbles on upper beach along with eolian ripples. High water is marked by the heavy mineral band in the lower left. Wallace Island site, June 24, 1988.



High water wave swash up to base of beach scarp at Wallace Island site. June 24, 1988.



Beach scarp that lies completely above high water, as interpreted by lack of swashed features, beach scarp and the occurrence of distinct eolian dunes down to the heavy mineral band in the extreme left. Surface bedforms suggest dominant wind direction is to the east, as at Price and Puget Islands.



Active beach scarp at Wallace Island site. Note eolian dunes above scarp and heavy mineral band with lobate swash pattern below, two distinct sedimentary environments.



Beach scarp exposing cross-bedding of eolian dunes.



Runnels at Puget Island site, occurring in site shore notch (profiles 3-9). Runnels form from the discharge of groundwater out of the beach. Groundwater is recharged at high water. Seepage out of the beach face is at a much lower rate than the tidally driven drop in the river's water level.



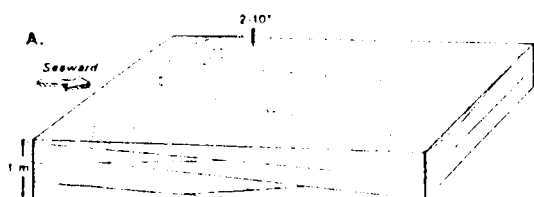
Micro-dendritic drainage patterns form cutting into the beach and moving sand down the beach face. Beach runnels occur below highest high water. The groundwater table lowers slower than the tide and releases water onto steeper slopes at lower tides, leading to runnels.



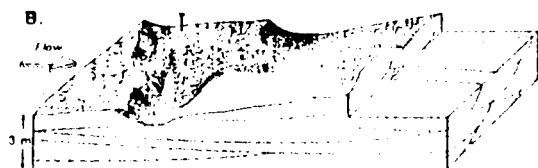
Distinct zone of heavy mineral accumulation on surface of beach face, associated with the high water line. Heavy minerals make up approximately 5-10 percent of the Columbia River sand.



Mineral separation patterns on beach face. Profile no.10, Puget Island site, June 13, 1988.



SWASH CROSS STRATIFICATION. Low-angle (2° - 10°) cross stratification, subparallel to bases of wedge-shaped sets. Stratification and set boundaries are formed parallel to changing slope of beachface and dip generally seaward.



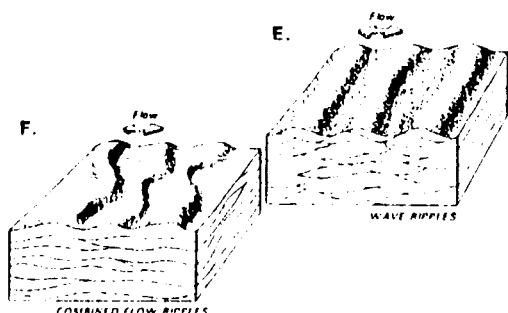
LARGE-SCALE TROUGH CROSS STRATIFICATION formed by subaqueous dunes or "megaripples". High-angle (25° - 30°) cross stratification, tangential to bases of trough-shaped sets. Cross strata dip parallel to flow direction.



TABULAR CROSS STRATIFICATION FORMED BY MIGRATING SAND WAVES. High-angle (near 30°) cross stratification in tabular sets. Cross strata are planar and angular to bases of sets where flow is steady but may be tangential under some conditions.



HUMMOCKY CROSS STRATIFICATION. Low-angle (less than 15°) cross stratification, subparallel to smooth, undulatory lower boundaries of sets. Similar appearance in all vertical orientations. Commonly associated with wave ripples.



WAVE RIPPLES. Ripple-trough profiles are symmetrical and rounded, and stratification dips in both directions of oscillatory flow.

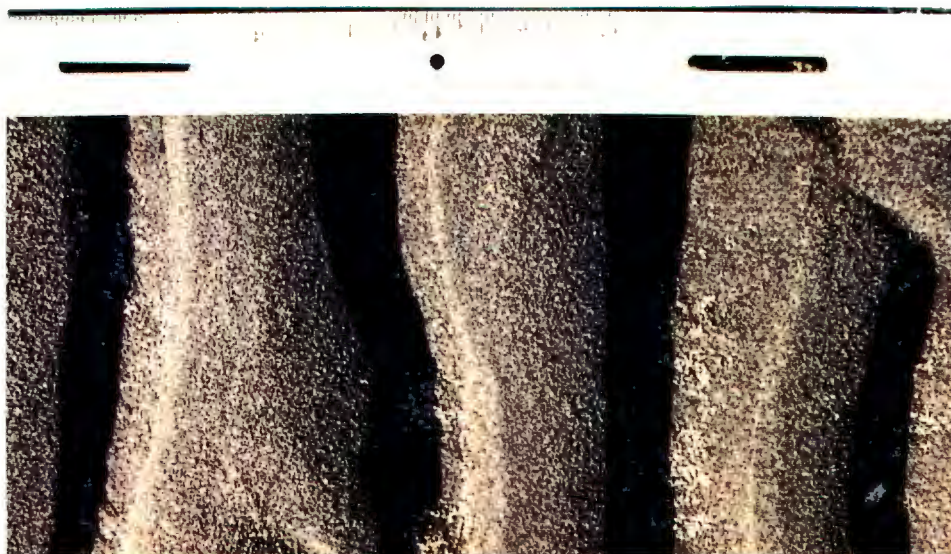


COMBINED-FLOW RIPPLES. Formed by superimposed wave and current action or by shoaling waves. Small-scale cross strata are curved and tangential, dipping in direction of dominant flow.

Common stratification types and associated bedforms in coastal-marine sands. Variations in form related to grain size, changing flow conditions, and rates of deposition (In: Scholle and Spearing, 1982, p.249). The study region shows excellent examples of the stratification patterns displayed in D, E, and F.



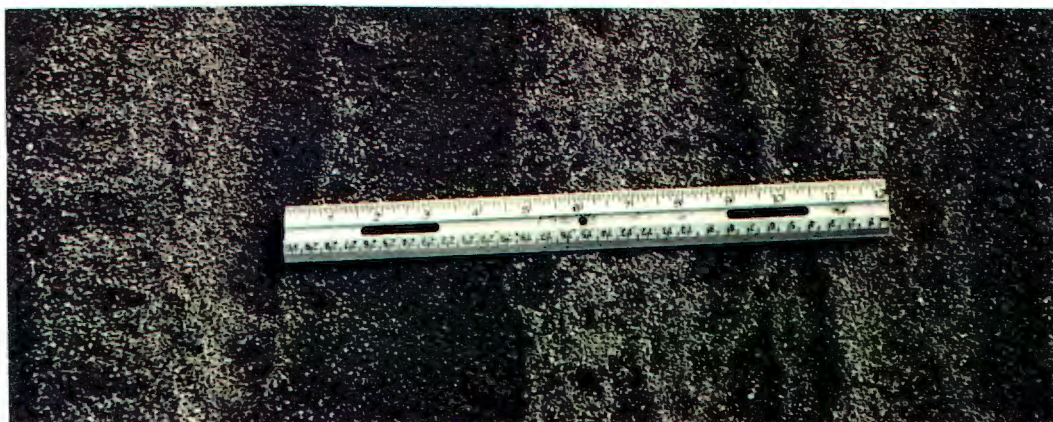
Looking down at preserved wind wave generated ripples on the beach face of Puget Island site profile no.11, September 16, 1987. Note bifurcating and symmetrical pattern characteristic of a wave dominated sedimentary environment.



Close-up of same ripples. Note flattening of ripple crests that occurs by swash action at the water's edge as the water level drops across the beach face. Pumice grains accumulate in the troughs.



Puget Island site beach face along profile no.11, 16SEP87. Waterline lies to the right of the photograph. This photo illustrates some interesting bedform development. The debris line visible in the upper left marks highest high water swash from run-up caused by a ship wave. The pumice swash delineates mean highest high water. No ripples are preserved in the upper beach, but as the rate of water level retreat increases during a drop in the tide, ripples become more completely preserved. Note that the most susceptible portion of the ripples are destroyed, their crests.



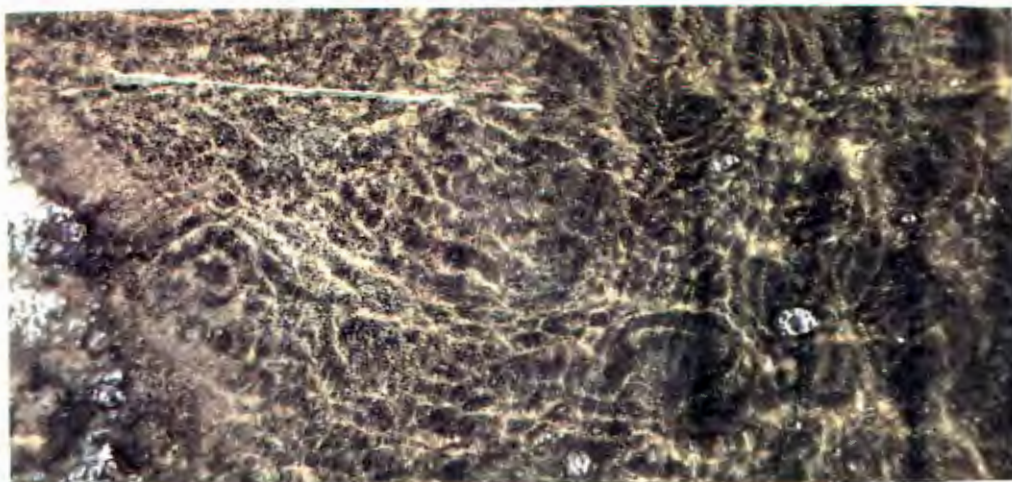
Close-up of same site exhibiting the pumice swash bands. Note the pumice grains are larger than the mean grain size. This size difference and the lower density of pumice grains makes the pumice very susceptible to entrainment and transport.



Conditions at the water's edge along beach face. Note lobate swash patterns delineated by pumice grains. The low density of the pumice and the larger size relative to the mean grain size of the sediment population, results in the pumice being easily moved. Thus the pumice ends up at the hydraulic boundary in which energy is delivered; the shoreline.



Active berm at the water's edge. Note distinct difference in grain size shoreward and riverward of this berm. This characteristic of the structures. The berm edge, slightly riverward of the water's edge was used as the water surface point in the level and rod surveying. Vista Park beach, Skamokawa, Washington, RK 54, 26AUG87.



Looking down at beach face just below the water's edge, which lies just to the left of the field of view. Note wind oscillatory wave ripples to the right. Edge of berm is marked by change between ripples to planar bed just left of center. Ruler is 1 foot (30.5cm) in length. Puget Island site, profile no.11, 16JUN87.



Looking down at beach face just above the water's edge, located at extreme right. Note the smooth, planar bed that is characteristic of the swash zone, especially the swash zone at tidal extremes where the water remains in one position for a longer period. Ripple preservation is apparently dependent upon the rate of water level regression down beach face. Puget Island site, profile no.11, 16JUN87.

APPENDIX C

SHIP WAVES

This appendix includes the data recorded by the low pressure transducer of ship waves at the Puget Island site. Information is also listed describing the ships, date and time, and tidal elevation.

Merchant Vessels^{1,2}

<u>Ship</u>	<u>Type</u>	<u>Date/time</u>	<u>draft</u>	<u>length</u>	<u>beam</u>	<u>displ.</u>
El Garen outbound	cargo	09/15/87	9.51	216.4	32.3	24,760
Ocean Beauty inbound	bulk	09/15/87 15:17	7.00	175.3 (BB)	23.4	16,636
Valdiva outbound	bulk	09/15/87 16:00	12.00	224.9 (BB)	32.3	61,161
Chevron Oregon inbound	tanker	09/17/87 12:54	10.67	198.1	29.3	37,602
Magnolia inbound	bulk	09/17/87 15:25	7.01	196.0 (BB)	29.6	30,127
Cordiality inbound	bulk	09/17/87 16:03	4.00	197.8 (BB)	24.3	12,548
Evelyn Maersk inbound	tanker	09/18/87	11.00	182.6 (BB)	32.2	45,636
Hyundai #108 inbound	car	09/18/87	7.20	173.7 (BB)	27.7	8,809
Kee Lung inbound	bulk	09/18/87 15:35	6.50	187.4 (BB)	28.3	22,612
Luna II inbound	bulk	10/29/87 13:30	9.54	182.8 (BB)	28.5	33,381
Lake River inbound	bulk	10/29/87 14:00	7.49	225.8 (BB)	32.3	38,815
Leonadros inbound	bulk	10/30/87 13:30	7.80	220.0 (BB)	32.3	34,446
European Hwy inbound	car	06/08/88 11:15	7.01	180.0	32.2	12,437
Coast Range inbound	tanker	06/09/88 13:00	7.32	220.7 (BB)	31.0	27,685

Merchant Vessels^{1,2}

<u>Ship</u>	<u>Type</u>	<u>Date/time</u>	<u>draft</u>	<u>length</u>	<u>beam</u>	<u>displ.</u>
Ocean Jade inbound	bulk	06/13/88 13:10	8.30	192.0 (BB)	30.0	28,950
Verranzano Br. inbound	cont.	06/13/88 11:33	6.13	264.5 (BB)	32.3	18,176
outbound		06/14/88 16:40	10.67	264.5	32.3	31,638
Indah Fuji inbound	bulk	06/14/88 12:30	6.72	160.0 (BB)	25.0	16,714

¹ Dimensions from Lloyd's Register, 1988-89.

² Drafts from Columbia River Pilots, 1988.

³ Dimensions from Janes Fighting Ships, 1987-88.

cont. = container ship

Br. = Bridge

Hwy = Highway

1988 Rose Festival Naval Vessels³

<u>Ship</u>	<u>Type</u>	<u>Date/time</u>	<u>draft</u>	<u>length</u>	<u>beam</u>	<u>displ.</u>
USN Chandler outbound	naval destroyer	06/14/88 16:00	6.20 ("Kidd" class)	171.6	16.8	6,210
USN Ford inbound	naval frigate	06/09/88 09:07	4.50 ("Oliver Hazard Perry" class)	135.6	13.7	2,750
USN Thach outbound	naval frigate	06/09/88 11:35	4.50 ("Oliver Hazard Perry" class)	135.6	13.7	2,750
USN Gray inbound outbound	naval frigate	06/09/88	7.80 ("Knox" class)	133.5	14.3	3,011
USN Kansas City inbound	naval oiler	06/08/88	10.20 (no wave record)	200.9	29.3	13,000
USN Mt. Vernon inbound	naval	06/08/88 11:30	6.00 dock landing ship	168.6	25.6	8,600
USN Ramsey inbound	naval frigate	06/09/88 09:45	4.60 ("Brooke" class)	126.3	13.5	2,640
USCG Boutwell outbound	cutter	06/13/88 13:45	6.10 ("Hamilton" and "Hero" class)	115.2	13.1	3,050
USCG Iris outbound	tender bouytender	06/13/88 13:52	4.00 "Balsam" class	54.9	11.3	935

¹ Dimensions from Lloyd's Register, 1988-89.

² Drafts from Columbia River Pilots, 1988.

³ Dimensions from Janes Fighting Ships, 1987-88.

cont. = container ship

Br. = Bridge

Hwy = Highway

Merchant Vessels^{1,2}

Ship	Velocity		<u>Bc</u>	<u>Bf</u>	<u>DD</u> (cm)	<u>H_{max}</u> (cm)	<u>T_{max}</u> (sec)	<u>DD</u> (s)	<u>d</u> (cm)
	<u>m/s</u>	<u>knots</u>							
El Garen outbound	8.7	16.8	0.37		-	-	-		
Ocean Beauty inbound	7.5	14.6	0.58	.022	36.3	27.0	4.10	26	119
Valdiva outbound	5.2	10.1	-		5.0	7.0	2.20	-	180
Chevron Oregon inbound	5.9	11.6	0.607	.041	34.0	17.1	2.14	37	96
Magnolia inbound	6.1	12.0	0.745	.028	23.6	38.1	3.74	55	150
Cordiality inbound	5.1	9.9	0.656	.013	4.0	17.1	2.43	-	122
Evelyn Maersk inbound	-	-							40
Hyundai #108 inbound	6.4	12.5	-	-	-	-			
Kee Lung inbound	7.1	13.9	0.651		33.0	15.0	3.76	30	122
Luna II inbound	5.9	11.5	0.673	.037	57.2	30.5	3.76		79
Lake River inbound	6.7	13.1	0.033	.033	26.5	16.0	4.14	40	79
Leonadros inbound	5.6	10.9	0.035	.035	26.7	15.2	3.38	-	104
European Hwy inbound	7.4	14.3	0.		38.0	30.0	4.80	35	113
Coast Range inbound	6.9	13.5	0.555	.029	25.0	11.0	4.50	30	155
Ocean Jade inbound	5.8	11.3	0.606	.033	15.2	27.8	3.76	40	110
Verranzano Br. inbound	6.0	11.9	0.35	.033	53.3	19.0	3.76	35	95
outbound (outbound record lost)	7.2	13.0	0.35	.045	157.0	61.0	4.60		
Indah Fuji inbound	6.6	12.9	0.622	.023	35.0	19.0	3.76	40	143

¹ Dimensions from Lloyd's Register, 1988-89.² Drafts from Columbia River Pilots, 1988.³ Dimensions from Janes Fighting Ships, 1987-88.

cont. = container ship

Br. = Bridge

Hwy = Highway

1988 Rose Festival Naval Vessels³

<u>Ship</u>	<u>Velocity</u>		<u>Bc</u>	<u>Bf</u>	<u>DD</u> (cm)	<u>H_{max}</u> (cm)	<u>T_{max}</u> (sec)	<u>d</u> (cm)
	<u>m/s</u>	<u>knots</u>						
USN Chandler outbound		13.8			22.9	20.9	3.76	143
USN Ford inbound		16.7			3.8	41.9	4.60	146
USN Thach outbound	7.2	14.0	0.429	.009	0.0	8.0	3.00	116
USN Gray inbound outbound	8.1	15.7			8.0	43.0	4.50	198
	6.6	11.9	0.478	.009	15.2	36.2	4.51	119
USN Mt. Vernon inbound		13.6			21.0	22.9	4.50	125
USN Ramsey inbound	7.8	15.2			0.0	38.1	4.50	168
USCG Boutwell outbound	8.1	15.7	0.331	.010	0.0	33.5	4.50	137
USCG Iris outbound	5.7	11.1	0.413	.006	0.0	22.9	3.76	137

¹ Dimensions from Lloyd's Register, 1988-89.

² Drafts from Columbia River Pilots, 1988.

³ Dimensions from Janes Fighting Ships, 1987-88.

cont. = container ship

Br. = Bridge

Hwy = Highway

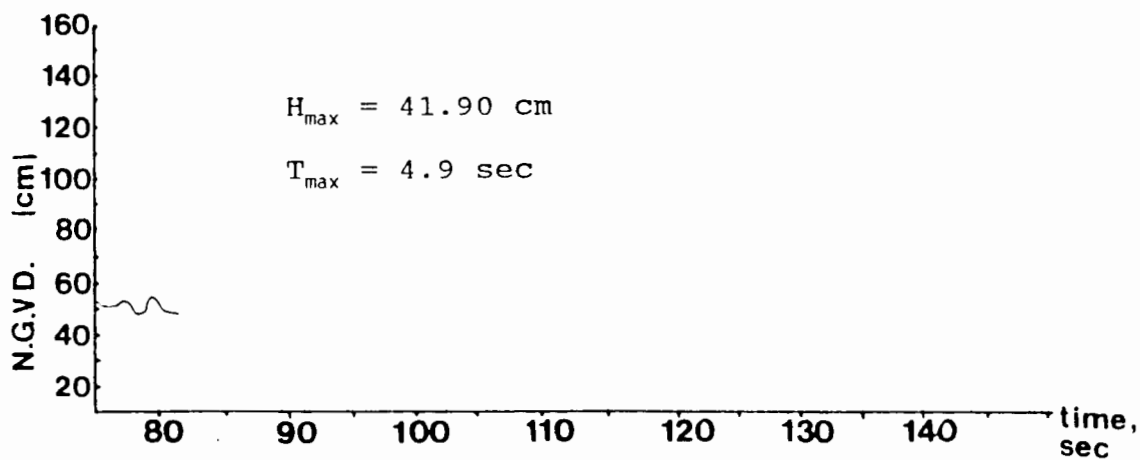
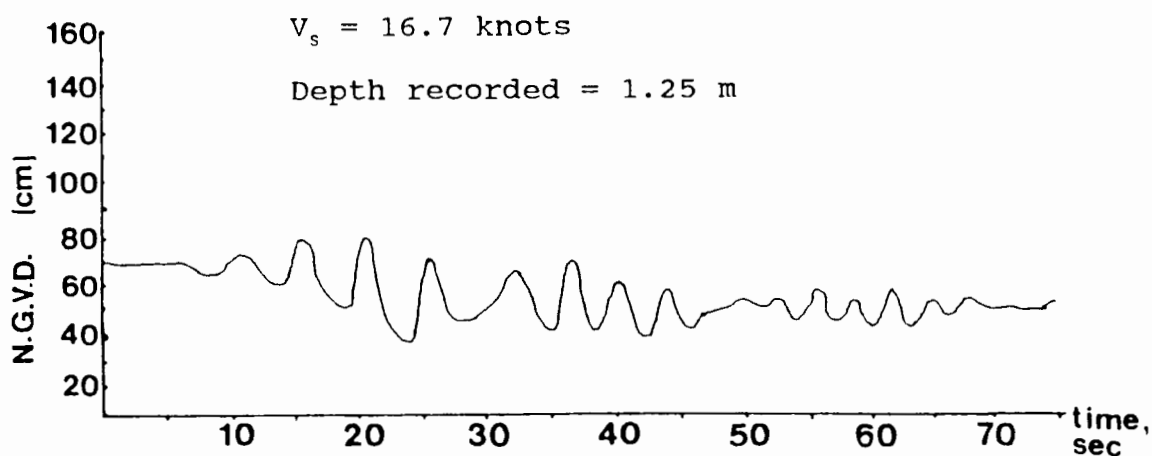
Maximum Design Draft and Deadweight Tonnage

From Lloyd's (1988) Listing of Ship Parameters

<u>Ship</u>	<u>Maximum Draft (m)</u>	<u>Deadweight (tonnes)</u>
El Garen	10.82	28,173
Ocean Beauty	10.41	24,740
Valdiva	12.92	65,785
Chevron Oregon	11.31	39,847
Magnolia	9.06	38,918
Cordiality	11.17	35,110
Evelyn Maersk	12.20	50,600
Hyundai #108	7.99	9,783
Kee Lung	10.75	37,389
Luna II	10.83	37,895
Lake River	13.20	68,407
Leandros	12.35	54,540
European Highway	8.20	14,569
Coast Range	10.74	40,631
Ocean Jade	10.67	37,217
Verranzano Bridge	12.04	35,582
Indah Fuji	10.00	24,872

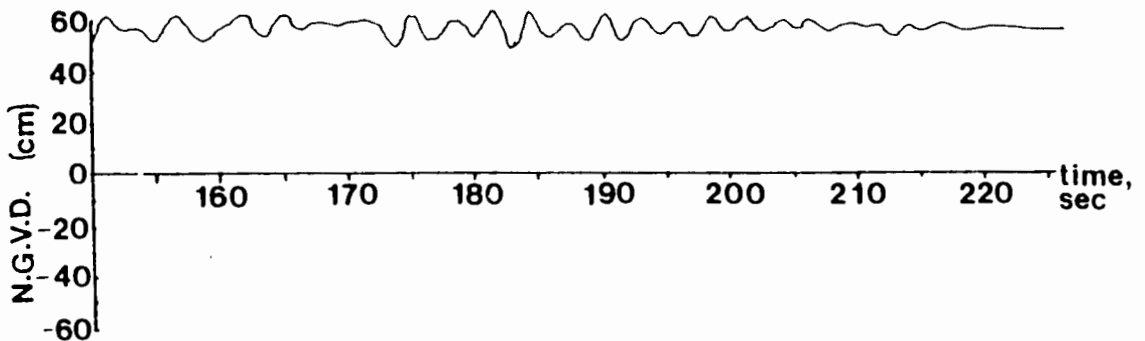
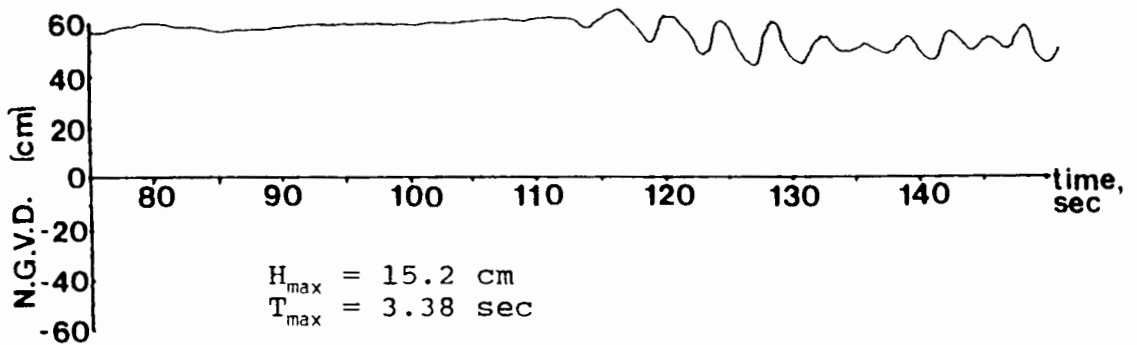
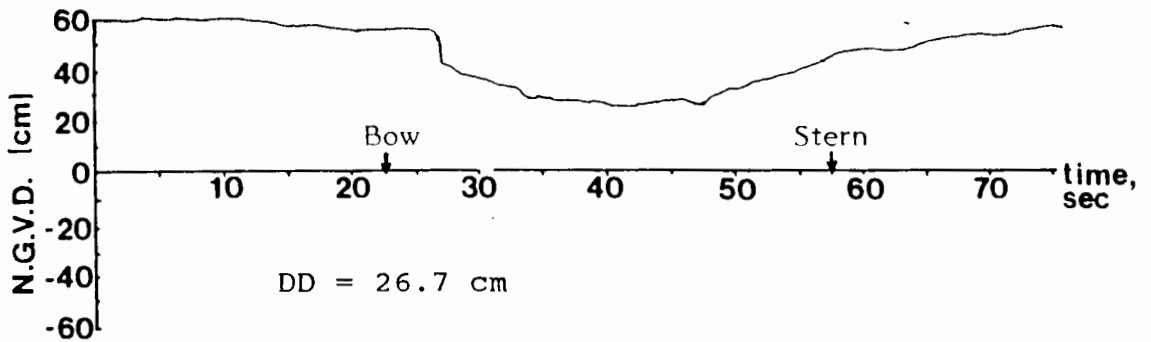
From Jane's Fighting Ships 1987-1988

	draft <u>(m)</u>	standard <u>displ. (tonnes)</u>
USN Chandler (996)	6.20	3,050
USN Ford (54)	4.50	2,750
USN Thach (43)	4.50	2,750
USN Gray (1054)	4.60	3,011
USN Kansas City (32)	10.20	12,500
USN Mt. Vernon (39)	6.00	8,600
USN Ramsey (2)	4.60	2,640
USCG Boutwell	6.10	3,050
USCG Iris	4.00	935

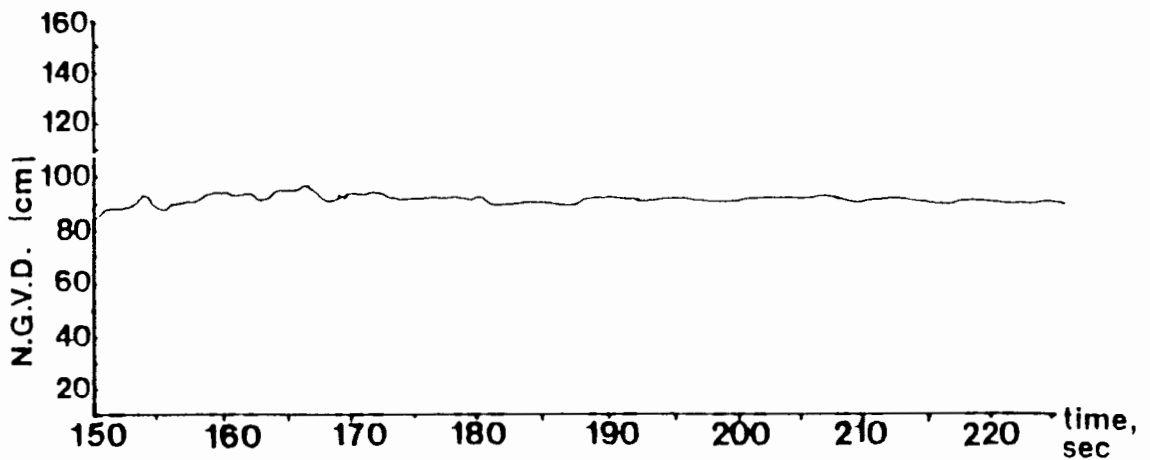
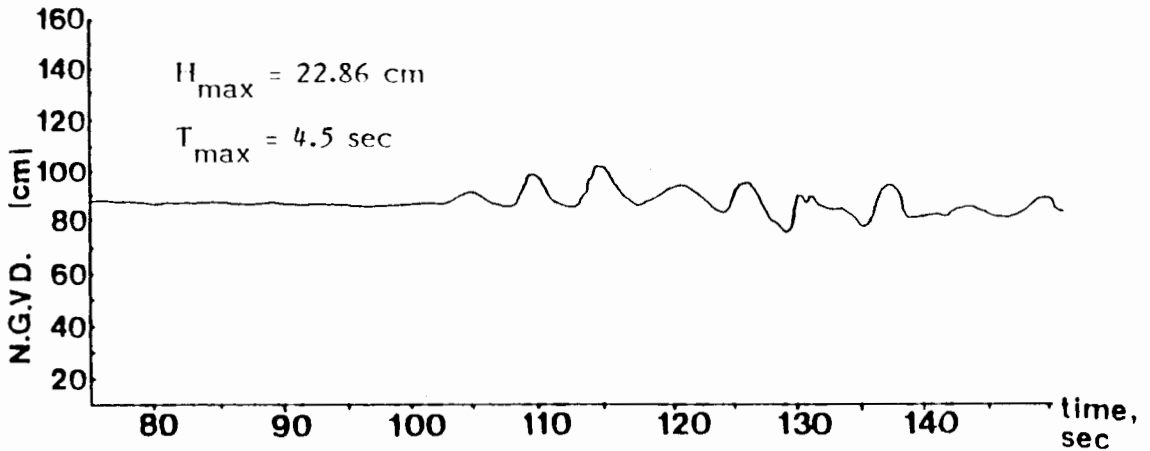
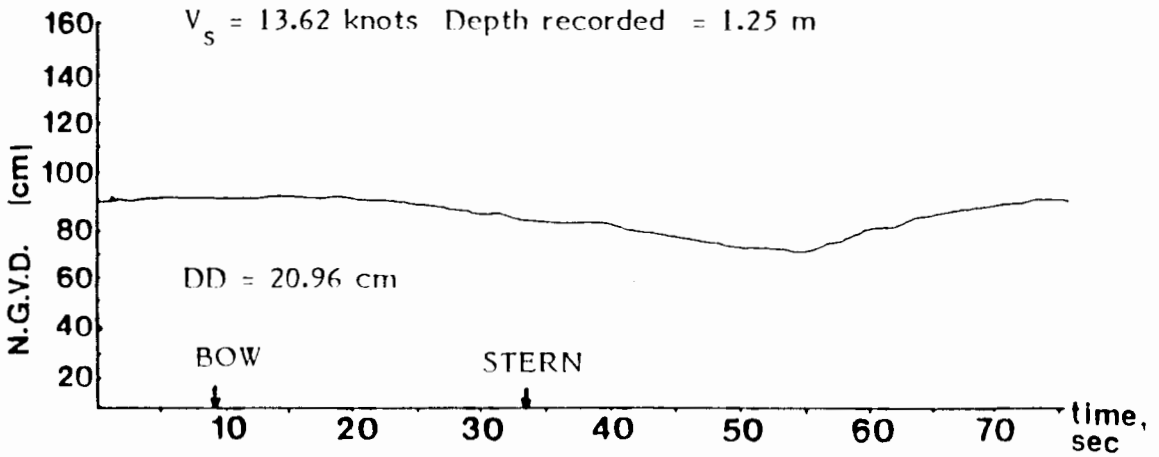


Ship wave record, Puget Island, WA RK 62
USN Ford 09JUN88 09:07 UPSTREAM

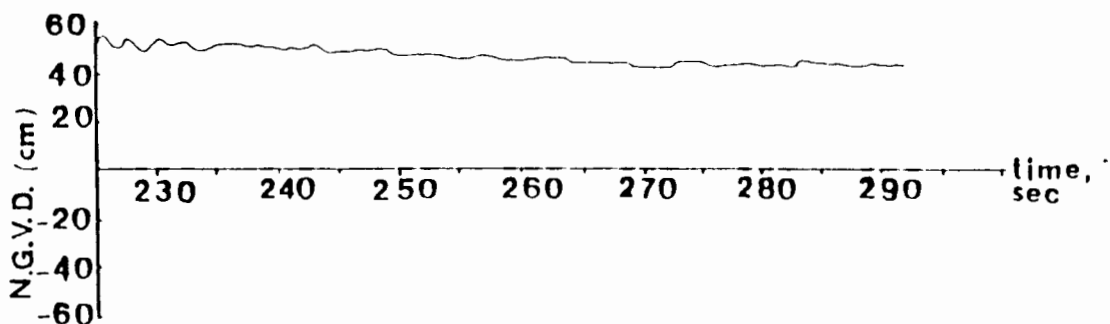
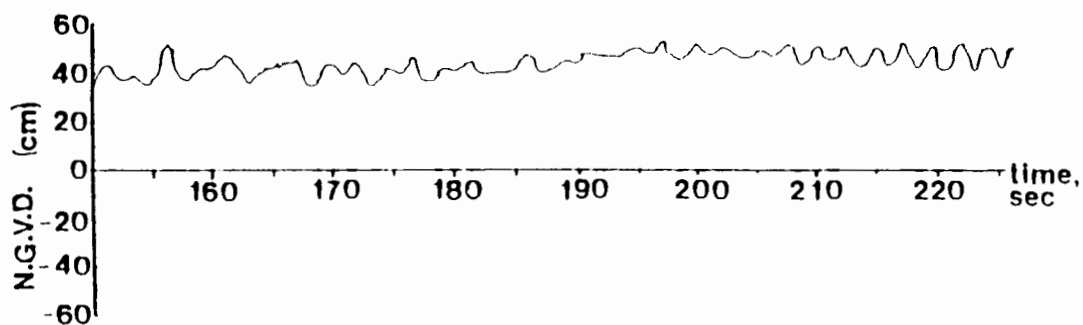
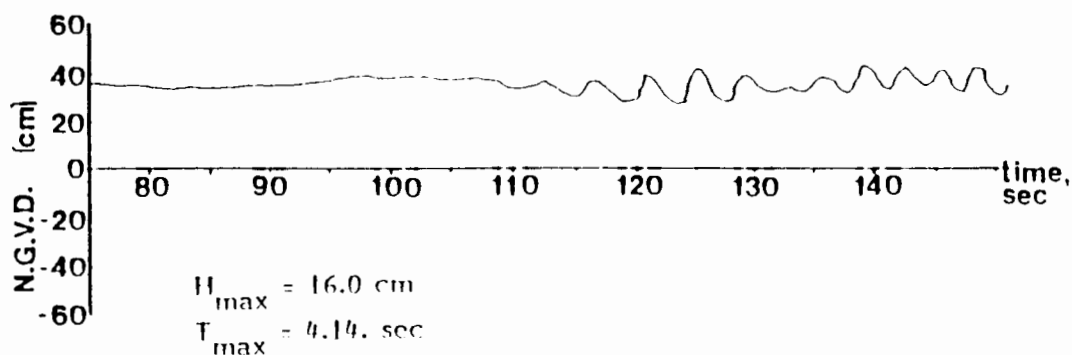
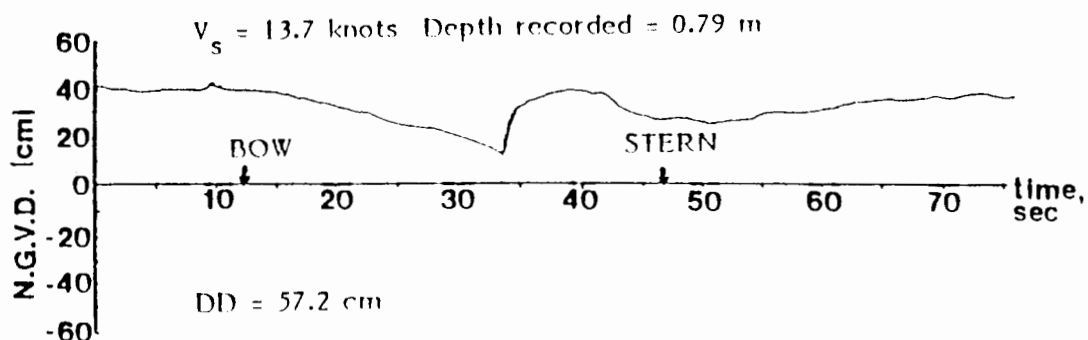
$V_s = 10.9$ knots
 Depth recorded = 1.04 cm



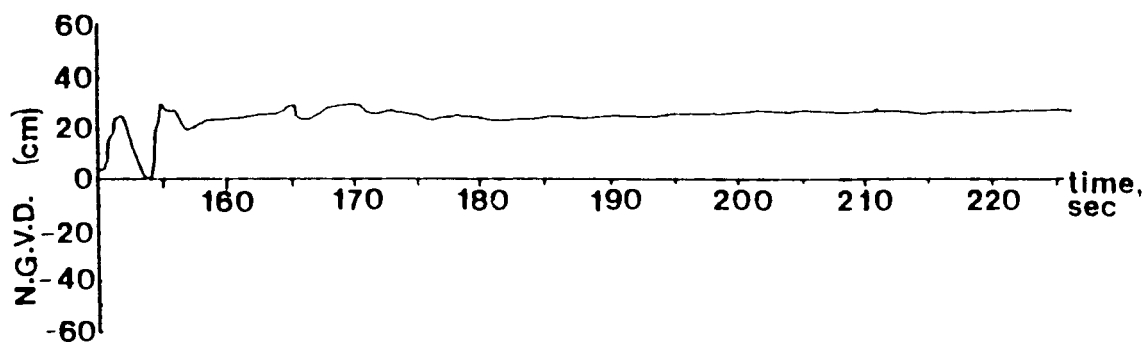
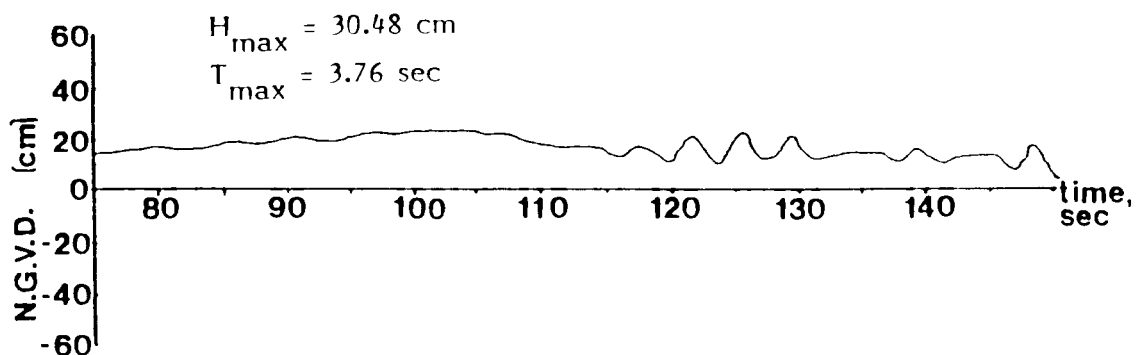
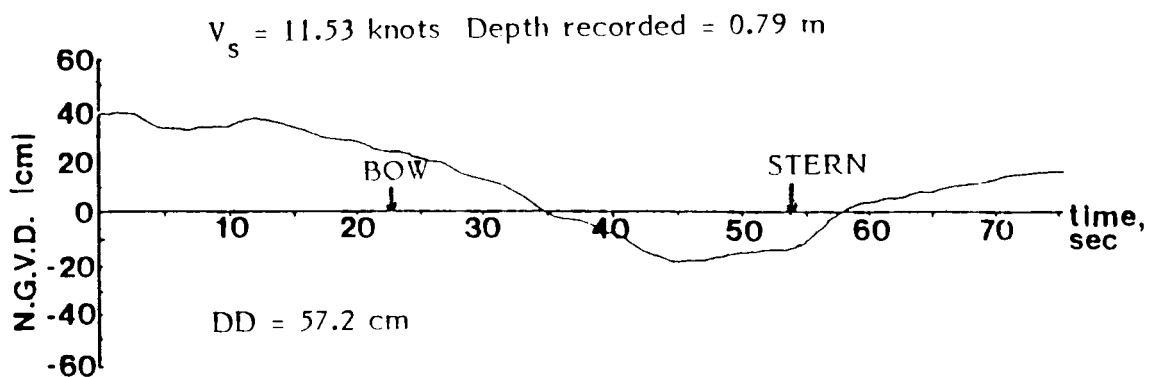
Ship wave record, Puget Island, WA RK 62
 Leonadros 30OCT87 UPSTREAM 13:30



Ship wave record, Puget Island, WA RK 62
USN Mt. Vernon (#39) 08JUN88 UPSTREAM 11:30

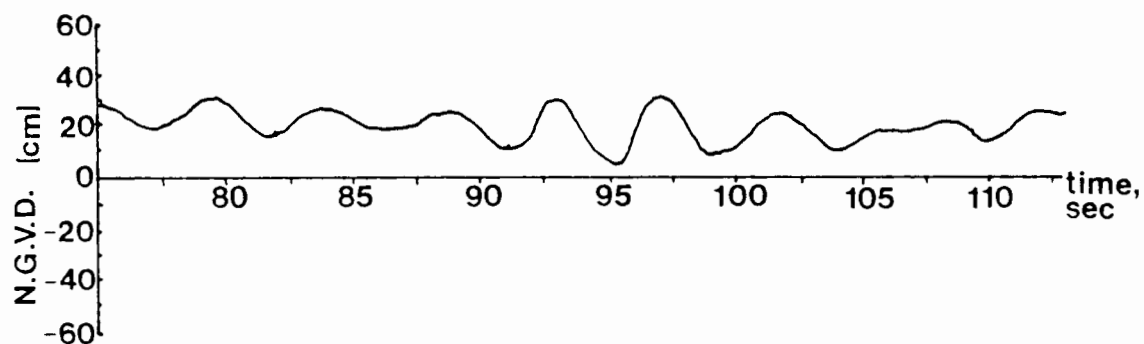
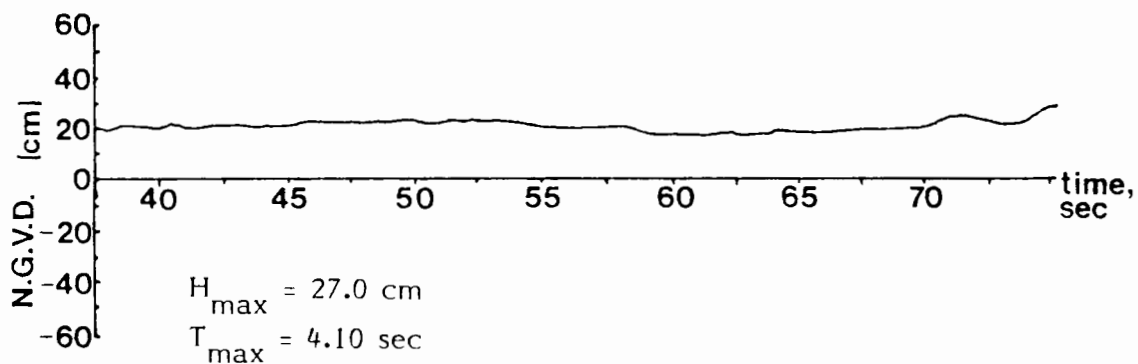
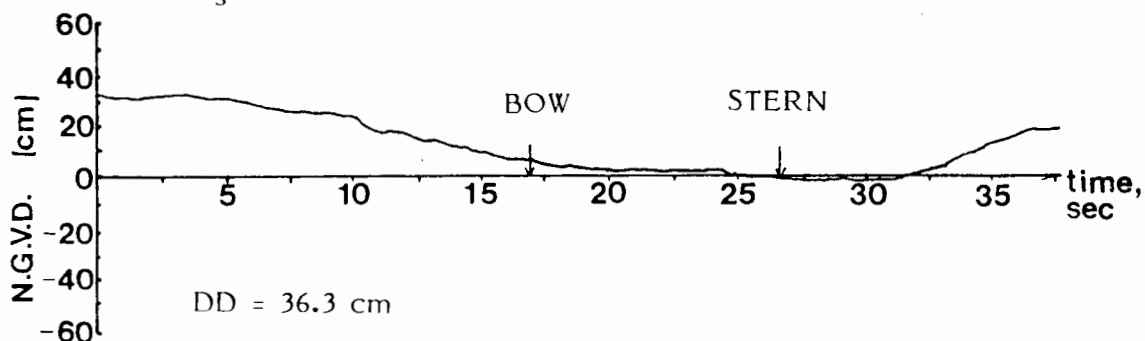


Ship wave record, Puget Island, WA RK 62
 Lake River 29OCT87 UPSTREAM 14:00

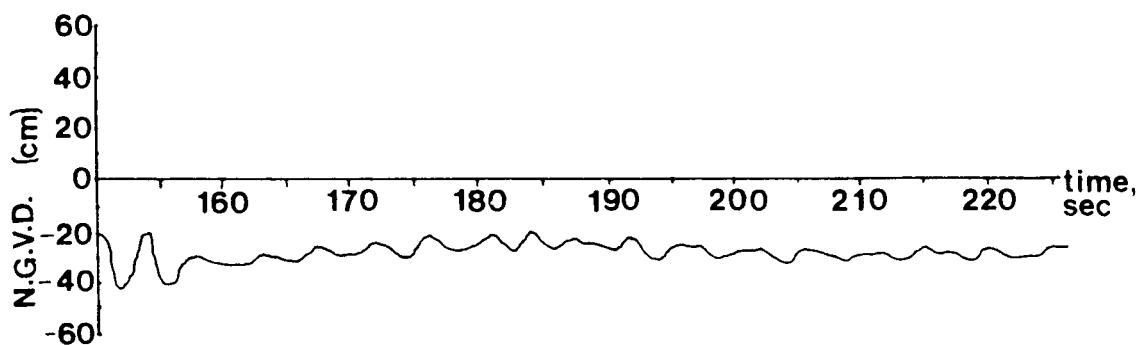
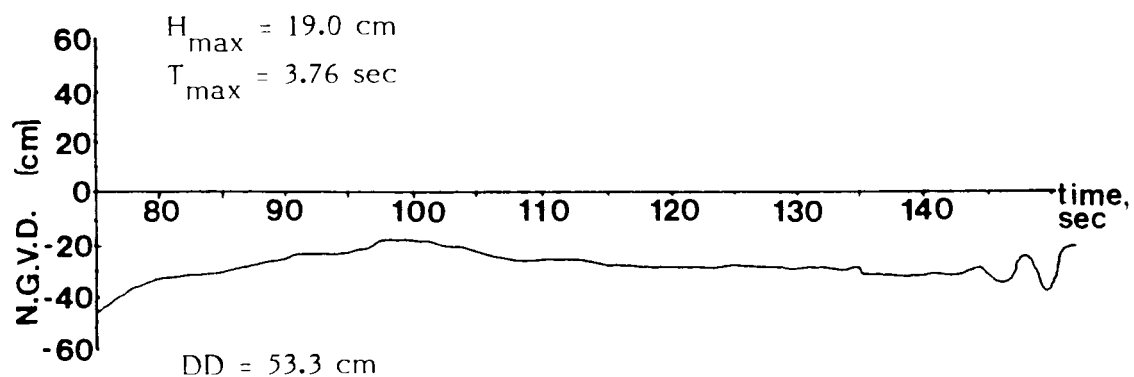
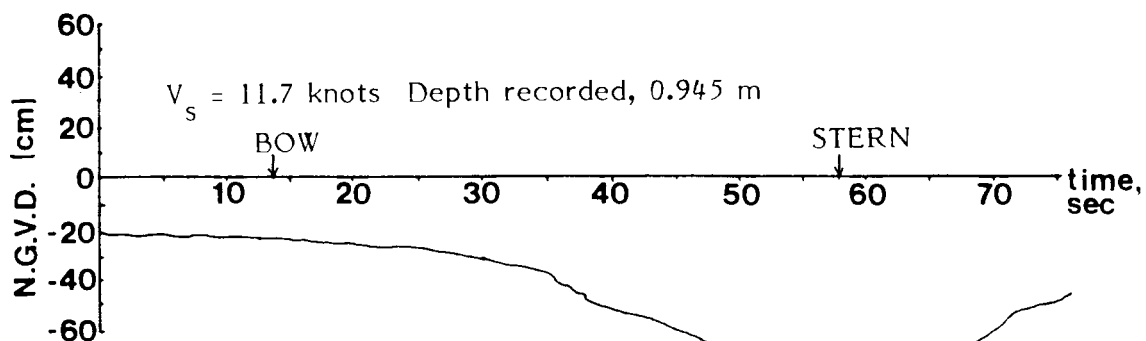


Ship wave record, Puget Island, WA RK 62
Luna II 29OCT87 UPSTREAM 13:30

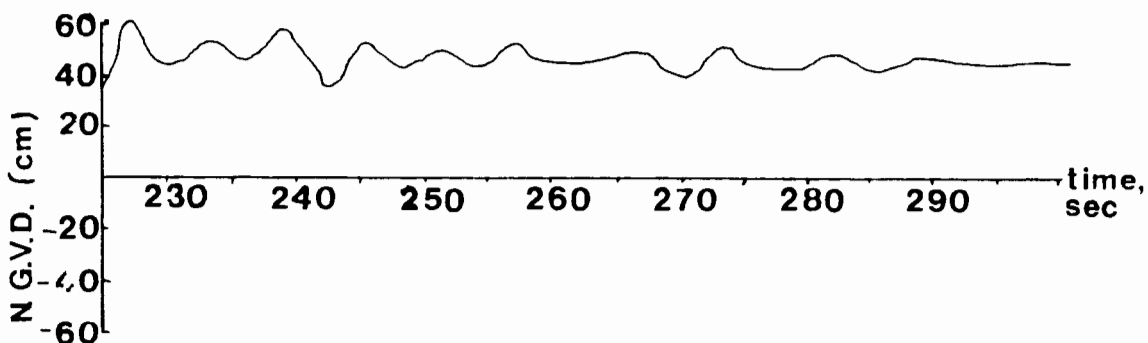
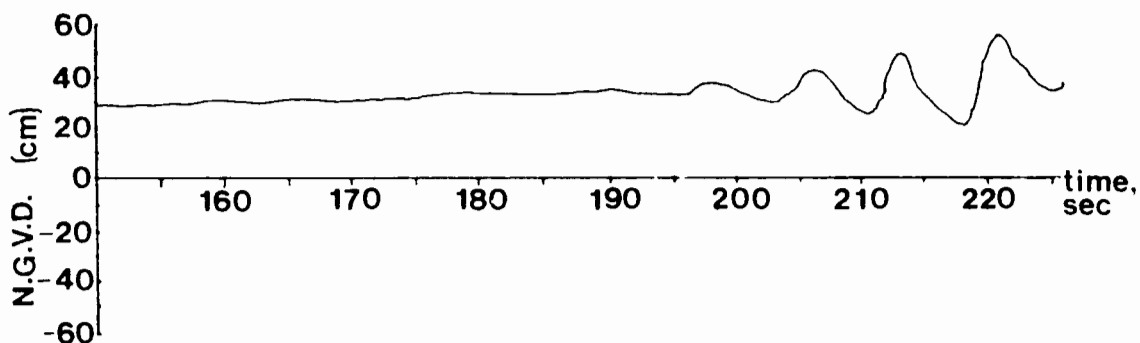
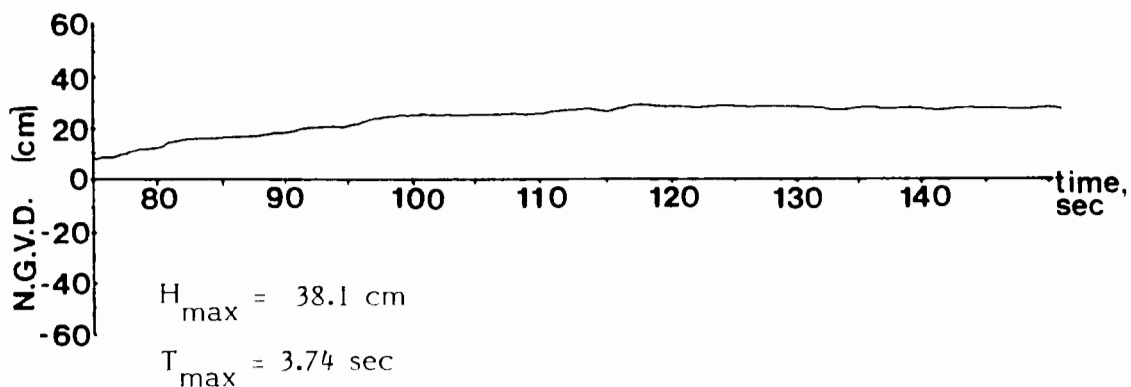
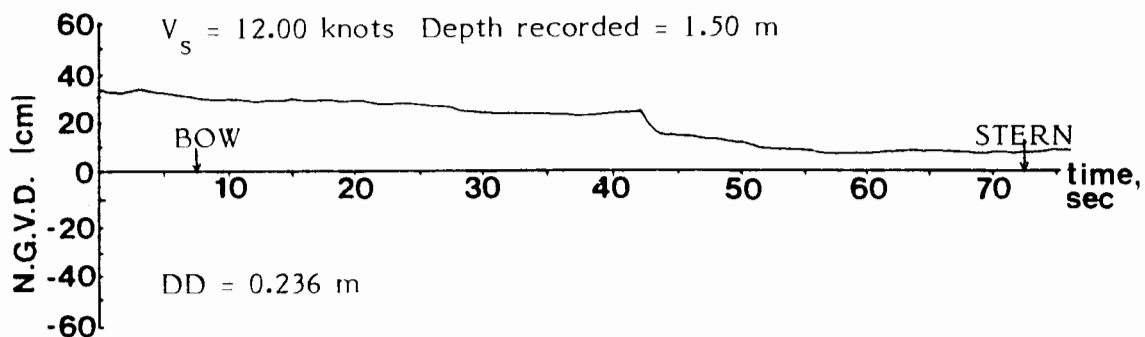
$V_s = 14.6$ knots Depth recorded = 1.19 m



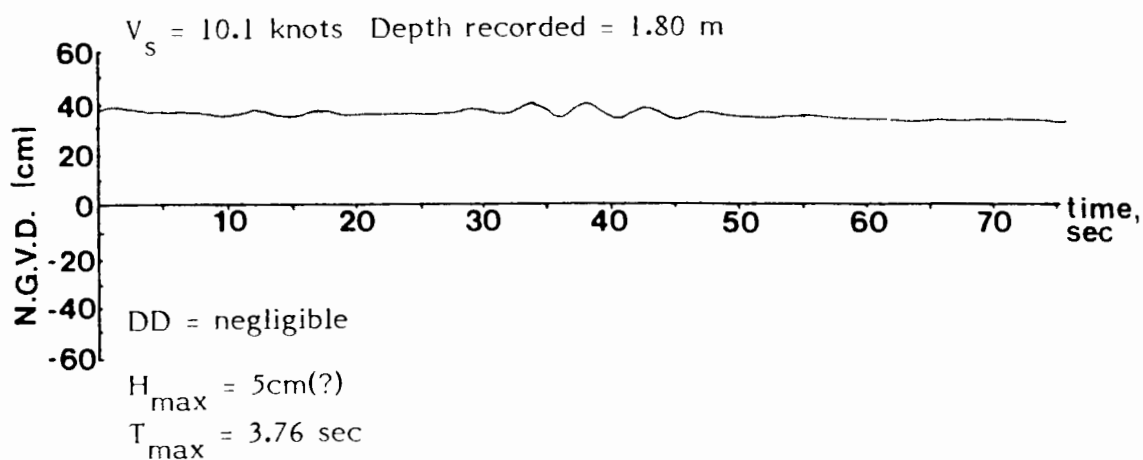
Ship wave record, Puget Island, WA RK 62
 Ocean Beauty 15SEP87 UPSTREAM 15:17



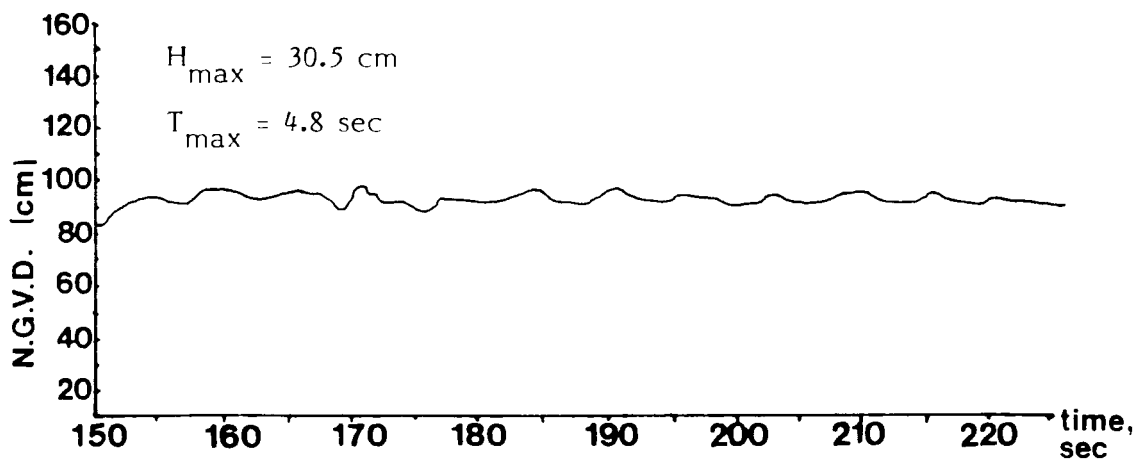
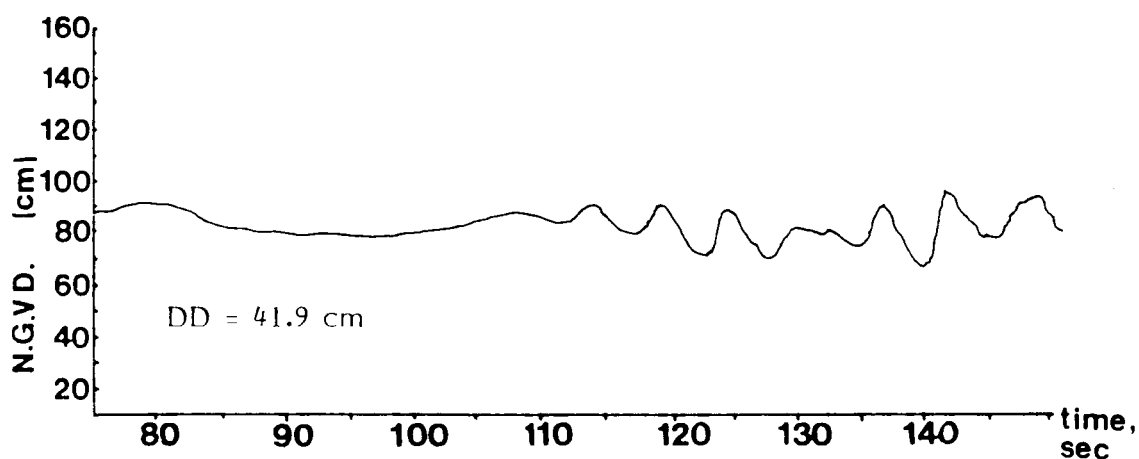
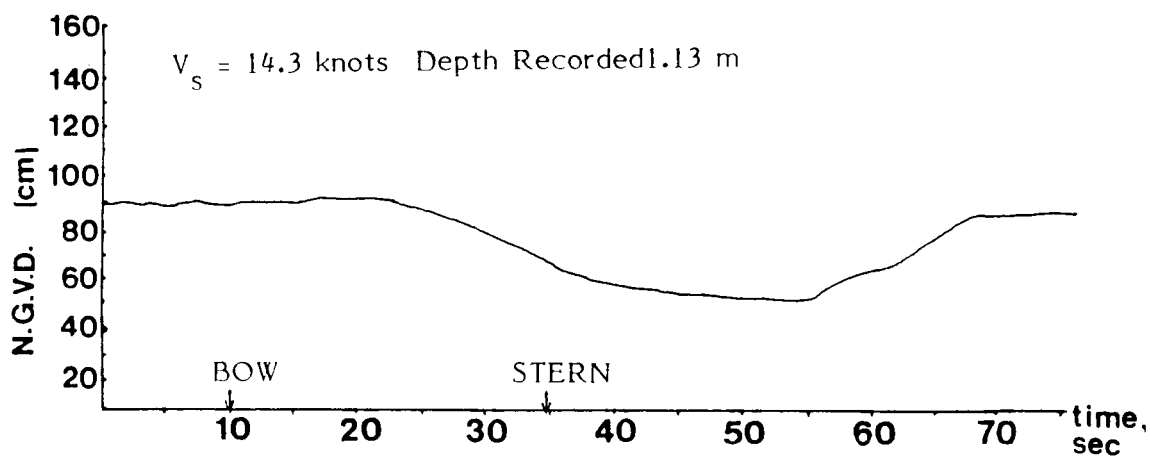
Ship wave record, Puget Island, WA RK 62
Verranzano Bridge 13JUN88 UPSTREAM 11:33



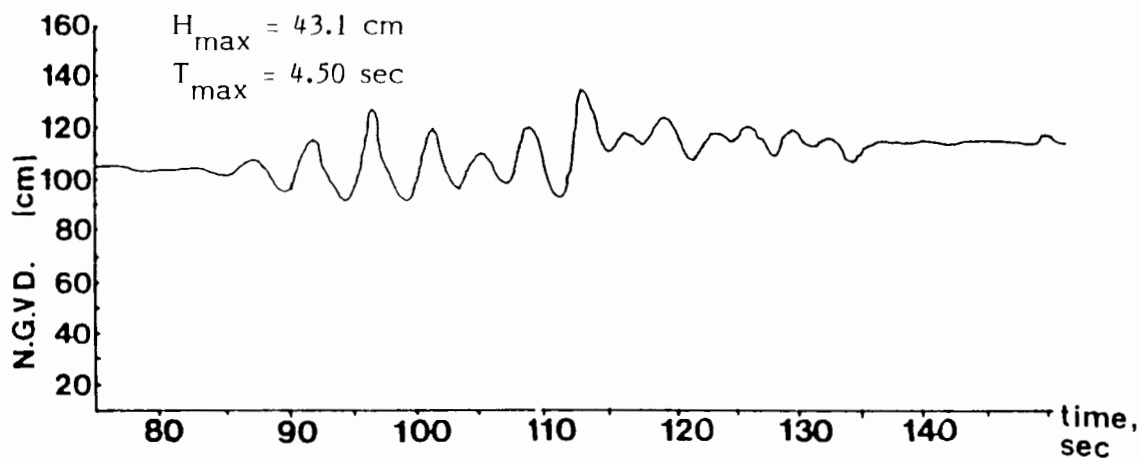
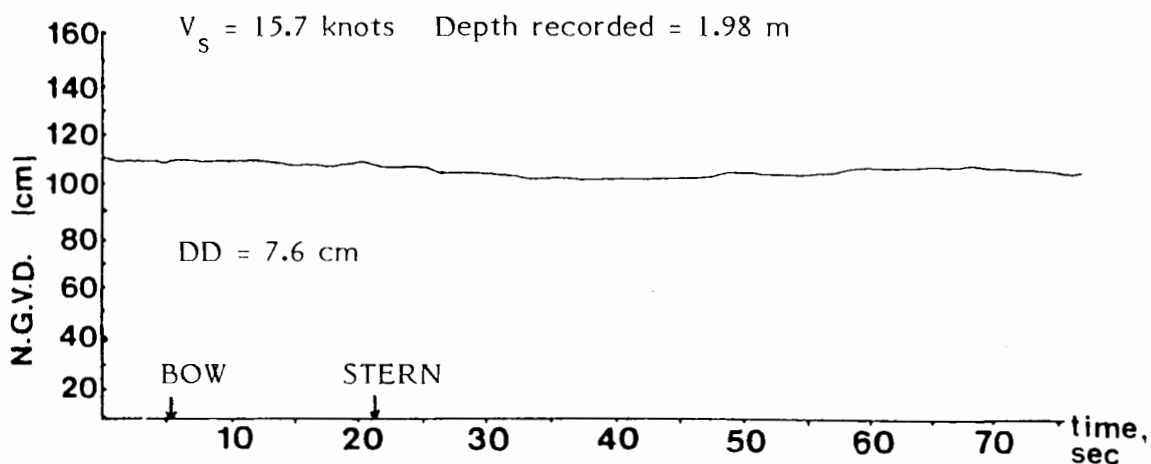
Ship wave record, Puget Island, WA RK 62
 Magnolia 17SEPT87 15:25



Ship wave record, Puget Island, WA RK 62
Valdiva 15SEPT87 DOWNSTREAM 16:00

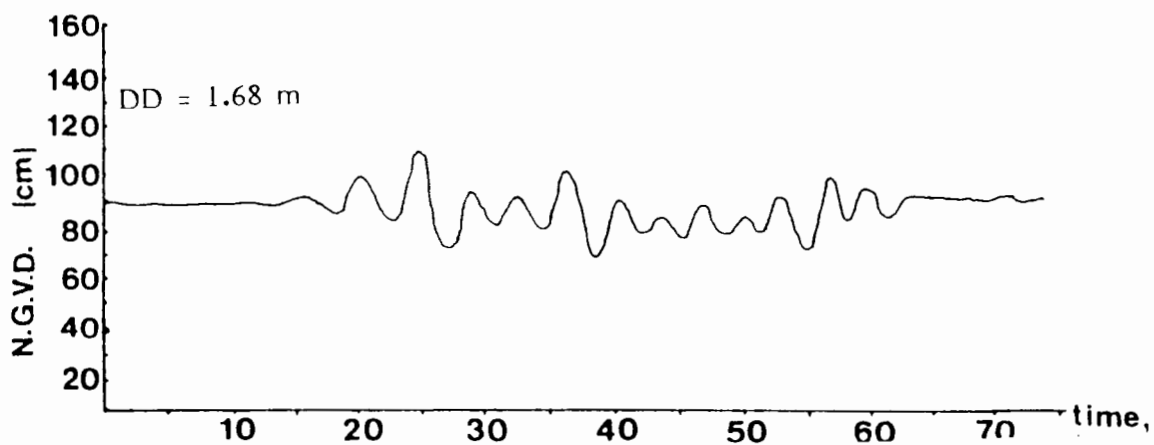


Ship wave record, Puget Island, WA RK 62
European Highway 08JUN88 UPSTREAM 11:15



Ship wave record, Puget Island, WA RK 62
USN Gray 09JUN88 UPSTREAM 10:23

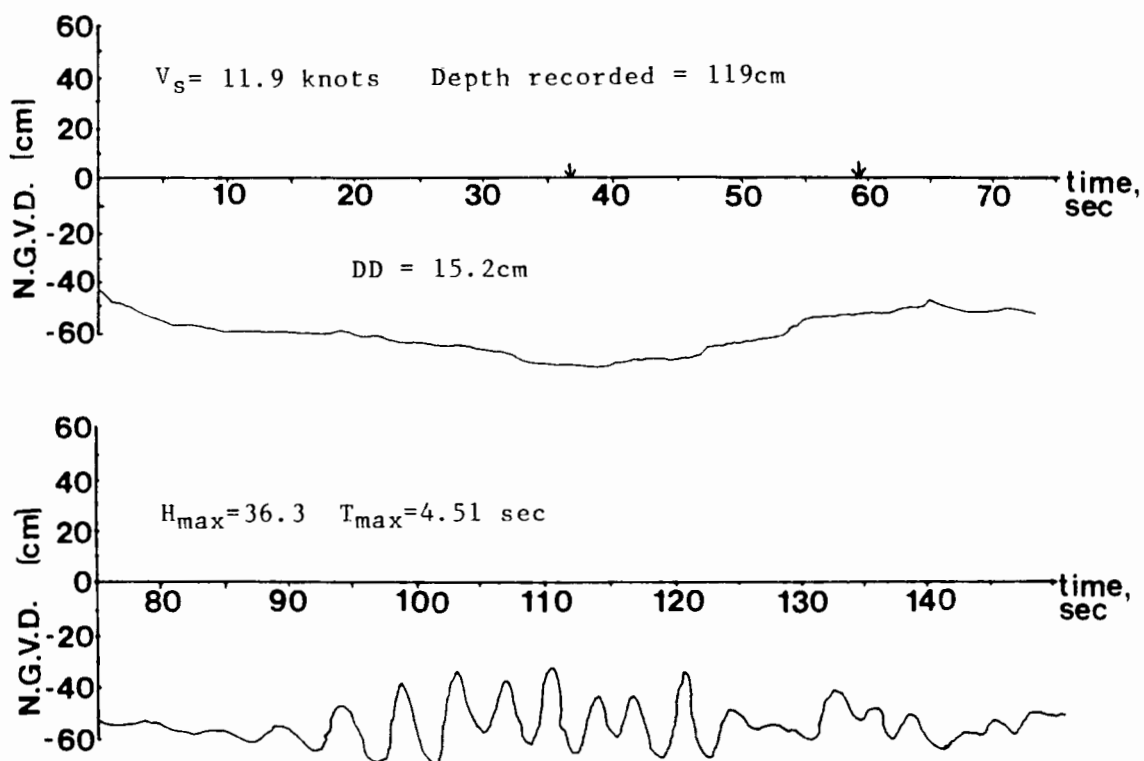
$V_s = 15$ knots Depth recorded 1.68 m



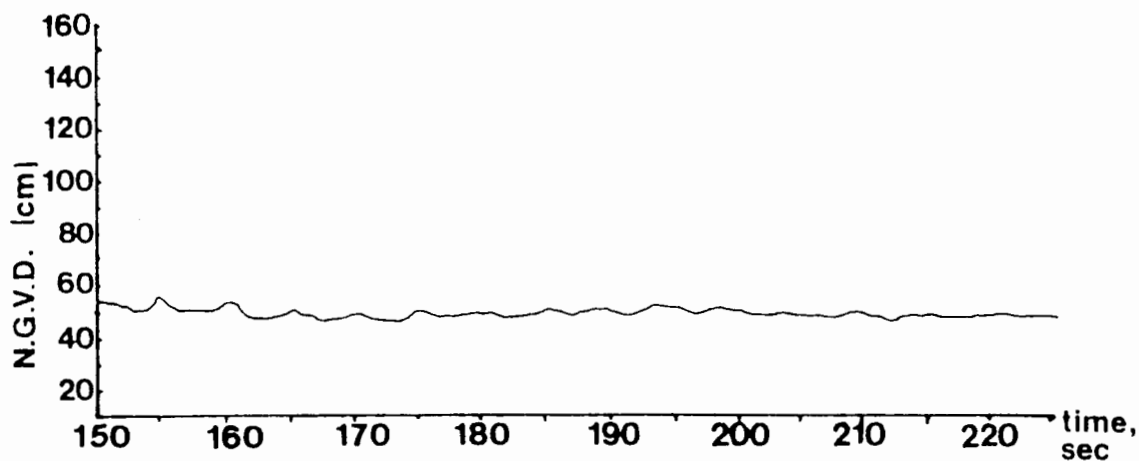
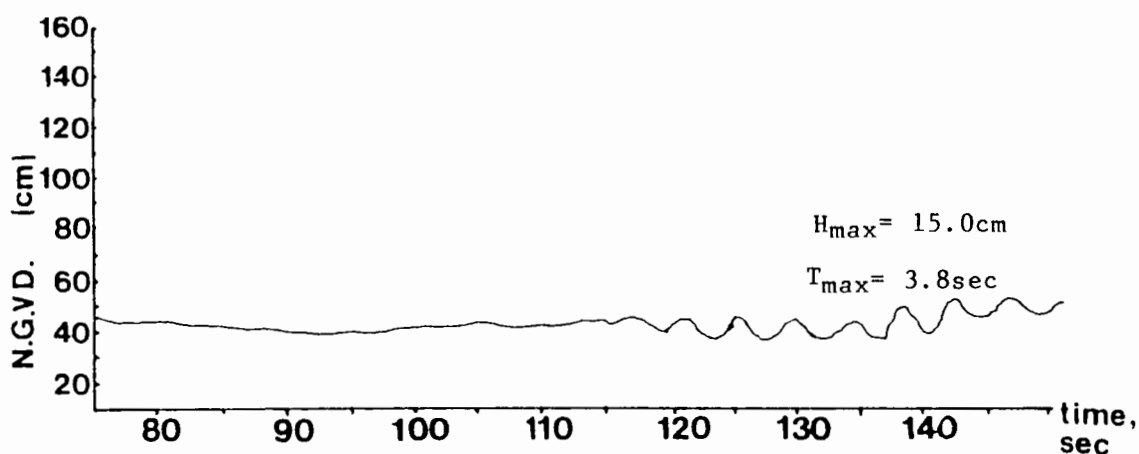
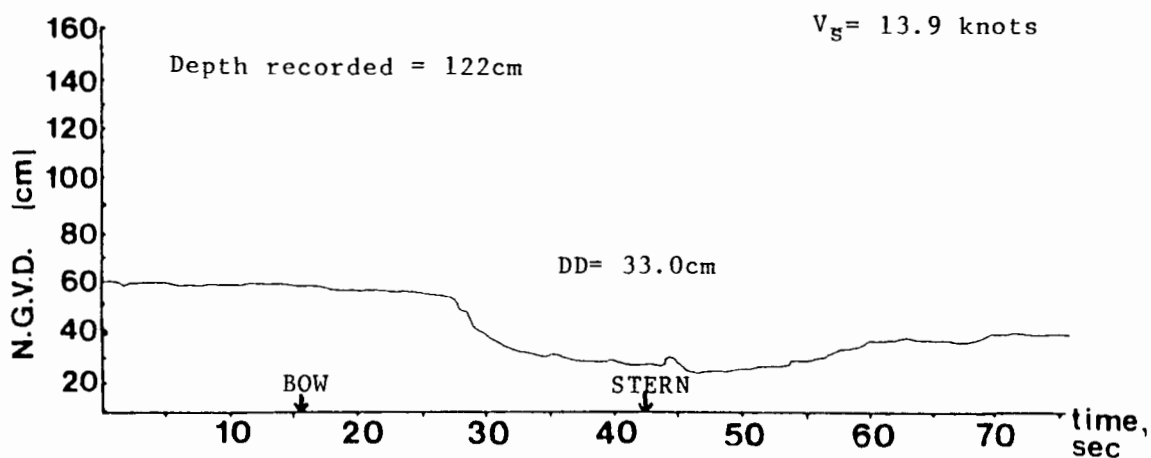
$H_{\max} = 38.1$ cm

$T_{\max} = 4.5$ sec

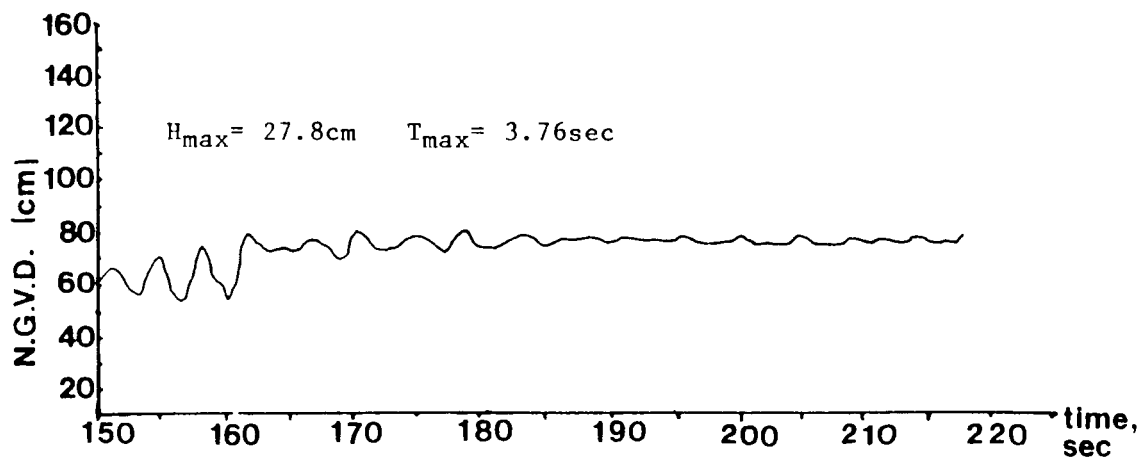
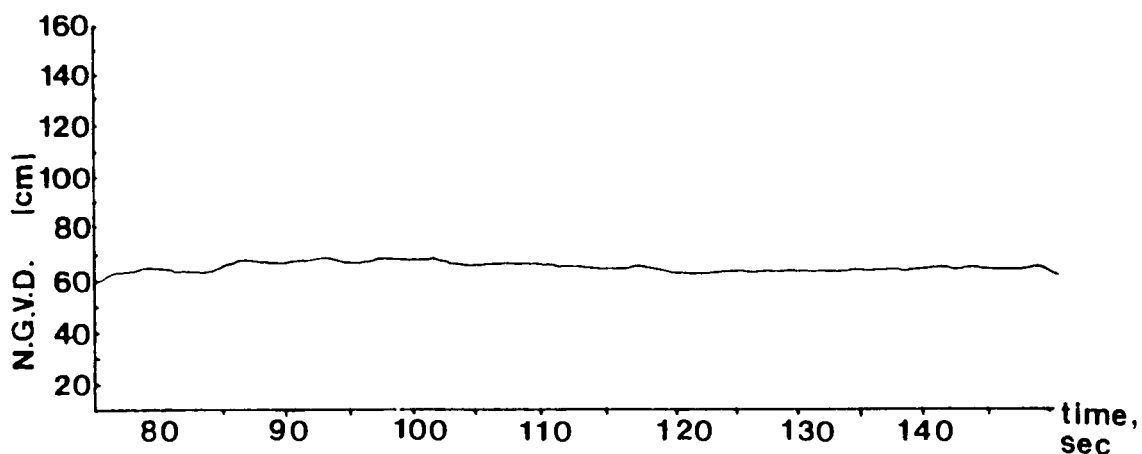
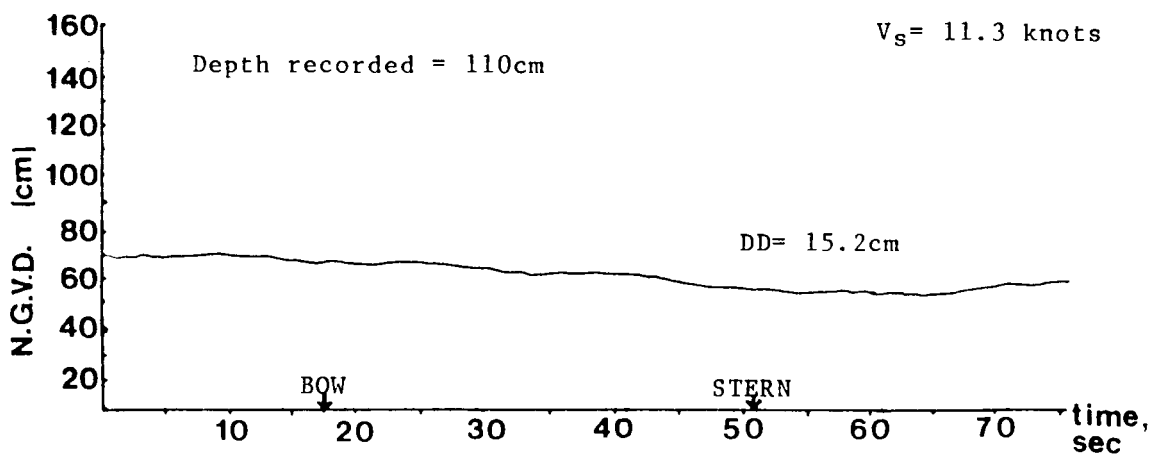
Ship wave record, Puget Island, WA RK 62
USN Ramsey 09JUN88 UPSTREAM 9:45



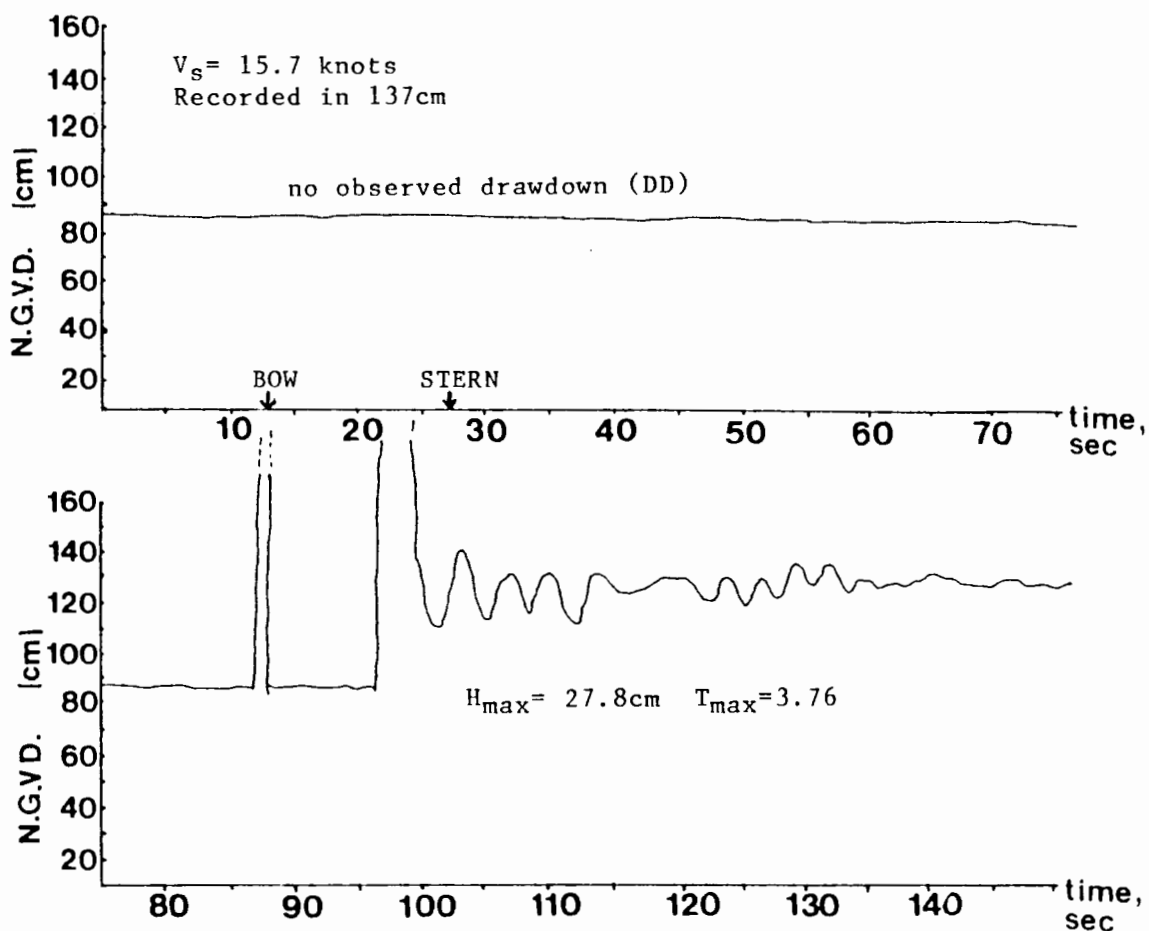
Ship wave record, Puget Island, WA RK 62
USN "Gray" (1054) 14JUN88 DOWNSTREAM 08:52



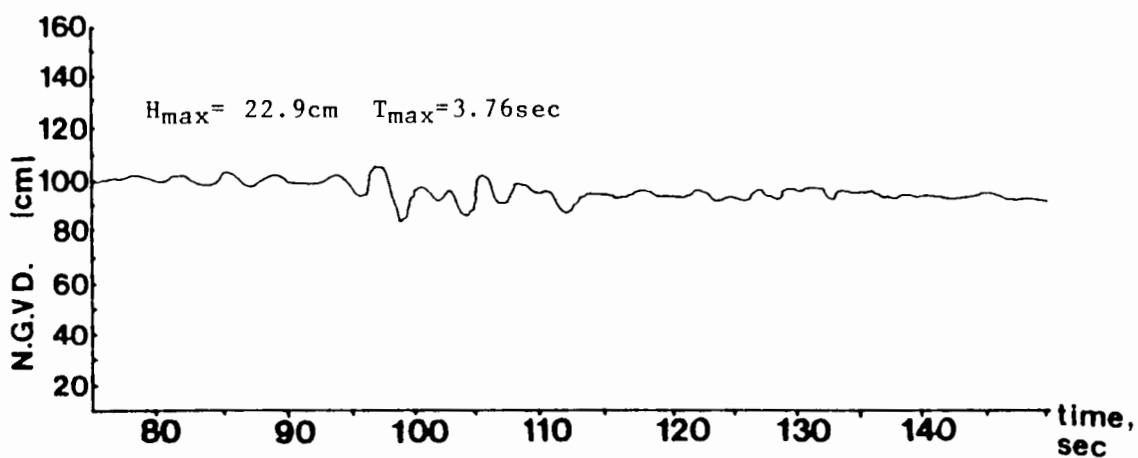
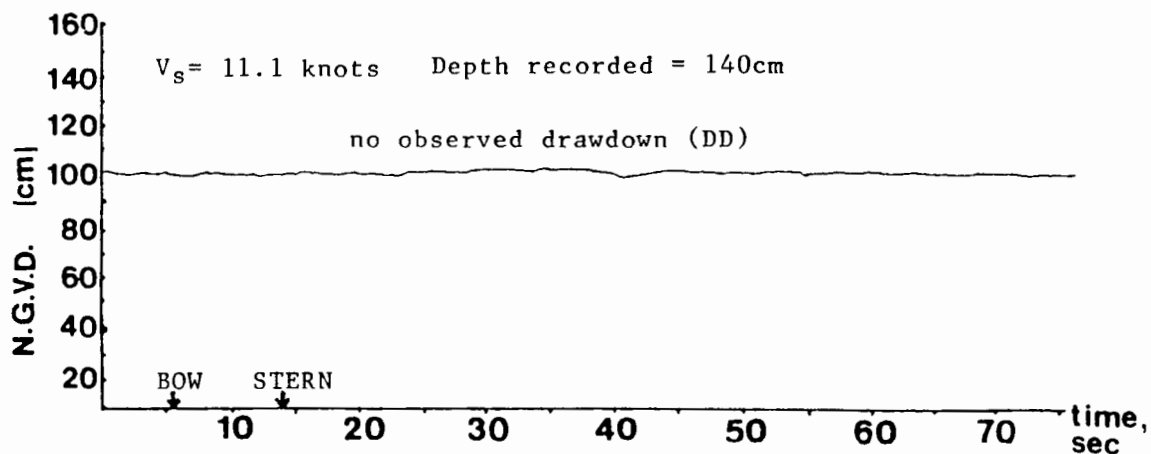
Ship wave record, Puget Island, WA RK 62
Kee Lung 18SEPT87 UPSTREAM 15:35



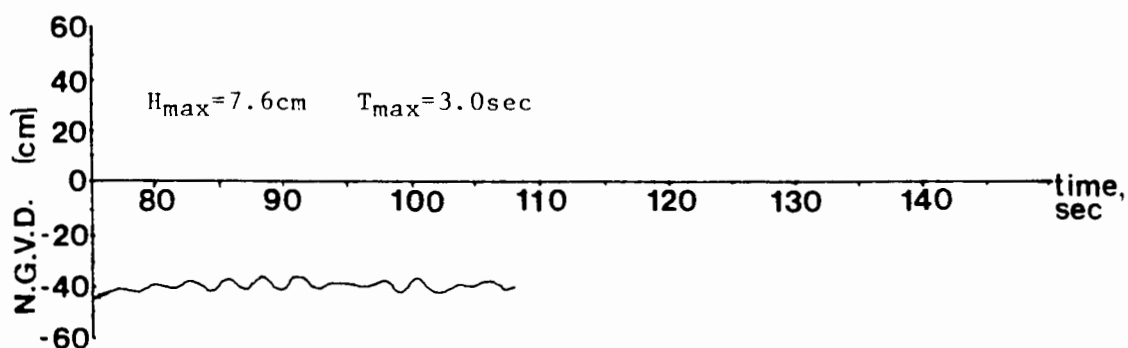
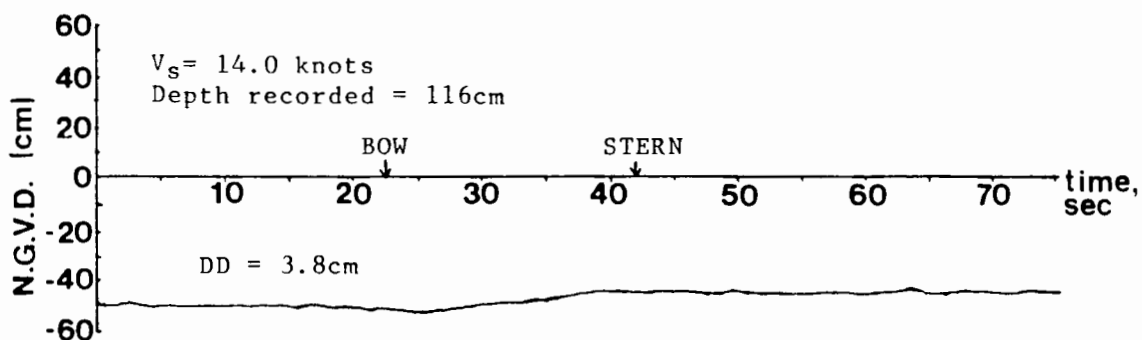
Ship wave record, Puget Island, WA RK 62
Ocean Jade 13JUN88 UPSTREAM 13:10



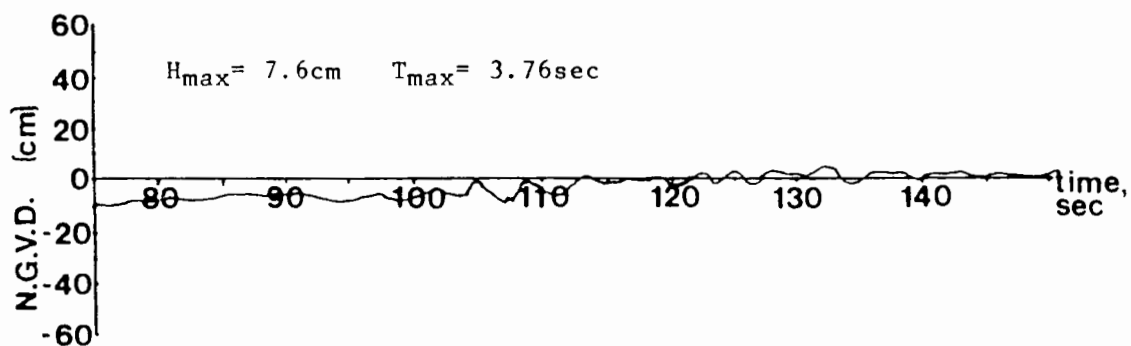
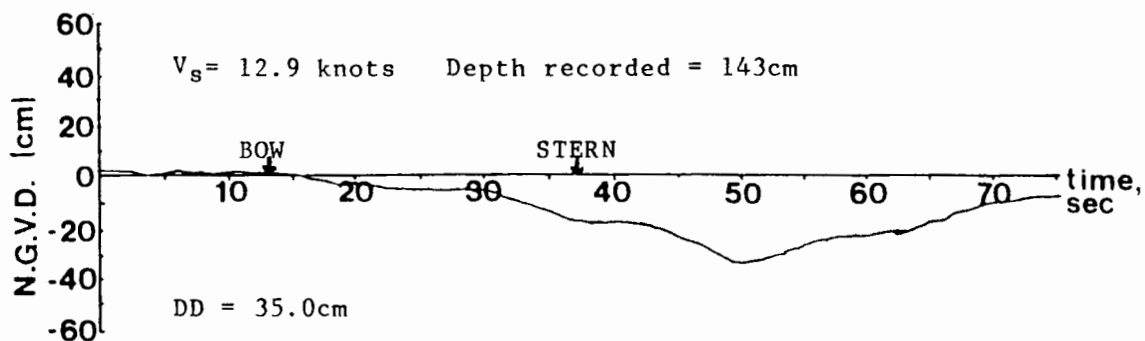
Ship wave record, Puget Island, WA RK 62
U.S.C.G. "Boutwell" (719) 13JUN88 DOWNSTREAM 13:45



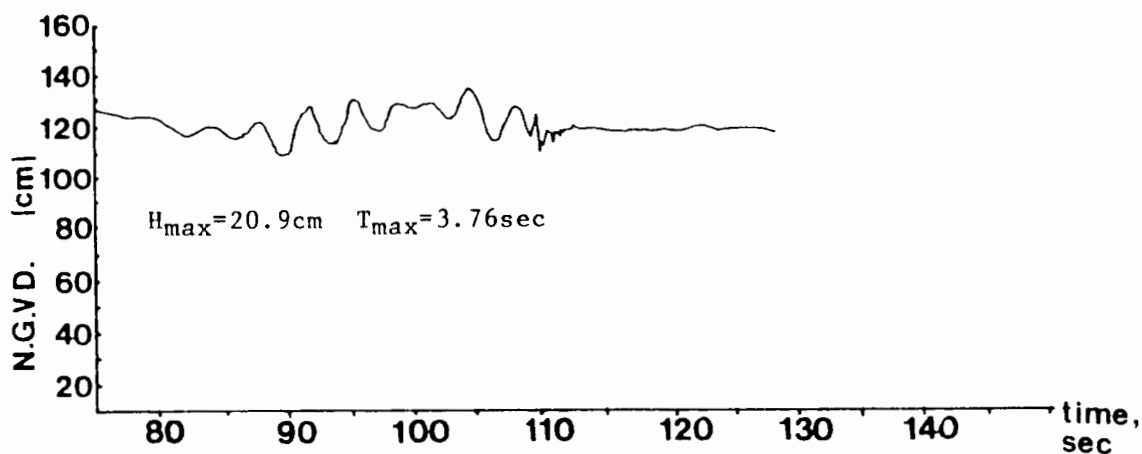
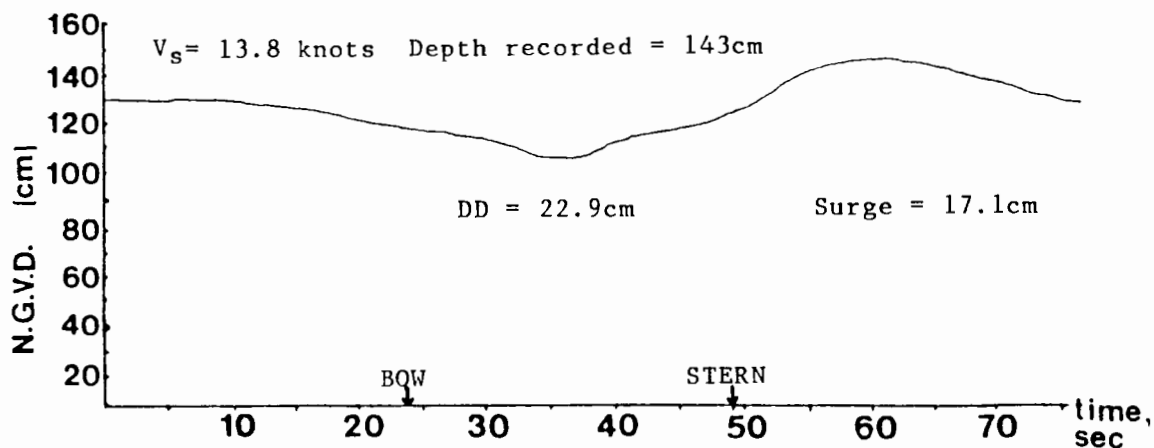
Ship wave record, Puget Island, WA RK 62
U.S.C.G. Bouytender 13JUN88 DOWNSTREAM 13:52



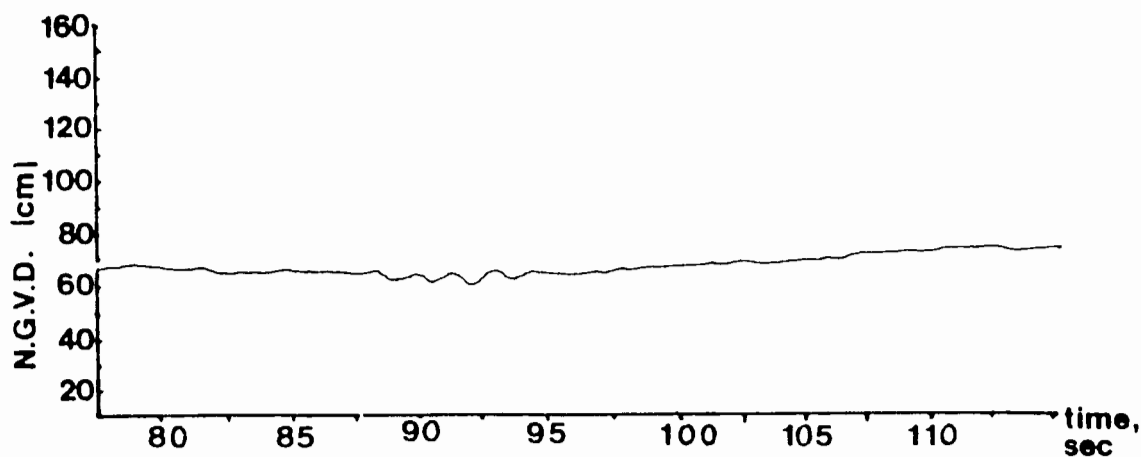
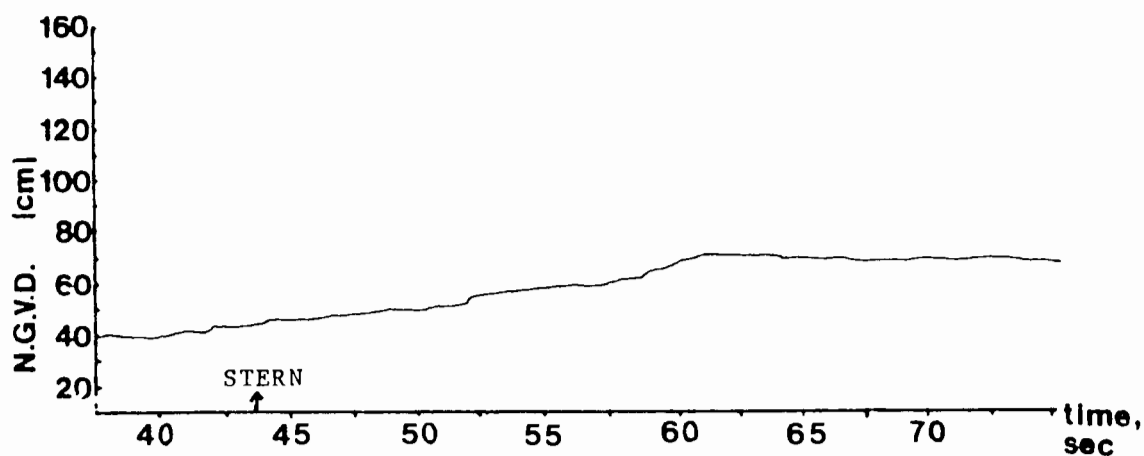
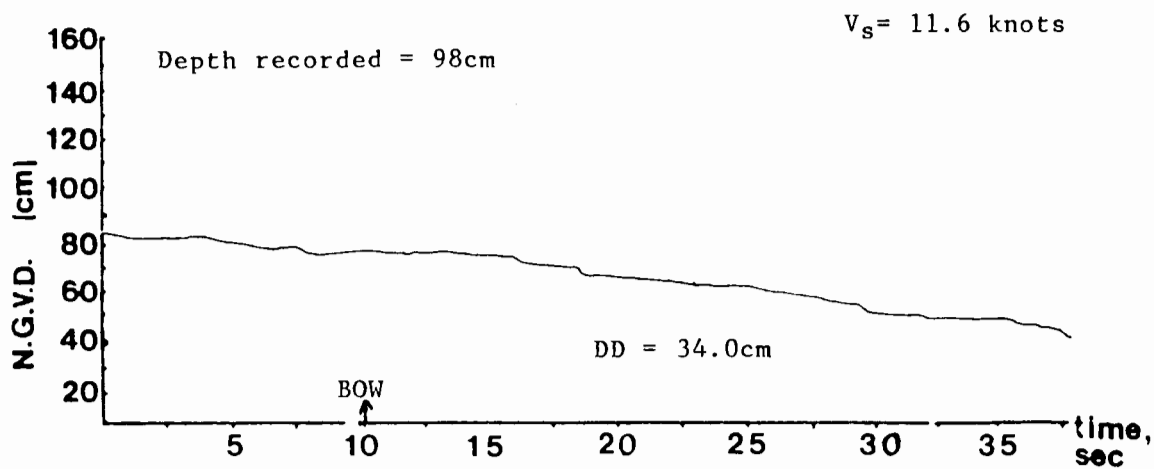
Ship wave record, Puget Island, WA RK 62
USN "Thach" (43) 14JUN88 DOWNSTREAM 11:35



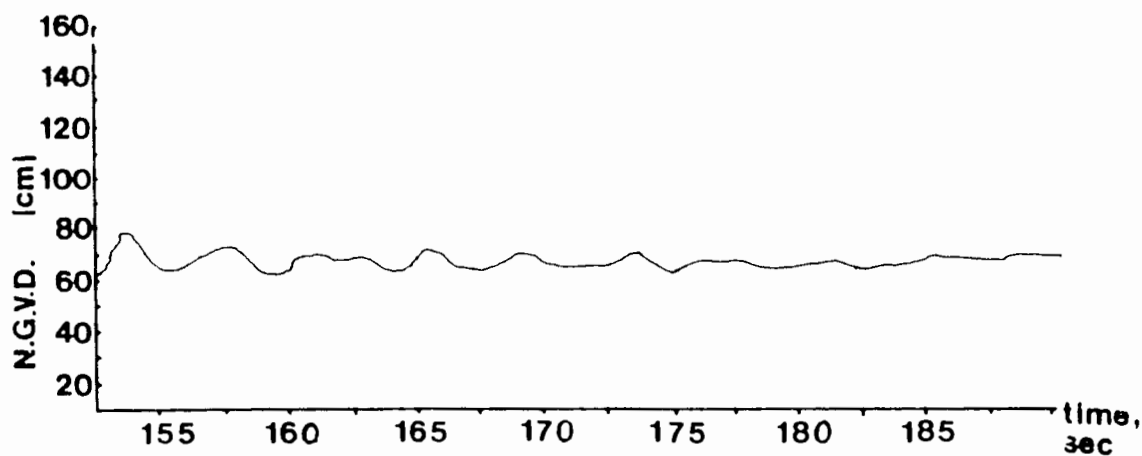
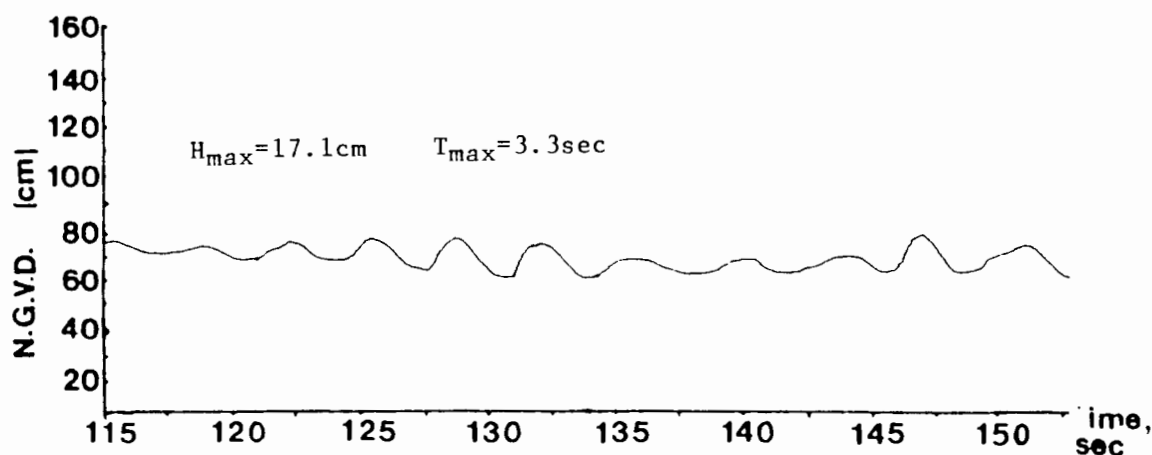
Ship wave record, Puget Island, WA RK 62
Indah Fuji (Happy Eager) 14JUN88 UPSTREAM 12:30



Ship wave record, Puget Island, WA RK 62
USN "Chandler" (996) 14JUN88 DOWNSTREAM 16:00



Ship wave record, Puget Island, WA RK 62
Chevron Oregon 17SEPT87 UPSTREAM 12:54



Ship wave record, Puget Island, WA RK 62
Chevron Oregon 17SEPT87 UPSTREAM 12:54 (continued)

The following eight photographs exhibit water motions in time sequence associated with the passage of a deep-draft ship.



The west end of Wallace Island (RM 47.8-OR) looking west. Note 16-foot (5 m) craft confronting a bore generated by the outbound passage of the container ship "Matsun" at 1230 hours, June 24, 1988. The bore seems to be the result of water just outside the shallow-water region to the left, in the lee of Wallace Island, similar to tidal bore.



Secondary wave train moving into same area. Note vessel in upper right is well past the site. Examining the waves we can deduce that there is a rapid shallowing of the river bottom, where the waves are beginning to break off the end of the island and where you see a rapid reduction in wave length toward the left of the photograph. Decrease in wave length and steepening of wave arc are indicative of waves moving into shallow water.



A fascinating phenomena that is interpreted the reflection of the initial bore or surge off the Oregon side moving back toward Wallace Island. Secondary waves are still attacking shore in foreground as the bore of water displaced by the ship moves toward us.



Surge



Bore starting to retreat off beach face. A complex set of water motions was still being observed all around the site, especially on the shallow water south side.



Approximately ten minutes after the vessel initially passed, the site returns to normal conditions. Event reactivated beach scarp on upper portion of beach. This event was one of several spectacular displays of complex water motions and large waves associated with vessel passage, but events such as this were NOT the norm. These large events did seem to be correlated to the downstream passage of large and fast container ships, but this statement cannot be substantiated with the limited data of this study. No equipment, such as the transducer system, was setup to record this event. Wallace Island, June 24, 1988.



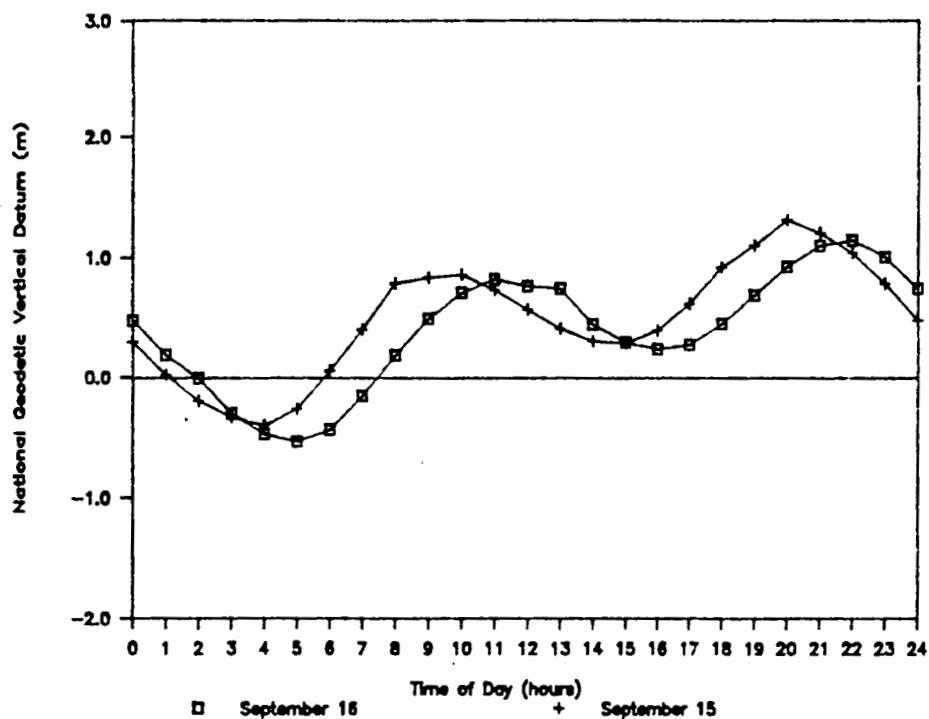
"Reflected bore" moving up beach face resembling severe wave runup. Mean water level during the event is just below secondary wave swash occurring in the lower right. Use log in foreground for reference.



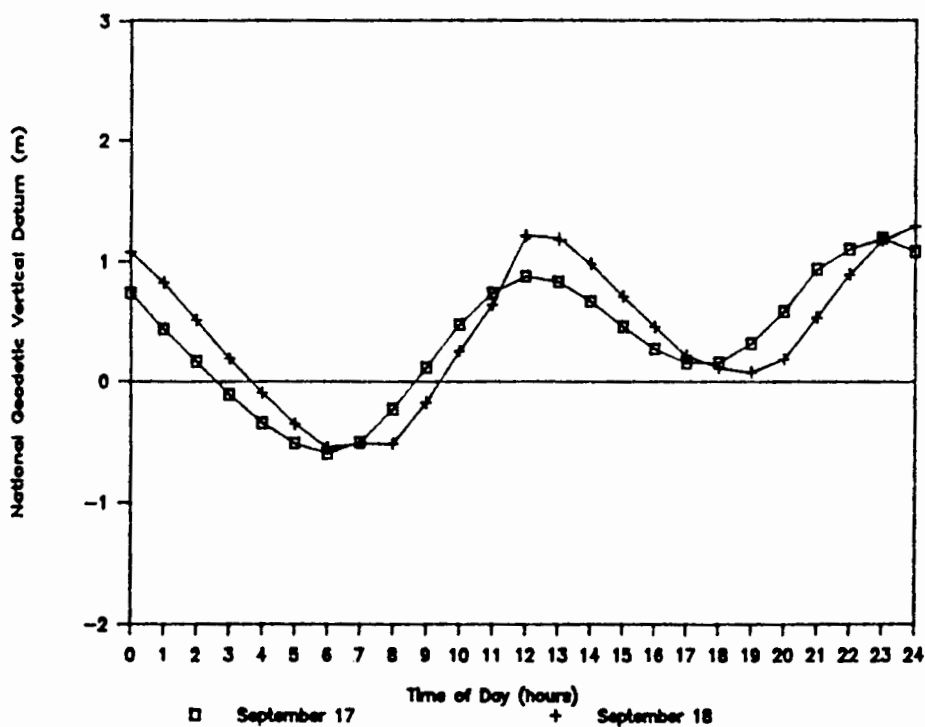
Bore easily reaching base of beach scarp, moving upstream around both sides of the island.

WAVE DESCRIPTION OF VESSEL PASSAGE

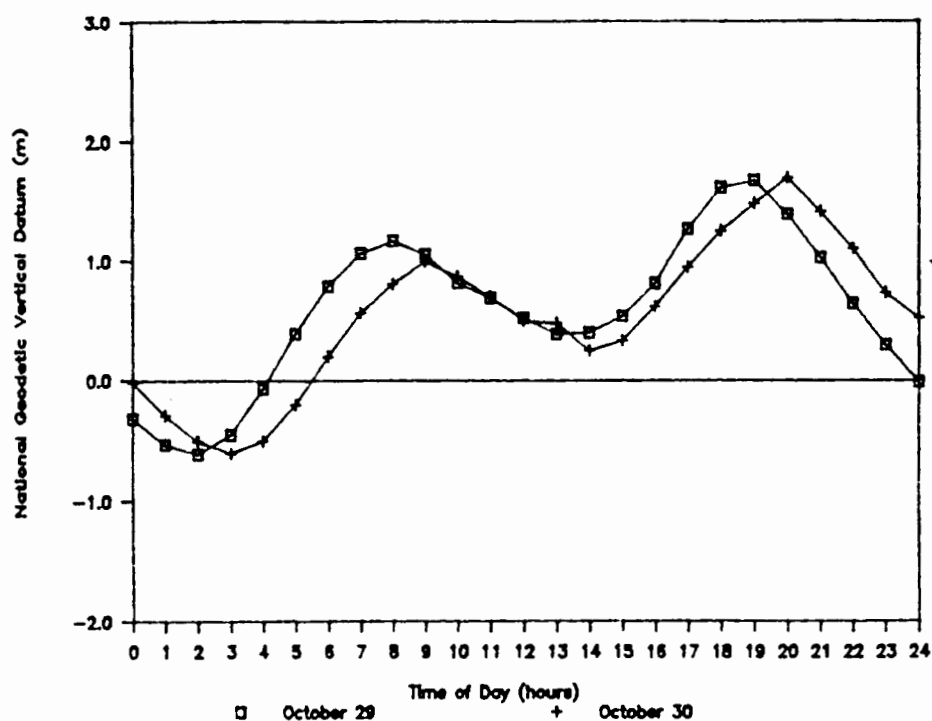
<u>Parameters</u>	<u>S1</u>	<u>S2</u>	<u>S3</u>	<u>S4</u>
Ship	Magnolia	Leandros	Verranzano Bridge	USN Ramsey
Ship Type	bulk	bulk	container	frigate
Direction	upstream	upstream	upstream	upstream
date	09-17-87	10-30-87	06-13-88	06-09-88
time	15:25	13:30	11:33	09:45
River KM	61.4	61.4	61.4	61.4
mean draft	7.0	7.8	6.1	4.6
length	196.0	220.0	264.5	126.3
beam	29.3	32.3	32.3	13.5
displacement	30,127	34,446	18,176	2,640
z_{tide} (NGVD)	0.33m	0.22m	-0.20m	0.90m
A_{ch}	7585m ²	7503m ²	7193m ²	8,005m ²
x_s	225m	225m	225m	225m
v_s	5.61m/s	6.17m/s	6.02m/s	7.9m/s
dd	24cm	27cm	53cm	0
dd _{time}	35sec	30sec	35sec	-
H_{max}	38cm	15cm	19cm	38cm
T_{max}	3.7sec	3.4sec	3.8sec	4.5sec
d_{meas}	150cm	104cm	96cm	168cm
α	15°	17°	0°	7°
bc	.745	.621	.347	.337
bf	.028	.035	.028	.008
m_{beach}	1:22.5	1:18.5	1:12.5	1:11.8



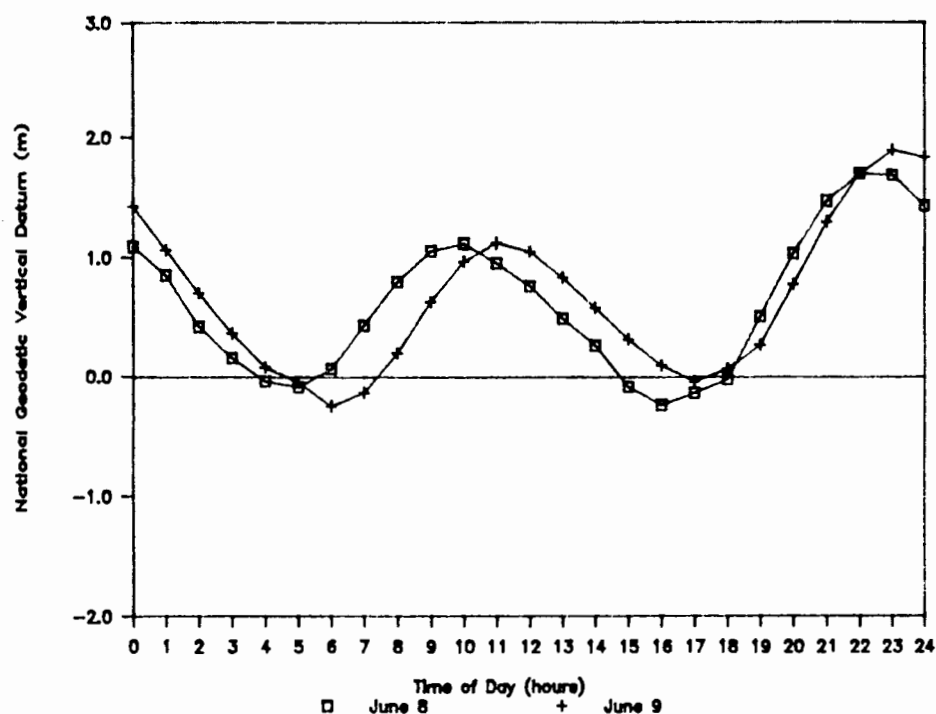
Puget Island Site Tidal Fluctuation
September 15-16, 1987



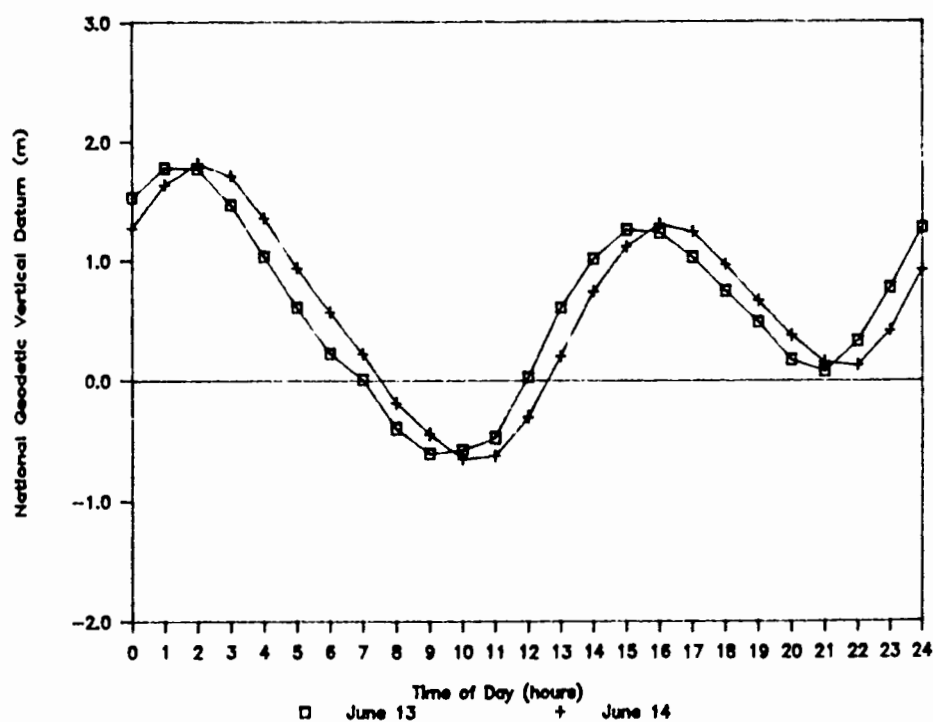
Puget Island Site Tidal Fluctuation
September 17-18, 1987



Puget Island Site Tidal Fluctuation
October 29-30, 1987



Puget Island Site Tidal Fluctuation
June 8-9, 1988



Puget Island Site Tidal Fluctuation
June 13-14, 1988

APPENDIX D

SAND TRANSPORT ON A BEACH FACE

This appendix includes data recorded by the shallow water sediment trap arrays set up on the beach face at the Puget Island site between profiles 9 and 11.

Shallow Water Sediment Trap Array Data

Trap mouth dimension: $3.81 \times 3.81 \text{ cm} = 14.4 \text{ cm}^2$

ON = Onshore transport, normal to shoreline

OF = Offshore transport, normal to shoreline

DD = Drawdown wave only

LS-D = Longshore transport downstream, parallel to shoreline

LS-U = Longshore transport upstream, parallel to shoreline

Sf = surface sample

α = angle of wave incidence

SHIP	DATE	DIRECTION				
Ocean Beauty	15SEPT87	Upstream 15:17	$\alpha = 5^\circ$			
Distance from Shore (m)	Depth (m)	SAMPLE DRY WEIGHT (grams)				
		Sampling Direction	Trap Elevation	Above Bed (cm)		
			1.9	9.5	17.1	
5.0	0.26	ON	89.7	8.5	0.8	
5.0	0.26	OF	172.4	5.4	0.7	
5.0	0.26	LS-U	6.5	0.7	1.0	

SHIP DATE DIRECTION
 Valdiva 15SEPT87 Upstream 16:03 $\alpha = 2^\circ$

Distance from Shore (m)	Depth (m)	SAMPLING Direction	SAMPLE DRY WEIGHT (grams)		
			Trap Elevation	Above Bed (cm)	
			1.9	9.5	17.1
3.3	0.17	OF	48.2	1.8	0.2
3.3	0.17	ON	59.9	0.5	0.5

Chevron Oregon 17SEPT87 Upstream 12:54 $\alpha = 12^\circ$

Distance from Shore (m)	Depth (m)	SAMPLING Direction	SAMPLE DRY WEIGHT (grams)		
			Trap Elevation	Above Bed (cm)	
			1.9	9.5	17.1
5.0	0.26	OF	23.2	1.1	0.4
5.0	0.26	ON	4.7	0.6	0.5
5.0	0.26	LS-U	8.5	2.0	1.0
7.0	0.37	LS-D	0.2	0.1	0.2
10.0	0.52	OF	4.0	0.5	0.03
10.0	0.52	ON	3.0	2.0	0.04

Magnolia 17SEPT Upstream 15:25 $\alpha = 18^\circ$

Distance from Shore (m)	Depth (m)	SAMPLING Direction	SAMPLE DRY WEIGHT (grams)		
			Trap Elevation	Above Bed (cm)	
			1.9	9.5	17.1
5.0	0.26	OF	31.4	13.9	4.4
5.0	0.26	ON	5.1	1.0	0.5
5.0	0.26	LS-U	186.0	117.7	74.5
10.0	0.52	OF	36.0	5.4	3.0
10.0	0.52	ON	26.1	4.0	1.8
10.0	0.52	LS-U	sum of 3 traps = 0.1		

SHIP DATE DIRECTION
 Cordiality 17SEPT87 Upstream 16:03 $\alpha = 10^\circ$

Distance from <u>Shore (m)</u>	Depth (m)	SAMPLING <u>Direction</u>	SAMPLE DRY WEIGHT (grams)		
			Trap	Elevation Above Bed	(cm)
			<u>1.9</u>	<u>9.5</u>	<u>17.1</u>
5.0	0.26	OF	23.2	0.4	0.2
5.0	0.26	ON	4.7	1.1	0.5
5.0	0.26	LS-U	8.5	2.0	1.0
10.0	0.52	OF	4.0	1.0	0.03
10.0	0.52	ON	5.4	3.0	2.0
7.0	0.52	LS-U	0.2	0.1	0.0

Evelyn Maersk 18SEPT87 Upstream $\alpha = 21^\circ$

Distance from <u>Shore (m)</u>	Depth (m)	SAMPLING <u>Direction</u>	SAMPLE DRY WEIGHT (grams)		
			Trap	Elevation Above Bed	(cm)
			<u>1.9</u>	<u>9.5</u>	<u>17.1</u>
5.0	0.26	OF	96.4	11.0	5.4
5.0	0.26	ON	6.1	3.9	1.7
5.0	0.26	LS-U	274.0	45.7	4.2
10.0	0.52	OF	78.0	4.6	0.8
10.0	0.52	ON	33.4	14.8	3.0

SHIP
Lake River

DATE
29OCT87

DIRECTION
Upstream $\alpha = 5^\circ$

Distance from <u>Shore (m)</u>	Depth (m)	SAMPLE DRY WEIGHT (grams)			
		<u>Sampling Direction</u>	<u>Trap Elevation</u> <u>1.9</u>	<u>Above Bed</u> <u>9.5</u>	<u>(cm)</u> <u>17.1</u>
5.0		OF	37.7	4.9	1.3
5.0		ON	8.0	0.9	1.2
5.0		LS-U	3.1	1.6	0.8
10.0		OF	16.4	1.3	0.3
10.0		ON	9.2	0.8	0.3

Leandros

30OCT87

Upstream $\alpha = 20^\circ$

Distance from <u>Shore (m)</u>	Depth (m)	SAMPLE DRY WEIGHT (grams)			
		<u>Sampling Direction</u>	<u>Trap Elevation</u> <u>1.9</u>	<u>Above Bed</u> <u>9.5</u>	<u>(cm)</u> <u>17.1</u>
5.0		OF	30.3	2.0	0.7
5.0		ON	8.0	1.9	1.2
5.0		DD	18.3	0.1	0.1
5.0		LS-U	23.4	18.9	10.8
10.0		OF	10.5	0.2	0.4
10.0		ON	5.4	0.7	0.5

SHIP DATE DIRECTION
European Highway 08JUN88 Upstream 11:15 $\alpha = 12^\circ$

Distance from Shore (m)	Depth (m)	SAMPLING Direction	SAMPLE DRY WEIGHT (grams)		
			Trap Elevation	Above Bed (cm)	
			1.9	9.5	17.1
5.8	0.33	OF	283.5	88.1	10.3
5.8	0.33	ON	175.0	52.7	35.7
5.8	0.33	LS-U	14.9	2.4	1.0
12.9	0.73	OF	10.1	4.4	1.5
12.9	0.73	ON	18.7	2.6	1.2
20.0	1.13	LS-U	3.3	0.4	0.1

USN Ford (54) 09JUN88 Upstream 9:07 $\alpha = 2^\circ$

Distance from Shore (m)	Depth (m)	SAMPLING Direction	SAMPLE DRY WEIGHT (grams)		
			Trap Elevation	Above Bed (cm)	
			1.9	9.5	17.1
14.0	0.79	OF	102.4	27.4	12.4
14.0	0.79	ON	80.0	21.4	9.7

USN Ramsey (2),
and USN 492, 493 09JUN88 Upstream 9:35 $\alpha = 5^\circ$

Distance from Shore (m)	Depth (m)	SAMPLING Direction	SAMPLE DRY WEIGHT (grams)		
			Trap Elevation	Above Bed (cm)	
			1.9	9.5	17.1
10.8	0.61	OF	146.3	81.2	47.2
10.8	0.61	ON	102.9	26.6	10.5
10.8	0.61	LS-U	3.1	1.7	1.6
16.1	0.91	OF	15.8	2.3	0.7
16.8	0.95	ON	24.9	5.1	0.2
18.4	1.04	LS-U	1.4	0.2	0.4

SHIP USN Thach (43) DATE 09JUN88 DIRECTION Upstream 10:10 $\alpha = 12^\circ$

Distance from <u>Shore (m)</u>	Depth (m)	SAMPLING <u>Direction</u>	SAMPLE DRY WEIGHT (grams)		
			Trap Elevation	Above Bed (cm)	
			<u>1.9</u>	<u>9.5</u>	<u>17.1</u>
7.6	0.43	OF	334.8	170.4	94.4
7.6	0.43	ON	56.0	31.4	14.5
8.7	0.49	LS-U	50.0	30.0	12.2
12.9	0.73	OF	33.9	1.7	0.8
14.0	0.79	ON	38.0	2.1	1.1
14.0	0.79	failed			

USN Gray (1054) 09JUN88 Upstream Time 10:23 $\alpha = 7^\circ$

Distance from <u>Shore (m)</u>	Depth (m)	SAMPLING <u>Direction</u>	SAMPLE DRY WEIGHT (grams)		
			Trap Elevation	Above Bed (cm)	
			<u>1.9</u>	<u>9.5</u>	<u>17.1</u>
7.6	0.43	OF	785.0	309.9	136.0
8.1	0.46	ON	219.3	116.9	75.7
9.2	0.52	LS-U	20.3	1.5	0.7

Coast Range 09JUN88 Upstream 13:00 $\alpha = 1^\circ$

Distance from <u>Shore (m)</u>	Depth (m)	SAMPLING <u>Direction</u>	SAMPLE DRY WEIGHT (grams)		
			Trap Elevation	Above Bed (cm)	
			<u>1.9</u>	<u>9.5</u>	<u>17.1</u>
5.0	0.33	OF	253.9	85.9	25.7
5.0	0.36	ON	166.5	74.1	26.6
5.0	0.33	DD	53.8	0.1	0.05
10.0	0.70	OF	11.7	0.6	0.65
10.0	0.76	ON	8.4	3.9	1.0
14.0	0.98	OF	6.0	0.3	0.4

SHIP
Coast Guard,
Boutwell
(719, Cutter)
and Iris
(Buoytender) 13JUN88 Downstream Time 11:00 $\alpha = 16^\circ$

Distance from <u>Shore (m)</u>	Depth <u>(m)</u>	SAMPLE DRY WEIGHT (grams) <u>Sampling Direction</u>	Trap Elevation Above Bed (cm)		
			<u>1.9</u>	<u>9.5</u>	<u>17.1</u>
5.0	0.35	OF	112.6	59.2	15.2
5.0	0.35	ON	45.3	1.3	3.2
5.0	0.35	LS-D	62.0	49.5	15.0
10.0	0.70	OF	10.8	1.0	0.7
10.0	0.70	ON	31.2	26.6	0.4
10.0	0.70	LS-D	1.0	0.2	0.1

Verrazano Bridge 13JUN88 Upstream 11:33 $\alpha = 3^\circ$

Distance from <u>Shore (m)</u>	Depth <u>(m)</u>	SAMPLE DRY WEIGHT (grams) <u>Sampling Direction</u>	Trap Elevation Above Bed (cm)		
			<u>1.9</u>	<u>9.5</u>	<u>17.1</u>
5.0	0.35	ON	8.9	1.8	0.7
5.0	0.35	OF	20.0	1.1	0.2
5.0	0.35	LS-U	0.6	0.3	0.2
10.0	0.70	OF	18.5	0.1	0.3
10.0	0.70	ON	1.8	0.3	0.1
10.0	0.70	LS-U	1.0	0.1	0.0

SHIP DATE DIRECTION
 Verrazano Bridge* 14JUN88 Downstream 16:40 $\alpha = 21^\circ$

Distance from Shore (m)	Depth (m)	SAMPLING Direction	SAMPLE DRY WEIGHT (grams)		
			Trap Elevation	Above Bed (cm)	
			1.9	9.5	17.1
11.0	0.76	LS-D	410.0	58.9	14.5
14.4	1.01	LS-D	335.9	49.1	14.9

*Because of large waves, traps were dislodged and data was disregarded.

RIVER FLOW SAND TRANSPORT IN THE NEAR SHORE REGION

06/14/89 11:10-11:22
 (3cm rise in water surface in that time)

Distance from Shore (m)	Depth (m)	SAMPLING Direction	SAMPLE DRY WEIGHT (grams)		
			Trap Elevation	Above Bed (cm)	
			1.9	9.5	17.1
10.4	0.73	LS-D	0.2	0.2	0.3
13.6	0.95	LS-D	15.2	0.1	0.1
17.0	1.19	LS-D	33.8	0.5	0.5

surface velocity at 1.22 m, 10:52 hrs. = 27.5 cm/s
 downstream

06/14/88 14:07-14:17

Distance from Shore (m)	Depth (m)	SAMPLING Direction	SAMPLE DRY WEIGHT (grams)		
			Trap Elevation	Above Bed (cm)	
			1.9	9.5	17.1
8.3	0.58	LS-U	0.1	0.0	0.0
10.6	0.76	LS-U	0.2	0.1	0.0
13.0	0.91	LS-U	5.9	0.2	0.1

surface velocity at 0.91 m, 13:50 hrs. = 14.1 cm/s upstream
 1.22 m, 13:56 hrs. = 15.1 cm/s upstream